

Electronic Thesis and Dissertation Repository

12-14-2023 5:00 PM

Imaging-Based Biomarkers for Evaluating Musculoskeletal Pain in the Hand and Wrist

Lauren Straatman, *Western University*

Supervisor: Lalone, Emily A, *The University of Western Ontario*

Co-Supervisor: Walton, David M, *The University of Western Ontario*

A thesis submitted in partial fulfillment of the requirements for the Doctor of Philosophy degree in Health and Rehabilitation Sciences

© Lauren Straatman 2023

Follow this and additional works at: <https://ir.lib.uwo.ca/etd>

Recommended Citation

Straatman, Lauren, "Imaging-Based Biomarkers for Evaluating Musculoskeletal Pain in the Hand and Wrist" (2023). *Electronic Thesis and Dissertation Repository*. 9883.

<https://ir.lib.uwo.ca/etd/9883>

This Dissertation/Thesis is brought to you for free and open access by Scholarship@Western. It has been accepted for inclusion in Electronic Thesis and Dissertation Repository by an authorized administrator of Scholarship@Western. For more information, please contact wlsadmin@uwo.ca.

Abstract

The defining symptom, and often the major reason for seeking medical treatment associated with most clinical disorders of the hand and wrist, is pain. However, pain mechanisms following MSK trauma are complex, multifactorial, and remain largely unknown. As such, this thesis sought to understand pain mechanisms in hand and wrist MSK pathologies, using imaging-based biomarkers and gold-standard pain evaluation techniques. Chapter 2 presents an exploratory analysis on the interacting influences of sex on multi-modal pain evaluation techniques that tap different pain domains. Our results highlight the importance of multiple pain measures when creating sex-specific intervention strategies, as the accuracy of predicting ones' clinical pain evaluation scores did not show true difference greater than chance. Chapter 3 explores the use of imaging-based biomarkers, namely subchondral volumetric bone mineral density (vBMD) and static joint contact area (JCA), to differentiate between two study cohorts. On average, our healthy cohort had a higher vBMD for all measured depths from the subchondral surface of the distal radius. Chapter 4 presents the relationship between subchondral vBMD and kinematic JCA throughout a range of motion in a healthy cohort of adults to understand the impact of joint contact on subchondral bone. In deep regions of subchondral bone, a higher vBMD was significantly correlated to a larger JCA, most notably during wrist extension. Lastly, Chapter 5 explores the preliminary association between structural and clinical disease progression, using pain evaluation measures and our imaging-based biomarkers, in a cohort of thumb carpometacarpal osteoarthritis (CMC OA) patients. Our preliminary results demonstrated that structural severity was significantly associated with a higher pain score and pain presentation was heterogeneous.

Keywords

Musculoskeletal pain, hand and wrist disorders, imaging-based biomarkers, pain evaluation techniques, pressure pain detection threshold, subchondral volumetric bone mineral density, joint contact area.

Summary for Lay Audience

The defining symptom, and often the major reason for seeking medical treatment associated with most clinical disorders of the hand and wrist, is pain. However, pain following hand and wrist musculoskeletal (MSK) trauma is likely due to several factors and remains largely unknown. The focus of this thesis is to explore underlying causes of pain associated with hand and wrist MSK trauma using imaging techniques and standard pain evaluation measures. The first project in this thesis was designed to explore the relationships between different forms of pain evaluation measures and how the sex of the participant may impact this relationship. We did this by comparing the results obtained from the pain measures between males and females, to determine whether there were consistencies (or differences) in the responses. Our results demonstrated the importance of using multiple pain measures to capture different aspects of the persons' pain experience. We also demonstrated that males and females likely respond to pain measures differently, and it is important to acknowledge this in studies moving forward. The second project in this thesis was designed to explore our imaging techniques in obtaining objective measures (biomarkers) to better understand pain. Specifically, we looked at bone density and the contact between bones as potential pain contributors. Bone density is thought to be a contributor to pain because of its rich blood and nerve supply. The contact between bones influences bone density, and as such we wanted to explore these two markers to differentiate between a healthy group of people and a group of people who have experienced some form of hand or wrist trauma. On average, the healthy group had an overall higher bone density than the hand or wrist trauma group. This finding encouraged us to explore this association further. The third project investigated the connection between bone density and joint movement in healthy adults, finding that a larger contact area between bones was linked to higher bone density, particularly during certain movements. The final project explored the connection between structural changes to the joint and pain in patients with thumb osteoarthritis. The initial findings from this project suggest that more severe structural changes to the thumb joint (such as a more progressed state of thumb osteoarthritis), were associated with more pain. Using the pain measures introduced in the first project, the results also demonstrated that pain symptoms varied among patients with thumb osteoarthritis. With all this information, we may be able to tailor treatment strategies aimed at minimizing pain following hand and wrist trauma.

Co-Authorship Statement:

Chapter 1:

Sole authorship: Lauren Straatman

Manuscript review: David Walton, Emily Lalone

Chapter 2:

Study design: Lauren Straatman, Michael Lukacs, David Walton

Data collection: Lauren Straatman, Michael Lukacs, Joshua Lee, David Walton

Data and statistical analysis: Lauren Straatman, David Walton

Manuscript preparation: Lauren Straatman

Manuscript review: David Walton, Emily Lalone, Michael Lukacs, Joshua Lee

Chapter 3:

Study design, data collection, statistical analysis: Lauren Straatman, Emily Lalone

Manuscript preparation: Lauren Straatman

Manuscript review: Nina Suh, Nikolas Knowles, David Walton, Emily Lalone

Chapter 4:

Study design: Lauren Straatman,

Data collection: Lauren Straatman, Megan Hutter, Randa Mudathir

Data and statistical analysis: Lauren Straatman, Elizabeth Norman

Manuscript preparation: Lauren Straatman

Manuscript review: Nina Suh, Nikolas Knowles, David Walton, Emily Lalone

Chapter 5:

Study Design: Lauren Straatman, Emily Lalone, David Walton

Data collection: Lauren Straatman, Megan Hutter, Randa Mudathir, Assaf Kadar

Data and statistical analysis: Lauren Straatman, David Walton

Manuscript preparation: Lauren Straatman

Manuscript review: Emily Lalone, David Walton

Chapter 6:

Sole authorship: Lauren Straatman

Manuscript review: Nina Suh, David Walton, Emily Lalone

Acknowledgments

The work completed in this thesis would not have been possible without the support and assistance from many. First and foremost, I would like to extend my deepest gratitude to my supervisors, Dr. Emily Lalone and Dr. David Walton. I am incredibly fortunate to have had the opportunity to work with two inspiring minds who have shaped me into the independent researcher I am today. Dr. Lalone has been truly monumental, and I owe much of the success of this work to her mentorship, assurance, and unmatched support in all walks of life. The brilliant insight and support from Dr. Walton has shaped my view of the importance of this work, and has inspired me to continue my academic career in the (currently), very murky world of pain. I would also like to acknowledge Dr. James Johnson, who hired me as an undergraduate research student many moons ago and saw the potential for me to succeed in research before I knew it was what I wanted. Thank you.

I also want to acknowledge my lab mates, current and past: Sydney Robinson, Carla DuToit, James Hunter, Kylie Paliani, Megan Hutter, Randa Mudathir, Maxwell Campbell, Elizabeth Norman, Josh Lee, Michael Lukacs, Zoe Leyland, Dorota Klubowicz, Iyad Al-Nasari, and Mohamad Fakhereddin. I want to extend my gratitude to Maxwell and Elizabeth; words cannot describe how grateful I am for your friendship and much needed support in times where I needed it most. Thank you both.

A very special thank you to my partner, Emily. Thank you for letting me practice all my presentations on you and for listening to me passionately discuss all aspects of my thesis weekly. Your unwavering support means the world and more.

Thank you to my friends and family, specifically my parents. Mom, thank you for your encouragement and constant reassurance that I do in fact “know what I’m doing with my life”. Dad, Dr. Tony Straatman, thank you for your invaluable mentorship. Your passion for academia has been instilled in me, and I am so proud to follow in your footsteps. Words can’t describe how fortunate I am to have role models like you.

Table of Contents

Abstract	ii
Summary for Lay Audience	iii
Co-Authorship Statement:	iv
Acknowledgments	v
Table of Contents	vi
List of Tables	xi
List of Figures	xii
List of Appendices	xiv
Chapter 1	1
1 Introduction	1
1.1 Understanding the Burden of Chronic Pain	2
1.1.1 The Influence of Sex and Gender on Chronic Pain	3
1.1.2 Musculoskeletal Pain	4
1.2 Anatomy of the Hand and Wrist	6
1.2.1 Osseous Anatomy	6
1.2.2 Subchondral Bone Tissue	8
1.2.3 Skeletal Anatomy: Hand and Wrist	11
1.2.4 Wrist Joints and Movement	20
1.3 Clinical Disorders of the Hand and Wrist	25
1.3.1 Wrist Fractures	25
1.3.2 Osteoarthritis	25
1.4 Evaluating Pain in Hand and Wrist Disorders	28
1.4.1 Patient Reported Outcome Measures	28
1.4.2 Quantitative Sensory Testing	31

1.4.3 Imaging Modalities	32
1.5 Thesis Rationale.....	35
1.6 Objectives and Hypotheses	36
1.7 Thesis Overview	37
Chapter 2.....	53
2 Are people good prognosticators of their own pain? An exploration of the relationship between sex-specific pain beliefs and clinical pain evaluation.....	53
2.1 Introduction.....	54
2.2 Methods.....	55
2.2.1 Participants.....	55
2.2.4 Testing Procedures	56
2.2.5 Statistical Analysis.....	58
2.2.6 Sample Size Estimation	60
2.3 Results	60
2.3.1 Participant Demographics	60
2.3.2 Study 1 – Healthy, Objective 1	63
<i>How accurate are sex-specific personal pain beliefs?</i>	63
2.3.3 Study 1 – Healthy, Objective 2	63
<i>Is accuracy of sex-specific personal pain beliefs different between sexes?</i>	63
2.3.4 Study 2 – Acute MSK Trauma, Objective 1	66
<i>How accurate are sex-specific personal pain beliefs?</i>	66
2.3.5 Study 2 – Acute MSK Trauma, Objective 2	66
<i>Is accuracy of sex-specific personal pain beliefs different between sexes?</i>	66
2.4 Discussion	69
2.5 Limitations	70
2.6 Conclusion	71

2.2	References.....	72
3	The Utility of Quantitative CT (QCT) To Detect Differences in Subchondral Bone Mineral Density Between Healthy People and People with Pain Following Wrist Trauma	74
3.1	Introduction.....	75
3.2	Methods.....	76
3.2.1	Study Protocol.....	76
3.2.2	CT Scanning.....	77
3.2.3	QCT Analysis.....	78
3.2.4	Statistical Analysis.....	81
3.3	Results	82
3.3.1	Participant Demographics	82
3.3.2	Volumetric Bone Mineral Density between Cohorts.....	85
3.3.3	Bilateral Volumetric Bone Mineral Density Comparison	86
3.4	Discussion	89
3.5	Limitations	91
3.6	Conclusion	92
3.7	References	93
	Chapter 4.....	98
4	Use it or lose it: The Relationship between Two Image-Based Biomarkers in Better Understanding Joint Adaptation in the Wrist.....	98
4.1	Introduction.....	99
4.2	Methods.....	100
4.2.1	Study Protocol.....	100
4.2.2	Quantitative Computed Tomography Analysis	103
4.2.3	Statistical Analysis.....	105
4.3	Results.....	106

4.3.1	Correlation Analysis	107
4.3.2	Regression Analysis.....	110
4.4	Discussion.....	112
4.5	Limitations	114
4.6	Conclusion	115
4.7	References.....	116
Chapter 5	121
5	Understanding Structural and Clinical Disease Severity in thumb CMC OA: A Preliminary Analysis Combining Image-Based Biomarkers and Pain Evaluation Techniques.	121
5.1	Introduction.....	122
5.2	Methods.....	124
5.2.1	Participants.....	124
5.2.2	Study Protocol.....	124
5.2.3	Quantitative CT Analysis.....	126
5.2.4	Patient-Reported Outcome Measure Analysis	127
5.2.5	Analyses	129
5.3	Results.....	129
5.3.1	Participant Demographics.....	129
5.3.2	Pain Evaluation Exploratory Analysis	132
5.4	Discussion	137
5.5	Limitations	139
5.6	Conclusion	139
5.7	References.....	141
Chapter 6	146
6	General Discussion and Conclusions.....	146
6.1	Summary.....	146

6.2 Future Directions 149

6.3 References 153

Appendices 155

Curriculum Vitae 199

List of Tables

Table 2-1: Participant Demographics	62
Table 2-2: Results from the independent samples t-test comparing sex-specific pain beliefs and clinical pain evaluations using z-transformations.	64
Table 2-3: AUC values and 95% Confidence Intervals from ROC curves. Independent groups analysis demonstrated the differences between males and females AUC values using a z-test.	67
Table 3-1: Participant Demographics.	83
Table 4-1: Pearson product-moment correlation (r).	108
Table 4-2: Model summary for the hierarchical regression analysis, with subchondral bone region as the dependent variable.....	111
Table 5-1: Summary statistics and results of vBMD (mg/K ₂ HPO ₄ cm ³), at each anatomical site for each normalized depth.	130

List of Figures

Figure 1-1: Anatomy of a Long Bone.....	7
Figure 1-2: Histology of Subchondral Bone.....	9
Figure 1-3: Subchondral bone remodeling.....	11
Figure 1-4 Bony Anatomy of Forearm, Wrist, and Hand.....	12
Figure 1-5: Bony anatomy of the Radius.....	14
Figure 1-6 Bony Anatomy of the 1st metacarpal.....	15
Figure 1-7 Bony Anatomy of the Carpals.....	17
Figure 1-8 Bony Anatomy of the Scaphoid.....	18
Figure 1-9 Bony Anatomy of the Lunate.....	18
Figure 1-10 Bony Anatomy of the Trapezium.....	19
Figure 1-11 Radiocarpal and Carpometacarpal Joints.....	21
Figure 1-12 Motions of the Wrist.....	22
Figure 1-13 First Carpometacarpal Joint.....	23
Figure 1-14 Motions of the Thumb.....	24
Figure 1-15 Scapholunate Advances Collapse Progression in the Hand.....	27
Figure 2-1: Accuracy of perceived ability to handle pain in predicting PPDT and CPT between a) males and b) females in the healthy cohort.....	65
Figure 2-2: Accuracy of perceived ability to handle pain in predicting BPI Severity and Interference between a) males and b) females in the acute MSK trauma cohort.....	68
Figure 3-1: Flow chart of the methodological sequence for QCT analysis.....	80

Figure 3-2: Representative data from a healthy participant (top rows) and a participant with previous wrist trauma (bottom rows).....	84
Figure 3-3: Mean vBMD comparison between the dominant wrist of the healthy cohort and the injured wrist of the trauma cohort.....	85
Figure 3-4: Bilateral vBMD differences in the healthy cohort.....	87
Figure 3-5: Bilateral vBMD differences in the trauma cohort.....	88
Figure 4-1: Static CT scan accompanied by calibration phantom.....	102
Figure 4-2: Wrist motions analyzed in 10-degree increments.....	104
Figure 4-3: Representative figure of healthy male data.....	109
Figure 5-1: Volumetric BMD between the healthy cohort and thumb CMC OA cohort.	131
Figure 5-2: Localized nociceptive pain phenotype.....	133
Figure 5-3: Widespread nociceptive pain phenotype.....	134
Figure 5-4: Localized neuropathic pain phenotype.....	135
Figure 5-5: Central nociplastic pain phenotype.....	136

List of Appendices

Appendix A: The Gender Role and Expectations of Pain Questionnaire (GREP).....	155
Appendix B: The Brief Pain Inventory	156
Appendix C: Calibration Phantom	158
Appendix D: The Patient-Rated Wrist Evaluation (PRWE)	159
Appendix E: Letter of Information and Consent (Ch. 5)	160
Appendix F: Study Specific Body Diagram	166
Appendix G: The Multidimensional Symptom Index (MSI)	167
Appendix H: The Self-Reported Leeds Assessment of Neuropathic Signs and Symptoms (S-LANSS)	168
Appendix I: Additional static subject-specific JCA and subchondral vBMD maps from Chapter 3 – Healthy Participants	169
Appendix J: Additional static subject-specific JCA and subchondral vBMD maps from Chapter 3 – Wrist Trauma Participants	174
Appendix K: Additional kinematic subject-specific JCA and subchondral vBMD maps from Chapter 4 – Healthy Participants	179

Chapter 1

1 Introduction

OVERVIEW

Imagine waking up every morning with a constant, nagging pain that never goes away. No matter what you do, it's always there, affecting your mood, your relationships, and your ability to enjoy life. This is the reality for millions of people around the world who suffer from chronic pain, a condition that can have a profound impact on every aspect of daily life. The purpose of this thesis is to explore pain evaluation techniques and the role of imaging-based biomarkers to better understand mechanisms underlying chronic pain in the hand and wrist. This introductory chapter provides an overview of chronic pain in the hand and wrist, hand and wrist skeletal and bone tissue anatomy, clinical disorders of the hand and wrist, evaluating pain in hand and wrist disorders, and the current state of literature regarding the role of imaging modalities on underlying bone changes and potential pain mechanisms.

1.1 Understanding the Burden of Chronic Pain

The defining symptom associated with most clinical disorders of the hand and wrist, and often the major reason for seeking medical treatment, is pain. While there have been numerous definitions of pain developed for the sake of understanding its myriad impacts, pain is one of the most multidimensional, complex, universal, human experiences, representing significant societal, economical, personal, and clinical burdens. Recognized as a deeply subjective experience, the International Association of the Study of Pain (IASP) provides a standardized definition of pain, re-defining pain as: “*An unpleasant sensory and emotional experience associated with, or resembling that associated with, actual or potential tissue damage.*”¹

Pain experience differs based on the duration and often the underlying cause. Acute pain is typically caused by a physical injury, serving as a warning signal to the body that something is wrong (for example spraining your ankle, cutting your finger, breaking a bone, etcetera). Acute pain usually resolves once the underlying physical injury or condition has healed, typically lasting between three to six weeks.^{2,3} However, when acute pain persists beyond six weeks, this is considered chronic pain. Chronic pain however does not always have a mechanism of onset or a warning function like acute pain, and can arise through several psychological, biological, and/or cultural variables.^{4,5} The point at which chronic pain can be diagnosed varies with the mechanism of injury, condition, or onset, but it is generally held that pain persisting beyond three months is most commonly the accepted definition of “chronic”.^{6,7}

It is estimated that chronic pain impacts 18.9% of adults in Canada, accounting for approximately \$43 billion CAD in annual costs associated with unemployment, productivity, and health care costs.⁷ Alongside the physical and financial effects of chronic pain, many studies have reported that a large proportion of chronic pain sufferers struggle with depression, anxiety, and feelings of isolation from family, occupation, and society.^{6,8-11} Taken together, the physical, financial, and emotional burden of chronic pain

significantly impacts patient quality of life, treatment effectiveness for chronic pain relief, and contributes to increasing health care costs.

Recent shifts towards biopsychosocial models of pain have provided new ways to understand this complex problem. Historically, a biomedical pain approach has been used by medical professionals treating pain, wherein the medical professional assesses the person physically using radiographic techniques to determine the injury, and then prescribes a treatment plan to target pathoetiology.¹² However, this insinuates that the physical injury is the only likely cause of the patients' pain, without consideration of any other aspects of the patient's life. The biopsychosocial model takes a holistic stance on pain assessment, by considering the psychological and social components (environment, culture, interpersonal dynamics), in addition to the biological components.¹³

1.1.1 The Influence of Sex and Gender on Chronic Pain

There are many patient demographics that influence or impact chronic pain research. Sex and gender are two demographics that hold significant merit, impacting chronic pain research, presentation, and response to pain evaluation techniques (further discussed in section 1.2.4). Sex and gender are terms commonly but erroneously used interchangeably. As defined by the Canadian Institute of Health Research (CIHR), *gender* is defined as “*socially constructed roles, behaviors, expressions and identities of girls, women, boys, men, and gender diverse people*”, while *sex* is defined as “*biological attributes in humans and animals*”.¹⁴ For ease of interpretation, we have conceptualized sex as a dichotomy of males and females (though acknowledge that a very small proportion of biologically intersex people exist), while gender will be conceptualized as identities existing along a socially constructed continuum of roles, behaviors, and beliefs.

The influence of *sex* on chronic pain prevalence is best represented by the prevalence rates of many musculoskeletal (MSK) pain conditions. For example, women are more likely to experience a variety of chronic MSK pain syndromes, outnumbering men in most chronic pain populations including headache, neck, shoulder, knee, back pain, and most notably osteoarthritis (OA) population-based studies by about a 2:1 ratio.^{4,12,15–19} Women are also more likely to experience multiple chronic pain conditions simultaneously, and report

more severe levels of pain at more anatomical locations in comparison to their male counterparts.^{4,15,17,18,20–26} There have been studies demonstrating biological differences between men and women (namely, hormonal and genetic differences), contributing to sex differences in pain presentation and experience.^{27–29} However, the cause-and-effect of these findings have not been established.

The experience of chronic pain is also influenced by *gender* norms and societal expectations. Since pain by definition is always subjective, it is inherently influenced by social factors that often stem from childhood.^{20,27,30} For example, studies have suggested that boys and girls are socialized along gender role expectations for how to respond to pain – girls are socialized to be careful, sensitive, and vocal regarding pain or discomfort, while boys are socialized to be stoic, and more tolerant of pain and painful experiences.^{20,24,27,29} Consequently, gender role expectations from childhood may influence pain presentation and expression in adulthood. However, the recent shift from binary concepts of gender (masculine v feminine, man v woman) to gender fluid identities, in addition to gender identities that are different from sex assigned at birth, require more rigorous analysis to better understand how these concepts are represented in chronic pain research.

Altogether, it is important to consider both *sex* and *gender* in chronic pain research, as neither concept alone can account for potential or observed differences in chronic pain presentation or expression. *Sex* and *gender* have complex and multi-faceted influences on chronic pain, therefore recognizing and acknowledging these influences is critical for equitable and just understandings of chronic pain.

1.1.2 Musculoskeletal Pain

Musculoskeletal (MSK) pain is characterized as pain that often arises from the bones, muscles, ligaments, tendons, and other structures that support the body's MSK system. MSK pain is a highly prevalent and costly problem on global health care systems,³¹ and is found to be a major cause of years living with pain and disability worldwide.^{32–34} It can be acute or chronic, caused by a variety of factors including injury, overuse, or inflammation. Pain that arises from *acute* MSK injuries such as a wrist fracture, are considered to

potentially have a strong peripheral nociceptive driving force – the break in the wrist bone resulted in damage to the bone tissue and surrounding joint structures, stimulating high-threshold nociceptors in the periphery that transmit signals of threat or harm towards the central nervous system.¹² It is of note that tissue damage is only potentially responsible for the pain experience, as tissue damage is neither necessary nor sufficient in isolation to explain the pain experience. *Chronic* MSK pain is not always as closely associated with a strong peripheral nociceptive input, though in some cases pathological lesions can be identified (e.g., osteoarthritis (OA)). Problems arise with chronic pain that is associated with MSK related disorders, as these conditions have a considerable effect on the health and well-being of the individual inflicted and have been described as an escalating problem in Canada and the United States.³⁵ Although common, there is a lack of understanding surrounding the mechanisms underlying chronic pain after MSK trauma and a lack of knowledge on the etiological factors behind nonmalignant but long-term pain in MSK related trauma.³⁵

1.1.2.1 Hand and Wrist MSK Pain

The hand and wrist are common sites of MSK pain and the most susceptible to injury in the upper limb.³⁶ Hand and wrist MSK pain are highly prevalent in young populations who partake in physically demanding activities, such as manual laborers and athletes, as well as older populations. Although it is not as common as other MSK pain complaints, hand and wrist pain represent a significant proportion of overall MSK burden.³¹

Distal radius fractures (DRF) are one such form of hand and wrist MSK injuries that commonly cause pain and disability (introduced in section 1.2.5.1).^{36,37} The societal effects of distal radius fractures extend to medical costs of hospital visits, decreased school attendance for the pediatric and adolescent population, lost work hours, loss of independence, and lasting pain and disability.^{36,38} While it has been found that most patients who sustained a DRF recover in the initial three to six months, approximately 22% of patients experience pain and disability one-year following fracture.³⁷

OA is the leading cause of insidious MSK pain in the hand and wrist, affecting approximately 13.6% of Canadians aged 20 years and older as of 2017.³⁹ The prevalence

of OA generally increases with age, and due to a growing and aging Canadian population the prevalence and burden of disability associated with OA are predicted to increase.³⁹⁻⁴¹ There is often discrepancy between the presence of the defining features of OA, namely degeneration of articular cartilage (explained in depth in section 1.3.2), and pain symptoms, as the articular cartilage itself is not an innervated tissue. This discrepancy highlights the complexity of this disease and the need for more rigorous exploration into the mechanisms underlying pain symptoms associated with OA in the hand and wrist. This concept will be discussed more in later sections of the introduction.

1.2 Anatomy of the Hand and Wrist

The subsequent chapters of this thesis focus on specific joints and movements in the hand and wrist. As such, this section of the introduction provides a brief overview of the bones, and associated joints and articulations that I will refer to for the remainder of this thesis.

1.2.1 Osseous Anatomy

Bone tissue is made up of a variety of cohesive tissues that work together to provide mechanical structure, stability, protection, support, and overall health maintenance to the human body. The human skeleton is split up into two major divisions: the axial skeleton, consisting of the head, neck and trunk, and the appendicular skeleton, consisting of the arms, legs, and girdles. Bones are classified based on their shape and mechanical ability, such as long and short bones of the extremities, flat bones of the sternum and skull, and irregular shaped bones such as the vertebrae.

Long bones are characterized as having a long shaft (diaphysis) and two wide ends (metaphyses) (Figure 1-1).⁴² Long bones make up most of the upper extremity, including the humerus, radius, ulna, and the metacarpals. The diaphysis is the long shaft of the bone, composed of a hard outer shell of cortical bone enclosing soft trabecular bone, all surrounding a marrow cavity filled with yellow bone marrow. Yellow marrow is composed of adipose tissue and plays an important role in energy storage and bone remodeling due to its ability to differentiate into various types of bone cells, namely osteoblasts (bone-forming cells) and chondrocytes (cartilage-repairing cells).⁴² Distal and proximal to the diaphysis are the metaphyses – the wide portions at the ends of the long

bones that are responsible for bone growth throughout development. Adjacent to the metaphyses are the epiphyses – the rounded ends of the long bones that articulate with adjacent bones to form a joint. Covered in articular cartilage to aid in frictionless and shock absorbing movement, the epiphyses are mostly composed of trabecular bone with a thin layer of cortical bone. Red bone marrow fills the spaces within the trabecular bone, facilitating the production of both red and white blood cells.⁴² This will be discussed further in section 1.2.2.1 where we look at the vascularity of the subchondral bone.

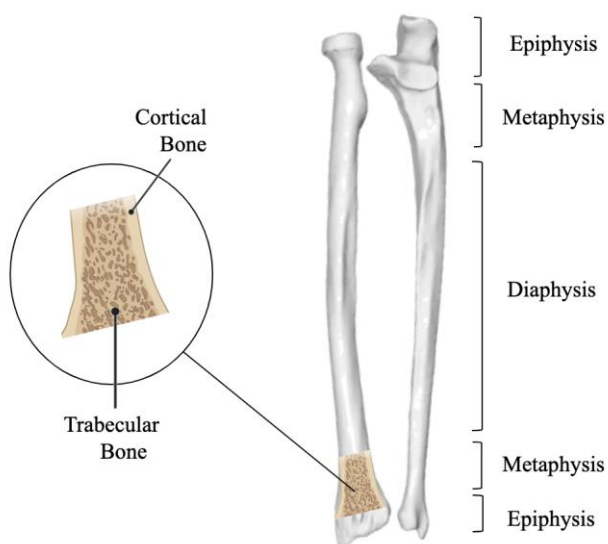


Figure 1-1: Anatomy of a Long Bone.

The long bone is characterized by proximal and distal metaphyses, epiphyses, and a diaphysis. The diaphysis is composed of a thick layer of cortical bone encasing trabecular bone. The metaphyses are composed mainly of trabecular bone, with a thin layer of cortical bone surrounding it.

Short bones are small, spherical-like bones mainly composed of trabecular bone with a thin layer of cortical bone and can be found in the wrist and feet. The eight carpal bones in the wrist are examples of short bones, where they serve as structural support and are integral for movement, shock absorption, and the distribution of load and pressure on the joint.^{43,44} As they are mainly composed of trabecular bone, short bones are also key contributors to blood cell production.⁴²

1.2.2 Subchondral Bone Tissue

Subchondral bone tissue is characterized as the bone tissue that lies directly beneath the articular cartilage covering the bone. The subchondral bone region is highly variable, depending on the function of the bone, but always consists of two different tissue types: cortical and trabecular bone tissue. Both types of bone tissue are essential for proper functioning, however, differ in their functionality, structure, and location within the bone.^{42,45} Cortical bone, also known as compact bone, is dense and hard bone tissue that makes up the outer surface of a bone and can vary in thickness (Figure 1-2). It is made up of tightly packed osteons that consist of concentric layers of bone tissue surrounding a central canal that contains blood vessels and nerves. Within the concentric layers are osteocytes, characterized as mature bone tissue that surround the osteons.⁴² Cortical bone makes up the bulk of the diaphysis of long bones and has a pronounced effect on the structural integrity of the bone, aiding in stress resistance produced by load and movement. Trabecular bone, also known as spongy or cancellous bone, is a less dense and more porous type of bone tissue that is protected by a covering of cortical bone (Figure 1-2). It is made up of a network of interconnecting trabeculae separated by spaces filled with bone marrow.⁴² As previously described, trabecular bone contains both yellow and red bone marrow – yellow marrow is an essential energy storage component while red bone marrow aids in blood cell production.^{42,45}

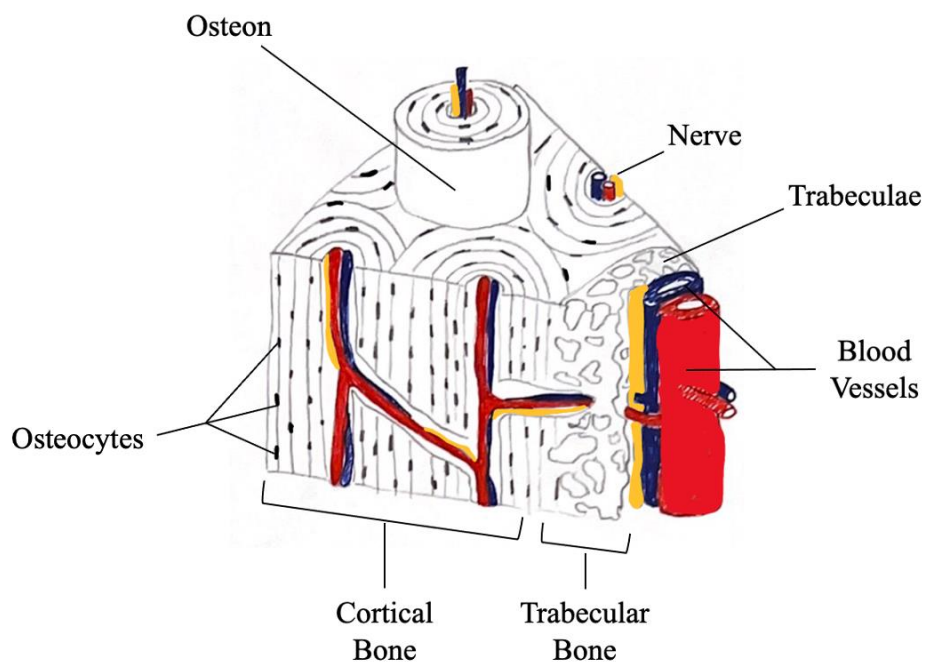


Figure 1-2: Histology of Subchondral Bone.

Subchondral bone tissue is made up of cortical and trabecular bone. Cortical bone is arranged in a series of osteons that contain blood vessels and nerves. Trabecular bone is composed of interconnecting trabeculae that are separated by bone marrow.

1.2.2.1 Vascularity and Innervation of Subchondral Bone

Subchondral bone is highly vascularized and innervated, supplied by a complex network of blood vessels and sensory nerves that are important for maintaining the health and function of the bone tissue (Figure 1-2).^{42,45,46} The blood supply to the bone is provided by arteries and vessels that penetrate the hollow spaces within the trabeculae. These blood vessels, which are abundant in regions of trabecular bone due to the high concentration of red bone marrow, supply nutrients and oxygen to the bone tissue. Sensory nerves accompany the blood vessels that supply the bone tissue, providing sensory information about movement, pressure, and mechanical changes, such as tension or tearing that occurs with fractures or bone tumors.^{42,46,47} Therefore, trabecular bone tissue has been found to serve as a major player in pain perception and supplying the bone tissue with nutrients.

1.2.2.2 Subchondral Bone Remodeling

Subchondral bone is a dynamic, metabolically active tissue that regularly undergoes bone remodeling (Figure 1-3).^{42,45} Bone remodeling is a continuous process of bone resorption and bone formation, tightly regulated by various factors including hormones, mechanical loading, and the type of bone tissue (cortical versus trabecular bone). Bone resorption is the removal of minerals and collagen fibers from bone by osteoclasts, resulting in the breakdown of the extracellular matrix of bone. Bone formation is the addition of minerals and collagen fibers to bone by osteoblasts, resulting in the formation of the extracellular matrix. The remodeling process is critical for the maintenance of bone health and integrity, where disruptions can lead to degenerative bone diseases, such as osteoporosis, characterized by low bone density and disrupted bone microarchitecture,⁴⁸ or OA, where morphological and biochemical changes associated with OA propagate bone tissue changes.^{49,50}

On average, 5-10 percent of the total bone mass in humans is remodeled each year, where the rate of renewal differs between the types of bone tissue.⁴² In cortical bone, four percent of bone tissue is remodeled each year compared to 20 percent of trabecular bone. Bone remodeling is triggered by exercise, lifestyle modifications, changes in diet, and is dependent upon body region.⁴² Due to its dynamic structure, subchondral bone adapts in

response to mechanical loads in order to bear said loads, becoming more dense and therefore stronger than other regions that are not mechanically stimulated.^{45,49,51,52} This effect can be seen when comparing weight-bearing joints, namely the lower extremities,^{53,54} to non-weight bearing joints, namely the upper extremity.^{45,55}

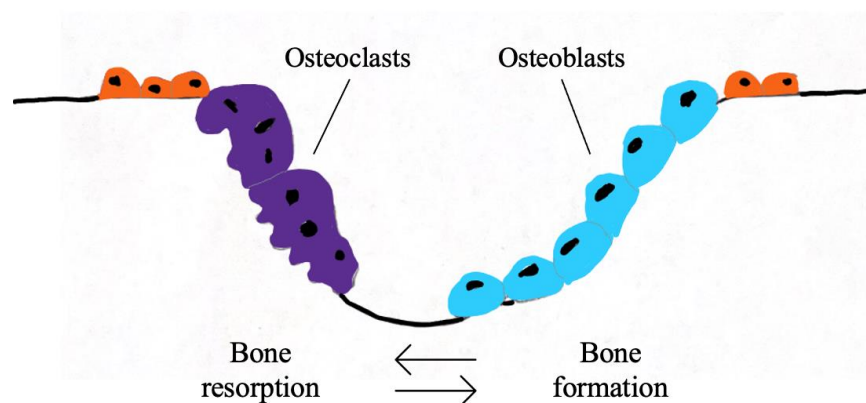


Figure 1-3: Subchondral bone remodeling.

Bone remodeling is a continuous process of bone resorption (through osteoclasts) and bone formation (through osteoblasts). Bone homeostasis is achieved through a balance of resorption and formation.

1.2.3 Skeletal Anatomy: Hand and Wrist

The hand and wrist are complex joints made up of four groups of bones: the forearm, carpus, metacarpus, and the phalanges (Figure 1-4).⁴² It is made up of two long bones and eight short bones called carpal bones, which are arranged in two rows. The carpal bones are connected to the two long bones in the forearm, the radius and ulna, and to the metacarpals and phalanges. The wrist is supported by ligaments, tendons and muscles that help to stabilize and move the joint.

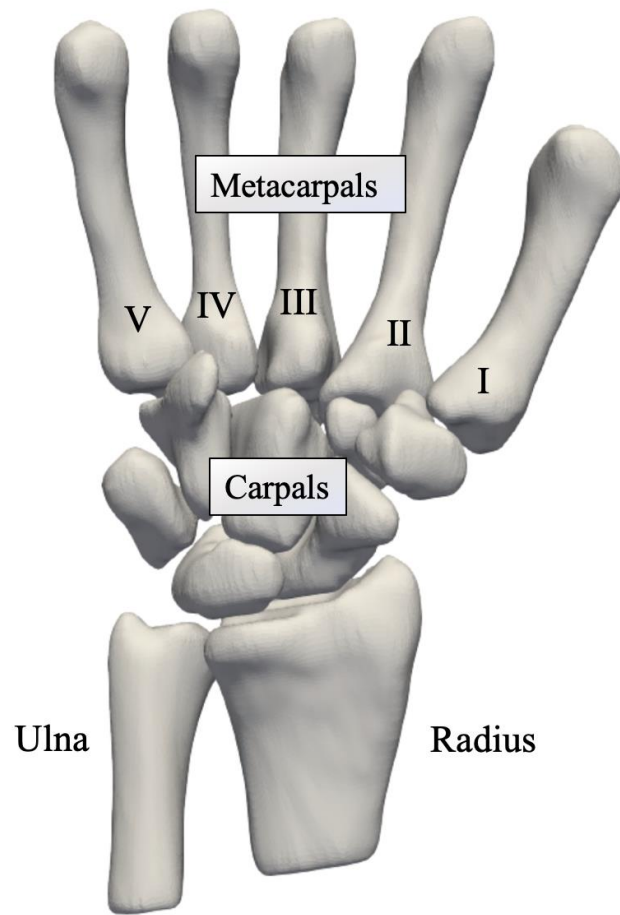


Figure 1-4 Bony Anatomy of Forearm, Wrist, and Hand.

Volar view of the skeletal anatomy of the right forearm, wrist, and hand.

1.2.3.1 Radius

The radius is a long bone located on the lateral aspect (thumb side) of the forearm and is characterized as the shorter of the two forearm bones (Figure 1-5). The radius articulates with four bones – the humerus, ulna, scaphoid, and lunate. The diaphysis of the radius presents as a rod-like bone, expanding at both proximal and distal ends. Proximally, the radius forms a golf-tee-like head that articulates with the radial notch on the ulna and the distal end of the humerus to allow for elbow movement.

Inferior to the head is the shaft of the radius, containing a roughened area on the volar aspect of the shaft that serves as a point of attachment for the tendon of the bicep brachii muscle. The volar surface of the radius is concave, while the dorsal surface is convex and grooved for extensor muscle tendons. Halfway down the dorsal surface of the radius is another roughened area that serves as a point of attachment for the pronator teres muscle, a superficial forearm muscle responsible for pronating the forearm. The medial side of the shaft has a distinct interosseous border, serving as an attachment site for the interosseous membrane that joins the shafts of the radius and ulna.

The distal radius expands into two articular surfaces allowing it to articulate with the scaphoid and lunate, forming the widest part of the bone and the major component of the wrist joint known as the radiocarpal joint. The medial aspect of the distal radius articulates with the ulna via the ulnar notch, forming the distal radioulnar joint (DRUJ).

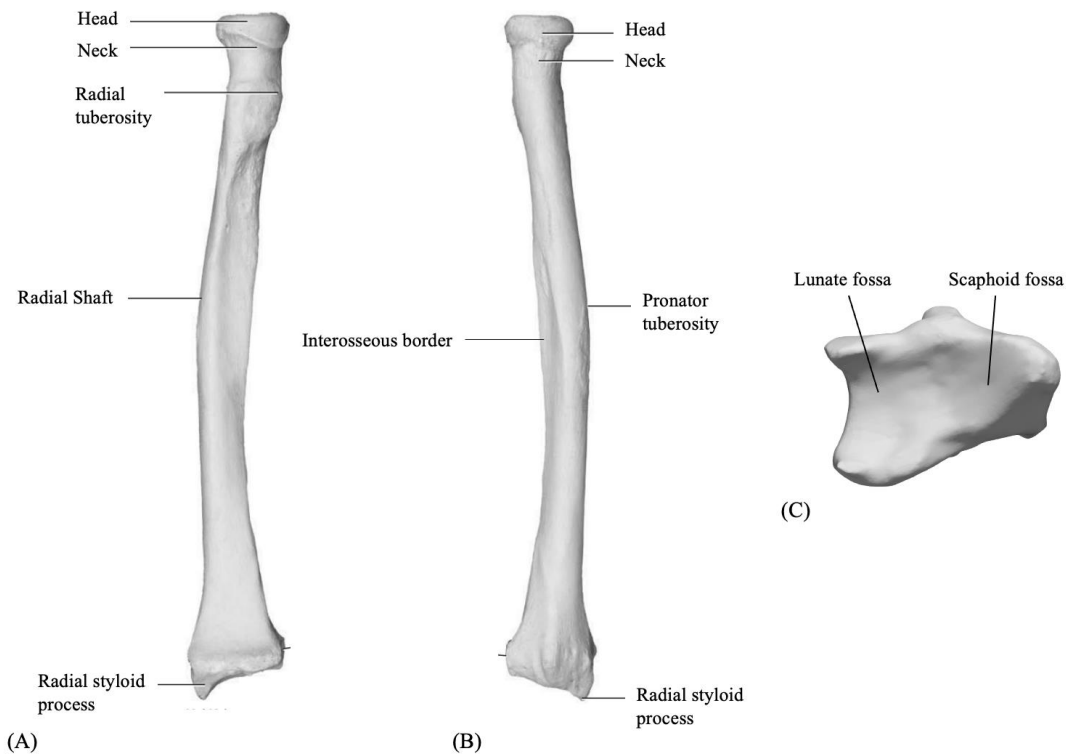


Figure 1-5: Bony anatomy of the Radius.

The bony anatomy of the radius in volar (A), dorsal (B), and distal surface (C) views.

1.2.3.2 First Metacarpal

The metacarpus is the intermediate region of the hand, consisting of five long bones called metacarpals (Figure 1-4). The metacarpals are numbered one to five, starting with the thumb. Like all long bones, the first metacarpal (MC) consists of a tubular shaft (diaphysis) with a proximal head and a distal articular base (metaphyses) (Figure 1-6). The first MC is medially rotated with respect to the remaining four metacarpals. Consequently, its dorsal surface faces radially and the palmar surface faces ulnarly.

The base of the first MC forms a saddle-like surface that articulates with the trapezium, forming the trapeziometacarpal (TMC) or first carpometacarpal (CMC1) joint. The head of the first MC is rounded and commonly forms the “knuckles” in the hand, articulating with the base of the first phalanx. Compared to the other metacarpals, the first MC is the shortest and thickest, consisting of a thicker layer of cortical bone encasing the trabecular bone. This is due to the independence and functionality of the CMC1 joint, serving to provide stability, load-bearing function that is unique to this joint (including gripping and grasping), and fine-motor skills which necessitate increased strength and dexterity.

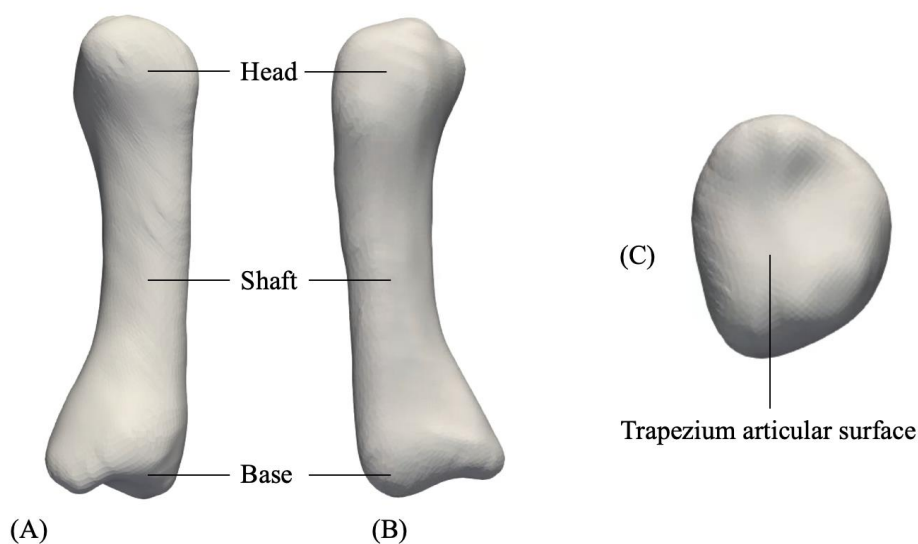


Figure 1-6 Bony Anatomy of the 1st metacarpal.

Bony anatomy of the right 1st MC in the volar (A), dorsal (B), and distal (C) views.

1.2.3.3 Carpal Bones

The carpus is composed of eight short bones arranged in two rows of four bones (Figure 1-7). Moving lateral to medial, the proximal row contains the scaphoid, lunate, triquetrum, and pisiform, and the distal row contains the trapezium, trapezoid, capitate, and hamate. This complex series of bones contains numerous articular surfaces that allow for movement about the carpals, metacarpals, and the forearm bones. The proximal row of the carpals articulates with the distal end of the radius and ulna to form the radiocarpal joints, while the distal row articulates with the metacarpals to form the carpometacarpal (CMC) joints.

The scaphoid is the largest short bone found in the proximal row of carpal bones and articulates with the distal radial surface to form the radioscapoid (RS) joint (Figure 1-8). The scaphoid is a stabilizing, boat-like bone that serves as a critical link for wrist movement and function. Much of its surface is articular, although it possesses a roughened dorsolateral surface at its waist and a palmar-laterally directed tubercle on the distolateral surface serving as a site for ligamentous attachment. The scaphoid has a large convex articular surface for the radius extending dorsally, a flat semilunar surface for the lunate medially, a large concave surface for the distal end of the capitate, and a generally triangular shaped distal surface for the trapezium and trapezoid. The scaphoid also serves as a major site of force transmission within the wrist joint.⁵⁶

The lunate is the second largest short bone found in the proximal row of carpal bones (Figure 1-9). It is characterized by a semilunar shape and like the scaphoid, has five articular surfaces. Proximally, the lunate has a large convex shape that articulates with the distal radius. Distally, the concave shape of the lunate articulates with the distal end of the capitate, similar to the scaphoid. The medial facet of the lunate articulates with the triquetrum, while the distomedial surface articulates with the hamate. Laterally, the flat semilunar surface articulates with the scaphoid, generating the bulk of the wrist joints stability and movement with the help of several ligaments that connect the bones together.

The trapezium is a small, irregularly shaped short bone found in the distal row of carpal bones, located at the base of the thumb (Figure 1-10). The flat, proximal surface of the

trapezium articulates with the scaphoid while the unique, saddle-shaped distal surface articulates with the base of the first MC. This saddle-shaped joint allows for a wide range of motion and flexibility within the thumb – FE, abduction and adduction, and circumduction. The distomedial surface articulates with the second MC, while the concave medial surface articulates with the trapezoid. Like the other carpal bones, the trapezium possesses tubercles on its volar surface containing a groove for tendon attachment and stability.⁴²

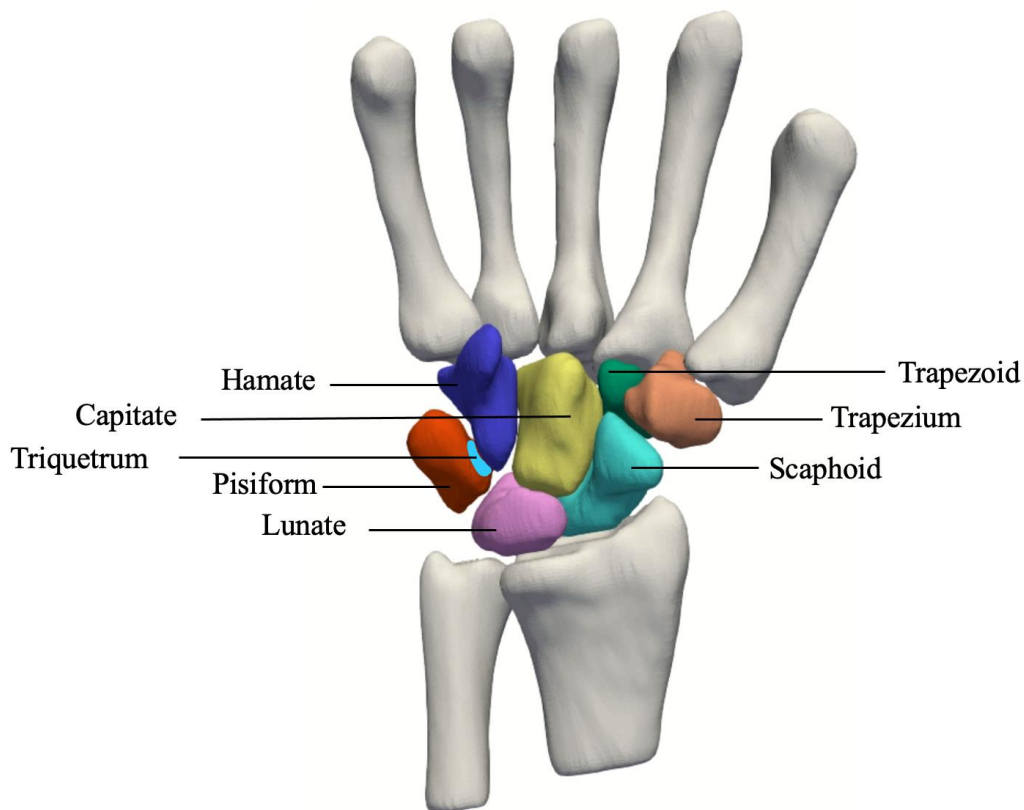


Figure 1-7 Bony Anatomy of the Carpals.

Bony anatomy of the right wrist in a volar view, demonstrating the proximal (scaphoid, lunate, pisiform, and triquetrum) and distal (trapezium, trapezoid, capitate, and hamate) rows of carpals.

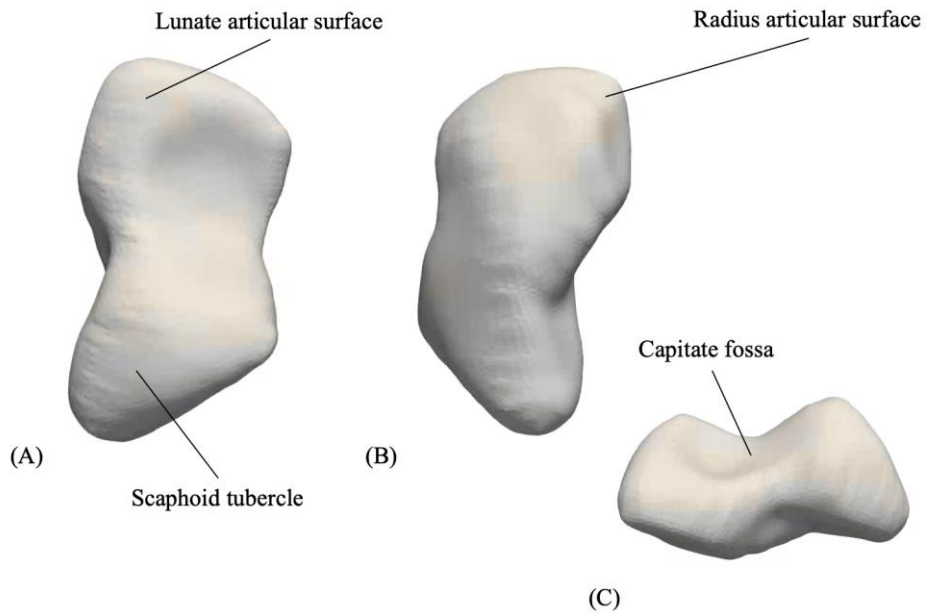


Figure 1-8 Bony Anatomy of the Scaphoid.

Bony anatomy of the right scaphoid in axial (A), dorsal (B), and medial (C) views.

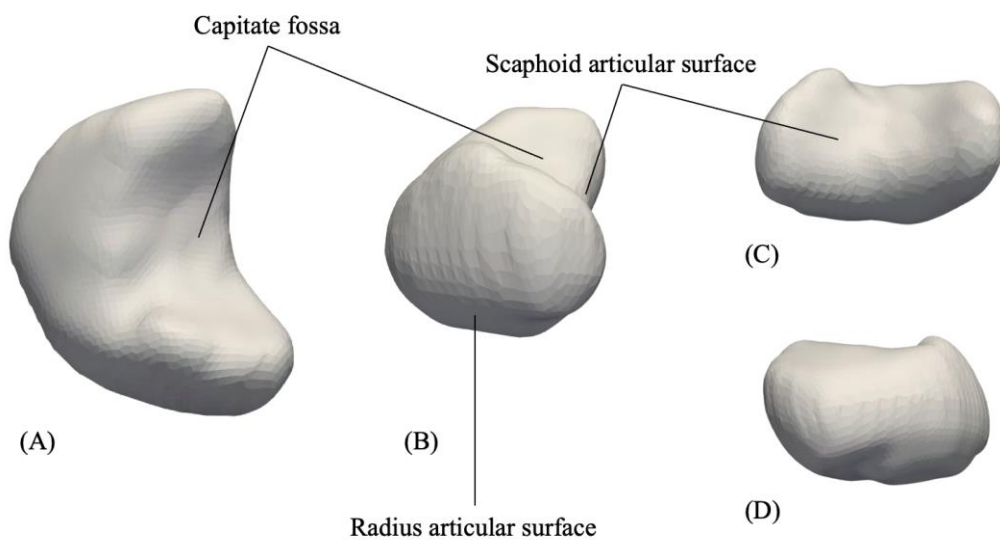


Figure 1-9 Bony Anatomy of the Lunate.

Bony anatomy of the right lunate in axial (A), volar (B), medial (C), and lateral (D) views.

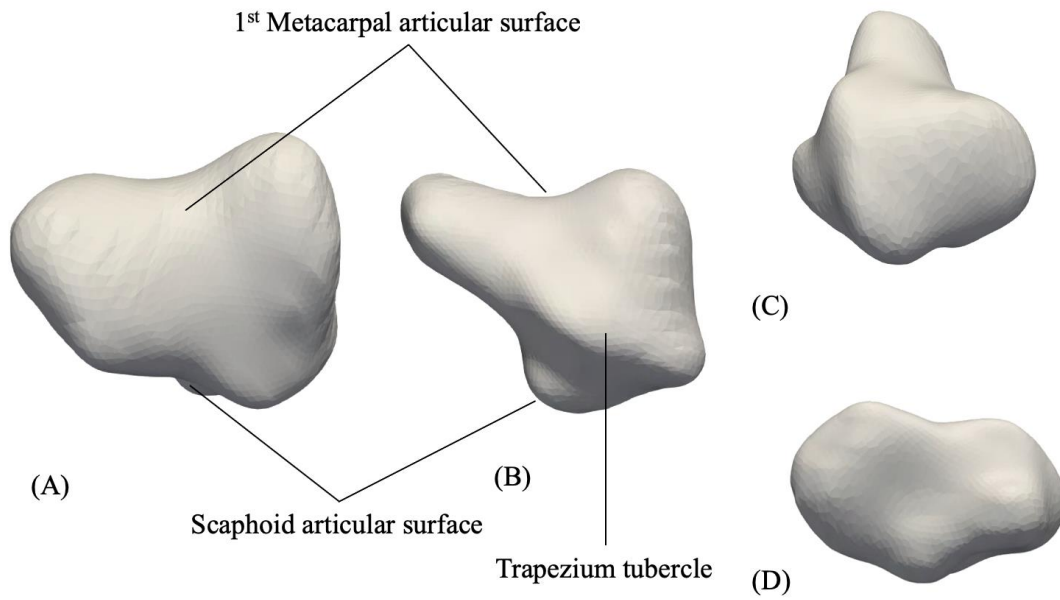


Figure 1-10 Bony Anatomy of the Trapezium.

Bony anatomy of the right trapezium in axial (A), medial (B), lateral (C), and dorsal (D) views.

1.2.4 Wrist Joints and Movement

The wrist and forearm are composed of numerous synovial joints, each with individual functions. The two main synovial joints in the wrist are the radiocarpal and carpometacarpal (CMC) joints. Within each synovial joint, there is a joint capsule that surrounds and seals the joint space between articulating bones. Each articulating end of the bone is covered in articular cartilage, and the joint space is filled and lined with synovial fluid and a synovial membrane, respectively. The articular cartilage, synovial fluid, and synovial membrane allow the joint to move smoothly, as well as aid in the structural integrity and health of the joint.

1.2.4.1 Radiocarpal Joints

The radiocarpal joint is the articulation between the distal end of the radius bone in the forearm and the proximal row of carpal bones in the wrist (Figure 1-11). The distal end of the radius has two distinct articular surfaces where the scaphoid (radioscaphoid joint (RS)) and lunate (radiolunate joint (RL)) sit. The radiocarpal joint is classified as a condyloid joint, allowing for the following movement – flexion and extension (FE), radioulnar deviation (RUD), and supination and pronation of the wrist (Figure 1-12).

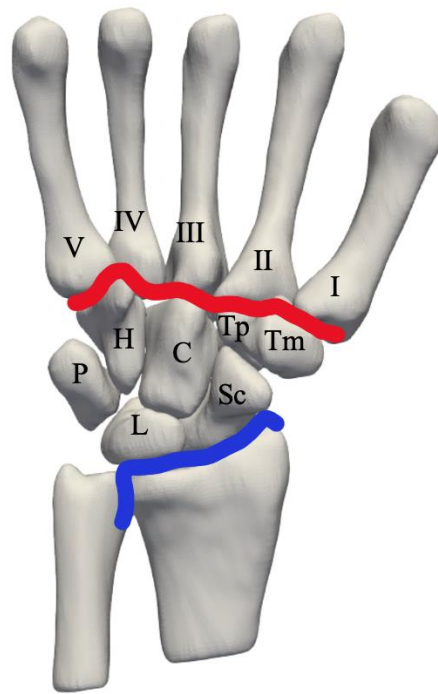


Figure 1-11 Radiocarpal and Carpometacarpal Joints.

Radiocarpal (blue line) and carpometacarpal (red line) joints within the hand and wrist.

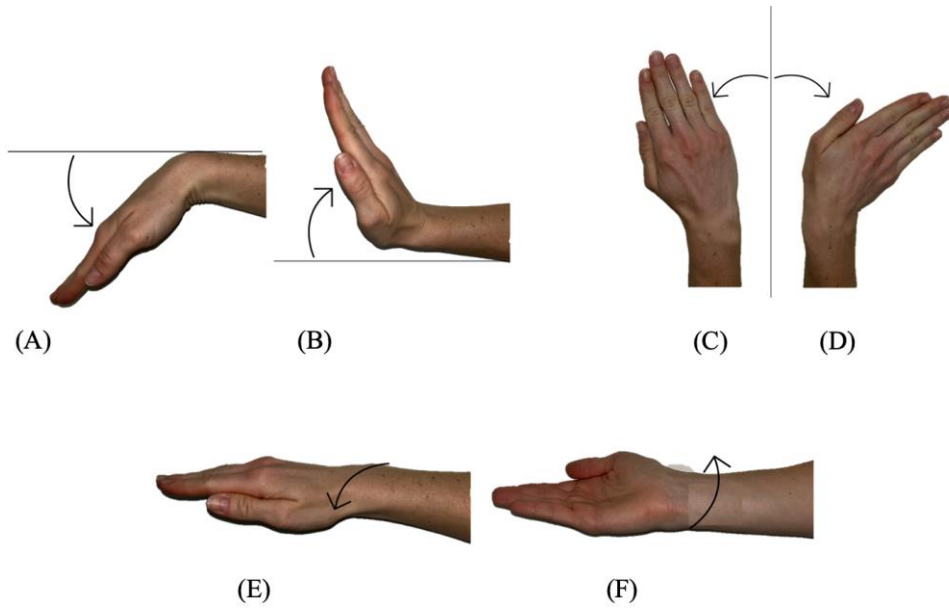


Figure 1-12 Motions of the Wrist.

Flexion (A), extension (B), radial deviation (C), ulnar deviation (D), pronation (E), and supination (F) of the right wrist.

1.2.4.2 Carpometacarpal Joints

The CMC joints comprise of five joints in the hand where the proximal bases of the metacarpal bones articulate with the distal row of carpal bones (Figure 1-11). All CMC joints are classified as gliding synovial joints, with the exception of the thumb. The thumb CMC joint is made up of the trapezium and the proximal base of the 1st metacarpal and is classified as a biconcave-convex synovial saddle joint (Figure 1-13). Both bones have a concave and convex surface, allowing for a wide range of motion including FE, abduction and adduction, opposition, and circumduction (Figure 1-14).⁴²

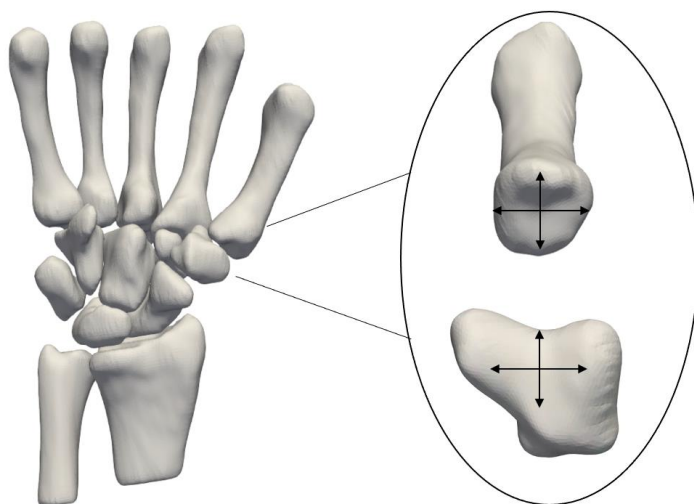


Figure 1-13 First Carpometacarpal Joint.

Right CMC1 joint demonstrating the planes of movement for the biconcave-convex saddle joint structure.

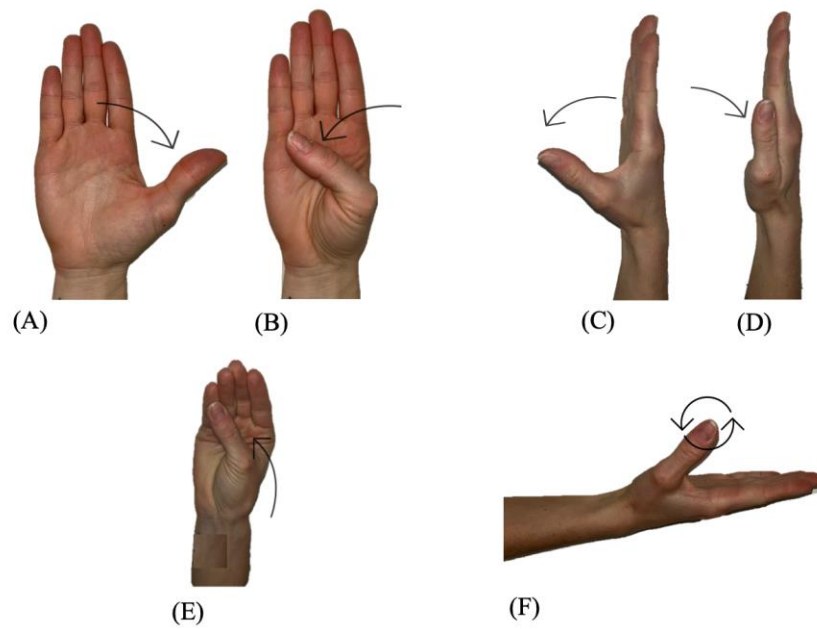


Figure 1-14 Motions of the Thumb.

Extension (A), flexion (B), abduction (C), adduction (D), opposition (E), and circumduction (F) of the right thumb.

1.3 Clinical Disorders of the Hand and Wrist

The wrist is the most frequently injured upper extremity joint, accounting for approximately 28% of all musculoskeletal^{2,37,57-59} and ligamentous trauma.^{44,60} Due to the number of bones and joints that make up the hand and wrist, it is vulnerable to a variety of injuries and conditions. The defining symptom associated with clinical disorders of the hand and wrist, and often the major reason for seeking medical treatment, is pain. Wrist fractures and arthritis are two of the most common types of injuries where pain is often the dominating symptom. Below we will introduce the hand and wrist pathologies we reference in this thesis.

1.3.1 Wrist Fractures

Wrist fractures are a common type of injury significantly impacting older adults and athletes involved in high-impact sports. The most common type of wrist fracture is a distal radius fracture (DRF), commonly occurring due to a fall on an outstretched hand (FOOSH) with a higher incidence rate in females compared to males. DRFs are common in isolation or in concert with other fractures and/or injuries. In 2022, there was a documented incidence rate of 67 upper extremity fractures per 10,000 people annually, with DRF accounting for approximately 25% of these fractures.^{61,62}

1.3.2 Osteoarthritis

Arthritis is a degenerative joint disease characterized by inflammation, pain, stiffness, and the degradation of articular cartilage, significantly impacting approximately one in every three adults.⁶³ As of 2019, approximately 73% of people living with osteoarthritis were older than 55 years, and approximately 60% were female.^{63,64} There are different types of arthritis often depending on the mechanism of disease progression, but the most common are OA, rheumatoid arthritis (RA), and post-traumatic arthritis. OA is the second most common disease worldwide and the most prevalent form of arthritis and has led to significant disability worldwide.¹⁶ In 2020, approximately 13.6% of Canadians over the age of 20 were diagnosed with OA, commonly impacting more females than males.^{16,65} Clinically, OA is characterized by joint pain and swelling, stiffness, and often a limited range of motion. Morphologically, OA is characterized by degeneration of articular

cartilage, subchondral bone alterations, osteophyte growth, and inflammation within the joint capsule. OA can affect any joint in the body but is commonly found in the distal joints of the hands, knees, hips, and spine – namely joints that are load- or weight-bearing.

Historically, OA was considered a disease of the articular cartilage – altered and repetitive joint loading results in degeneration of the articular cartilage between joints, causing further cartilage breakdown, joint pain, and limited range of motion. Current literature, however, supports a new hypothesis that subchondral bone changes may precede cartilage degeneration in OA, due to the metabolic activity, innervation, and vascularity of subchondral bone. To date, this hypothesis has been tested in weight-bearing joints, such as the knee and hip, as these bones physiologically represent the loading history of the joint, thereby demonstrating alterations and adaptations from normal loading patterns.

1.3.2.1 Thumb Carpometacarpal Osteoarthritis

Thumb carpometacarpal OA (CMC OA) is a type of OA that affects the joint at the base of the thumb. Thumb CMC OA is more prevalent in post-menopausal females, where studies have demonstrated that age and biological female sex are undisputed risk factors of thumb CMC OA.⁶⁴ Specifically, 11% of men and 33% of women between the ages of 50 to 60 are affected by thumb CMC OA, while 90% of people over the age of 80 years are affected.⁶⁶ The progression of thumb CMC OA is characterized by pain, reduced strength, functional impairments, and morphological changes to the saddle structure of the joint.^{49,66} Structural progression of thumb CMC OA is characterized by pathological changes in joint tissues, namely articular cartilage degeneration, subchondral bone alterations, osteophyte growth, and inflammation within the joint capsule.^{46,67–69}

1.3.2.2 Scapholunate Advanced Collapse

Scapholunate (SL) injuries are the most frequent ligamentous wrist injury that commonly leads to instability, pain, and functional disability, having a significant impact on patient quality of life.^{71–75} SL injuries are prevalent in a middle-aged male patient population with a history of working in manual labor, due to the chronic, repetitive conditions often impacting the wrist joint.⁷¹ It is generally held that if an SL injury is left untreated, the resultant consequence is wrist instability and abnormal motion between the bones,

resulting in a form of secondary OA known as Scapholunate Advanced Collapse (SLAC).^{71,73-76} There are four stages of SLAC that are based on the extent of the damage to the radiocarpal joint (Figure 1-15). However, the progression of SLAC is often dependent on individual factors such as the mechanism and severity of injury, as well as the effectiveness of treatment and rehabilitative strategies.^{72,75}

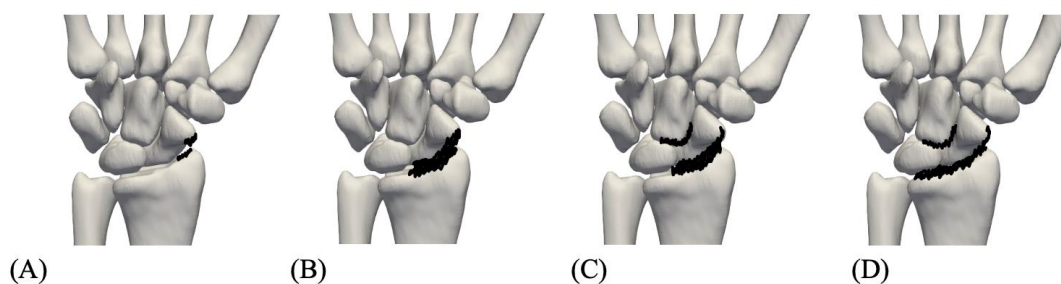


Figure 1-15 Scapholunate Advances Collapse Progression in the Hand.

Four stages of SLAC progression in the wrist, where the arthritis is confined to the radial styloid (A), arthritis impacts the entire RS joint (B), arthritis impacts the RS and capitolunate joint (C), and the arthritis involves the entire radiocarpal joint and the capitolunate and capitolunate joints (D).

1.4 Evaluating Pain in Hand and Wrist Disorders

Due to its subjectivity, pain is always a personal experience that is often influenced by varying degrees of biological, psychological, and social factors.¹ This allows us to appreciate pain as a latent construct – it cannot be directly observed, rather interpreted or inferred.¹² However, there are sources of information that can be obtained from the patient to enhance our understanding of their pain experience and presentation, some of which will be explained below.

It is of note that there are inherent biases and limitations associated with all pain evaluation measures, as they are dependent on the patient to complete. Response and/or social desirability bias impact patient self-report based on the mood the patient is in, the degree to which the patient is trying to please the provider, the context to which the report is given in, and any number of other influences that may impact patient responses.^{12,23} Subjectivity and interpretation of the pain evaluation techniques are also limitations, including the degree to which the patient was following instruction, the interpretation of the questions or instructions given, individual experiences that may influence how respondents perceive the questions asked, and the importance of the pain measures to the respondent. Given the extensive list, it's important to recognize and acknowledge these biases and limitations, while also considering that when administered to the same patient over time these biases may become systemic rather than random, thereby mitigating the effects of the biases. However, it is also important to reduce the impact of these inherent biases and limitations by maintaining anonymity and confidentiality of pain measures to alleviate patient concerns with their responses being shared, by giving consistent instructions of pain measures between and within participants, and by using multiple pain measures to triangulate pain scores and provide a more comprehensive understanding of their pain experience.²⁴

1.4.1 Patient Reported Outcome Measures

As there is no objective measure of pain, the patient perspective is considered as close to a gold standard as is currently available.¹² The most common form of subjective pain measurement strategies are patient-reported outcome measures (PROMs). PROMs are an

umbrella term for self-reported pain measures, ranging from questionnaires to visual analogue scales to numeric rating scales, intended to inform the clinician on the patients' pain experience. PROMs are integral to understanding the patients' pain experience, and for the sake of this thesis, select PROMs will be discussed in detail.

The Patient Rated Wrist Evaluation (PRWE): The PRWE is one of the most common self-reported pain rating scales developed for the upper extremity.^{70,71} In its infancy, the PRWE was developed for assessing pain and disability following a DRF, but has since been validated for use in other upper extremity conditions, such as OA in the hand and wrist,^{72,73} carpal tunnel syndrome and carpectomy,⁷⁴ as well as wrist pain resulting from different pathologies,⁷⁵ enhancing its overall clinical applicability.⁷⁰ The PRWE is a valid, reliable, and responsive 15-item scale with two subscales that address pain and function in the aforementioned pathologies.^{37,71} The pain subscale is composed of five items covering the severity, intensity, and frequency of pain during the preceding two weeks. The function subscale is composed of 10 items which are further divided into two sections – specific activities (six items), including turning a doorknob, fasten buttons on a shirt, etc., and usual activities (four items), including household work or recreational activities. The scoring on the PRWE is a simple sum of the two subscales, where a maximum of 50 points can be summed for both the five pain items and 10 function items. The score on the PRWE ranges from 0 to 100, where higher scores represent more pain or functional disability. The full PRWE questionnaire is appended in **appendix D**.

Brief Pain Inventory (BPI): The BPI is another widely used self-report outcome measure containing two quantifiable subscales aimed at measuring pain interference and pain severity.⁷⁶ Initially developed for use in measuring cancer-related pain, the BPI is widely accepted as a valid, reliable, and responsive outcome measure for measuring pain interference and severity for a variety of different pain-related clinical pathologies.^{26,77} The pain severity subscale is a four item temporally focused severity scale ranging from 0 to 10, where 0 represents no pain and 10 represents worst imaginable pain, at its least, worst, on average, and right now. The pain interference subscale is a seven-item scale inquiring how pain interferes with daily functioning (e.g., walking, sleeping, usual work),

where 0 indicates that pain does not interfere and 10 represents complete interference of daily functioning. The full BPI is appended in **appendix B**.

Gender Role and Expectations of Pain Scale (GREP): The GREP was introduced by Robinson and colleagues as a pain-oriented scale designed to capture self-rated pain expectations and experiences, in relation to one's perception of the typical male or female.¹⁸ The GREP is a multi-subscale tool where each separate section is to be interpreted in isolation.¹⁷ It is composed of three-items aimed at pain sensitivity, endurance for pain, and willingness to report pain, where the respondent has five response options: not at all, very little, somewhat, a lot, or extremely. The following section prompts respondents to provide introspection into their beliefs on sex-based sensitivity to pain, endurance for pain, and willingness to report pain with five response options: men-a lot more, men-a little more, no difference, women-a little more, and women-a lot more. Finally, the last section asks respondents to indicate how well they handle pain compared to others of the same sex, with three response options: less well, the same, or better than. While arguably conflating the difference between sex and gender, previous work has used the GREP to descriptively explore the ways in which male and female respondents think about sex-based differences in pain sensitivity, endurance, and willingness to report pain.^{14,15} The GREP has also been used to evaluate gender role impacts on responses to experimental pain.^{6-8,16} For example, Wise and colleagues demonstrated that willingness to report pain predicted heat pain threshold, tolerance and pain unpleasantness.⁷ Defrin and colleagues found that sensitivity to pain and willingness to report pain could predict heat pain tolerance but not heat pain threshold.⁶ Alabas and colleagues further demonstrated the ability of sensitivity to pain and endurance for pain to predict mechanical pain threshold, and endurance for pain to predict pain tolerance.⁸ All results were found in both males and females.

Multidimensional Symptom Index (MSI): The MSI is a recently developed PROM intending to capture patients' pain experiences with 10 listed symptoms. The MSI serves to identify symptoms that have the greatest impact on the patients' experience, allowing exploration and phenotyping of the patients' pain.⁷⁸ The 10 symptoms can be dichotomized into separate classes – somatic symptoms (e.g., sharp or dull pain,

weakness, or stiffness), and non-somatic symptoms (e.g., environmental sensitivity, nausea, or low mood). The MSI has two parallel scales for each symptom – the frequency of each named symptom (never, rarely, often, or always), followed by the extent to which the symptom impacts normal functioning (barely, somewhat, quite a bit, or completely). Several metrics can be obtained from the MSI, including the Somatic and Non-Somatic symptoms scores in addition to the Number of symptoms experienced (any symptom experienced at a frequency greater than “never”), the Mean frequency of symptoms (sum of frequency scores/Number of symptoms), and the Mean interference (sum of interference scores/ Number of symptoms). The full MSI is appended in **appendix G**.

Self-Reported Leeds Assessment of Neuropathic Symptoms and Signs (S-LANSS): In line with the ability to phenotype patients’ pain experiences, the self-completed S-LANSS was developed to identify pain of predominately neuropathic origin, distinct from nociceptive pain.⁷⁹ The S-LANSS is seven-items long with a binary response (a simple yes or no), to the presence of symptoms (five items) or clinical signs (two items) of neuropathic pain. Each item is given a score, where “no” represents 0 and “yes” represents scores ranging from one to five depending on the symptom. A total score of 12 or greater has shown 74% sensitivity and 76% specificity for identifying pain of primarily neuropathic origin.⁷⁹ The full S-LANSS is appended in **appendix H**.

1.4.2 Quantitative Sensory Testing

Quantitative sensory testing (QST) is a psychophysical measure that systematically documents alterations in the nervous systems response to a stimulus. Slightly different from PROM’s, QST provides a quantifiable measure of hypo- and hyper sensory function; common symptoms in people with chronic pain.⁸⁰⁻⁸² The method of using QST for experimental pain measure is a multi-step process that can involve different sensory modalities on a variety of tissues, such as thermal, mechanical, electrical, and chemical modalities applied to skin, muscle, viscera, and bone.⁸⁰

Pressure Pain Detection Threshold (PPDT): PPDT is an example of a mechanical modality that is used to measure pain threshold (pain sensitivity), in deep somatic structures.^{83,84} Pressure pain threshold is defined as the minimum pressure applied that causes unpleasant

or uncomfortable sensations. The terms “unpleasant” or “uncomfortable” are used as they align with the IASP definition of pain while avoiding saying “pain”, so as not to imply that the test will be painful.^{1,84} Using a digital handheld algometer, PPDT has demonstrated predictive validity and reliability in patient populations with neck pain and whiplash-associated disorder (WAD),^{83–87} wrist fracture,⁸⁸ CMC1 OA,⁶⁷ myofascial pain,^{89,90} and other chronic pain disorders.⁹¹ Generally consistent results in the literature indicate that PPDT in females is lower, indicating more sensitivity to pain, in comparison to their male counterparts.^{17,21,84,85} Standardized instruction for PPDT is required for reliable and valid measures and is explained in depth in Chapters 2 and 5.

Cold Pressor Task (CPT): CPT is an example of a thermal QST measure used to measure cold pain sensitivity. Cold pressor pain is induced by the submergence into cold water, typically performed on the hand and forearm. CPT is found to be reliable and valid in myriad pain conditions,⁹² including WAD, pain related to neuropathies⁹³, and has been used in conditioned pain modulation (CPM), a technique used to evaluate the functioning of pain inhibitory pathways in people with chronic pain.^{94–96} Standardized instruction and methodological implementation of CPT is explained in depth in Chapter 2.

1.4.3 Imaging Modalities

Efforts to quantify pain using imaging modalities are ongoing, albeit far from eliminating the patient self-report from serving as the gold standard to which to compare diagnostic imaging. MSK disorders are often solely diagnosed using diagnostic imaging; that is, acute MSK disorders such as a fracture, sprain, strain, etc., have a strong physiological influence that is likely “causing” the patient to be in pain. However, the magnitude of pain is not synonymous with the magnitude of tissue damage, indicating that whatever is happening at the tissue level may not be accurately represented by the patients’ pain experience.

1.4.3.1 Imaging and Hand and Wrist Disorders

Accurate diagnosis of hand and wrist disorders is important for providing the most effective, timely intervention to mitigate the risk of pain and suffering among patients. As mentioned previously, the hand and wrist joints are the most frequently injured upper

extremity joints. Due to the complex structure of ligaments, bones, and numerous articulations within the joint, misdiagnosis is common. This makes it challenging to visualize subtle abnormalities using static imaging modalities.

1.4.3.1.1 Conventional Ultrasound

Conventional US imaging is characterized as a two-dimensional (2D) US imaging technique that is widely used due to its bedside accessibility and low cost to purchase and use. The greatest utility of US imaging in hand and wrist MSK disorders is related to ligament or tendon disorders/ injuries, muscles and joint structures, and inflammatory disorders such as carpal tunnel syndrome and arthritis.⁹⁹ As US imaging is real-time, images are continuously acquired while the transducer is manually agitated along the anatomical region of interest. This allows for simultaneous assessment of the internal structures associated with the MSK disorder.

However, US imaging is limited in its ability to detect individual joints, as the field of view is limited to the scope of the transducer. Therefore, multiple images are often required to visualize the entire joint structure, resulting in an increased scanning time and an increased risk of error in diagnosing MSK disorders due to multiple images. In addition, as is true for all 2D imaging modalities, acquiring 2D images of three-dimensional (3D) anatomy increases the risk of misdiagnosis as it relies on the technician's interpretation of the images.

1.4.3.1.2 Radiography

Radiography, also known as x-ray, is a static, 2D imaging modality that produces 2D representations of complex 3D anatomical pathology.¹⁰¹⁻¹⁰³ The high attenuation of x-ray allows for the 2D imaging of bone and associated joint space and joint angles between articulating bones. As it is a static 2D projection of a 3D image, x-ray is limited to detecting bone fractures, bony growths, and malalignment among bony structures. Using static, radiographic techniques increases the risk of misdiagnosis in hand and wrist injuries, due to the inability to assess dynamic abnormalities, subtle bony changes, as well as the extent of the abnormality.¹⁰¹⁻¹⁰³

1.4.3.1.3 Computed Tomography

CT is an x-ray technique that collects imaged “slices” of the body, where multiple adjacent slices are reconstructed to create 3D images. Traditional 3DCT imaging allows for the visualization, assessment, and modelling of complex 3D anatomy, effective for observing static abnormalities.^{104,105} Studies have used 3DCT to model bone fractures, contact mechanics between articulating bones, and surface area measures of joint contact.^{104,105} However, in isolation, the use of a static imaging modality can only represent abnormal bone position without the possibility of analyzing abnormal motion.

Four-dimensional CT (4DCT) is a dynamic imaging technique that incorporates three spatial dimensions + time. 4DCT can capture dynamic, unconstrained data that represents true physiological joint motion. Imaging during active motion is of particular value in the recognition and analysis of dynamic pathology in the hand and wrist, where the majority of such disorders can only be diagnosed dynamically. In the wrist, 3D bone scans of the moving joint are continuously acquired, producing a large spectrum of joint motion with subtle changes between frames. Clinically, the advantages of 4DCT lie in its ability to detect injuries early, when only subtle bony motion changes are occurring,^{57,102,105} allowing for timely interventions and therapeutic strategies to aid in better prognosis. There are myriad other advantages to using 4DCT over other imaging modalities, namely precise analysis of individual carpal motion,⁴³ the ability to detect dynamic instabilities and asymptomatic conditions,^{57,106,107} and more recently, the ability to describe joint contact measures qualitatively and quantitatively throughout motion, a metric with significant impact on wrist instability and OA.^{57,108}

Joint contact area (JCA) is a CT-derived measure used to describe the surface area on articulating bone structures. There are many terms that can be used interchangeably when describing JCA, namely interbone distance, joint surface area, joint congruency, or joint proximity are terms used predominately. This approach assumes that regions of higher contact pressure within the joint correspond to regions of closest proximity and assumed largest joint contact.^{109,110} 4DCT is not a reliable soft tissue imaging device, therefore JCA is limited to osseous structures (subchondral bone) and as such does not include the influence of articular cartilage.

Quantitative CT (QCT) is a method for measuring BMD using a standard CT scanner with a calibrated reference phantom to convert Hounsfield Units (HU) into equivalent volumetric BMD (vBMD) values (Appendix C). QCT is capable of distinguishing between subchondral bone tissue types (cortical and trabecular bone), allowing for analysis on different bone regions and depths of bone. Referring to section 1.2.3, the importance of subchondral bone lies in its inherent ability to adapt and respond to mechanical loads, and its vascularity and innervation. These depth-specific imaging techniques have the potential to make distinctions between subchondral bone layers, which researchers are turning to as potential contributors to the pain experience in myriad musculoskeletal (MSK) injuries due to the vascularity of the subchondral bone.⁴⁵ In addition, Apergis and colleagues¹¹¹ found that subchondral BMD represents the loading history of the joint, wherein altered BMD patterns are often in line with pathological changes in the bone, such as injury. Previous research on the lower extremity (namely, knees and hips), have demonstrated the ability of QCT to analyze bone geometry measurements' predictive ability of bone strength in the knee¹¹², lower bone density in the patella¹¹³, femur¹¹⁴ and tibia¹¹⁵ of patients with OA and its association with pain, as well as accelerated bone loss after ligamentous injuries in the knee.¹¹⁶

1.5 Thesis Rationale

The mechanisms underlying chronic pain following various MSK hand and wrist disorders remains unknown. Diagnostic imaging is crucial for identifying abnormalities to provide the best possible course of treatment. Although far from eliminating the patient self-report from serving as the gold standard to which to compare diagnostic imaging, when an abnormality is present that aligns with the patient self-report of pain, it is logical to assume the abnormality is a contributor. Using 4DCT and QCT, two robust imaging techniques in MSK disorders, combined with gold-standard pain evaluation techniques, our work aims to examine adaptive joint changes following various forms of wrist trauma to better understand potential pain mechanisms. 4DCT allows for the identification of kinematic joint congruency, or JCA, providing information on how far apart articulating bones are throughout motion and if bones are moving together or separate from one another, highlighting subtle changes or abnormalities with motion. QCT allows for the

quantification of depth-specific subchondral bone layers – regions of interest as potential mechanisms underlying pain due to the rich blood and nerve supply in the subchondral bone. We believe that the synergistic interaction between JCA and subchondral vBMD is likely greater than the individual effect of both metrics.

The goal of this thesis is to investigate JCA and subchondral vBMD, combined with gold-standard pain evaluation strategies, as potential contributors to the patient's pain experience. With the collaboration of hand surgeons, radiologists, and researchers spanning both biomedical engineering and physical therapy, these findings will help to inform investigators of the effectiveness and application of image-based biomarkers in conjunction with various PROM's. Ultimately, these findings aim to inform researchers and clinicians alike of potential underlying mechanisms of pain, and treatment and intervention strategies aimed at mitigating the risk of chronic pain.

The work from this thesis is presented in four separate but related main chapters, aiming to address and fill knowledge gaps surrounding chronic MSK pain in hand and wrist disorders.

1.6 Objectives and Hypotheses

The objectives of this thesis are as follows:

1. To explore the correlation between sex-specific personal pain beliefs and clinical pain evaluation within and between biological sex.
2. To demonstrate the utility of QCT in comparing subchondral vBMD between a healthy cohort and a cohort of chronic pain patients following various forms of wrist trauma.
3. To evaluate the correlation between kinematic JCA and subchondral vBMD in a cohort of healthy people, as it relates to depth from the subchondral surface.
4. To explore the association between clinical and structural disease severity in patients with thumb CMC OA, using our image-based biomarkers, sex of the

participant, and patient-reported outcome measures. We will also explore pain phenotypes within this cohort.

The specific hypotheses for this thesis correlate to each objective, and are as follows:

1. The correlation between sex-specific pain beliefs and clinical pain evaluation will be greater within biological females compared to their male counterparts.
2. Patients with chronic pain following wrist trauma will have lower subchondral vBMD for all depths from the subchondral surface.
3. A larger JCA will be significantly correlated to a higher subchondral vBMD measure, within all depth-specific layers.
4. Synergistic interactions between image-based biomarkers, sex, and pain evaluation techniques will aid in the understanding of thumb CMC OA pain.

1.7 Thesis Overview

Chapter 2: Describes the relationship between sex-specific pain beliefs and clinical pain evaluation. As pain is influenced by myriad factors, this chapter aims to understand how these influences impact a person's self-reported pain.

Chapter 3: Demonstrates the utility of QCT in detecting differences in depth-specific subchondral vBMD between healthy people and people with pain lasting longer than three months post wrist trauma.

Chapter 4: Demonstrates the relationship between subchondral vBMD and kinematic JCA while the wrist is moving through a range of motion.

Chapter 5: Investigates the relationship between clinical and structural disease severity in patients with thumb CMC OA. A sub-analysis of this work aims to characterize thumb CMC OA patients' pain, to better understand pain phenotypes associated with this clinical cohort.

Chapter 6: General summary, discussion, and conclusion of the work presented in this thesis.

References

1. Raja SN, Carr DB, Cohen M, et al. The Revised IASP definition of pain: concepts, challenges, and compromises. *Pain*. 2020;161(9):1976.
doi:10.1097/J.PAIN.0000000000001939
2. Bruno F, Arrigoni F, Palumbo P, et al. The Acutely Injured Wrist. *Radiol Clin North Am*. 2019;57(5):943-955. doi:10.1016/j.rcl.2019.05.003
3. Management of chronic pain in the acute care setting. *Emerg Med Clin North Am*. 2005;23(2):307-338. doi:http://dx.doi.org/10.1016/j.emc.2004.12.004
4. Defrin R, Shramm L, Eli I. Gender role expectations of pain is associated with pain tolerance limit but not with pain threshold. *Pain*. 2009;145(1-2):230-236.
doi:10.1016/j.pain.2009.06.028
5. Fillingim RB. Sex, gender, and pain: women and men really are different. *Curr Rev Pain*. 2000;4(1):24-30. doi:10.1007/s11916-000-0006-6
6. Andrew R, Derry S, Taylor RS, Straube S, Phillips CJ. The Costs and Consequences of Adequately Managed Chronic Non-Cancer Pain and Chronic Neuropathic Pain. *Pain Practice*. 2014;14(1):79-94. doi:10.1111/PAPR.12050
7. Lynch ME. The need for a Canadian pain strategy. *Pain Research & Management : The Journal of the Canadian Pain Society*. 2011;16(2):77.
doi:10.1155/2011/654651
8. Turk DC, Okifuji A, Scharff L. Chronic pain and depression: role of perceived impact and perceived control in different age cohorts. *Pain*. 1995;61(1):93-101.
doi:10.1016/0304-3959(94)00167-D
9. Wilson AT, George SZ, Bialosky JE. Patient-defined outcomes for pain, fatigue, emotional distress, and interference with activities did not differ by age for

- individuals with musculoskeletal pain. *Pain Rep.* 2019;4(6):e798.
doi:10.1097/pr9.0000000000000798
10. Qiao-Tasserit E, Vuilleumier P, Corradi-Dell'Acqua C. The good, the bad, and the suffering. Transient emotional episodes modulate the neural circuits of pain and empathy. *Neuropsychologia.* 2018;116:99-116.
doi:http://dx.doi.org/10.1016/j.neuropsychologia.2017.12.027
 11. Lerman SF, Rudich Z, Brill S, Shalev H, Shahar G. Longitudinal associations between depression, anxiety, pain, and pain-related disability in chronic pain patients. *Psychosom Med.* 2015;77(3):333-341.
doi:10.1097/PSY.0000000000000158
 12. Walton DM, Elliott JM. *Musculoskeletal Pain - Assessment, Prediction and Treatment.* HANDSPRING PUBLISHING LIMITED; 2019.
 13. Engel GL. The Need for a New Medical Model: A Challenge for Biomedicine. *Science (1979).* 1977;196(4286):129-136. doi:10.1126/SCIENCE.847460
 14. What is gender? What is sex? - CIHR. Accessed August 17, 2020. <https://cihr-irsc.gc.ca/e/48642.html>
 15. LeResche L. Defining gender disparities in pain management. *Clin Orthop Relat Res.* 2011;469(7):1871-1877. doi:10.1007/s11999-010-1759-9
 16. Osteoarthritis in Canada - Canada.ca. Accessed May 17, 2023.
<https://www.canada.ca/en/public-health/services/publications/diseases-conditions/osteoarthritis.html#>
 17. Wise EA, Price DD, Myers CD, Heft MW, Robinson ME. Gender role expectations of pain: Relationship to experimental pain perception. *Pain.* 2002;96(3):335-342. doi:10.1016/S0304-3959(01)00473-0

18. Robinson ME, Riley JL, Myers CD, et al. Gender role expectations of pain: Relationship to sex differences in pain. *Journal of Pain*. 2001;2(5):251-257. doi:10.1054/jpai.2001.24551
19. Walton DM, Macdermid JC, Giorgianni AA, Mascarenhas JC, West SC, Zammit CA. Risk factors for persistent problems following acute whiplash injury: Update of a systematic review and meta-analysis. *Journal of Orthopaedic and Sports Physical Therapy*. 2013;43(2):31-43. doi:10.2519/jospt.2013.4507
20. Templeton KJ. Sex and Gender Issues in Pain Management. *J Bone Joint Surg Am*. 2020;102:32-35. doi:10.2106/JBJS.20.00237
21. Robinson ME, Gagnon CM, Riley JL, Price DD. Altering gender role expectations: Effects on pain tolerance, pain threshold, and pain ratings. *Journal of Pain*. 2003;4(5):284-288. doi:10.1016/S1526-5900(03)00559-5
22. Wandner LD, Scipio CD, Hirsh AT, Torres CA, Robinson ME. The perception of pain in others: How gender, race, and age influence pain expectations. *Journal of Pain*. 2012;13(3):220-227. doi:10.1016/j.jpain.2011.10.014
23. Ghodrati M, Walton DM, MacDermid JC. Exploring the Domains of Gender as Measured by a New Gender, Pain and Expectations Scale. *Women's Health Reports*. 2021;2(1):87-96. doi:10.1089/whr.2020.0109
24. Straatman LN, Lukacs MJ, Lee JY, Ghodrati M, Lalone EA, Walton DM. Are people good prognosticators of their own pain? An exploration of the relationship between sex-specific pain beliefs and clinical pain evaluation. *Musculoskelet Sci Pract*. 2022;62:102667. doi:10.1016/J.MSKSP.2022.102667
25. Kindler LL, Valencia C, Fillingim RB, George SZ. Sex differences in experimental and clinical pain sensitivity for patients with shoulder pain. *European Journal of Pain*. 2011;15(2):118-123. doi:10.1016/j.ejpain.2010.06.001
26. Bartley EJ, Fillingim RB. Sex differences in pain: A brief review of clinical and experimental findings. *Br J Anaesth*. 2013;111(1):52-58. doi:10.1093/bja/aet127

27. Samulowitz A, Gremyr I, Eriksson E, Hensing G. “Brave Men” and “Emotional Women”: A Theory-Guided Literature Review on Gender Bias in Health Care and Gendered Norms towards Patients with Chronic Pain. *Pain Res Manag.* 2018;2018. doi:10.1155/2018/6358624
28. Fillingim RB, King CD, Ribeiro-Dasilva MC, Rahim-Williams B, Riley JL. Sex, Gender, and Pain: A Review of Recent Clinical and Experimental Findings. *Journal of Pain.* 2009;10(5):447-485. doi:10.1016/j.jpain.2008.12.001
29. Greenspan JD, Craft RM, LeResche L, et al. Studying sex and gender differences in pain and analgesia: A consensus report. *Pain.* 2007;132(SUPPL. 1):S26-S45. doi:10.1016/J.PAIN.2007.10.014
30. Diamond LM. Gender Fluidity and Nonbinary Gender Identities Among Children and Adolescents. *Child Dev Perspect.* 2020;14(2):110-115. doi:10.1111/cdep.12366
31. Ferguson R, Riley ND, Wijendra A, Thurley N, Carr AJ, Bjf D. Wrist pain: a systematic review of prevalence and risk factors- what is the role of occupation and activity? *BMC Musculoskelet Disord.* 2019;20(1):1-13. doi:10.1186/S12891-019-2902-8/FIGURES/3
32. Phillips CJ. The Cost and Burden of Chronic Pain. *Rev Pain.* 2009;3(1):2-5. doi:10.1177/204946370900300102
33. Woolf AD, Pfleger B. Burden of major musculoskeletal conditions. *Bull World Health Organ.* 2003;81(9):646-656. doi:10.1590/S0042-96862003000900007
34. Woolf CJ. Central sensitization: Implications for the diagnosis and treatment of pain. *Pain.* 2011;152(SUPPL.3):S2-S15. doi:http://dx.doi.org/10.1016/j.pain.2010.09.030
35. Bergman S, Herrström P, Högström K, Petersson IF, Svensson B, Jacobsson LT. *Chronic Musculoskeletal Pain, Prevalence Rates, and Sociodemographic.* Vol 28.; 2001. Accessed March 26, 2020.

<http://www.jrheum.org/content/28/6/1369><http://www.jrheum.org/alerts1>. Signup for TOCs and other alerts <http://jrheum.com/faq> www.jrheum.org Downloaded from

36. Leng S, Zhao K, Qu M, An KN, Berger R, McCollough CH. Dynamic CT technique for assessment of wrist joint instabilities. *Med Phys*. 2011;38(S1):S50-S56. doi:10.1118/1.3577759
37. Nellans KW, Kowalski E, Chung KC. The Epidemiology of Distal Radius Fractures. *Hand Clin*. 2012;28(2):113-125. doi:10.1016/j.hcl.2012.02.001
38. MacDermid JC, Roth JH, Richards RS. Pain and disability reported in the year following a distal radius fracture: A cohort study. *BMC Musculoskelet Disord*. 2003;4(1):1-13. doi:10.1186/1471-2474-4-24
39. Swart E, Nellans K, Rosenwasser M. The effects of pain, supination, and grip strength on patient-rated disability after operatively treated distal radius fractures. *Journal of Hand Surgery*. 2012;37(5):957-962. doi:10.1016/j.jhsa.2012.01.028
40. Osteoarthritis in Canada - Canada.ca. Accessed June 4, 2023. <https://www.canada.ca/en/public-health/services/publications/diseases-conditions/osteoarthritis.html#>
41. Woolf AD. Global burden of osteoarthritis and musculoskeletal diseases. *BMC Musculoskeletal Disorders* 2015 16:1. 2015;16(1):1-1. doi:10.1186/1471-2474-16-S1-S3
42. Birtwhistle R, Morkem R, Peat G, et al. Prevalence and management of osteoarthritis in primary care: an epidemiologic cohort study from the Canadian Primary Care Sentinel Surveillance Network. *Canadian Medical Association Open Access Journal*. 2015;3(3):E270-E275. doi:10.9778/CMAJO.20150018
43. Roiger D, Bullock N. *Anatomy, Physiology, & Disease*. Third Edition. McGraw Hill LLC; 2023.

44. Rainbow MJ, Wolff AL, Crisco JJ, Wolfe SW. Functional kinematics of the wrist. *Journal of Hand Surgery: European Volume*. 2016;41(1):7-21. doi:10.1177/1753193415616939
45. Padmore C, Stoesser H, Langohr GD, Johnson J, Suh N. Carpal Kinematics following Sequential Scapholunate Ligament Sectioning. *J Wrist Surg*. 2019;08(02):124-131. doi:10.1055/s-0038-1676865
46. Madry H, van Dijk CN, Mueller-Gerbl M. The basic science of the subchondral bone. *Knee Surgery, Sports Traumatology, Arthroscopy*. 2010;18(4):419-433. doi:10.1007/s00167-010-1054-z
47. Barr AJ, Campbell TM, Hopkinson D, Kingsbury SR, Bowes MA, Conaghan PG. A systematic review of the relationship between subchondral bone features, pain and structural pathology in peripheral joint osteoarthritis. *Arthritis Research & Therapy*. 2015;17(1). doi:10.1186/S13075-015-0735-X
48. Sun Q, Li G, Liu D, et al. Peripheral nerves in the tibial subchondral bone THE ROLE OF PAIN AND HOMEOSTASIS IN OSTEOARTHRITIS. *Bone Joint Res*. 2022;11(7):439-452. doi:10.1302/2046-3758.117.BJR
49. Sozen T, Ozisik L, Calik Basaran N. An overview and management of osteoporosis. *Eur J Rheumatol*. 2017;4(1):46-56. doi:10.5152/eurjrheum.2016.048
50. Morton AM, Peipert LJ, Moore DC, et al. Bone morphological changes of the trapezium and first metacarpal with early thumb osteoarthritis progression. *Clinical Biomechanics*. 2022;100:105791. doi:10.1016/j.clinbiomech.2022.105791
51. Neogi T. Clinical significance of bone changes in osteoarthritis. *Ther Adv Musculoskelet Dis*. 2012;4(4):259-267. doi:10.1177/1759720X12437354
52. Brand RA. Biographical sketch: julius wolff, 1836-1902. *Clin Orthop Relat Res*. 2010;468(4):1047-1049. doi:10.1007/s11999-010-1258-z

53. Wolff J. The Classic: On the Theory of Fracture Healing. *Clin Orthop Relat Res.* 2010;468(4):1052-1055. doi:10.1007/s11999-010-1240-9
54. Sampath SA, Lewis S, Fosco M, Tigani D. Trabecular orientation in the human femur and tibia and the relationship with lower-limb alignment for patients with osteoarthritis of the knee. *J Biomech.* 2015;48(6):1214-1218. doi:10.1016/j.jbiomech.2015.01.028
55. Zhou GQ, Pang ZH, Chen QQ, et al. Reconstruction of the biomechanical transfer path of femoral head necrosis: A subject-specific finite element investigation. *Comput Biol Med.* 2014;52:96-101. doi:10.1016/j.combiomed.2014.04.002
56. Straatman L, Knowles N, Suh N, Walton D, Lalone E. The Utility of Quantitative Computed Tomography to Detect Differences in Subchondral Bone Mineral Density Between Healthy People and People With Pain Following Wrist Trauma. *J Biomech Eng.* 2022;144(8). doi:10.1115/1.4053594
57. Hoogbergen MM, Schots JMP, Niessen WJ, Schuurman AH, Spauwen PHM, Kauer JMG. Subchondral bone mineral density patterns representing the loading history of the wrist joint after a proximal row carpectomy. *Eur J Plast Surg.* 2008;31(3):101-107. doi:10.1007/s00238-008-0230-6
58. Zhao K, Breighner R, Holmes D, Leng S, McCollough C, An KN. A technique for quantifying wrist motion using four-dimensional computed tomography: Approach and validation. *J Biomech Eng.* 2015;137(7). doi:10.1115/1.4030405
59. Shores JT, Demehri S, Chhabra A. Kinematic “4 Dimensional” CT Imaging in the Assessment of Wrist Biomechanics Before and After Surgical Repair. *Eplasty.* 2013;13:e9. Accessed July 15, 2020. <https://www.ncbi.nlm.nih.gov/pmc/articles/PMC3589877/>
60. Garcia-Elias M, Folgar MÁV. The management of wrist injuries: An international perspective. *Injury.* 2006;37(11):1049-1056. doi:10.1016/j.injury.2006.07.025

61. Wang P, Stepan JG, An T, Osei DA. Equivalent Clinical Outcomes Following Favored Treatments of Chronic Scapholunate Ligament Tear. *HSS Journal*. 2017;13(2):186-193. doi:10.1007/s11420-016-9525-5
62. MacIntyre NJ, Dewan N. Epidemiology of distal radius fractures and factors predicting risk and prognosis. *Journal of Hand Therapy*. 2016;29(2):136-145. doi:10.1016/j.jht.2016.03.003
63. London DA, Calfee RP. Distal Radius Fractures. *Skeletal Trauma of the Upper Extremity*. Published online February 5, 2023:470-484. doi:10.1016/B978-0-323-76180-2.00060-X
64. Theodosakis J, Buff S. *The Arthritis Cure*. St. Martin's Press ; 2004.
65. Haugen IK, Englund M, Aliabadi P, et al. Prevalence, incidence and progression of hand osteoarthritis in the general population: the Framingham Osteoarthritis Study. *Ann Rheum Dis*. 2011;70(9):1581-1586. doi:10.1136/ARD.2011.150078
66. Zhang Y, Jordan JM. Epidemiology of Osteoarthritis. *Clin Geriatr Med*. 2010;26(3):355-369. doi:10.1016/J.CGER.2010.03.001
67. Schreiber JJ, McQuillan TJ, Halilaj E, et al. Changes in Local Bone Density in Early Thumb Carpometacarpal Joint Osteoarthritis. *Journal of Hand Surgery*. 2018;43(1):33-38. doi:10.1016/j.jhsa.2017.09.004
68. Chiarotto A, Fernandez-de-Las-Penas C, Castaldo M, Villafane JH. Bilateral pressure pain hypersensitivity over the hand as potential sign of sensitization mechanisms in individuals with thumb carpometacarpal osteoarthritis. *Pain Med*. 2013;14(10):1585-1592. doi:https://dx.doi.org/10.1111/pme.12179
69. Grassel S, Muschter D, Pitsillides A, Zaucke F. Recent advances in the treatment of osteoarthritis [version 1; peer review: 3 approved]. Published online 2020. doi:10.12688/f1000research.22115.1
70. Health Canada. Arthritis in Canada An Ongoing Challenge. Published online 2003.

71. Murphy BD, Nagarajan M, Novak CB, Roy M, McCabe SJ. The Epidemiology of Scapholunate Advanced Collapse. *Hand*. 2020;15(1):23-26. doi:10.1177/1558944718788672
72. Andersson JK. Treatment of scapholunate ligament injury: Current concepts. *EFORT Open Rev*. 2017;2(9):382-393. doi:10.1302/2058-5241.2.170016
73. Pomeranz SJ, Salazar P. Scapholunate advanced collapse. *J Surg Orthop Adv*. 2015;24(2):140-143. doi:10.1016/j.ocl.2015.08.002
74. Kuo CE, Wolfe SW. Scapholunate Instability: Current Concepts in Diagnosis and Management. *Journal of Hand Surgery*. 2008;33(6):998-1013. doi:10.1016/j.jhsa.2008.04.027
75. Shah CM, Stern PJ. Scapholunate advanced collapse (SLAC) and scaphoid nonunion advanced collapse (SNAC) wrist arthritis. *Curr Rev Musculoskelet Med*. 2013;6(1):9-17. doi:10.1007/s12178-012-9149-4
76. O’Meeghan CJ, Stuart W, Mamo V, Stanley JK, Trail IA. The natural history of an untreated isolated scapholunate interosseus ligament injury. *Journal of Hand Surgery*. 2003;28(4):307-310. doi:10.1016/S0266-7681(03)00079-2
77. Mehta SP, Macdermid JC, Richardson J, Macintyre NJ, Grewal R. A systematic review of the measurement properties of the patient-rated wrist evaluation. *Journal of Orthopaedic and Sports Physical Therapy*. 2015;45(4):289-298. doi:10.2519/JOSPT.2015.5236/ASSET/IMAGES/LARGE/JOSPT-289-FIG001.JPEG
78. MacDermid JC. Development of a scale for patient rating of wrist pain and disability. *Journal of Hand Therapy*. 1996;9(2):178-183. doi:10.1016/S0894-1130(96)80076-7
79. Bicknell RT, MacDermid J, Roth JH. Assessment of Thumb Metacarpophalangeal Joint Arthrodesis Using a Single Longitudinal K-Wire. *J Hand Surg Am*. 2007;32(5):677-684. doi:10.1016/J.JHSA.2007.02.010

80. MacDermid JC, Wessel J, Humphrey R, Ross D, Roth JH. Validity of self-report measures of pain and disability for persons who have undergone arthroplasty for osteoarthritis of the carpometacarpal joint of the hand. *Osteoarthritis Cartilage*. 2007;15(5):524-530. doi:10.1016/J.JOCA.2006.10.018
81. Kwon BC, Choi SJ, Shin J, Baek GH. Proximal row carpectomy with capsular interposition arthroplasty for advanced arthritis of the wrist. *Journal of Bone and Joint Surgery - Series B*. 2009;91(12):1601-1606. doi:10.1302/0301-620X.91B12.22335/LETTERTOEDITOR
82. Michlovitz S, Hun L, Erasala GN, Hengehold DA, Weingand KW. Continuous low-level heat wrap therapy is effective for treating wrist pain. *Arch Phys Med Rehabil*. 2004;85(9):1409-1416. doi:10.1016/J.APMR.2003.10.016
83. Cleeland C. The Brief Pain Inventory. *Pain Research Group*. Published online 1991:3-66. Accessed April 2, 2020. www.mdanderson.org/departments/prg
84. Cleeland CS, Ryan KM. Pain assessment: global use of the Brief Pain Inventory. *Ann Acad Med Singap*. 1994;23(2):129-138. Accessed July 5, 2020. <http://www.ncbi.nlm.nih.gov/pubmed/8080219>
85. Walton DM, Marsh J. Reliability, Discriminative, and Prognostic Validity of the Multidimensional Symptom Index in Musculoskeletal Trauma. *Clin J Pain*. 2020;36(9):700-706. doi:10.1097/AJP.0000000000000856
86. Bennett MI, Smith BH, Torrance N, Potter J. The S-LANSS score for identifying pain of predominantly neuropathic origin: Validation for use in clinical and postal research. *J Pain*. 2005;6(3):149-158. doi:10.1016/J.JPAIN.2004.11.007
87. Arendt-Nielsen L, Yarnitsky D. Experimental and Clinical Applications of Quantitative Sensory Testing Applied to Skin, Muscles and Viscera. *Journal of Pain*. 2009;10(6):556-572. doi:10.1016/j.jpain.2009.02.002

88. Eisenberg E, Backonja M, RB F, et al. Quantitative sensory testing for spinal cord stimulation in patients with chronic neuropathic pain. *Pain Practice*. 2006;6(3):161-165. doi:10.1111/j.1533-2500.2006.00080.x
89. Uddin Z, MacDermid JC, Woodhouse LJ, Triano JJ, Galea V, Gross AR. The Effect of Pressure Pain Sensitivity and Patient Factors on Self-Reported Pain-Disability in Patients with Chronic Neck Pain. *Open Orthop J*. 2014;8(1):302-309. doi:10.2174/1874325001408010302
90. Walton D, Macdermid J, Nielson W, Teasell R, Reese H, Levesque L. Pressure pain threshold testing demonstrates predictive ability in people with acute whiplash. *Journal of Orthopaedic and Sports Physical Therapy*. 2011;41(9):658-665. doi:10.2519/jospt.2011.3668
91. Walton D, MacDermid J, Nielson W, Teasell R, Chiasson M, Brown L. Reliability, Standard Error, and Minimum Detectable Change of Clinical Pressure Pain Threshold Testing in People With and Without Acute Neck Pain. *Journal of Orthopaedic & Sports Physical Therapy*. 2011;41(9):644-650. doi:10.2519/jospt.2011.3666
92. Sterling M, Treleaven J, Edwards S, Jull G. Pressure pain thresholds in chronic whiplash associated disorder: Further evidence of altered central pain processing. *J Musculoskelet Pain*. 2002;10(3):69-81. doi:10.1300/J094v10n03_05
93. Sterling M, Jull G, Vicenzino B, Kenardy J. Sensory hypersensitivity occurs soon after whiplash injury and is associated with poor recovery. *Pain*. 2003;104(3):509-517. doi:10.1016/S0304-3959(03)00078-2
94. Rolke R, Magerl W, Campbell KA, et al. Quantitative sensory testing: A comprehensive protocol for clinical trials. *European Journal of Pain*. 2006;10(1):77. doi:10.1016/j.ejpain.2005.02.003
95. Naterstad IF, Bjordal JM, Joensen J, Saebo H, Stausholm Humaira; ORCID: <http://orcid.org/0000-0001-8882-014X> MBAOS. Reliability of pain pressure

- threshold algometry in persons with conservatively managed wrist fractures. *Physiother Res Int*. 2020;25(1):e1797. doi:<http://dx.doi.org/10.1002/pri.1797>
96. Schneider M. Changes in pressure pain sensitivity in latent myofascial trigger points in the upper trapezius muscle after a cervical spine manipulation in pain-free subjects. *J Manipulative Physiol Ther*. 2008;31(3):251-252. doi:<https://dx.doi.org/10.1016/j.jmpt.2008.02.011>
97. Ruiz-Saez M, Fernandez-de-las-Penas C, Blanco CR, Martinez-Segura R, Garcia-Leon R. Changes in pressure pain sensitivity in latent myofascial trigger points in the upper trapezius muscle after a cervical spine manipulation in pain-free subjects. *J Manipulative Physiol Ther*. 2007;30(8):578-583. <http://ovidsp.ovid.com/ovidweb.cgi?T=JS&PAGE=reference&D=med6&NEWS=N&AN=17996549>
98. Amiri M, Alavinia M, Singh M, Kumbhare D. Pressure Pain Threshold in Patients with Chronic Pain: A Systematic Review and Meta-Analysis. *Am J Phys Med Rehabil*. 2021;100(7):656-674. doi:10.1097/PHM.0000000000001603
99. Edens JL, Gn KM. Experimental Induction of Pain: Utility in the Study of Clinical Pain. *Behav Ther*. 1995;26:197-216.
100. Traynor R, MacDermid JC. Immersion in cold-water evaluation (ICE) and self-reported cold intolerance are reliable but unrelated measures. *Hand*. 2008;3(3):212-219. doi:10.1007/s11552-008-9085-3
101. Lewis GN, Rice DA, McNair PJ. Conditioned Pain Modulation in Populations With Chronic Pain: A Systematic Review and Meta-Analysis. *J Pain*. 2012;13(10):936-944. doi:10.1016/J.JPAIN.2012.07.005
102. Kennedy DL, Kemp HI, Ridout D, Yarnitsky D, Rice ASC. Reliability of conditioned pain modulation: a systematic review. *Pain*. 2016;157(11):2410. doi:10.1097/J.PAIN.0000000000000689

103. Nir RR, Yarnitsky D. Conditioned pain modulation. *Curr Opin Support Palliat Care*. 2015;9(2):131-137. doi:10.1097/SPC.0000000000000126
104. Peyron R, Laurent B, García-Larrea L. Functional imaging of brain responses to pain. A review and meta-analysis (2000). *Neurophysiologie Clinique/Clinical Neurophysiology*. 2000;30(5):263-288. doi:10.1016/S0987-7053(00)00227-6
105. Davis KD, Flor H, Greely HT, et al. Brain imaging tests for chronic pain: medical, legal and ethical issues and recommendations. *Nature Reviews Neurology* 2017 13:10. 2017;13(10):624-638. doi:10.1038/nrneurol.2017.122
106. Holsbeeck M van, ... SSAJ of, 2021 undefined. Advanced musculoskeletal ultrasound techniques: what are the applications? *researchgate.net*. doi:10.2214/AJR.20.22840
107. Shakoor D, Hafezi-Nejad N, Haj-Mirzaian A, et al. Kinematic analysis of the distal radioulnar joint in asymptomatic wrists using 4-dimensional computed tomography-motion pattern and interreader reliability. *J Comput Assist Tomogr*. 2019;43(3):392-398. doi:10.1097/RCT.0000000000000839
108. Mat Jais IS, Tay SC. Kinematic analysis of the scaphoid using gated four-dimensional CT. *Clin Radiol*. 2017;72(9):794.e1-794.e9. doi:10.1016/J.CRAD.2017.04.005
109. Kramer A, Allon R, Werner F, Lavi I, Wolf A, Wollstein R. Distinct Wrist Patterns Founded on Measurements in Plain Radiographs. *J Wrist Surg*. 2018;07(05):366-374. doi:10.1055/S-0038-1660811
110. Kamal RN, Rainbow MJ, Akelman E, Crisco JJ. In Vivo Triquetrum-Hamate Kinematics Through a Simulated Hammering Task Wrist Motion. *J Bone Joint Surg Am*. 2012;94(12):e85. doi:10.2106/JBJS.J.01644
111. Kobayashi M, Berger RA, Nagy L, et al. Normal kinematics of carpal bones: A three-dimensional analysis of carpal bone motion relative to the radius. *J Biomech*. 1997;30(8):787-793. doi:10.1016/S0021-9290(97)00026-2

112. Tay SC, Primak AN, Fletcher JG, et al. Four-dimensional computed tomographic imaging in the wrist: Proof of feasibility in a cadaveric model. *Skeletal Radiol.* 2007;36(12):1163-1169. doi:10.1007/S00256-007-0374-7
113. Kakar S, Breighner R, Leng S, et al. The Role of Dynamic (4D) CT in the Detection of Scapholunate Ligament Injury. *J Wrist Surg.* 2016;05(04):306-310. doi:10.1055/s-0035-1570463
114. Robinson S, Straatman L, Lee TY, Suh N, Lalone E. Evaluation of four-dimensional computed tomography as a technique for quantifying carpal motion. *J Biomech Eng.* 2021;143(6). doi:10.1115/1.4050129
115. Lalone EA, McDonald CP, Ferreira LM, Peters TM, King GW, Johnson JA. Development of an image-based technique to examine joint congruency at the elbow. *Comput Methods Biomech Biomed Engin.* 2013;16(3):280-290. doi:10.1080/10255842.2011.617006
116. Crisco JJ, Moore DC, Marai GE, et al. Effects of distal radius malunion on distal radioulnar joint mechanics - An in vivo study. *Journal of Orthopaedic Research.* 2007;25(4):547-555. doi:10.1002/jor.20322

Chapter 2

2 Are people good prognosticators of their own pain? An exploration of the relationship between sex-specific pain beliefs and clinical pain evaluation.

OVERVIEW

Under-explored to date are the interacting influences of patient sex on multi-modal evaluation techniques that tap different domains of the pain experience. This chapter aimed to explore the impact of sex on how pain is experienced and evaluated. Overall, this study suggests that pain is a complex experience that cannot be evaluated using only one technique. It is important to consider all available clinical pain evaluations, as different aspects of pain may be more accurately represented by different evaluation techniques.¹

¹*A version of this work has been published in the Musculoskeletal Science and Practice Journal, and presented at the following conferences: The Canadian Bone and Joint Conference, and the Orthopedic Research Society Conference.*

2.1 Introduction

As described in the introductory chapter, section 1.2, pain represents major social, economic, personal, and clinical burdens. It is recognized as a deeply subjective experience affected by biology, culture, environment, and prior life experiences.¹ Owing to its subjectivity, prior research has found many clinicians are uncomfortable treating pain, particularly complex or chronic pain problems, as there are no objective markers that can be consistently used for diagnosis, or for tracking treatment effectiveness.^{2,3} Currently, the closest gold standard measure for pain is patient narrative,² meaning it is subject to the same influences on patient reporting as is any personal experience. Pain evaluation techniques are increasingly employed to provide clinicians with quantifiable metrics of pain, from the ubiquitous Numeric Pain Rating Scale (NPRS) to quantitative sensory testing like pressure pain detection threshold (PPDT). This is in accordance with recent emphasis on mechanism-based pain assessment, through which authors have endorsed the use of multi-modal evaluation techniques that tap different domains of the pain experience, such as both pain ratings and quantitative sensory tests.⁴⁻⁶ Under-explored to date are the interacting influences of patient sex and gender on quantitative pain sensitivity and pain ratings that could influence interpretation of these evaluations.

Introduced in section 1.1.1, there are good reasons to further explore the potential for sex- and gender-based influences on clinical pain ratings and pain sensitivity. Across the field, results from both clinical and experimental pain studies have consistently found a tendency for women to rate on average more severe pain, or more sensitivity to pain stimuli, compared to men.^{5,7,8} Mechanisms to explain the differences remain unclear, though both theoretical and empirical evidence exists to support a multitude of interacting influences, from differences in processing of peripheral nociceptive afferents³, to the differences in how men and women are culturally ‘primed’ to express their pain.⁹ Measurement in the field of gender-based pain studies is difficult most notably owing to fluctuating conceptualizations of the construct as cultural mindsets shift, but this has not stopped the development of some tools for this purpose. Introduced in section 1.4.1, the *Gender Role and Expectations of Pain* (GREP) questionnaire is a pain-oriented scale designed to capture self-rated pain expectations and experiences, in relation to one’s

perception of the typical male or female.¹⁰ Despite previous work exploring the role of sex and gender on responses to experimental pain,^{4-6,11,12} comparing oneself to the believed “typical” male or “typical” female, as is done using the GREP, requires considerable experience and introspection about one’s own experiences and behaviours with pain and beliefs about pain in others of the same and opposite sex.

To contribute to this field, we conducted two studies to compare pain beliefs within and between the sexes. In the first study a healthy cohort participated in a quantitative pain threshold testing protocol with results compared against sex-specific beliefs about their own pain sensitivity in relation to others. The primary objective of Study 1 was to explore the accuracy of sex-specific personal pain beliefs in relation to quantitative pain indicators within sexes, and the secondary objective was to compare the accuracy of sex-specific personal pain beliefs in relation to quantitative pain indicators between sexes. In the second study a clinical cohort with acute musculoskeletal (MSK) pain completed both the GREP and a standardized self-report pain severity and interference scale. The primary objective of Study 2 was to explore the accuracy of sex-specific personal pain beliefs and self-rated pain severity within sexes. The secondary objective of Study 2 was to compare sex-specific personal pain beliefs and pain severity ratings between sexes.

2.2 Methods

2.2.1 Participants

This was a cross-sectional analysis of secondary data. Data were extracted from two studies that used the same sex-based pain and expectations questions.

2.2.2 Study 1: Healthy Cohort

Participants were recruited from a university campus in London Ontario, Canada. Inclusion criteria were: age ≥ 18 years, able to speak conversational English, no major systemic health condition affecting pain sensitivity, and no other major organ disease or active cancer. Participants completed a study-specific demographics form and a new Gender, Pain, and Expectations Scale (GPES)¹³, that includes four items from the GREP questionnaire.⁷ For the purpose of this analysis, only one GREP item (participants ability

to handle pain compared to the typical male or typical female), was extracted to allow comparison of our findings with prior work using the same tool or item. All participants provided informed, written consent prior to participation, and the study was approved by the local institutional review board prior to initiation.

2.2.3 Study 2: Acute MSK Trauma Cohort

The second study used data from a longitudinal study of adults recruited through an urgent care centre of a local hospital in London Ontario, Canada (clinicaltrials.gov registration number NCT02711085). Inclusion criteria were: age ≥ 18 , recent (within 3 weeks) injury affecting the MSK system, able to speak conversational English or French, free of significant systemic comorbidities that would affect physiological reactions to trauma or likelihood of recovery such as cancer, neuromuscular disorders (e.g. stroke, multiple sclerosis, amyotrophic lateral sclerosis or related disorders), uncontrolled mental health disorders (e.g. major depressive disorder or anxiety disorder not currently under the management of a professional) or severe organ disease (e.g. end-stage liver, kidney, heart or lung disease). Eligible MSK injuries were a slip and fall, motor vehicle collision, awkward lift, sporting injury, or other such injuries that did not require surgery or inpatient admission. Participants were invited to the study after being medically cleared and discharged but before leaving the urgent care centre. All participants completed a study-specific demographics form, the Brief Pain Inventory (BPI)¹⁴, and the same scale including the GREP questionnaire.⁷ The parent data collection was approved by the local institutional review board prior to initiation.

2.2.4 Testing Procedures

From both databases responses to the same GREP question were used to explore our study objectives. The question asks participants to indicate their ability to handle pain compared to the typical male and typical female. Responses are rated on a three-point opinion-based scale with the response categories: “better than”, “no different than” or “worse than” compared to typical males or females. For the purpose of our analysis, we analyzed the responses that compared each respondent to another person of their sex;

females were analyzed based on their perceived and observed ability to handle pain compared to other females, and same for males.

2.2.4.1 Study 1: Healthy Cohort

Following the completion of the GREP, participants underwent pressure pain detection threshold (PPDT) and cold pressor task (CPT) testing. The PPDT was tested at the upper trapezius on the dominant side following a standardized protocol.¹⁵ In brief, a digital algometer (Wagner FDX-25, Wagner Instruments, Greenwich, CT) with a 1cm² round rubber tip was applied to the skin over the angle of the upper trapezius muscle of the dominant hand. The algometer was calibrated before use and was found to have a linear response to force application between 0 – 1300 kilopascals (kPa). The rater was trained to apply force at a rate of 50 kPa/s. Standardized instructions asked participants to verbally express when the sensation changed from pressure to pain. The algometer was then immediately removed and PPDT was recorded as the maximum force applied at reporting threshold in kPa. Three measurements were taken and PPDT was the mean of all three.

For CPT, we followed a similar protocol to Kaunisto and colleagues.¹⁶ The dominant hand was submerged in an insulated container filled with ten centimeters of cooled ice water held at a temperature of two to four degrees centigrade, monitored throughout the test with a water-safe digital thermometer with additional ice added as needed. The cooler was outfitted with a mesh screen that separated the ice from the hand of each participant. As we were also measuring electrodermal response through high-sensitivity finger-based recording electrodes for a separate research question, we did not use an electric pump to circulate the water as it caused interference with those readings. Accordingly, the water in the cooler was manually agitated with a wooden stir stick by an investigator to prevent localized warming around the hand. Each participant was instructed to keep the hand submerged up to the wrist until the pain experienced reached a severity of 8 out of 10 on a numeric pain rating scale (0 = no pain, 10 = worst pain), or until a maximum of 90 seconds was reached, whichever came first. Only one trial of the CPT was conducted, wherein the amount of time (seconds) the hand was submerged was recorded as an indicator of cold pain endurance, with an upper limit of 90 seconds for safety. The same (male) investigator performed all measures of the CPT and PPDT on all participants.

2.2.4.2 Study 2: Acute MSK Trauma Cohort

Following the completion of the GREP participants also completed the BPI. The BPI is a widely recognized self-report tool used as a generic patient-reported outcome for capturing pain severity and pain-related interference.¹⁸ The BPI includes two quantifiable subscales; a 4-item, 0-10 temporally focused pain severity scale, where 0 represents “no pain” and 10 represents “worst pain imaginable” at its least, worst, on average, and right now. The second is a 7-item pain interference scale asking how pain interferes with daily functional activities, where 0 represents “no interference” and 10 represents “complete interference”. These data were captured from participants within 3 weeks of an acute MSK trauma. No PPDT or CPT testing was performed on the clinical cohort.

2.2.5 Statistical Analysis

Descriptive statistics (mean \pm standard deviation, percentage) were used to summarize participant demographics within both cohorts.

2.2.5.1 Study 1 – Healthy, Objective 1

How accurate are sex-specific personal pain beliefs when responses to the GREP item on perceived ability to handle pain are compared to PPDT and CPT, independent of sex?

The PPDT and CPT values for each participant were transformed into a z-value based on the mean and standard deviation of all participants within the same category of sex.

Therefore, all participant values are expressed as the number of standard deviations away from the mean of all other participants of the same sex for that indicator. This effectively removed the effect of sex for this analysis to allow for direct comparison. Within the three available response categories to the one GREP question regarding one’s ability to handle pain compared to others of the same sex, the response category ‘worse than’ demonstrated five or fewer responses for both study cohorts. To allow meaningful comparisons, this category was collapsed into the ‘no different’ response category. The subsequent analyses therefore compared those who believed they could handle pain ‘better than’ others of their same sex against those who believed they handled pain ‘no different than’ or ‘worse than’ others. After ensuring adequate data normality through Shapiro-Wilks test, a set of independent t-tests were conducted to identify differences in

z-transformed PPDT and CPT measures, across the two levels of responses to the GREP question. We hypothesized that, if our participants held accurate beliefs about their ability to handle pain compared to others, then both PPDT and CPT should be significantly different (higher PPDT, longer CPT) between the ‘better than’ respondents vs. those who selected one of the other two responses.

2.2.5.2 Study 1 – Healthy, Objective 2

Is accuracy of sex-specific personal pain beliefs different between sexes?

Receiver Operating Characteristic (ROC) curves were used to compare the accuracy of males and females when predicting their own pain. Each participant was first assigned a dichotomous variable based on whether they perceived themselves as being better able to handle pain (1) or no different/ worse (2) compared to others of the same sex. The reference category to which the comparisons were made was variable 1. ROC curves (plotting sensitivity vs. 1-specificity for each of PPDT and CPT) were first constructed for males and females separately, with area under the curve (AUC) used as an omnibus indicator of accuracy. Here an AUC statistically greater than 0.50 was an indicator of the ability of the overall group to significantly compare their pain sensitivity against others. We then compared the sex-specific AUC, once for PPDT and once for CPT, using a z-test. A significant difference ($p < 0.05$) was used to indicate that one group (males or females) were more accurate predictors for that indicator based on their ability to handle pain.

2.2.5.3 Study 2 – Acute MSK Trauma, Objective 1

How accurate are sex-specific self-beliefs of ‘ability to handle pain’ when a clinical pain rating is used in an acute MSK injury sample?

Where Study 1 used PPDT and CPT in otherwise healthy participants, Study 2 used clinical pain ratings collected from people with recent-onset MSK pain. Similar to Study 1, BPI Pain Severity and Interference ratings were transformed into a z-value based on the mean and standard deviation of all participants within the same category of sex, effectively removing the effect of sex for this analysis. Similar to Study 1, there were five or fewer respondents who indicated their ability to handle pain was ‘worse than’ others of

the same sex, so again we collapsed the three response categories into two: those indicating they were able to handle pain ‘better than’ others of the same sex and those indicating ‘no different/ worse than’. After ensuring adequate data normality through Shapiro-Wilks test, a set of independent t-tests were conducted to identify differences in the z-transformed BPI Pain Severity and Interference ratings, across the two levels of responses to the GREP question. We hypothesized that, if our participants held accurate beliefs about their ability to handle pain compared to others, then both BPI Severity and BPI Interference should be significantly different (lower scores), between the ‘better than’ response category vs. those who selected one of the other two responses.

2.2.5.4 Study 2 – Acute MSK Trauma, Objective 2

Is accuracy of sex-specific personal pain beliefs different between the sexes?

Similar to Study 1 – Objective 2, ROC curves were constructed independently for males and females, in which ‘ability to handle pain’ was the reference category and ROC curves plotting sensitivity vs. 1 – specificity for each of BPI Pain Severity and BPI Pain Interference were constructed. AUC with 95% confidence intervals was calculated for each, and accuracy was compared between the sexes using a z-test in which a point estimate of one sex not included within the confidence intervals of the other was considered a significantly different accuracy of self-rated pain beliefs.

2.2.6 Sample Size Estimation

Sample size estimates were based on objective 1 from both studies. Using an expected power of 80%, an alpha error rate of 0.05, and a medium effect size of 0.5 following guidelines associated with clinical significance using patient-reported outcome measures,¹⁷ a total sample of 128 participants divided equally between two groups for each independent t-test was considered optimal for avoiding beta error.

2.3 Results

2.3.1 Participant Demographics

Descriptive characteristics are presented in table 2-1. All participants (Study 1 and Study 2) identified as their sex assigned at birth, where sex is characterized by the biological

difference between males and females. Across both cohorts, 48% of respondents described themselves as being able to handle pain 'better than' with the remainder indicating 'no different/worse than' (52%).

Table 2-1: Participant Demographics

Characteristics	Healthy Cohort (n = 50)	Acute MSK Trauma Cohort (n = 111)
Age, y*	24.5 (\pm 3.3)	43.2 (\pm 14.8)
Sex (%)		
Male	25 (50)	45 (40)
Female	25 (50)	66 (60)
<i>GREP Frequency Count (%)**</i>		
Male		
Better Than	11 (44)	24 (53)
No Different/ Worse	14 (56)	21 (47)
Female		
Better Than	9 (36)	34 (52)
No Different/ Worse	16 (64)	32 (48)
<i>Clinical Pain Evaluations (\pmSD)</i>		
PPDT (kPa, SD)		
Male	475.2 (\pm 214.2)	
Female	369.7 (\pm 172.2)	
CPT (sec., SD)		
Male	67.9 (\pm 26.9)	
Female	74.2 (\pm 21.5)	
BPI Pain Severity		
Male		4.0 (\pm 2.1)
Female		4.6 (\pm 2.0)
BPI Pain Interference		
Male		26.4 (\pm 16.0)
Female		26.7 (\pm 17.1)

*Values for total sample within each cohort, with values for subgroups in the following categories.

**Indicates the frequency of responses on the one GREP question used to explore our objectives.

2.3.2 Study 1 – Healthy, Objective 1

How accurate are sex-specific personal pain beliefs?

In Study 1, 40% of participants indicated they were better able to handle pain compared to another person of their own sex (table 2-2). Z-transformed PPDT was not significantly different between the ‘better than’ ($Z = 0.02$, 95%CI -0.50 to 0.50) compared to the ‘no difference/ worse than’ groups ($Z = -0.10$, 95%CI -0.40 to 0.30, $t(48) = 0.10$, $p = 0.90$). In total, twenty-six participants ($n = 12$ males and $n = 14$ females) reached the maximum cold immersion time of 90 seconds for the CPT. Cold immersion time did not statistically differ between those rating a better than ability to handle pain ($Z = 0.10$, 95%CI -0.30 to 0.50) compared to those self-rating no difference/ worse than ability ($Z = -0.10$, 95% CI -0.50 to 0.30, ($t(48) = 0.71$, $p = 0.48$).

2.3.3 Study 1 – Healthy, Objective 2

Is accuracy of sex-specific personal pain beliefs different between sexes?

Overall, 36% of females indicated their ability to handle pain was ‘better than’ other females, while 46% of males indicated they handle pain ‘better than’ other males (table 1). Table 2-3 presents the results of the ROC analyses for the between-sex comparisons, and the independent groups analysis. Figures 2-1a and 2-1b demonstrate the ROC curves for PPDT and CPT for males and females, respectively. Across PPDT and CPT, males were descriptively more accurate predictors of their clinical pain evaluations than were females though none of the between sex comparisons were statistically significant ($p > 0.05$).

Table 2-2: Results from the independent samples t-test comparing sex-specific pain beliefs and clinical pain evaluations using z-transformations.

Pain Indicator (n)/Group	Z-score	95% CI	T-statistic	P-value
Study 1 (n = 50)				
PPDT (z-score)				
<i>Better than (20)</i>	0.02	-0.50 to 0.50	0.10	0.90
<i>No Different/ Worse than (30)</i>	-0.10	-0.40 to 0.30		
CPT (z-score)				
<i>Better than (20)</i>	0.10	-0.30 to 0.50	0.71	0.48
<i>No Different/ Worse than (30)</i>	-0.10	-0.50 to 0.30		
<hr/>				
Study 2 (n = 111)				
BPI Pain Severity (z-score)				
<i>Better than (58)</i>	-0.01	-0.03 to 0.01	1.49	0.14
<i>No Different/ Worse than (53)</i>	-0.30	-0.30 to -0.20		
BPI Pain Interference (z-score)				
<i>Better than (58)</i>	0.02	0.01 to 0.03	0.40	0.69
<i>No Different/ Worse than (53)</i>	-0.10	-0.11 to -0.10		

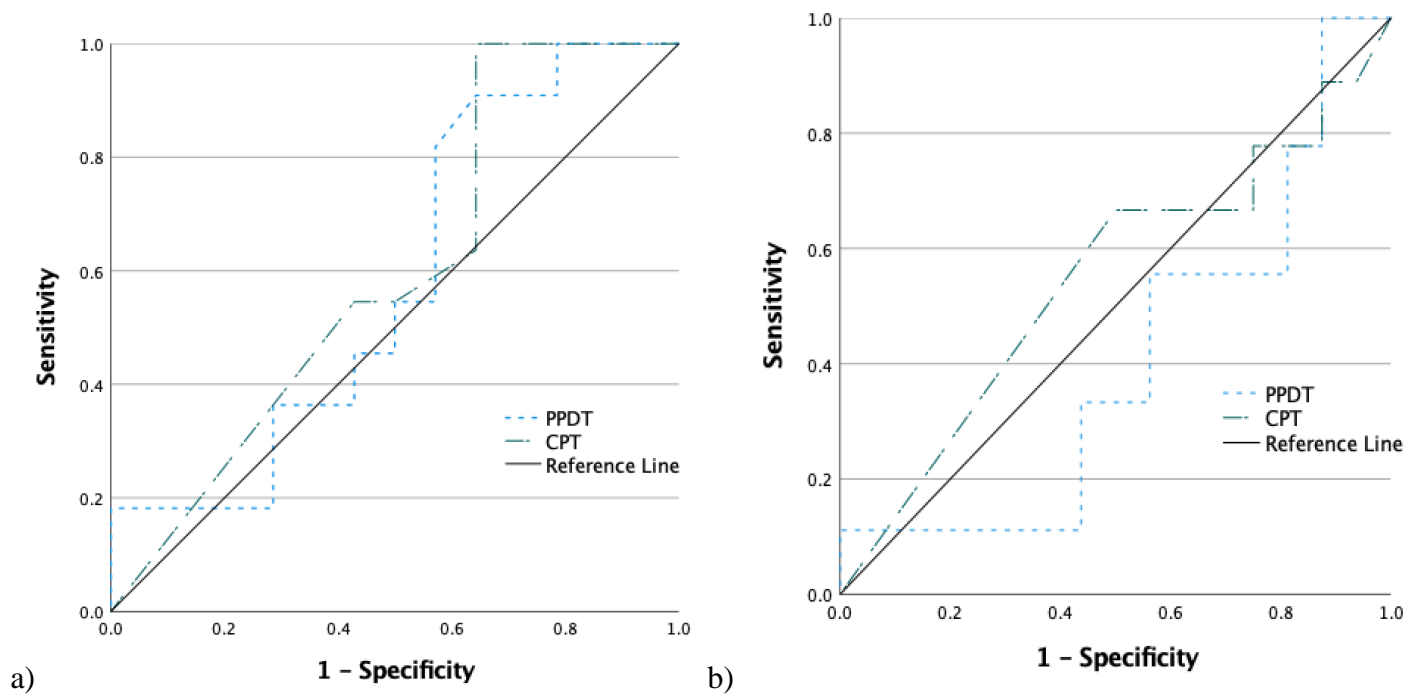


Figure 2-1: Accuracy of perceived ability to handle pain in predicting PPDT and CPT between a) males and b) females in the healthy cohort.

Males are descriptively more accurate in their predictions, however the between sex comparisons were not statistically significant.

2.3.4 Study 2 – Acute MSK Trauma, Objective 1

How accurate are sex-specific personal pain beliefs?

In Study 2, 52% of respondents overall indicated they were better able to handle pain than others of their same sex. There were no statistically significant differences in mean BPI Severity scores between those self-rating a better than ability to handle pain ($Z = -0.01$, 95%CI -0.03 to 0.01) compared to those who self-rated no difference/worse than ability ($Z = -0.30$, 95%CI -0.30 to -0.20, $t(109) = 1.49$, $p = 0.14$). There were also no significant differences in mean BPI Interference scores between those self-rating a better than ability to ‘handle’ pain ($Z = 0.02$, 95%CI 0.01 to 0.03) compared to those self-rating a no difference/ worse than ability ($Z = -0.10$, 95%CI -0.11 to 0.10, $t(109) = 0.40$, $p = 0.69$). See table 2-2 for all results.

2.3.5 Study 2 – Acute MSK Trauma, Objective 2

Is accuracy of sex-specific personal pain beliefs different between sexes?

In Study 2, 52% of females and 53% of males indicated they were better able to handle pain compared to others of the same sex (table 1). Table 2-3 presents the AUCs and Figures 2a and 2b are the ROC curves for BPI Severity and Interference plotted against belief in ability to handle pain for males and females, respectively. Similar to Study 1, males were descriptively more accurate predictors of their pain compared to females, however the between-sex comparisons were not statistically significant ($p > 0.05$). Across both pain indicators, the only group that was able to accurately predict their clinical pain evaluations compared to others at a level statistically better than chance was males in Study 2 when BPI Severity was the indicator (AUC = 0.67, 95%CI 0.50 to 0.83, $p = 0.04$).

Table 2-3: AUC values and 95% Confidence Intervals from ROC curves. Independent groups analysis demonstrated the differences between males and females AUC values using a z-test.

Pain Indicator	ROC Analysis		Independent Group Analysis	
	AUC	95% CI	Z-statistic	P-value
Study 1				
PPDT (kPa)				
<i>Females</i>	0.40	0.17 to 0.64	1.06	0.29
<i>Males</i>	0.58	0.35 to 0.81		
CPT (sec.)				
<i>Females</i>	0.55	0.30 to 0.79	0.31	0.76
<i>Males</i>	0.60	0.37 to 0.82		
Study 2				
BPI Pain Severity				
<i>Females</i>	0.52	0.38 to 0.67	1.31	0.19
<i>Males</i>	0.67*	0.50 to 0.83*		
BPI Pain Interference				
<i>Females</i>	0.50	0.35 to 0.65	0.97	0.33
<i>Males</i>	0.60	0.43 to 0.77		

*Indicates statistical significance at $p < 0.05$.

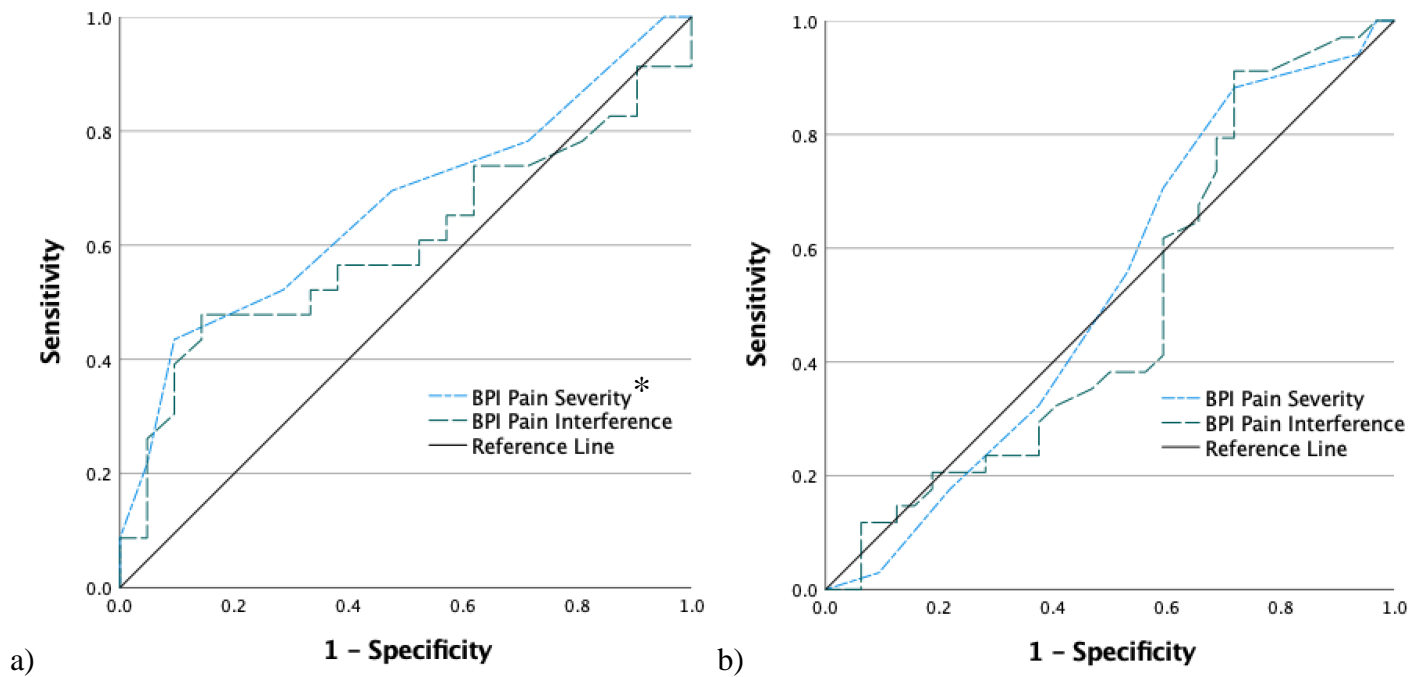


Figure 2-2: Accuracy of perceived ability to handle pain in predicting BPI Severity and Interference between a) males and b) females in the acute MSK trauma cohort.

Across all pain indicators, when BPI severity was the indicator, males demonstrated accurate predictions of their ability to handle pain ($p = 0.04$). This is indicated on the graph with an asterisk.

2.4 Discussion

Using two study cohorts, we demonstrated that sex-specific pain beliefs were not accurate predictors of performance on two quantitative sensory tests in otherwise healthy participants (PPDT, CPT (Study 1)) or clinical ratings of BPI Severity and Interference (Study 2). Both studies provide insight into different types of clinical pain evaluations, how they compare to the GREP, and the ability of one item on the GREP to predict different clinical pain evaluations between males and females. Looking across all analyses, males were descriptively more accurate in predicting clinical pain evaluations compared to other males than were females when comparing themselves to other females. However, the inferential statistics did not show this to be a true difference greater than chance.

Our results demonstrated that the perceived ability to handle pain better than a “typical” person of the same sex did not indicate a higher PPDT, longer CPT, or a lower BPI Severity or Interference score, compared to those who perceived themselves as no different or worse in their ability to handle pain. One potential explanation is the inability to recall experiences or events that would inflict similar pain as that experienced during PPDT or CPT. More specifically, recalling a specific instance where pain sensitivity or pain endurance was “tested” may not correlate to how one believes they are able to handle pain. The perceived ability to handle pain is likely a more general perception about one’s overall pain sensitivity, rather than a situational pain experience, as is measured using PPDT and CPT. A surprising finding was the lack of a relationship between one’s perceived ability to handle pain and the BPI Severity and Interference scales. Considering a shared method variance (self-reported questionnaires), it was more likely we would have found a significant relationship; those that indicated they were better able to handle pain would have lower pain severity and interference scores, and vice versa. This was not the case for Study 2, and the disparate associations may lie in the nature of the questionnaires. As described, the BPI is a specific measure of pain severity and interference, while the GREP item refers to a more general orientation towards pain tolerance. The lack of association between the two scales may highlight the importance of

administering more than one patient-reported outcome measure to capture the person's pain experience.

Previous research has found a relationship between experimental pain measures and items from the GREP, demonstrating that gender-role (or arguably sex-based), expectations of pain do play a role in predicting individual's experimental pain report.^{17,18} However methodologically, prior studies differ from the present study wherein we compared one's perceived ability to handle pain compared to the typical person of all others of the same sex, rather than comparing pain beliefs to a typical person of the opposite sex. This resulted in a new finding from our studies, where the males in Study 2 demonstrated greater accuracy for predicting BPI Severity scores using the GREP. Following AUC guidelines however, the predictive ability is small, and the difference between males and females was not statistically significant. Overall, females demonstrated the lowest predictive ability across all clinical pain evaluations. This may be the result of how sex-based pain beliefs are formed. Females may be more influenced by stereotypical implications that they are less able to handle pain, while the results from the clinical pain evaluations demonstrate otherwise. Developmentally, males *may* have been more exposed to, or observed more, instances where pain or pain-related experiences were inflicted upon other males, for example through sport. Observing how other people of the same sex *seem* to react to injury or pain, may lead to thoughts and perceptions about how you compare to them. Overall, males and females are likely responding to patient-reported clinical pain evaluations through different contextual lenses in light of different life experiences.¹² Our results further acknowledge that pain beliefs, reports, and intervention strategies therein, will likely be different, on average, between males and females, and further highlights the importance of considering all available pain measures when cultivating sex-specific intervention strategies.

2.5 Limitations

Our primary analysis relies on participant self-report; therefore, our results are subject to social desirability bias. To minimize this effect, survey responses were kept anonymous. Further, it is acknowledged that an upper limit of 90 seconds of cold immersion time for the CPT test could lead to a ceiling effect within our data. However, the percent of people

to reach the upper limit was similar for both sexes and the absence of significant differences between sexes proves unlikely that this had an impact on our findings. Finally, our *a priori* sample size estimation indicated a sample of 128 people (divided equally between two groups for each independent t-test), was sufficient to obtain 80% power for our analysis. However, as this was a secondary analysis on previously collected data we were unable to ensure a minimum of $n = 64$ participants within each group to maintain sufficient power. Our results therefore do not demonstrate definitive conclusions, rather encourage future work in this area.

2.6 Conclusion

Our study demonstrates that sex-specific pain beliefs were not accurate predictors of clinical pain evaluations. The purpose of identifying whether people can predict their pain when compared to others of the same sex is important for clinical settings as it is becoming increasingly important that multi-modal pain evaluation techniques that tap different domains of the pain experience, such as both pain ratings and quantitative sensory tests, are employed. This work also highlights the importance of considering all available clinical pain evaluations when creating interventions and treatment strategies, as one pain measurement technique is unlikely to represent the entirety of the patients' pain experience. Future work should target large, diverse samples to better understand the magnitude and significance of sex differences in pain beliefs and clinical pain evaluations, with a sub-aim focused on age-related changes that may play a role in the ability to accurately predict pain.

2.2 References

1. González-Fernández M, Ghosh N, Ellison T, McLeod JC, Pelletier CA, Williams K. Moving beyond the limitations of the visual analog scale for measuring pain: Novel use of the general labeled magnitude scale in a clinical setting. *Am J Phys Med Rehabil.* 2014;93(1):75-81. doi:10.1097/PHM.0b013e31829e76f7
2. Vader K, Bostick GP, Carlesso LC, et al. The Revised IASP Definition of Pain and Accompanying Notes: Considerations for the Physiotherapy Profession. *Physiotherapy Canada.* 2021;73(2):103-106. doi:10.3138/ptc-2020-0124-gee
3. Walton DM, Elliott JM. *Musculoskeletal Pain - Assessment, Prediction and Treatment.* HANDSPRING PUBLISHING LIMITED; 2019.
4. Defrin R, Shramm L, Eli I. Gender role expectations of pain is associated with pain tolerance limit but not with pain threshold. *Pain.* 2009;145(1-2):230-236. doi:10.1016/j.pain.2009.06.028
5. Wise EA, Price DD, Myers CD, Heft MW, Robinson ME. Gender role expectations of pain: Relationship to experimental pain perception. *Pain.* 2002;96(3):335-342. doi:10.1016/S0304-3959(01)00473-0
6. Alabas OA, Tashani OA, Tabasam G, Johnson MI. Gender role affects experimental pain responses: A systematic review with meta-analysis. *European Journal of Pain (United Kingdom).* 2012;16(9):1211-1223. doi:10.1002/j.1532-2149.2012.00121.x
7. Robinson ME, Riley JL, Myers CD, et al. Gender role expectations of pain: Relationship to sex differences in pain. *Journal of Pain.* 2001;2(5):251-257. doi:10.1054/jpai.2001.24551
8. Fillingim RB. Sex, gender, and pain: women and men really are different. *Curr Rev Pain.* 2000;4(1):24-30. doi:10.1007/s11916-000-0006-6

9. Garcia E, Godoy-Izquierdo D, Godoy JF, Perez M, Lopez-Chicheri I. Gender differences in pressure pain threshold in a repeated measures assessment. *Psychol Health Med*. 2007;12(5):567-579. doi:10.1080/13548500701203433
10. Robinson ME, Riley JL, Myers CD, et al. Gender role expectations of pain: Relationship to sex differences in pain. *Journal of Pain*. 2001;2(5):251-257. doi:10.1054/jpai.2001.24551
11. Robinson ME, Riley JL, Myers CD, et al. *Gender Role Expectations of Pain: Relationship to Sex Differences in Pain*. Vol 2. Churchill Livingstone Inc.; 2001:251-257. doi:10.1054/jpai.2001.24551
12. Sivagurunathan M, MacDermid J, Chuang JCY, Kaplan A, Lupton S, McDermid D. Exploring the role of gender and gendered pain expectation in physiotherapy students. *Canadian Journal of Pain*. 2019;3(1):128-136. doi:10.1080/24740527.2019.1625705
13. Ghodrati M, Walton DM, MacDermid JC. Exploring the Domains of Gender as Measured by a New Gender, Pain and Expectations Scale. *Women's Health Reports*. 2021;2(1):87-96. doi:10.1089/whr.2020.0109
14. Cleeland C. The Brief Pain Inventory. *Pain Research Group*. Published online 1991:3-66. Accessed April 2, 2020. www.mdanderson.org/departments/prg
15. Walton D, Macdermid J, Nielson W, Teasell R, Nailer T, Maheu P. A descriptive study of pressure pain threshold at 2 standardized sites in people with acute or subacute neck pain. *Journal of Orthopaedic and Sports Physical Therapy*. 2011;41(9):651-657. doi:10.2519/jospt.2011.3667
16. Kaunisto MA, Jokela R, Tallgren M, et al. Pain in 1,000 women treated for breast cancer: a prospective study of pain sensitivity and postoperative pain. *Anesthesiology*. 2013;119(6):1410-1421. doi:10.1097/ALN.0000000000000012
17. Wilson D, CA MLTO, Sage U, 2001 U. Practical meta-analysis. *rogeriofvieira.com*. Published online 2001. Accessed July 22, 2020. <http://rogeriofvieira.com/wp-content/uploads/2016/05/Wilson.pdf>

Chapter 3

3 The Utility of Quantitative CT (QCT) To Detect Differences in Subchondral Bone Mineral Density Between Healthy People and People with Pain Following Wrist Trauma

OVERVIEW

Studying subchondral bone is important in pain research because it has been suggested to be a potential contributor to chronic pain following musculoskeletal trauma. Subchondral bone is rich in blood and nerve supply and plays a critical role in supporting and nourishing the overlying cartilage. Changes in subchondral bone structure and density can lead to alterations in cartilage mechanics and joint loading, which may ultimately result in pain and disability. Therefore, understanding the role of subchondral bone in the development of pain can lead to improved diagnosis, treatment, and management of musculoskeletal conditions.

This chapter presents the utility of QCT to measure the density of depth-specific subchondral bone in the wrists of 10 participants, five of whom had experienced a wrist injury and are still experiencing pain, and five who had not. This study demonstrated the ability of QCT to distinguish between different types of subchondral bone and has proven useful for future work to study patient populations with degenerative conditions.¹

¹*A version of this work has been published in the Journal of Biomechanical Engineering and presented at the following conferences: IASP World Congress of Pain, Orthopedic Research Society Conference, the Health and Rehabilitation Science Conference, and the Canadian Pain Society Conference.*

3.1 Introduction

As introduced in Chapter 1, the wrist is the most frequently injured upper extremity joint, ¹⁻⁵ accounting for approximately 28% of all musculoskeletal (MSK) trauma.² The prevalence of chronic wrist pain after wrist trauma varies depending on the mechanism of injury,^{2,6-9} but has been found to affect up to one third of the population, especially older adults.¹⁰ The adverse effects associated with chronic wrist pain following trauma include functional and socioeconomic interference such as, functional limitations, emotional and psychological suffering, and lost hours of work.¹⁰⁻¹³

Bone fractures and ligamentous injuries in the wrist may result in bone mal-tracking. This can result in permanent damage to the joint with lasting pain and disability. Surgical approaches and treatment strategies target anatomical restoration within the joint following trauma, while traditional radiographic imaging, such as planar x-rays, are used to monitor joint alignment.^{14,15} Some studies have demonstrated that anatomical malalignment of the articulating joints can lead to mal-tracking. This mal-tracking leads to altered joint contact mechanics with overloading and under-loading of some articular regions.^{14,16-19} With time, the abnormal joint loading is a contributing factor to degeneration of the articular cartilage, and typical arthritic patterns can occur.^{9,14,16-19} However, other studies have stated that some malalignment within the joint is tolerated, without arthritic progression.^{14,20} Grewal et al.²⁰ concluded that malalignment should be considered a gradient risk of poor outcomes rather than an all-or-none phenomenon. In addition, Lalone et al.¹⁴ found that altered joint loading in a cohort of unilateral wrist fracture participants did not lead to the development of post-traumatic arthritis, or increased pain and disability within the study timeframe. As previously indicated in Chapter 1, cartilage is avascular and aneural, meaning that there are no blood vessels or nerves that supply the articular cartilage structure.²¹ The consequence of malalignment and its relationship to pain following wrist trauma is therefore unclear.

Recent studies in the knee have demonstrated that altered joint loading may induce changes to bone density and associated pain following trauma, due to the vascularity of the subchondral bone.^{22,23} In order to examine subchondral bone changes, a depth-specific imaging technique using quantitative computed tomography (QCT) has been

used.²⁴⁻²⁷ Prior research has explored the utility of depth-specific imaging in the knee with a specific focus on osteoarthritis (OA)-related knee pain^{22,27} and longitudinal effects of anterior cruciate ligament tears on vBMD.^{26,28} More specific to the hand and wrist, Hoogbergen et al²⁵ demonstrated that in ten cadaveric wrists, bone density patterns reflect long-term force transmission. The authors further concluded that pathologically altered cadaveric wrists (due to trauma, fractures, or degenerative diseases), demonstrated a shift in bone density laterally, towards the scaphoid.²⁵ As this was performed in cadaveric wrists, the ability to elucidate pain mechanisms is absent.

We propose the use of a QCT imaging technique to examine the relationship between static, *in vivo* joint-specific articular contact area (JCA) and depth-specific subchondral volumetric bone mineral density (vBMD) to characterize quantitative differences between people with a history of wrist trauma compared to healthy wrists. Our primary objective is to demonstrate the utility of the imaging technique in a small cohort of adults following a traumatic wrist event and compare these results to a healthy cohort. Our second objective is to examine bilateral differences in depth-specific subchondral vBMD.

3.2 Methods

3.2.1 Study Protocol

This was a cross-sectional exploratory analysis on prospectively collected data. Our analysis included two study cohorts: a healthy cohort and a wrist trauma cohort.

Healthy Cohort: The first cohort was recruited via newspaper ads and word of mouth. Inclusion criteria were: 18 years of age or older, able to speak conversational English, no previous history of hand or wrist trauma, and sufficient shoulder mobility that allowed the arm to be outstretched while lying in a prone position.

Wrist Trauma Cohort: The second cohort was recruited from a tertiary academic upper extremity orthopedic center. Inclusion criteria were: 18 years of age or older, able to speak conversational English, a history of a unilateral injury to either wrist, no reconstructive surgery to the hand or wrist, and sufficient shoulder mobility that allowed

the arm to be outstretched while lying in a prone position. Our study was approved by the institutional ethics review board at Western University, Canada (REB# 111702), and informed consent was obtained from all participants included in the study.

Following recruitment, all participants underwent CT scans of their dominant and non-dominant (healthy cohort), or injured and uninjured (trauma cohort) distal forearm and hand. This consisted of a localizer scan to determine the wrist location in space, and static neutral scans accompanied by a calibration phantom with known material densities calibrated against a liquid dipotassium phosphate (K_2HPO_4) solution. Participants were positioned on their stomach with their arm outstretched above their head into the scanner for the duration of the scans. Participants also filled out a study-specific demographics form and the *Patient-Rated Wrist Evaluation* (PRWE), a common patient-reported outcome measure specific to wrist pain and functional disability. A higher score is indicative of more pain and functional disability, with a total possible score of 100.²⁹ For descriptive purposes, and following work by Mehta et al.,¹⁰ we considered a score of $\leq 25/100$ as having little to no pain and functional disability, and a score of $>26/100$ was considered as having significant pain and functional disability following wrist trauma.

3.2.2 CT Scanning

A clinical CT scanner (Revolution CT Scanner, GE Healthcare, USA) was used to acquire static images of the distal forearm and hand in neutral position using a routine wrist scan protocol (120 kVp, 125 effective mAs, 0.35 s rotation time, and helical pitch of 1)¹. A calibration phantom (Model 3 calibration phantom, Mindways Software Inc, Austin, TX, USA) with known material densities was used as an accessory in the CT scanner and placed under the distal forearm and hand (Figure 3-1A). The phantom was used to transform grayscale CT Hounsfield Units (HU) to equivalent vBMD ($mg K_2HPO_4/cm^3$). Scanned image volumes included the distal radius and ulna, the carpals, metacarpals and phalanges. For the purpose of this analysis, only the volumes of the distal radius, lunate and scaphoid were analyzed.

CT scanning parameters included: an image volume of 16 cm, configured as a 512 x 512 matrix, and 0.625 mm thick slices. The total scan time was 40 s for a total of 160 0.625

mm thick slices. The voxel volume was 0.625 mm^3 for the static scans. The total skin dose was 0.2 mGy from the hand scans. The participant and CT technologist were both required to wear a lead apron and neck band, therefore the scatter dose from the scanner was 0.04 mGy of radiation for the duration of the testing.

3.2.3 QCT Analysis

The DICOM (digital imaging and communications in medicine) images obtained from the CT scans were reconstructed in 3D and used to create bone models of the distal radius, lunate and scaphoid using Materialise Mimics Software (v. 22, Leuven, Belgium) (Figure 3-1B). In brief, the global segmentation threshold was manually selected, and each slice was manually outlined according to the anatomical geometry of the bone. Previous work within our lab demonstrated that the inter- and intra-rater reliability using Mimics is high, with an error rate of less than or equal to 0.36 mm and 0.26 mm, respectively.³⁰ Post-processing procedures were used to ensure surface smoothness and uniform bone shape, following a previously established protocol.³¹ The resultant image was overlaid on the CT scan to ensure qualitative congruency.

3.2.3.1 Radiocarpal joint contact area

To illustrate regional JCA, static inter-bone distances (a CT-derived measure of joint contact) were calculated for the RL and RS joints using a previously validated Python algorithm.¹⁵ In brief, a proximity of less than or equal to 2.0 mm was used as it approximates the entire articular surface of the radius and its articular joints. The resultant inter-bone distance was visualized using an iso-contoured proximity map, with colors that represent the distance between articulating bones. A scale of red (0 mm) to blue (2 mm) was chosen to represent all inter-bone distances that are less than or equal to 2 mm, while all distances greater than 2 mm are shown as dark blue (Figure 3-1C).¹⁵ Post-processing procedures were used to obtain the weighted average normal surface vector of the point with the most JCA for each participant. In brief, values of proximity were used as a weighting factor with any scalar values that were greater than 2 mm excluded from the analysis, and any scalar values less than 2 mm (indicating more AC) weighted more heavily (Figure 3-1D). This process allowed for subject-specific

comparison, by considering subject-specific AC. The use of this surface vector will be described in detail in the subsequent section.

3.2.3.2 Subchondral bone mineral density analysis

To determine subchondral vBMD of the radius, we applied a depth-specific image-processing technique. To determine K_2HPO_4 equivalent density, circular regions of interest of $\sim 150\text{mm}^2$ were overlaid within each of the reference phantom cylinders to determine a patient-specific calibration equation. These linear regression equations, developed from known material densities within the cylinders of the calibration phantom,²² were applied to convert grayscale HU units obtained from the 3D bone model to equivalent vBMD ($\text{mg } K_2HPO_4/\text{cm}^3$) (Figure 3-1A, 3-1B). To define the subchondral bone surface, articular sites on the distal radius (RL and RS) were manually defined in 3-Matic software (v.14, Leuven, Belgium) (Figure 3-1E), using the articular contact maps (Figure 3-1C) as a qualitative reference. The x,y,z values from the subject-specific weighted average normal surface vector were used to extrude the volumized articular slice in the direction of the most contact at a uniform thickness of 2.5 mm (Figure 3-1F).

Average vBMD within three normalized layers (0 to 2.5 mm, 2.5 to 5 mm and 5 to 7.5 mm) were measured in relation to depth from the subchondral surface for each RL and RS articular surface (Matlab, 2019a, Natick, ME, USA), and representative vBMD measures are presented qualitatively (using vBMD colored scatterplots (Figure 3-1G)) and quantitatively (using percentage differences and effect sizes). Similar to the inter-bone distance color maps, a scale of red ($1600 \text{ mg } K_2HPO_4/\text{cm}^3$) to blue ($0 \text{ mg } K_2HPO_4/\text{cm}^3$) was chosen.

A series of regional analyses were performed on each normalized layer (0 to 2.5 mm, 2.5 to 5 mm, and 5 to 7.5 mm), including mean bilateral vBMD comparison, and a comparison between the dominant wrist in participants in the healthy cohort to the injured wrist of participants in the trauma cohort. Since all participants in the trauma cohort had injured their dominant wrist, they were compared to the dominant wrist of the healthy participants for an accurate comparison.

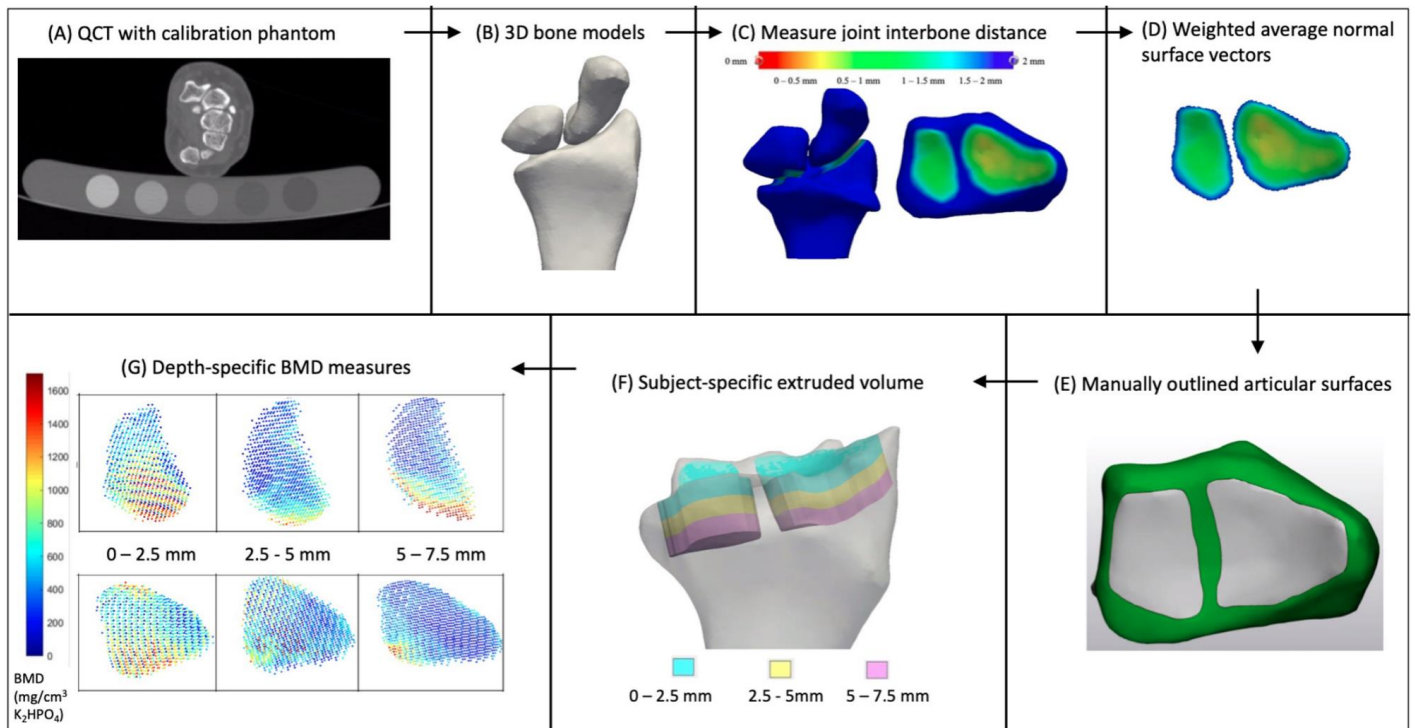


Figure 3-1: Flow chart of the methodological sequence for QCT analysis.

Flow chart of the methodological sequence for QCT analysis in the wrist using a calibration phantom with known densities (A), followed by the segmenting of the radius, lunate, and ulna to create 3D bone models (B). Bone models were used to create iso-contoured proximity maps to analyze articular contact (C). The articular contact maps were used to calculate the weighted average normal surface vector for each participant (D) and as a qualitative reference to manually define the radiolunate (RL) and radioscapoid (RS) regions on the radius (E). The weighted average normal surface vector values were used to extrude the RL and RS in the direction of the most contact at a uniform thickness of 2.5mm across three normalized layers (F). Colour maps from each layer represent the highest (red) and lowest (blue) regions of vBMD (G).

3.2.4 Statistical Analysis

For both objectives, we computed the percentage differences for each normalized layer to identify the largest joint-specific regional differences between vBMD measures. We also calculated Cohen's *d* effect sizes to determine the magnitude of the between-group differences in relation to the pooled standard deviation. We considered an absolute Cohen's *d* larger than 0.5 to be an effect size with clinical significance. Since this is an exploratory study, we opted to take a more conservative approach by adopting a moderate effect size so as not to risk the dismissal of potential important relationships and differences within our data.

To demonstrate the reliability of obtaining vBMD, estimates of intra-rater reliability were calculated using a two-way mixed-effects intra-class correlation coefficient (ICC). The data used for this calculation were from one rater manually segmenting the articular surfaces (RL and RS), and obtaining the vBMD from one study participant consecutively, five times. Following standard ICC guidelines, an ICC of less than 0.5 is indicative of poor reliability, 0.5 to 0.7 indicates moderate reliability, and values between 0.8 to 0.9 or greater are indicative of excellent reliability.³²

3.2.4.1 Volumetric Bone Mineral Density between Cohorts

To demonstrate the utility of QCT as our analysis method, we computed percentage differences between the dominant wrist of our healthy cohort and the injured wrist of our trauma cohort (healthy minus trauma divided by healthy). This was done for both articular surfaces (RL and RS). We computed Cohen's *d* effect sizes to determine the magnitude of the differences between groups, for all depths. A positive percentage difference and a positive Cohen's *d* demonstrates that the mean vBMD in the healthy participants is higher than the mean vBMD of the trauma participants.

3.2.4.2 Bilateral Volumetric Bone Mineral Density Comparison

We examined bilateral subchondral vBMD in our healthy cohort by computing the percentage difference between the dominant and non-dominant wrist vBMD for both articular surfaces (dominant RL minus non-dominant RL divided by dominant RL, and

the same for the RS). In our wrist trauma cohort, we computed percentage differences between the injured wrist and uninjured wrist vBMD for both articular surfaces (injured RL minus uninjured RL divided by injured RL, and the same for the RS). For this analysis, a positive percentage difference and a positive Cohen's *d* effect size demonstrates that the mean vBMD in the dominant or injured wrist is higher than the mean vBMD in the non-dominant or uninjured wrist.

3.3 Results

3.3.1 Participant Demographics

The sample was comprised of 10 participants: five healthy (4 males; 1 female, mean age, 70.4 ±6.5 years), and five participants with a history of wrist trauma (2 males; 3 females, mean age, 56.2 ±11.7 years). All participants in the healthy cohort demonstrated a PRWE score of ≤21.5/100 (little to no functional disability), while all participants in the wrist trauma cohort demonstrated a PRWE score of ≥35.0/100 (significant functional disability). Descriptive information (age, sex, mechanism of injury, scan date, and PRWE score) of each participant is presented in Table 3-1.

Overall, the healthy participants demonstrated higher vBMD compared to the wrist trauma participants, for both articular surfaces and all normalized depths. Results from our intra-rater reliability analysis for obtaining vBMD demonstrated excellent reliability, with an ICC of 0.99 (95% CI, 0.94 to 1.0). Qualitatively, vBMD patterns across the RL and RS joints appeared to differ for all regional analyses (0 to 2.5 mm, 2.5 to 5 mm, and 5 to 7.5 mm). Figure 3-2 demonstrates representative data from a healthy participant (top rows) and a participant with previous wrist trauma (bottom rows).

Table 3-1: Participant Demographics.

Participant	Age	Sex	Mechanism of Injury	Date of Injury	Date of Scan	PRWE score (/100)
1 - 71	68	Male	Healthy	N/A	Feb. 2020	0
2 - 72	82	Male	Healthy	N/A	Feb. 2020	21.5
3 - 73	67	Female	Healthy	N/A	Feb. 2020	16.0
4 - 75	68	Male	Healthy	N/A	Mar. 2020	0
5 - 78	67	Male	Healthy	N/A	Mar. 2020	0
6 - 105	60	Male	SL Injury (6 weeks prior)	Sept. 2020	Oct. 2020	35.0
7 - 108	45	Female	Distal Radius Malunion Elbow Fracture	Sept. 2018 Sept. 2019	Nov. 2020	58.0
8 - 109	58	Female	Right Pisiform Excision due to Pisotriquetral Arthritis	Oct. 2020	Nov. 2020	83.5
9 - 110	45	Male	SLAC wrist (4-5 years post SL injury)	Nov. 2015	Nov. 2020	44.0
10 - 113	73	Female	Distal Radius Malunion	June 2020	Dec. 2020	69.0

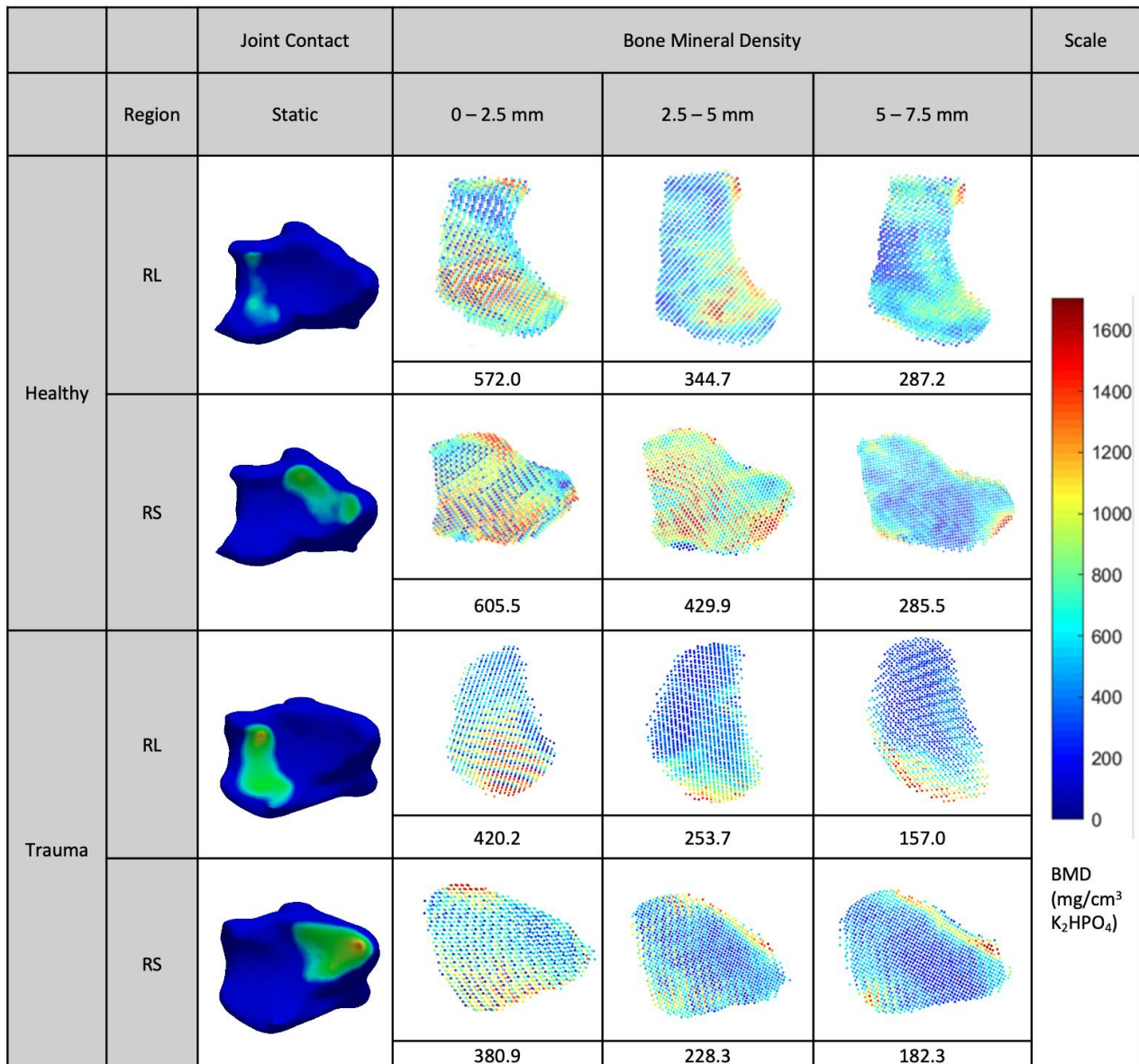


Figure 3-2: Representative data from a healthy participant (top rows) and a participant with previous wrist trauma (bottom rows).

Proximity maps of average BMD for the radiolunate (RL) and radioscapoid (RS) joints with respective bone mineral density (BMD) scatter plots and numeric measure at depths of 0 – 2.5mm, 2.5 – 5mm, and 5 – 7.5mm. Sex-matched representative data from one participant's wrist was used to demonstrate results from the healthy cohort (top row) and one participant's injured wrist was used to demonstrate results from the trauma cohort (bottom row). Both were participant's dominant hand.

3.3.2 Volumetric Bone Mineral Density between Cohorts

When comparing the dominant wrist of the healthy cohort to the injured wrist of the trauma cohort, percentage differences ranged from 7.3 to 26.7 % in the RL joint, and 15.0 to 20.6 % in the RS joint, demonstrating a higher vBMD in the dominant wrist of the healthy cohort. Furthermore, Cohen's *d* effect sizes demonstrated small to large differences ranging from 0.2 to 1.4, with larger effect sizes, and therefore more vBMD, in the dominant wrist of the healthy cohort. The most significant differences were noted 0 to 2.5 mm and 5 to 7.5 mm from the subchondral surface for both RL and RS joints. The largest magnitude of difference was demonstrated 0 to 2.5 mm from the surface in the RL joint, indicated by an overall percentage difference of 26.7% higher vBMD in the RL joint of the healthy cohort, and an effect size of 1.4 (Figure 3-3).

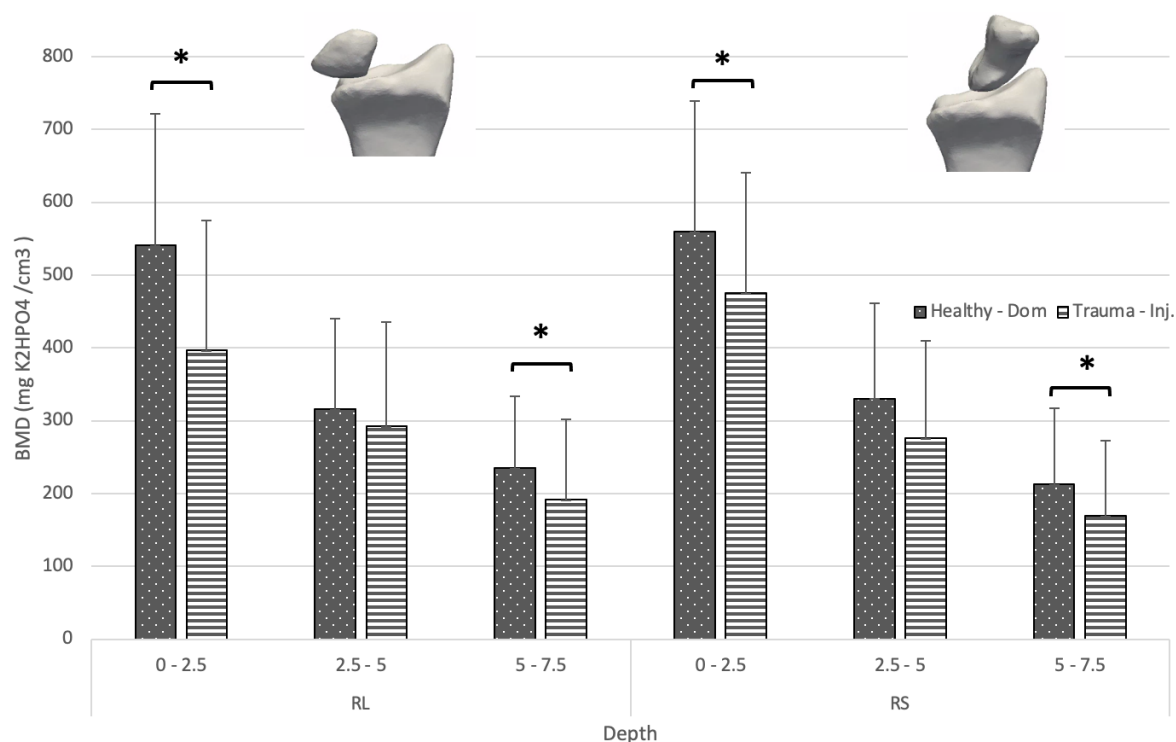


Figure 3-3: Mean vBMD comparison between the dominant wrist of the healthy cohort and the injured wrist of the trauma cohort.

Overall, the healthy participants have a higher vBMD for all depths. The largest magnitude of difference was demonstrated at depth 0 to 2.5 mm and 5 to 7.5 mm and is indicated on the graph with an asterisk.

3.3.3 Bilateral Volumetric Bone Mineral Density Comparison

In the RL joint of the healthy cohort, vBMD in the 0 to 2.5 mm region was higher in the dominant wrist, demonstrated by a 6.5% difference, while the vBMD in the non-dominant wrist was higher in the deeper regions, demonstrated by a -12.8 to -32.1% difference. The RS joint followed the same pattern, wherein the vBMD in the dominant wrist was higher in the 0 to 2.5 mm region (9.3%), while the vBMD in the non-dominant wrist was higher in the deeper regions, demonstrated by a -18.1% to -31.4% difference. Cohen's *d* effect sizes indicated moderate differences between the dominant and non-dominant wrists, with values ranging from 0.3 to -0.7. The largest differences were demonstrated 2.5 to 5mm from the subchondral surface for both the RL and RS joints, with higher vBMD found in the non-dominant RL and RS joints (Figure 3-4).

In the RL joint of the trauma cohort, vBMD in the 2.5 to 5 mm and 5 to 7.5 mm regions was higher in the injured wrist, demonstrated by a 0.4% to 2.0% difference, while the uninjured wrist demonstrated a higher vBMD in the shallow region, demonstrated by a -9.3% difference. In the RS joint, vBMD was higher in the injured wrist in the 0 to 2.5 mm region with a 4.8% difference, while vBMD in the uninjured wrist was higher in the deeper regions, demonstrated by -10.8% to -22.8% difference. Cohen's *d* effect sizes demonstrated small to moderate differences between the injured and uninjured wrists, with values ranging from 0.2 to -0.4 (Figure 3-5).

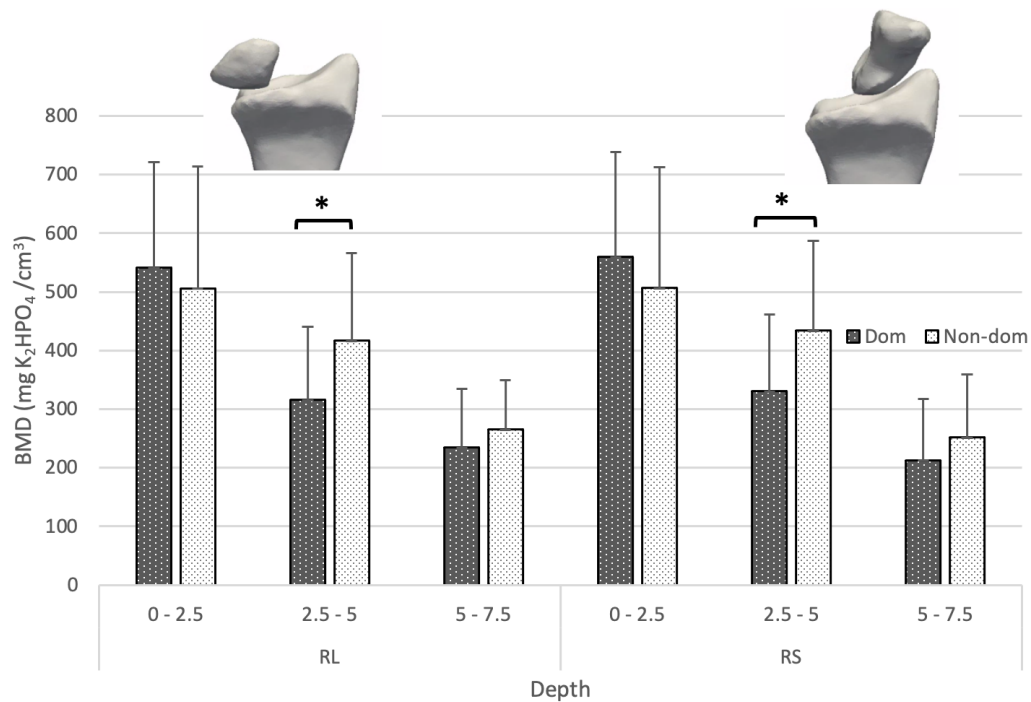


Figure 3-4: Bilateral vBMD differences in the healthy cohort.

Clinically significant differences were demonstrated 2.5 – 5 mm from the subchondral surface for the RL and RS. The graph demonstrates a trend in vBMD, wherein vBMD in the dominant wrist is highest at 0 – 2.5mm, while the non-dominant wrist demonstrates a higher vBMD at depths of 2.5 – 5 and 5 – 7.5 mm.

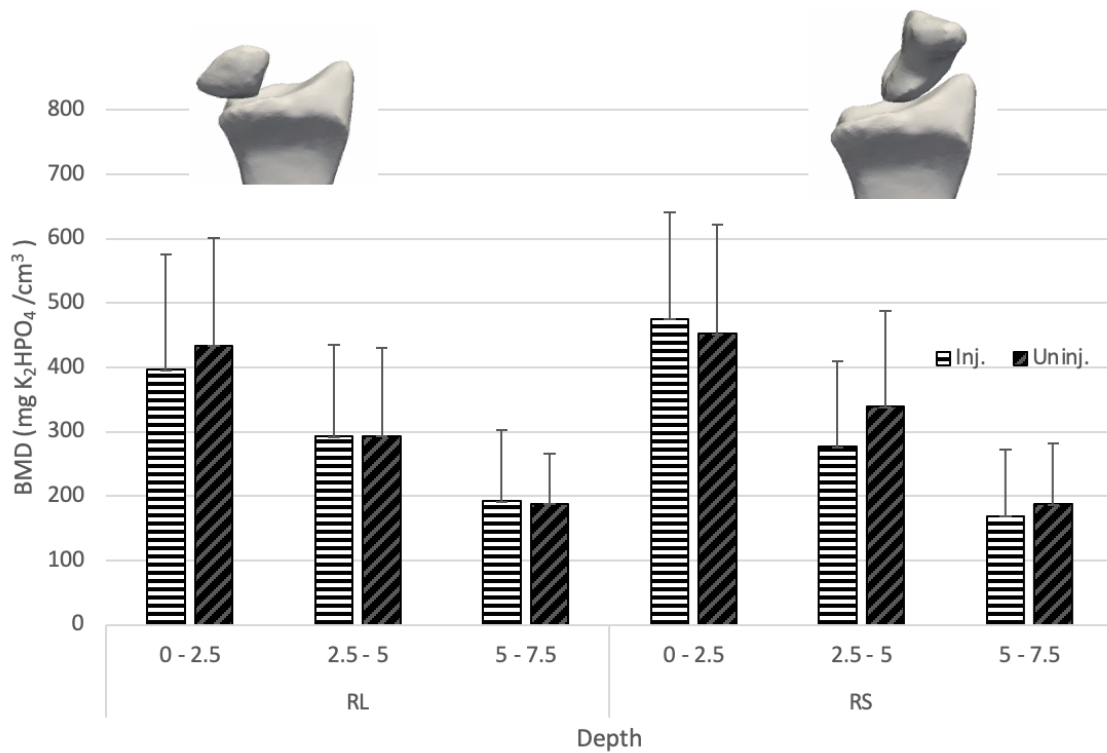


Figure 3-5: Bilateral vBMD differences in the trauma cohort.

There are no clinically significant differences in bilateral BMD in participants with pain. The BMD measures are similar for all depths for both the injured and uninjured wrists.

3.4 Discussion

The purpose of Chapter 3 was to demonstrate the utility of a QCT imaging technique to examine subchondral vBMD in the wrist. This image-based tool provides reliable subject-specific, depth-specific, and joint-specific measures of vBMD within the wrist. This study presented quantitative vBMD measures in a cohort of healthy participants and in patients with a history of wrist trauma.

Subject-specific differences in joint contact is an important element to incorporate into our analysis of vBMD, as joint contact mechanics has been shown to be directly related to bone density in the underlying subchondral bone. Previous studies in the knee have examined the relationship between altered jointing loading and vBMD as it relates to long-term effects of loading and contact mechanics.³³ In this study, we took this analysis further by including subject-specific models of our participants and examining vBMD in key regions in the subchondral bone that are experiencing more load (more contact), compared to other regions in the subchondral bone, using the subject-specific identification of the weighted average normal surface vector. Future work will examine the relationship between joint contact area throughout the full range of motion and the underlying subchondral bone.

The depth-specific analysis allowed us to differentiate vBMD across three normalized layers from the subchondral surface. Preliminary data from our cohort showed a decrease in vBMD for all study participants, however the wrist trauma cohort demonstrated a greater decrease in vBMD across the subchondral bone layers when compared to our healthy cohort. Both findings are consistently supported in the literature.^{22,26-28,34-36} Our technique further highlighted potential bone remodeling in subchondral cortical versus trabecular bone following wrist trauma, wherein the largest difference in vBMD between the healthy cohort and the wrist trauma cohort was found in the superficial layer of bone (0 to 2.5 mm). This region is primarily composed of subchondral cortical bone. It is important to analyze this region of bone as subchondral cortical bone is susceptible to abnormal wear patterns on the articular cartilage that is adjacent to the subchondral cortical bone,¹⁹ and has a pronounced effect on the structural integrity of the joint.³⁷ Abnormal contact patterns and increased wear on the joint following injury is directly

related to a decrease in subchondral cortical bone. Previous work in the knee demonstrated that the deepest regions (2.5 to 5.0 and 5.0 to 7.5 mm) had the largest differences between vBMD in OA-related knee pain in the patella^{22,27} or tibia,^{26,28} and knee pain associated with ACL tears^{26,28} when compared to a healthy cohort. These regions are primarily composed of subchondral trabecular bone, wherein trabecular bone is found to be more metabolically active, adaptive to change, and has a higher bone turnover rate when compared to subchondral cortical bone.²⁷ However, loading patterns in the knee are very different from loading patterns in the wrist, therefore it is unlikely that changes to the subchondral bone in these joints following trauma will be the same. It is acknowledged that a reduction in vBMD in our wrist trauma cohort could be due to a decrease in physical activity that exacerbates bone loss in the injured wrist. Future research should therefore employ this depth-specific imaging technique in longitudinal studies focused on vBMD following trauma to better understand the healing process of the subchondral bone.

Our methodology also highlighted joint-specific or regional differences in vBMD across the articular surface. This is important as differences in contact area between the regions exist.²⁵ The radiocarpal joint describes the articulation of the distal radius with the scaphoid (RS) and lunate (RL). Our methodology allowed us to differentiate between these specific joint contact regions, which could have been missed if the entire joint surface was analyzed. Specifically, previous work from Hoogbergen et al.,²⁵ demonstrated that pathological changes to the wrist resulted in a shift of bone density towards the scaphoid. As we were able to directly compare the vBMD beneath the RL and RS joint surfaces, our results demonstrated that the vBMD beneath the RS joint was descriptively greater than the vBMD beneath the RL. These results are promising, as the RS joint is the main site of force transmission while the RL joint plays a lesser role.²⁵ Therefore, while the joint-specific comparison within our analysis was advantageous *between* study participants (namely, the RL to RL and RS to RS comparisons), future work should employ this technique to study the relationship between the vBMD beneath the RL versus the RS *within* study participants.

Our QCT imaging analysis also demonstrates potential clinical implications. Using our methodology, the ability to distinguish between normalized layers from the subchondral surface may aid in a better understanding of the relationship between vBMD, OA progression, and pain. OA progression and severity is usually monitored using radiographic features near the joint surface (primarily, the subchondral cortical bone), however previous studies have found signs of OA severity within the deeper regions of the subchondral bone, namely, studies performed in the knee.^{22,25,27,28} This methodology enables us to monitor depth-specific changes in the wrist that may be indicative of structural or clinical changes associated with OA, and allow for timely interventions to mitigate the progression of OA. In addition, all participants with a history of wrist trauma, regardless of the elapsed time since injury, scored higher on the PRWE (indicating more pain and functional disability), compared to those in the healthy group. Lower vBMD measures were consistently associated with higher PRWE scores in our study sample and may therefore be a more robust explanation for lasting pain and disability following wrist trauma compared to the consequence of malalignment. However, it is cause for further investigation into the relationship between low subchondral vBMD, pain, and OA progression by implementing this imaging technique into a larger sample that is analyzed longitudinally to better understand the changes occurring throughout the course of recovery.

3.5 Limitations

Volumetric BMD is a measurement that is also indirectly affected by inflammatory markers (for example, cytokines) that naturally occur in the bone following injury.³⁸ These markers could change the attenuation of the tissue being scanned; the scan incorporates the marrow space between the trabeculae, and infiltration of blood or other fluids into the marrow space. Therefore, since we are measuring where the trauma would have occurred, we are exposing ourselves to the potential of artificially inflating or decreasing the vBMD measures. However, we didn't analyze these participants over time, and we therefore can't make any conclusions on the timeframe that these changes would occur, and if these factors impact the vBMD measures as a result. Moreover, the manual segmentation of the articular surfaces within our methodology introduces

potential reliability error, wherein the manually segmented articular surfaces are used to obtain the underlying subchondral vBMD. However, the results from our intra-rater ICC analysis suggest that our methodology can be undertaken reliably. Given that these results were obtained from one rater, it is unknown whether other raters would achieve the same vBMD measures. Finally, while we intentionally analyzed vBMD as it relates to a static wrist position, it is acknowledged that analyzing variations in vBMD according to AC throughout motion would provide more specific information on the wrist positions that most impact subchondral vBMD.

3.6 Conclusion

Chapter 3 demonstrated the utility of a QCT imaging technique in characterizing quantitative differences in subchondral vBMD between our study cohorts. This methodology highlighted the differences between subject-specific, depth-specific, and joint-specific vBMD in healthy people and people who have experienced wrist trauma. Overall, the healthy cohort demonstrated higher vBMD across all three depths and both articular surfaces. This imaging technique further distinguished between subchondral cortical and trabecular bone wherein clinical implications can be drawn from these distinctions in future work. The largest difference and effect size between the healthy and trauma cohort was demonstrated 0 to 2.5 mm from the surface, demonstrating that remodeling following wrist trauma may occur in the subchondral cortical bone region. Our study supports the utility of a QCT imaging technique in detecting differences in depth-specific vBMD. The next step with this work is to understand how joint motion, or kinematic JCA, contributes to alterations in vBMD in a cohort of healthy adults.

3.7 References

1. Zhao K, Breighner R, Holmes D, Leng S, McCollough C, An KN. A technique for quantifying wrist motion using four-dimensional computed tomography: Approach and validation. *J Biomech Eng.* 2015;137(7). doi:10.1115/1.4030405
2. Shores JT, Demehri S, Chhabra A. Kinematic “4 Dimensional” CT Imaging in the Assessment of Wrist Biomechanics Before and After Surgical Repair. *Eplasty.* 2013;13:e9. Accessed July 15, 2020.
<https://www.ncbi.nlm.nih.gov/pmc/articles/PMC3589877/>
3. Bruno F, Arrigoni F, Palumbo P, et al. The Acutely Injured Wrist. *Radiol Clin North Am.* 2019;57(5):943-955. doi:10.1016/j.rcl.2019.05.003
4. Garcia-Elias M, Folgar MÁV. The management of wrist injuries: An international perspective. *Injury.* 2006;37(11):1049-1056. doi:10.1016/j.injury.2006.07.025
5. MacDermid JC, Roth JH, Richards RS. Pain and disability reported in the year following a distal radius fracture: A cohort study. *BMC Musculoskelet Disord.* 2003;4(1):1-13. doi:10.1186/1471-2474-4-24
6. MacDermid JC, Roth JH, Richards RS. Pain and disability reported in the year following a distal radius fracture: A cohort study. *BMC Musculoskelet Disord.* 2003;4:1-13. doi:10.1186/1471-2474-4-24
7. Shah CM, Stern PJ. Scapholunate advanced collapse (SLAC) and scaphoid nonunion advanced collapse (SNAC) wrist arthritis. *Curr Rev Musculoskelet Med.* 2013;6(1):9-17. doi:10.1007/s12178-012-9149-4
8. Murphy BD, Nagarajan M, Novak CB, Roy M, McCabe SJ. The Epidemiology of Scapholunate Advanced Collapse. *Hand.* 2020;15(1):23-26. doi:10.1177/1558944718788672

9. O’Meehan CJ, Stuart W, Mamo V, Stanley JK, Trail IA. The natural history of an untreated isolated scapholunate interosseus ligament injury. *Journal of Hand Surgery*. 2003;28(4):307-310. doi:10.1016/S0266-7681(03)00079-2
10. Mehta SP, Macdermid JC, Richardson J, MacIntyre NJ, Grewal R. Baseline pain intensity is a predictor of chronic pain in individuals with distal radius fracture. *Journal of Orthopaedic and Sports Physical Therapy*. 2015;45(2):119-127. doi:10.2519/jospt.2015.5129
11. Ospina M, Harstall C. Prevalence of chronic pain: an overview HTA 29 Health Technology Assessment Alberta Heritage Foundation for Medical Research. Published online 2002.
12. Elliott AM, Smith BH, Penny KI, Smith WC, Chambers WA. The epidemiology of chronic pain in the community. *Lancet*. 1999;354(9186):1248-1252. doi:10.1016/S0140-6736(99)03057-3
13. Cimmino MA, Ferrone C, Cutolo M. Epidemiology of chronic musculoskeletal pain. *Best Pract Res Clin Rheumatol*. 2011;25(2):173-183. doi:10.1016/j.berh.2010.01.012
14. Lalone EA, MacDermid J, King G, Grewal R. The Effect of Distal Radius Fractures on 3-Dimensional Joint Congruency. *Journal of Hand Surgery*. 2021;46(1):66.e1-66.e10. doi:10.1016/j.jhsa.2020.05.027
15. Lalone EA, McDonald CP, Ferreira LM, Peters TM, King GW, Johnson JA. Development of an image-based technique to examine joint congruency at the elbow. *Comput Methods Biomech Biomed Engin*. 2013;16(3):280-290. doi:10.1080/10255842.2011.617006
16. Lalone E, MacDermid J, Grewal R, King G. Patient Reported Pain and Disability Following a Distal Radius Fracture: A Prospective Study. *Open Orthop J*. 2017;11(1):589-599. doi:10.2174/1874325001711010589

17. Crisco JJ, Moore DC, Marai GE, et al. Effects of distal radius malunion on distal radioulnar joint mechanics - An in vivo study. *Journal of Orthopaedic Research*. 2007;25(4):547-555. doi:10.1002/jor.20322
18. Rainbow MJ, Wolff AL, Crisco JJ, Wolfe SW. Functional kinematics of the wrist. *Journal of Hand Surgery: European Volume*. 2016;41(1):7-21. doi:10.1177/1753193415616939
19. Laulan J, Marteau E, Bacle G. Wrist osteoarthritis. *Orthopaedics and Traumatology: Surgery and Research*. 2015;101(1):S1-S9. doi:10.1016/j.otsr.2014.06.025
20. Grewal R, MacDermid JC. The Risk of Adverse Outcomes in Extra-Articular Distal Radius Fractures Is Increased With Malalignment in Patients of All Ages but Mitigated in Older Patients. *Journal of Hand Surgery*. 2007;32(7):962-970. doi:10.1016/j.jhsa.2007.05.009
21. Madry H, van Dijk CN, Mueller-Gerbl M. The basic science of the subchondral bone. *Knee Surgery, Sports Traumatology, Arthroscopy*. 2010;18(4):419-433. doi:10.1007/s00167-010-1054-z
22. Burnett W, Kontulainen S, McLennan C, et al. Patella bone density is lower in knee osteoarthritis patients experiencing moderate-to-severe pain at rest. *Journal of Musculoskeletal Neuronal Interactions*. 2016;16(1):33-39. Accessed March 17, 2020. <http://www.ncbi.nlm.nih.gov/pubmed/26944821>
23. Burnett WD, Kontulainen SA, McLennan CE, et al. Proximal tibial trabecular bone mineral density is related to pain in patients with osteoarthritis. *Arthritis Res Ther*. 2017;19(1):1-9. doi:10.1186/s13075-017-1415-9
24. Johnston JD. *DEVELOPMENT OF A NOVEL NON-INVASIVE IMAGING TECHNIQUE FOR CHARACTERIZING SUBCHONDRAL BONE DENSITY AND STIFFNESS*. 2010. doi:10.14288/1.0071564
25. Hoogbergen MM, Schots JMP, Niessen WJ, Schuurman AH, Spauwen PHM, Kauer JMG. Subchondral bone mineral density patterns representing the loading history of the

- wrist joint after a proximal row carpectomy. *Eur J Plast Surg*. 2008;31(3):101-107. doi:10.1007/s00238-008-0230-6
26. Kroker A, Zhu Y, Manske SL, Barber R, Mohtadi N, Boyd SK. Quantitative in vivo assessment of bone microarchitecture in the human knee using HR-pQCT. *Bone*. 2017;97:43-48. doi:10.1016/j.bone.2016.12.015
 27. Burnett WD, Kontulainen SA, McLennan CE, Hunter DJ, Wilson DR, Johnston JD. Regional depth-specific subchondral bone density measures in osteoarthritic and normal patellae: In vivo precision and preliminary comparisons. *Osteoporosis International*. 2014;25(3):1107-1114. doi:10.1007/s00198-013-2568-2
 28. Kroker A, Besler BA, Bhatla JL, et al. Longitudinal Effects of Acute Anterior Cruciate Ligament Tears on Peri-Articular Bone in Human Knees Within the First Year of Injury. *Journal of Orthopaedic Research*. 2019;37(11):2325-2336. doi:10.1002/jor.24410
 29. MacDermid JC. Development of a scale for patient rating of wrist pain and disability. *Journal of Hand Therapy*. 1996;9(2):178-183. doi:10.1016/S0894-1130(96)80076-7
 30. Robinson SM. 4DCT to Examine Carpal Motion. *Electronic Thesis and Dissertation Repository*. Accessed September 27, 2021. <https://ir.lib.uwo.ca/etd://ir.lib.uwo.ca/etd/7801>
 31. Robinson S, Straatman L, Lee TY, Suh N, Lalone E. Evaluation of four-dimensional computed tomography as a technique for quantifying carpal motion. *J Biomech Eng*. 2021;143(6). doi:10.1115/1.4050129
 32. Koo TK, Li MY. A Guideline of Selecting and Reporting Intraclass Correlation Coefficients for Reliability Research. *J Chiropr Med*. 2016;15(2):155. doi:10.1016/J.JCM.2016.02.012
 33. Apergis E, Darmanis S, Theodoratos G, Maris J. Subchondral bone mineral density patterns representing the loading history of the wrist joint. *Journal of Hand Surgery*. 2002;27 B(2):150-154. doi:10.1054/jhsb.2001.0714

34. Burghardt AJ, Buie HR, Laib A, Majumdar S, Boyd SK. Reproducibility of direct quantitative measures of cortical bone microarchitecture of the distal radius and tibia by HR-pQCT. *Bone*. 2010;47(3):519-528. doi:10.1016/j.bone.2010.05.034
35. Johnston JD, Masri BA, Wilson DR. Computed tomography topographic mapping of subchondral density (CT-TOMASD) in osteoarthritic and normal knees: methodological development and preliminary findings. *Osteoarthritis Cartilage*. 2009;17(10):1319-1326. doi:10.1016/j.joca.2009.04.013
36. Kontulainen S, Liu D, Manske S, Jamieson M, Sievänen H, McKay H. Analyzing Cortical Bone Cross-Sectional Geometry by Peripheral QCT: Comparison With Bone Histomorphometry. *Journal of Clinical Densitometry*. 2007;10(1):86-92. doi:10.1016/j.jocd.2006.07.007
37. Kontulainen S, Liu D, Manske S, Jamieson M, Sievänen H, McKay H. Analyzing Cortical Bone Cross-Sectional Geometry by Peripheral QCT: Comparison With Bone Histomorphometry. *Journal of Clinical Densitometry*. 2007;10(1):86-92. doi:10.1016/j.jocd.2006.07.007
38. Meyer U, De Jong JJ, Bours SG, et al. Early changes in bone density, microarchitecture, bone resorption, and inflammation predict the clinical outcome 12 weeks after conservatively treated distal radius fractures: An exploratory study. *Journal of Bone and Mineral Research*. 2014;29(9):2065-2073. doi:10.1002/jbmr.2225

Chapter 4

4 Use it or lose it: The Relationship between Two Image-Based Biomarkers in Better Understanding Joint Adaptation in the Wrist.

OVERVIEW

Subchondral bone tissue is influenced by its mechanical environment and adapts in response to mechanical loads acting on it. This is evident in weight-bearing joints, such as the knee and hip. Building off Chapter 3, this chapter sought to understand how joint motion contributes to subchondral bone mineral density in a cohort of healthy adults. We demonstrated that subchondral bone changes in the wrist are influenced by wrist position and may likely serve to bear load similar to the knee and hip.¹

¹ *A version of this work has been published in the Journal of Biomechanics and presented at the following conferences: The Canadian Orthopedic Research Conference, Orthopedic Research Society Conference, Imaging Network Ontario Conference, Canadian Bone and Joint Conference, Ontario Biomechanics Conference, and the Canadian Arthritis Society Conference.*

4.1 Introduction

In Chapter 1, osteoarthritis (OA) is introduced as a chronic joint disease characterized by degeneration of articular cartilage between joints and subchondral bone alterations, including bony growth outside the joint (osteophytes).¹⁻⁴ OA has serious impacts on patient quality of life and as there is no cure for OA, early detection and preventative measures are paramount. Understanding biological mechanisms underlying OA are therefore crucial. As discussed in Chapter 3, previous literature has focused on joint mal-tracking as an underlying mechanism leading to post-traumatic OA.⁵⁻⁹ Specifically, Laulan et al.,⁷ demonstrated that traumatic injuries resulting in malalignment within the wrist are consistently followed by the development of OA within approximately 5 – 10 years due to the over and under loading of some articular regions within the joint. However, other studies have demonstrated that malalignment should be considered a gradient risk of OA progression rather than an all-or-none phenomenon, as some degree of malalignment can be tolerated without typical arthritic progression.^{5,9}

As discussed in Chapter 3, knee research using variations of a QCT analysis demonstrated that altered joint loading leads to alterations in subchondral bone mineral density (BMD) and associated pain therein. Notably, the following studies on the knee indicated alterations in trabecular bone tissue (introduced in Chapter 1 as metabolically active and adaptive bone tissue¹⁰). Specifically, OA-related knee pain was consistently associated with lower BMD,^{11,12} and unloading of the injured knee due to OA-related knee pain resulted in irreversible bone loss.^{13,14} It was further demonstrated that bone tissue changes (as a result of altered loading), may precede cartilage degeneration in OA-related research.^{11,12} Some of these trabecular bone changes in the knee may be attributed to post-injury disuse in the load-bearing joints. Understanding whole joint changes in non-weight-bearing joints are essential to elucidate key factors that may contribute to structural and/or clinical OA initiation and progression.

According to Wolff's law, bone tissue is influenced by its mechanical environment and adapts in response to the mechanical load that acts on it,^{15,16} due to the dynamic, metabolically active structure of bone tissue. Repetitive joint loading therefore leads to adaptive changes in the underlying bone that enable it to cope with varying loads. These

bone alterations have been supported by studies analyzing bone adaptation in weight-bearing joints, namely that of the knee^{11-13,17} and hip,¹⁸ where an increased mechanical load led to adaptations in the trabecular bone specifically. In Chapter 3, we provided an in-depth analysis on the use of a quantitative computed tomography (QCT) imaging technique, to detect depth-, joint-, and subject-specific differences in subchondral volumetric BMD (vBMD) of the wrist.¹⁹ Our sample was composed of people with previous wrist injury and healthy people. The greatest differences in vBMD were found in regions mainly composed of trabecular bone, while lower vBMD was also correlated with higher amounts of pain. This study was performed while the wrist was in a static, neutral position and therefore has limited ability to elucidate the contribution of loading patterns on subchondral vBMD within the joint.

Building off the results from Chapter 3, the purpose of this study is to examine relationships between subchondral bone and kinematic joint contact area (JCA) throughout a range of motion within the wrist. Our primary objective is to evaluate the correlation between kinematic joint contact and subchondral vBMD, as it relates to depth from the subchondral surface. Assuming that JCA is highly correlated with joint loading,²⁰ we hypothesize that an increase in joint loading, (measured as an increase in JCA), will result in an increase in vBMD within all depth-specific layers from the subchondral surface. Where a relationship between subchondral vBMD and kinematic JCA exists, our secondary objective is to determine the amount of additional variance that can be explained by the sex and age of the participant.

4.2 Methods

4.2.1 Study Protocol

This was a cross-sectional analysis on prospectively collected data. Our study included a cohort of healthy adults, recruited via newspaper and word of mouth. Inclusion criteria were: 18 years of age or older, able to speak conversational English, no previous history of hand or wrist trauma, and sufficient shoulder mobility that allowed the arm to be outstretched while lying in a prone position. Our study was approved by the institutional

ethics review board (REB# 111702), and informed consent was obtained from all participants included in the study.

Following recruitment, all participants underwent three sets of CT scans (Revolution CT Scanner, GE Healthcare, Waukesha, WI) of their dominant distal forearm and hand. The first was a localizer scan to determine the wrist location in space, followed by a static neutral scan using the same protocol as described in Chapter 3 (section 3.2.2). Briefly, a calibration phantom (model three calibration phantom, Mindways Software, Austin, TX) with known material densities was used as an accessory in the static CT scans and placed under the distal forearm and hand (Figure 4-1). Calibrated against a liquid dipotassium phosphate (K_2HPO_4) solution, the phantom was used to transform grayscale CT Hounsfield Units (HU) into equivalent vBMD ($mg K_2HPO_4/cm^3$). Scanned image volumes included the distal radius and ulna, carpals, metacarpals, and phalanges. For this analysis, only the distal radius, lunate, and scaphoid were analyzed.

The third set of scans included a kinematic scan (four-dimensional (3DCT + time) scans), where the participant performed unconstrained maximum extension to maximum flexion while in the scanner, using a routine wrist scan protocol (80 kV, 125 effective mAs, 0.35 second rotation time, voxel size 0.625 x 0.625 x 1.25 mm).²¹ Participants underwent an initial training session where they were positioned on their stomach with their arm outstretched above their head into the scanner, and they were instructed to perform maximum wrist extension to maximum flexion, at the prescribed speed (listed below). This process rendered a more standardized range of motion amongst our study participants. Reducing our kV to 80 kV reduced radiation exposure and helped to enhance image contrast to differentiate between structures obtained from the images. Continuous data acquisition during the 4DCT scan yields a total of 24 frames per pass of motion (maximum extension to maximum flexion), in approximately eight seconds. This speed was determined through previous analysis to ensure minimal blurring effects.²² The angular speed for flexion to extension and the reverse was estimated at $13 \pm 2^\circ$ degrees/second. The common range of motion for all participants was 40 degrees of extension to 40 degrees of flexion, therefore, this was the range of motion analyzed in this study. The participant and CT technologist were required to wear a lead apron and

neck band to decrease the scatter dose from the scanner to 40 mGy of radiation for the duration of testing.

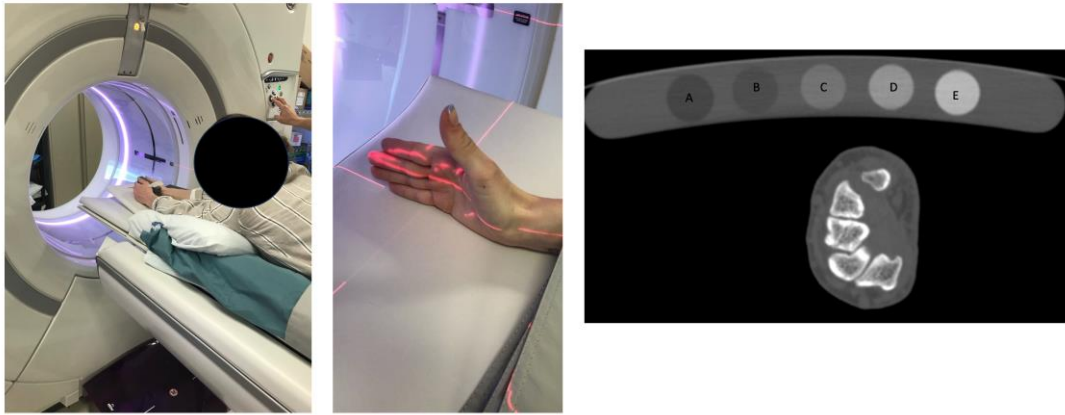


Figure 4-1: Static CT scan accompanied by calibration phantom.

Static CT scan demonstrating hand, wrist, and shoulder position, accompanied by the calibration phantom with rods composed of known material densities embedded in a plastic covering. The densities were calibrated against a liquid dipotassium phosphate (K_2HPO_4) solution. The rod densities range from the lowest (A) to the highest (E) density, to represent equivalent volumetric bone mineral density in the bones of interest.

4.2.2 Quantitative Computed Tomography Analysis

Similar to data analyzed in Chapter 3, the digital imaging and communications in medicine (DICOM) images obtained from the CT scans were reconstructed in 3D and used to create bone models of the distal radius, lunate and scaphoid using Materialize Mimics Software (v. 22, Leuven, Belgium) and 3D Slicer (version 4.11.0, an open-source medical image processing software available at <http://www.slicer.org>). In both software, the global segmentation threshold was manually set to 226 HU, and each slice was manually outlined according to the anatomical geometry of the bone. Previous work within our lab demonstrated the mean error rate in bone models between Mimics and 3D Slicer, and the error rate in our JCA algorithm,²³ was less than or equal to 0.3mm.²⁴ In addition, the inter- and intrarater reliability using Mimics is high, with an error rate of less than or equal to 0.36mm and 0.26mm, respectively.^{19,24} Postprocessing procedures were used to ensure surface smoothness and uniform bone shape in both software, and the resultant image was overlaid on the CT scan to ensure qualitative congruency.

4.2.2.1 Post Processing (Frame Determination)

The motion was analyzed in 10-degree increments from 40 degrees of extension (-40-degrees) to 40 degrees of flexion (Figure 4-2), allowing for a detailed examination of joint motion. The decision to analyze a -40-to-40-degree trajectory despite the ability of some participants to achieve greater range, was to allow a standard, achievable range of motion amongst all participants. As such, nine frames of motion were analyzed to represent the 10-degree increments of motion. The approximate neutral position was determined through alignment of the capitate with the long axis of the radius and subsequent 10-degree increments were identified through examination of the capitate position using ImageJ (open-source image processing program available at <https://imagej.nih.gov/ij/index.html>).^{25,26} 3D models of the radius and capitate were reconstructed in 3DSlicer for both the static and kinematic frames. The static frames were then registered to the position of the kinematic frames using a two-step registration, landmark and ICP.²² Through registration, transformation matrices were obtained and subsequently input into an adapted Matlab code to calculate the helical axis of the

capitate throughout motion.^{27,28} The rotations of the capitate about the helical axis confirmed the 10-degree increments of motion.

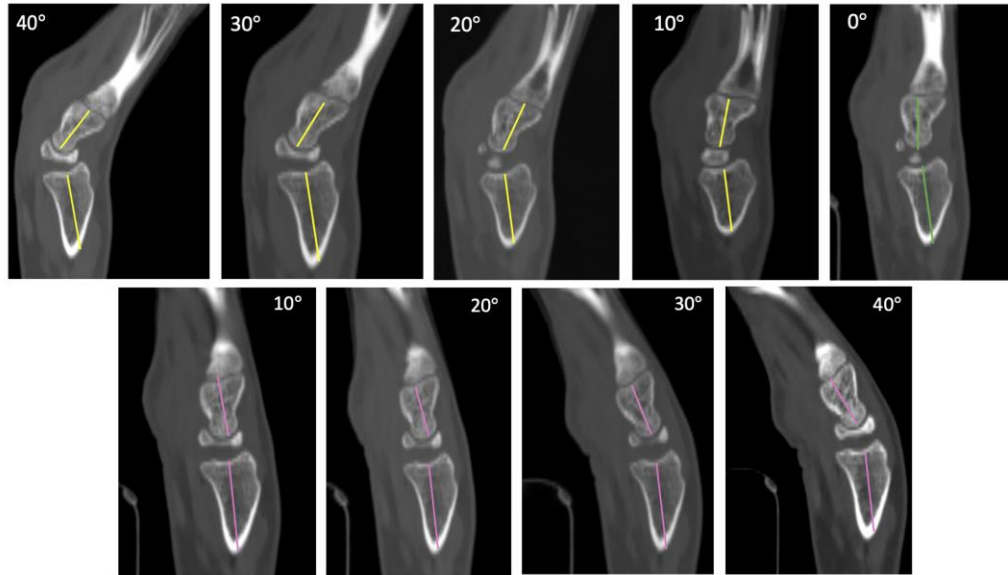


Figure 4-2: Wrist motions analyzed in 10-degree increments.

Angles were determined from a mid-sagittal cross-section, where a line was extended from the central head to central base of the capitate, and the center of the distal radius along the bisection of the shaft of the radius. The neutral position (green line at 0 degrees) was identified first. Extension angles are represented in yellow and flexion angles are represented in purple.

4.2.2.2 Radiocarpal Joint Contact Area

Chapter 3 demonstrated the process for estimating JCA. Briefly, kinematic interbone distances for every 10 degrees of motion (starting at 40 degrees extension) were calculated for the radiolunate (RL) and radioscapoid (RS) joints, using an inter bone proximity of less than or equal to 2.0mm to approximate the entire surface of the radius and its articulations.^{20,23} The resultant image was an iso-contoured proximity map with colors that represent regions of highest and lowest joint contact between articulating bones; a scale of red (0mm) to blue (2.0mm) was chosen, respectively. All regions in dark blue demonstrate that the distance between articulating bones is greater than 2.0mm.

Within the set threshold (0mm to 2.0mm), JCA measures (in mm^2) were obtained to represent the surface area of the contact between articulating bones.

4.2.2.3 Subchondral Volumetric Bone Mineral Density Analysis

All participants underwent static CT scans; however the calibration phantom was used as an accessory for 50% of participant scans. Estimated density is known to vary with CT parameters; CT settings are found to predict calibration terms.²⁹ The CT scanning parameters were the same for all participants and therefore the calibration terms were input based on the averaged rod intensities from the scans that included the calibration phantom. The standard deviation of the averaged rod intensities was calculated as 1.21 HU to 4.7 HU (95% CI 1.1 to 5.2 HU).

To determine subchondral vBMD of the radius, we applied the same depth-specific image-processing technique described in detail in Chapter 3.¹⁹ In brief, circular regions of interest of $\sim 150\text{mm}^2$ were overlaid within each of the reference phantom cylinders. Linear regression equations developed from known material densities within the cylinders of the phantom were applied to convert HU units obtained from the 3D bone model to equivalent vBMD ($\text{mg K}_2\text{HPO}_4/\text{cm}^3$). Articular sites on the distal radius (RL and RS) were then manually outlined using SolidWorks (SolidWorks Education Edition v. 2022) using static joint contact maps as qualitative references.

Average vBMD within three normalized layers from the subchondral surface (0 to 2.5mm, 2.5 to 5mm, and 5 to 7.5mm) were measured for each RL and RS articular surface. Similar to the JCA maps, a scale of red ($1600 \text{ mg K}_2\text{HPO}_4/\text{cm}^3$) to blue ($0 \text{ mg K}_2\text{HPO}_4/\text{cm}^3$) was used to demonstrate the regions of highest and lowest vBMD, respectively.

4.2.3 Statistical Analysis

Descriptive statistics were calculated to describe the sample. To determine the relationship between vBMD and kinematic JCA in the RL and RS, Pearson product-moment correlation coefficients were calculated. Volumetric BMD was the dependent variable, and the independent variable included in the analysis was JCA (mm^2) while in

extension at 40, 30, 20, and 10 degrees of motion, neutral position at 0 degrees, and flexion at 40, 30, 20, and 10 degrees of motion.

Independent variables that contributed significantly to the variance in vBMD were assessed with a regression model. To examine the proportion of explained variance in vBMD measures, a hierarchical regression was used. The independent variables were entered into the model in the following steps: (1) significant correlations (between kinematic JCA and vBMD), (2) sex, and (3) age. The sex and age of the participant was not analyzed using the Pearson product-moment correlation coefficient, as these independent variables are significantly correlated to changes and adaptations in the bone.^{30,31} Changes in adjusted R^2 were noted after each independent variable to determine the association with the additional variables. The significance criterion for all statistical tests was set at $p < 0.05$.

To demonstrate the reliability of obtaining JCA (mm^2), estimates of intrarater reliability were calculated using a two-way mixed effects intraclass correlation coefficient (ICC). The data used for this calculation were from one rater manually segmenting the radius, lunate, and scaphoid from one study participant, followed by the calculation of the interbone distances for the radiolunate (RL) and radioscapoid (RS) joints. A total of five repetitions of this process were performed. Following standard ICC guidelines, an ICC of less than 0.5 indicates poor reliability, 0.5-0.7 indicates moderate reliability, and values between 0.8-0.9 or greater indicate excellent reliability.³²

4.3 Results

The sample was composed of 20 participants; 9 males (mean age 56 ± 24 years; range 22 to 82 years) and 11 females (mean age 42 ± 25 years; range 22 to 80 years). Descriptive statistics demonstrated more JCA and higher vBMD in the RS joint compared to the RL joint for all degrees of motion and all depths from the subchondral surface, respectively. Results from our intrarater reliability analysis for obtaining JCA (mm^2) demonstrated excellent reliability, with an ICC of 0.91 (95% CI 89.41 – 97.21 mm^2).

4.3.1 Correlation Analysis

Significant correlations between vBMD and kinematic JCA were demonstrated in the middle (2.5 to 5mm) and deep (5 to 7.5mm) layers of subchondral bone, however there were no significant correlations in the superficial layer (0 to 2.5mm) of bone. A significant, positive correlation demonstrates a higher JCA is significantly associated with higher vBMD, specifically in the middle (RS joint), and deepest layers (RL and RS joints) from the subchondral surface. Specifically in the RL joint, there were significant, positive correlations between vBMD in region three (5 to 7.5mm) and extension at 40, 30, 20 and 10 degrees ($p < 0.05$), and flexion at 30 and 10 degrees ($p < 0.05$).

In the RS joint, there were significant, positive correlations between vBMD in region two (2.5 to 5mm) and extension at 40, 30, and 10 degrees ($p < 0.05$), and flexion at 30 and 20 degrees ($p < 0.05$). In region three (5 to 7.5mm) of the RS joint, there were significant, positive correlations in extension at 40, 30, and 10 degrees ($p < 0.05$), and flexion at 30 degrees ($p < 0.05$). Table 4-1 demonstrates the complete results from all correlation analyses. Figure 4-3 demonstrates representative data from one male participant's vBMD plots at a depth of 5 to 7.5mm, and the kinematic JCA proximity maps at extension and flexion for every 10 degrees of motion.

Table 4-1: Pearson product-moment correlation (r).

Every 10-degrees of motion from extension to flexion (top), depth of subchondral bone (left) as it relates to articular surface. Significant correlations are represented in bold and with an asterisk.

	Extension				Neutral	Flexion			
	40	30	20	10	0	10	20	30	40
RL									
0 – 2.5	0.20	0.09	0.02	0.09	-0.02	0.16	-0.15	0.10	0.28
2.5 – 5	0.36	0.41	0.37	0.39	0.16	0.38	0.15	0.44	0.39
5 – 7.5	0.54*	0.56*	0.48*	0.53*	0.25	0.51*	0.23	0.55*	0.41
RS									
0 – 2.5	0.25	0.12	0.001	0.24	-0.13	0.04	0.26	0.06	-0.09
2.5 – 5	0.65**	0.61**	0.41	0.57*	0.24	0.36	0.50*	0.50*	0.20
5 – 7.5	0.66**	0.59**	0.42	0.56*	0.25	0.29	0.44	0.46*	0.17

** $p < 0.05$, ** $p < 0.01$*

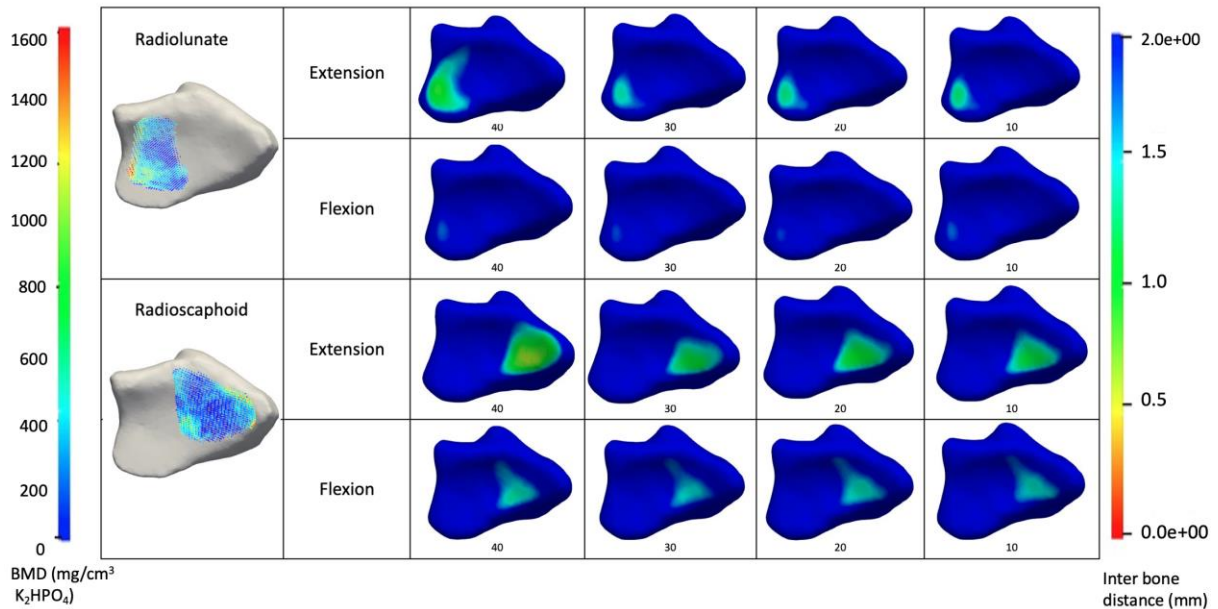


Figure 4-3: Representative figure of healthy male data.

Demonstrates qualitative comparison between subchondral bone at 5 to 7.5 mm from the surface and JCA at every 10 degrees of motion from extension to flexion. The scale on the left is representative of vBMD (mg/cm^3 K_2PHO_4), where blue is indicative of a low BMD and red is indicative of a high BMD. The scale on the right represents inter bone distance (mm), where dark blue represents no joint contact and red represents the highest joint contact.

4.3.2 Regression Analysis

Table 4-2 demonstrates the hierarchical regression analyses conducted in this study. The hierarchical regression demonstrated no statistically significant variance in vBMD in region three (5 to 7.5mm) of the RL joint, for any of the models included in the analysis. In the RS joint, 38% of the variance in vBMD in the middle layer (2.5 to 5mm) can be explained by JCA in extension at 40, 30, and 10 degrees, and flexion at 30 and 20 degrees of motion ($p = 0.04$). Sex contributed an additional 13% of variance, and when combined with the significant degrees of motion, 51% of the variance in vBMD can be explained ($R^2 = 0.67$, adjusted $R^2 = 0.51$, $F = 4.11$, $p = 0.02$). Age did not contribute to the variance. In region three (5 to 7.5mm) of the RS joint, 33% of the variance can be explained by JCA in extension at 40, 30 and 10 degrees, and flexion at 30 degrees of motion ($p = 0.04$). Sex contributed an additional 7% of the variance, and when combined with the significant degrees of motion, explained 40% of the variance in vBMD ($R^2 = 0.57$, adjusted $R^2 = 0.40$, $F = 3.43$, $p = 0.03$). Age did not contribute to the variance.

Table 4-2: Model summary for the hierarchical regression analysis, with subchondral bone region as the dependent variable.

RL 5 – 7.5 mm				
Model	R ²	Adjusted R ²	F	P
1	0.36	0.05	1.15	0.40
2	0.58	0.31	2.12	0.13
3	0.60	0.28	1.87	0.17
RS 2.5 – 5mm				
Model	R ²	Adjusted R ²	F	P
1	0.55	0.38	3.22	0.04*
2	0.67	0.51	4.11	0.02*
3	0.67	0.47	3.23	0.04*
RS 5 – 7.5mm				
Model	R ²	Adjusted R ²	F	P
1	0.48	0.33	3.25	0.04*
2	0.57	0.40	3.43	0.03*
3	0.57	0.36	2.70	0.07

Note: R² = proportion of variance in the dependent variable explained by the independent variable(s); adjusted R² = adjusted proportion of variance to account for multiple independent variables; F statistic = tests overall fit of regression model for the data; P = significance of the correlation at 0.05.

* $p < 0.05$

Model 1: Constant, significant correlations

Model 2: Constant, significant correlations, sex

Model 3: Constant, significant correlations, sex, age

4.4 Discussion

The purpose of Chapter 4 was to investigate the relationship between depth-specific vBMD and kinematic JCA in the wrists of healthy adults, to better understand how joint contact impacts the underlying bone. The correlation analysis successfully demonstrated that a large JCA was significantly correlated to higher vBMD, specifically in the middle and deeper layers of subchondral bone during wrist extension, supporting our hypothesis. The regression analysis demonstrated that in the RS joint specifically, variance in the middle and deep layers of bone can be explained by varying degrees of kinematic JCA and the sex of the participant.

Previous research at the elbow,²³ demonstrated that JCA in a loaded versus unloaded condition was not significantly different, concluding that JCA was similar in both testing conditions. Compared to joints such as the elbow where resting state joint contact is minimal,²³ JCA in the wrist is always present. In the wrist, the distal radius and carpal bones are always in contact due to the physiological nature of the joint.³³ This is also evident in the results demonstrated in Chapter 3, where we reported on JCA in a static, neutral positioned wrist.¹⁹ Wrist extension is the position the wrist is most loaded during activities of daily living, where previous research has demonstrated that during dynamic wrist loading (for example, a pushup), an average of 70% body weight is loaded on the upper extremity.³⁴ Findings from this study further indicated that forces were found to travel mainly through the radiocarpal joints (namely, the RS joint), in the wrist. Similarly, our results indicated that wrist extension was significantly correlated to subchondral vBMD in the RS joint specifically. It can therefore be assumed that JCA can be linked with joint loading in the wrist, wherein our study demonstrated that the underlying bone in our healthy population was highest where JCA was largest, namely in the deeper regions of bone. This further demonstrates Wolff's law in the wrist, highlighting that the wrist may serve to bear load similar to the knee and hip despite different loading patterns. We can conclude that subchondral bone changes are therefore influenced by wrist position in a healthy cohort.

Our methodology allowed us to differentiate between the RL and RS, an important implication as differences in contact area and loading patterns between these regions

exists.^{19,35} The RS joint is the main site of force transmission in the wrist when compared to the RL joint.³⁵ Specifically, Majima and colleagues demonstrated that in a neutral wrist position, the force transmission ratio (described as the amount of force within each fossa (RL and RS), relative to the total amount of force through the radiocarpal joint), was 52% in the RS joint and 42% in the RL joint. During extension, the force transmission ratio increased from 52% to 62% in the RS joint and decreased from 42% to 36% in the RL joint.³³ Our results demonstrated a larger number of statistically significant correlations in the RS joint, indicating that an increased JCA in the RS joint was significantly correlated to a larger vBMD in comparison to the RL joint. This may be due to the concentration of forces at the scaphoid that occurs during wrist extension.^{33,34} These results further highlight the influence of wrist position and load on subchondral bone changes.

Our hierarchical regression analysis demonstrated that sex impacted the variance in the relationship between kinematic JCA and vBMD. Previous research has demonstrated that sex contributes to the differences in subchondral BMD, wherein biological females generally have lower overall subchondral BMD when compared to their biological male counterparts.^{30,31,36} Our research is an extension of this finding, highlighting that sex contributed to the variance in the relationship between vBMD and kinematic JCA. We are limited in our ability to conclude the clinical implications of this finding; however subsequent work will use the sex of the participant as a moderator variable to determine the magnitude to which sex impacts this relationship clinically. Interestingly, age did not impact the variance in the relationship between kinematic JCA and vBMD. Previous literature has demonstrated that age-related changes to bone are specific to the cortical bone region, namely the first region of bone in our analysis. As our regression was specific to the deep regions of bone mainly composed of trabecular bone, this could be why age did not have an independent effect on subchondral bone variations. With age, bone turnover rate slows down, and the bones do not rebuild themselves at a comparable rate to a younger population. However, the older participants in our study did not sustain traumatic injuries or adjacent diseases that would cause the bones to adapt, likely maintaining a normal bone turnover rate throughout their lifespan. The absence of pathological changes to the joint that would cause the bone to adapt to the new load may therefore explain why age did not play a role in the variance. Since OA is highly

prevalent in an older population, these results are foundational for future work in a patient population with OA, to better understand the differences in a normal aging joint versus a joint undergoing osteoarthritic change.

As discussed in Chapter 1 and Chapter 3, the deep regions of bone that consist primarily of trabecular bone are adaptive to change and metabolically active. This was supported in our study wherein the regions deepest from the subchondral surface (2.5 to 7.0mm) were significantly correlated to JCA; a higher vBMD was correlated to a larger JCA. Our results are further supported by previous work in the knee,¹¹⁻¹⁴ and it is therefore logical to believe that subchondral bone is impacted following pathological changes to the wrist, for example OA. Establishing this relationship in the wrist serves as a strong foundation wherein more rigorous analysis in the depth-specific regions of the joint may highlight adaptive changes to the structure of the bone that precede typical arthritic patterns in the wrist, similar to what was found in the knee. Establishing the significance of this relationship is paramount to future OA research, wherein malalignment and altered joint loading following traumatic injuries could result in acute changes in vBMD, preceding the degeneration of articular cartilage seen through traditional radiographs. More rigorous analysis of deeper structures may aid in early detection of post-traumatic OA and may facilitate greater efforts to rehabilitate the joint soon after injury to prevent or decrease its progression and degenerative nature within the joint.

4.5 Limitations

Using averaged rod intensities risks inputting inaccurate data into the linear regression equation that converts HU values into equivalent vBMD. However, previous research demonstrated that CT settings play the largest role in calibrating the phantom, therefore highlighting the importance of consistent CT settings for all consecutive scans.²⁹ Since all participants underwent CT scanning under the same conditions and settings, using the averaged rod intensities is warranted. The manual segmentation of the articular surfaces within our methodology introduces potential reliability error, as the segmented articular surface is used to obtain vBMD. However, our previous intrarater reliability analysis for obtaining vBMD demonstrated excellent reliability, with an ICC of 0.99.¹⁹ In addition, manually verifying neutral position through alignment of the capitate with the long axis

of the radius introduces potential reliability error. Despite automated techniques for identifying neutral position,³⁷ the initial training session reduced the risk of variable motion, and the manual identification of position neutral was to verify our alignment. Our analysis was also limited to bone and did not include evaluation of soft tissues. Therefore, the contribution of cartilage thickness and soft-tissue interactions could not be included in this analysis. Lastly, our analysis was limited to a -40-to-40-degree trajectory of extension to flexion, yielding a 37% dose efficiency by analyzing 9 out of a possible 24 frames of motion. However, to sufficiently compare our data, this was the achievable range of motion among all participants.

4.6 Conclusion

Our results demonstrate correlation between kinematic JCA and depth-specific subchondral vBMD in the wrists of healthy adults. This relationship is important to characterize in a healthy population to provide baseline data that can be compared to populations that experience bone remodeling following injury or disease, such as OA. This methodology allows us to analyze deeper regions of the bone that adapt to forces and loads acting on it, and therefore enable us to detect acute changes in the bone that may be indicative of the development of OA within 5 – 10 years following injury. Historically, anatomical malalignment does not indicate poor prognosis. Therefore, when coupled with changes to depth-specific layers of subchondral bone, this relationship demonstrates a more robust examination of acute changes following wrist trauma, and potentially early signs of OA therein. The next steps with this work are to characterize the relationship between our imaging-based biomarkers in a clinical cohort of participants undergoing pathological change, and how these correlate to clinical symptoms as measured using pain evaluation techniques.

4.7 References

1. Chiarotto A, Fernandez-de-Las-Penas C, Castaldo M, Villafane JH. Bilateral pressure pain hypersensitivity over the hand as potential sign of sensitization mechanisms in individuals with thumb carpometacarpal osteoarthritis. *Pain Med.* 2013;14(10):1585-1592. doi:<https://dx.doi.org/10.1111/pme.12179>
2. Fontana L, Neel S, Claise JM, Ughetto S, Catilina P. Osteoarthritis of the Thumb Carpometacarpal Joint in Women and Occupational Risk Factors: A Case-Control Study. *Journal of Hand Surgery.* 2007;32(4):459-465. doi:10.1016/j.jhsa.2007.01.014
3. Linde KN, Puhakka KB, Langdahl BL, et al. Bone Mineral Density is Lower in Patients with Severe Knee Osteoarthritis and Attrition. *Calcif Tissue Int.* 2017;101(6):593-601. doi:10.1007/s00223-017-0315-y
4. Schreiber JJ, McQuillan TJ, Halilaj E, et al. Changes in Local Bone Density in Early Thumb Carpometacarpal Joint Osteoarthritis. *Journal of Hand Surgery.* 2018;43(1):33-38. doi:10.1016/j.jhsa.2017.09.004
5. Grewal R, MacDermid JC. The Risk of Adverse Outcomes in Extra-Articular Distal Radius Fractures Is Increased With Malalignment in Patients of All Ages but Mitigated in Older Patients. *Journal of Hand Surgery.* 2007;32(7):962-970. doi:10.1016/j.jhsa.2007.05.009
6. Lalone EA, MacDermid J, King G, Grewal R. The Effect of Distal Radius Fractures on 3-Dimensional Joint Congruency. *Journal of Hand Surgery.* 2021;46(1):66.e1-66.e10. doi:10.1016/j.jhsa.2020.05.027
7. Laulan J, Marteau E, Bacle G. Wrist osteoarthritis. *Orthopaedics and Traumatology: Surgery and Research.* 2015;101(1):S1-S9. doi:10.1016/j.otsr.2014.06.025

8. Madry H, van Dijk CN, Mueller-Gerbl M. The basic science of the subchondral bone. *Knee Surgery, Sports Traumatology, Arthroscopy*. 2010;18(4):419-433. doi:10.1007/s00167-010-1054-z
9. Lalone E, MacDermid J, Grewal R, King G. Patient Reported Pain and Disability Following a Distal Radius Fracture: A Prospective Study. *Open Orthop J*. 2017;11(1):589-599. doi:10.2174/1874325001711010589
10. Roiger D, Bullock N. *Anatomy, Physiology, & Disease*. Third Edition. McGraw Hill LLC; 2023.
11. Burnett WD, Kontulainen SA, McLennan CE, Hunter DJ, Wilson DR, Johnston JD. Regional depth-specific subchondral bone density measures in osteoarthritic and normal patellae: In vivo precision and preliminary comparisons. *Osteoporosis International*. 2014;25(3):1107-1114. doi:10.1007/s00198-013-2568-2
12. Burnett W, Kontulainen S, McLennan C, et al. Patella bone density is lower in knee osteoarthritis patients experiencing moderate-to-severe pain at rest. *Journal of Musculoskeletal Neuronal Interactions*. 2016;16(1):33-39. Accessed July 15, 2021. /pmc/articles/PMC5089452/
13. Kroker A, Zhu Y, Manske SL, Barber R, Mohtadi N, Boyd SK. Quantitative in vivo assessment of bone microarchitecture in the human knee using HR-pQCT. *Bone*. 2017;97:43-48. doi:10.1016/j.bone.2016.12.015
14. Kroker A, Besler BA, Bhatla JL, et al. Longitudinal Effects of Acute Anterior Cruciate Ligament Tears on Peri-Articular Bone in Human Knees Within the First Year of Injury. *Journal of Orthopaedic Research*. 2019;37(11):2325-2336. doi:10.1002/jor.24410
15. Brand RA. Biographical sketch: julius wolff, 1836-1902. *Clin Orthop Relat Res*. 2010;468(4):1047-1049. doi:10.1007/s11999-010-1258-z
16. Wolff J. The Classic: On the Theory of Fracture Healing. *Clin Orthop Relat Res*. 2010;468(4):1052-1055. doi:10.1007/s11999-010-1240-9

17. Sampath SA, Lewis S, Fosco M, Tigani D. Trabecular orientation in the human femur and tibia and the relationship with lower-limb alignment for patients with osteoarthritis of the knee. *J Biomech*. 2015;48(6):1214-1218. doi:10.1016/j.jbiomech.2015.01.028
18. Zhou GQ, Pang ZH, Chen QQ, et al. Reconstruction of the biomechanical transfer path of femoral head necrosis: A subject-specific finite element investigation. *Comput Biol Med*. 2014;52:96-101. doi:10.1016/j.combiomed.2014.04.002
19. Straatman L, Knowles N, Suh N, Walton D, Lalone E. The Utility of Quantitative Computed Tomography to Detect Differences in Subchondral Bone Mineral Density Between Healthy People and People With Pain Following Wrist Trauma. *J Biomech Eng*. 2022;144(8). doi:10.1115/1.4053594
20. Crisco JJ, Moore DC, Marai GE, et al. Effects of distal radius malunion on distal radioulnar joint mechanics - An in vivo study. *Journal of Orthopaedic Research*. 2007;25(4):547-555. doi:10.1002/jor.20322
21. Zhao K, Breighner R, Holmes D, Leng S, McCollough C, An KN. A technique for quantifying wrist motion using four-dimensional computed tomography: Approach and validation. *J Biomech Eng*. 2015;137(7). doi:10.1115/1.4030405
22. Robinson SM. 4DCT to Examine Carpal Motion. *Electronic Thesis and Dissertation Repository*. Accessed September 27, 2021. <https://ir.lib.uwo.ca/etd://ir.lib.uwo.ca/etd/7801>
23. Lalone EA, McDonald CP, Ferreira LM, Peters TM, King GW, Johnson JA. Development of an image-based technique to examine joint congruency at the elbow. *Comput Methods Biomech Biomed Engin*. 2013;16(3):280-290. doi:10.1080/10255842.2011.617006
24. Robinson S, Straatman L, Lee TY, Suh N, Lalone E. Evaluation of four-dimensional computed tomography as a technique for quantifying carpal motion. *J Biomech Eng*. 2021;143(6). doi:10.1115/1.4050129
25. Neu CP, Crisco JJ, Wolfe SW. In vivo kinematic behavior of the radio-capitate joint during wrist flexion–extension and radio-ulnar deviation. *J Biomech*. 2001;34(11):1429-1438. doi:10.1016/S0021-9290(01)00117-8

26. Patterson RM, Nicodemus CL, Viegas SF, Elder KW, Rosenblatt J. High-speed, three-dimensional kinematic analysis of the normal wrist. *J Hand Surg Am.* 1998;23(3):446-453. doi:10.1016/S0363-5023(05)80462-9
27. Kettler A, Marin F, Sattelmayer G, et al. Finite helical axes of motion are a useful tool to describe the three-dimensional in vitro kinematics of the intact, injured and stabilised spine. *European Spine Journal.* 2004;13(6):553-559. doi:10.1007/S00586-004-0710-8/FIGURES/5
28. Wolfe SW, Neu C, Crisco JJ. In vivo scaphoid, lunate, and capitate kinematics in flexion and in extension. *J Hand Surg Am.* 2000;25(5):860-869. doi:10.1053/JHSU.2000.9423
29. Reeves JM, Knowles NK, Athwal GS, Johnson JA. Methods for post Hoc quantitative computed tomography bone density calibration: Phantom-only and regression. *J Biomech Eng.* 2018;140(9). doi:10.1115/1.4040122
30. Khosla S, Riggs L, Atkinson EJ, et al. Effects of Sex and Age on Bone Microstructure at the Ultradistal Radius: A Population-Based Noninvasive In Vivo Assessment. *J Bone Miner Res.* 2006;21:124-131. doi:10.1359/JBMR.050916
31. Riggs L, Melton LJ, Robb RA, et al. Population-Based Study of Age and Sex Differences in Bone Volumetric Density, Size, Geometry, and Structure at Different Skeletal Sites. *J Bone Miner Res.* 2004;19:1945-1954. doi:10.1359/JBMR.040916
32. Koo TK, Li MY. A Guideline of Selecting and Reporting Intraclass Correlation Coefficients for Reliability Research. *J Chiropr Med.* 2016;15(2):155-163. doi:10.1016/j.jcm.2016.02.012
33. Majima M, Horii E, Matsuki H, Hirata H, Genda E. Load Transmission Through the Wrist in the Extended Position. *J Hand Surg Am.* 2008;33(2):182-188. doi:10.1016/J.JHSA.2007.10.018
34. Polovinets O, Wolf A, Therapy RWJ of H, 2018 undefined. Force transmission through the wrist during performance of push-ups on a hyperextended and a neutral wrist. *Elsevier.* Accessed June 26, 2023.
https://www.sciencedirect.com/science/article/pii/S0894113017301217?casa_token=EkigNSXfBW8AAAAA:BUuYcJUNlzQYxHpaUxm3PW9SWH_VeSG7_IM-Mm0CVE1XsnAjH9cuSvyIOBLMvjcdAH62NRAwiRY

35. Hoogbergen MM, Schots JMP, Niessen WJ, Schuurman AH, Spauwen PHM, Kauer JMG. Subchondral bone mineral density patterns representing the loading history of the wrist joint after a proximal row carpectomy. *Eur J Plast Surg*. 2008;31(3):101-107. doi:10.1007/s00238-008-0230-6
36. Shanbhogue V V, Brixen K, Hansen S. Age- and Sex-Related Changes in Bone Microarchitecture and Estimated Strength: A Three-Year Prospective Study Using HRpQCT. *Journal of Bone and Mineral Research*. 2016;31(8):1541-1549. doi:10.1002/jbmr.2817
37. Dobbe JGG, De Roo MGA, Visschers JC, Strackee SD, Streekstra GJ. Evaluation of a Quantitative Method for Carpal Motion Analysis Using Clinical 3-D and 4-D CT Protocols. *IEEE Trans Med Imaging*. 2019;38(4):1048-1057. doi:10.1109/TMI.2018.2877503

Chapter 5

5 Understanding Structural and Clinical Disease Severity in thumb CMC OA: A Preliminary Analysis Combining Image-Based Biomarkers and Pain Evaluation Techniques.

OVERVIEW

Understanding the mechanisms underlying pain in thumb CMC OA is crucial towards targeting affected individuals with appropriate therapy and treatment strategies aimed to mitigate symptoms of pain. We will consider structural changes that occur with OA that may be linked with pain, to better understand potential mechanisms underlying chronic pain in thumb CMC OA. In addition, we will explore a variety of potential pain phenotypes associated with thumb CMC OA, to provide more insight into appropriate treatment strategies targeting pain symptoms. No therapies have been able to halt or reverse the progression of OA. It's important to apply therapies at the early stages of the disease prior to major structural or functional damage in the joint, however without a deep understanding of the role each tissue plays in the structural and clinical progression of OA, the therapeutic interventions cannot target biomarkers responsible. The discrepancy between OA progression and pain presentation is a major player in the complexity of curating patient-specific treatment strategies for OA.

5.1 Introduction

Introduced in Chapter 1 and Chapter 4, osteoarthritis (OA) is the most common musculoskeletal (MSK) condition worldwide, and the leading cause of chronic pain in Canada, accounting for approximately three times the proportion of individuals with other chronic conditions.^{1,2} Chapter 1 introduced thumb carpometacarpal (CMC) OA as a major cause of functional morbidity, associated with pain at the base of the thumb, and a disease that disproportionately affects post-menopausal women.²⁻⁵ Specifically, females have 30% higher odds of developing radiographic thumb CMC OA than males.² Structural progression of thumb CMC OA is characterized by pathological changes in joint tissues, namely the degeneration of articular cartilage, subchondral bone alterations, osteophyte growth, and inflammation within the joint capsule.^{1-3,6,7} However, there is a discrepancy between structural thumb CMC OA progression and its relationship to pain. It is widely recognized that there is poor concordance between structural disease severity and symptoms of pain.⁸⁻¹⁰ Although pain is often the dominant and defining symptom of thumb CMC OA, and often the driving force behind seeking care, the mechanisms underlying thumb CMC OA pain are unclear.

To date, patients with thumb CMC OA represent a cohort of people with upper extremity arthritis likely to undergo surgery.¹¹ However, the effectiveness of surgery for improving hand function and reducing pain is highly variable, with an adverse event rate of chronic-pain related conditions between 10% and 22%.^{11,12} OA pain is heterogenous, spanning a multitude of potential etiologies, including social, environmental, physical, and biological factors that may impact the patients pain experience. The experience of pain is neither uniform across patients nor during the structural progression of the disease.¹ Efforts to understand mechanisms underlying OA-related pain predominately in the knee have been made, demonstrating that knee OA-related pain is associated with structural factors including subchondral bone (bone marrow lesions (BMLs)), synovitis, and effusion.^{1,13-15} However, mechanisms underlying thumb CMC OA pain are less clear.

Identifying different domains of OA pain is an important component of directing the course of treatment and therapy, as pain domains differ in presentation and manifestation. For example, nociceptive pain is characterized as pain arising from an external stimulus, activating the pain receptors in the periphery that are capable of processing noxious- or potentially noxious-level

stimuli of mechanical, thermal, or chemical nature.¹⁶ On the other hand, pain of primarily neuropathic origin is characterized as damage directly to sensory nerves, resulting in varying sensations such as burning, stabbing, or tingling.^{1,2} Peripheral and central sensitization represent an increased response to nociception, either at the level of the periphery or the central nervous system, respectively.^{13,16} Nociceptive and neuropathic pain are distinct pain domains that have been associated with knee OA,^{13-15,17} while peripheral and central sensitization are distinct pain domains that have been associated with knee and thumb CMC OA.³⁻⁵ Specific to thumb CMC OA, Chiarotto and colleagues demonstrated the complex interplay between sensory and cognitive processes in thumb CMC OA, identifying a bilateral hypersensitivity to pain, suggesting peripheral sensitization.³ This work was performed on people with symptomatic thumb CMC OA. However, how this relates to the structural progression of thumb CMC OA has not yet been studied.

Introduced in Chapters 1, 3, and 4, subchondral bone has been the subject of recent MSK pain research due to its rich blood and nerve supply,⁵⁻⁹ highlighting its potential to provide pertinent information on pain mechanisms. Specifically, subchondral bone is innervated by high-threshold afferent nociceptors capable of transducing noxious level stimuli. Mechanical alterations in the joint are sensed by the afferent nociceptors, thereby serving as a potential mechanism in pain perception.¹⁶ Chapter 3 demonstrated the use of quantitative computed tomography (QCT) in detecting depth-, joint-, and subject-specific differences in subchondral bone between healthy people and people with previous wrist trauma.¹⁰ Following this work, Chapter 4 demonstrated that joint contact area and volumetric bone mineral density (vBMD) are correlated in the wrists of healthy adults, demonstrating that a large joint contact area (JCA) was significantly associated with a higher vBMD, specifically in wrist positions that are most commonly loaded during activities of daily living. However, subchondral bone research has been limited to providing insight into early morphological changes that may be associated with structural OA initiation and progression, highlighting the need for analysis on the relationship between subchondral bone and clinical severity (pain) of OA.

Using exploratory methods, the purpose of this study is to explore pain mechanisms in thumb CMC OA using our imaging-based biomarkers and clinical pain evaluation techniques, and to explore pain phenotypes among patients with thumb CMC OA. Using our imaging-based

biomarkers, we propose to differentiate between potential pain phenotypes within our thumb CMC OA cohort. We suspect that our imaging-based biomarkers will provide pertinent information on clinical disease severity longitudinally.

5.2 Methods

5.2.1 Participants

This was an exploratory, cross-sectional analysis on data that are part of a larger longitudinal study. Our study included two cohorts: a cohort of healthy adults, and a cohort of adults with varying stages of thumb CMC OA.

Healthy cohort: Our healthy participants were recruited via newspaper advertisements and word of mouth. Inclusion criteria were as follows: 18 years of age or older, able to speak conversational English, no previous history of hand or wrist trauma, and sufficient shoulder mobility that allowed their arm to be outstretched while lying in a prone position.

Clinical cohort: Patients presenting with pain at the base of their thumb or with previously diagnosed thumb CMC OA were recruited from the Roth|McFarlane Hand and Upper Limb clinic in Ontario Canada. Inclusion criteria were as follows: 18 years of age or older, able to speak conversational English, sufficient shoulder mobility that allowed their arm to be outstretched while lying in a prone position, and pain at the base of the thumb. Based on radiographic indicators using the Eaton-Littler grading, patients were diagnosed with CMC OA by a fellowship-trained hand surgeon (AK). Patients who were scheduled to receive or had already received a corticosteroid injection within a three-month period were eligible to participate only after the three-month drug activation period.

The protocol was approved by the institutional ethics review board at Western University (REB# 121960), and all patients provided written and informed consent before baseline participation.

5.2.2 Study Protocol

Following recruitment, all participants underwent a series of static CT scans (Revolution CT Scanner, GE Healthcare, Waukesha, WI) of their distal forearm and hand. The first was a static localizer scan to determine the wrist location in space, followed by a static neutral scan of

participants bilateral thumbs. The static scan was acquired in a neutral position using a routine wrist scanning protocol (120 kVp, 125 effective mAs, 0.35 s rotation time, and helical pitch of 1, voxel size 0.625 x 0.625 x 0.625 mm).¹¹ The static CT scanning parameters were the same for all participants and have been published previously.¹⁰ Briefly, a calibration phantom (model three calibration phantom, Mindways Software, Austin, TX)(**Appendix C**) with known material densities was used as an accessory to the static CT scan, placed underneath the distal forearm and hand. The phantom was calibrated against a liquid dipotassium phosphate solution (K_2HPO_4) using the CT scanning parameters mentioned previous. The phantom was used to transform grayscale Hounsfield Units (HU) into equivalent vBMD ($mg K_2HPO_4/cm^3$). For this analysis, scanned image volumes of the first metacarpal (MC1), trapezium (TPM), and the 3rd MC (MC3) were used.

Participants then filled out pain specific patient-reported outcome measures (PROM). Both study cohorts completed the Patient-Rated Wrist Evaluation (PRWE), while the thumb CMC OA cohort also completed the Multidimensional Symptom Index (MSI), the Short-Form Leeds Assessment for Neuropathic Signs and Symptoms (S-LANSS), and underwent pressure pain detection threshold (PPDT) testing. All PROMs are described in detail in Chapter 1 (section 1.41) and included in the appendices of this thesis. PPDT was used to measure pain sensitivity in deep somatic structures following a standardized protocol.^{18,19} In brief, a digital algometer (Commander Echo, JTECH Medical, Midvale, UT) with a 1cm² round rubber tip was applied bilaterally at the base of the thumb, and the tibialis anterior muscle belly of the dominant leg for all participants. The algometer was calibrated before use and found to have a linear response to force application between 0 to 13 kilogram-force (kgf). The rater was trained to apply force at a rate of 0.5 kgf/s. Following standardized instructions, participants were asked to verbally indicate when the sensation changed to an uncomfortable pressure. The algometer was then removed and PPDT was recorded as the maximum pressure applied before cessation. Three measurements were taken at each site, and PPDT was reported as the average threshold at each anatomical site.

The Eaton-Littler grading (EL-grade) was based on the grading definitions outlined by Eaton and Glickel.^{7,20} This classification system describes the four stages of thumb CMC OA arthritis. Stage I shows subtle CMC joint space widening, likely attributed to synovitis, effusion, or laxity

of the surrounding ligamentous structure. Stage II shows mild CMC joint space narrowing, sclerosis, and cystic changes with the presence of osteophytes smaller than 2mm in diameter. Stage III shows moderate to severe CMC joint space narrowing, sclerosis, and cystic changes with the presence of osteophytes larger than 2mm in diameter. Stage IV includes all aspects of stage III but extends to scaphotrapezial arthritis.

5.2.3 Quantitative CT Analysis

The QCT protocol used in this study is the same as the protocol demonstrated in Chapter 3, section 3.2, and Chapter 4, section 4.2. Briefly, the DICOM images obtained from the CT scans were reconstructed into 3D images and used to create bone models of the first metacarpal (MC1), the trapezium (TPM), and the third metacarpal (MC3) using Materialize Mimics Software (v.26. Leuven, Belgium) and 3D Slicer (version 4.11.0, an open-source medical image processing software available at <http://www.slicer.org>). The global segmentation threshold was manually set to 226 HU in both software, and each slice was manually segmented according to the anatomical geometry of the bone. The mean error rate between Mimics and 3D Slicer, and the error rate in our JCA algorithm was less than or equal to 0.3mm,^{21,22} and the inter- and intra-rater reliability using Mimics demonstrated an error rate less than or equal to 0.36mm and 0.26mm, respectively.^{21,23} Post processing procedures were used to ensure surface smoothness and uniform bone shape in both software.

5.2.3.1 Carpometacarpal Joint Contact Area

To estimate JCA, a similar protocol to the one listed in Chapter 3 section 3.2 and Chapter 4 section 4.2 was used.²² Static inter bone distances (a CT-derived measure of joint contact) were calculated for the thumb CMC joint. Briefly, an inter bone distance of less than or equal to 2.0mm was used to approximate the entire surface of the thumb CMC joint.²⁴ The resultant image was an iso-contoured distance map with colors representing regions of high and low joint contact – a scale of red (0mm) to dark blue (2.0mm) was chosen, respectively. Within this set threshold, JCA (in mm²) was obtained to represent the surface area of the contact between the MC1 and TPM. Given the potential for variability within our JCA (mm²), intrarater reliability has been calculated previously to demonstrate the reliability of obtaining JCA (mm²),

demonstrating an intraclass correlation coefficient (ICC) of 0.91 (95% CI 89.41 to 97.21 mm²) using a two-way mixed effects model.²⁵

5.2.3.2 Subchondral Volumetric Bone Mineral Density

To determine subchondral vBMD of the MC1, TPM, and MC3, we applied a variation of a depth-specific image-processing technique described in detail in Chapter 3.²³ In brief, ~150mm² circular regions of interest were overlaid within each of the reference phantom cylinders. Linear regression equations developed from known material densities within the cylinders of the phantom were applied to convert HU units obtained from the 3D bone models into equivalent vBMD (mg K₂HPO₄/cm³). The articular site on the MC1, TPM, and MC3 were then manually outlined using SolidWorks (SolidWorks Education Edition v. 2022), using static joint contact maps as a qualitative reference.

Due to the difference in bone composition between long and short bones (Chapter 1 section 1.2.1), average vBMD of the MC1 and MC3 were analyzed in three normalized layers of 2.5mm slice thickness (0 to 2.5mm, 2.5 to 5mm, and 5 to 7.5mm), while vBMD of the TPM was analyzed in five normalized layers of 1.25mm thickness (0 to 1.25mm, 1.25 to 2.5mm, 2.5 to 3.75mm, 3.75 to 5mm, and 5 to 6.25mm). Similar to the JCA iso-contoured color maps, a scale of red (1600 mg K₂HPO₄/cm³) to blue (0 mg K₂HPO₄/cm³) was used to demonstrate the regions of highest and lowest vBMD, respectively.

5.2.4 Patient-Reported Outcome Measure Analysis

The PRWE is a 15-item patient-reported outcome measure specific to wrist pain and functional disability.²⁶ It contains two subscales that address pain and function associated with the hand and wrist: the pain subscale is composed of five items covering the severity, intensity, and frequency of pain during the preceding two weeks, and the function subscale is composed of 10 items which are further divided into specific and usual activities, addressing the difficulty with each activity. The scoring of the PRWE is a simple sum of the two subscales, with a total possible score out of 100 where higher scores represent more pain and functional disability.²⁶ The PRWE will be used to characterize clinical severity within our study.

A study-specific body diagram was used to collect the distribution of pain symptoms. Participants were instructed to shade (color) the areas of the body they are experiencing pain, circle the areas in which they feel tingling, pricking, or burning sensations, and finally to place an “N” near the areas where they are feeling numbness, heaviness, or other sensations. The results from the body diagram are characterized as symptom distribution. As such, we dichotomized pain distribution into localized versus widespread pain, where localized pain is characterized as pain below the elbow of the affected hand(s), and widespread pain is characterized as pain that extends beyond the elbow of the affected hand(s). Tingling and numbness were dichotomized as present or absent, representing any tingling, pricking, burning, or numbness that is widespread or localized.

The Multidimensional Symptom Index (MSI) is a 10-item self-report tool that provides an indication of total number of symptoms experience, the mean frequency of those experiences, and the mean interference of those.²⁷ Two summary scores can be extracted, ‘Somatic Symptoms’ (*sharp pain, dull ache, weakness or giving way, stiffness of restricted movement, and numbness or pins and needles* symptoms), and ‘Non-Somatic Symptoms’ or ‘Central’ subscale (*sensitivity to light, noise, odor or temperature, fatigue, fogginess, poor appetite or nausea, nervousness, anxiety, or sadness, and numbness or pins and needles*). Scores are presented as a percentage of maximum possible score with higher values indicating greater problems. As there is no specified cut score for the MSI, based on previous literature using similar somatic symptom²⁸ or central symptom²⁹ scales, a percent score of 40% on either scale was considered a high likelihood of presenting with somatic or central pain symptoms. A percent score less than 40% was therefore considered low.

The self-report version of the Leeds Assessment of Neuropathic Signs and Symptoms (S-LANSS) is seven-items long with a binary response (a simple yes or no), to the presence of symptoms (five items) or clinical signs (two items) of neuropathic pain.³⁰ Each item is given a score, where “no” represents 0 and “yes” represents scores ranging from one to five depending on the symptom. A total score greater than 12 has been previously endorsed as indicating pain of primarily neuropathic origin. As such, we classified S-LANSS scores as low (<6.0), moderate (7.0 to 11.0), and high (>12.0) likelihood of a neuropathic pain component.

Pressure Pain Detection Threshold (PPDT) was collected through digital algometry over the locally-painful site (base of the thumb, bilaterally) and over an anatomically-distinct region (muscle belly of tibialis anterior) as a comparator site. Interpretation of PPDT scores (kgf) are based on available normative values. Specifically, PPDT scores (kgf) in the affected and unaffected hands of females and males, were classified as low (<2.0 kgf (females) or <3.0 kgf (males)), moderate (2.1 to 4.0 kgf (females) or 3.1 to 5.0 kgf (males)), or high (> 4.1 kgf (females) or > 5.0 kgf (males)) pain threshold.³¹ The PPDT scores (kgf) of the tibialis anterior muscle belly are based on normative values for males and females collectively, and were classified as low (< 2.5), moderate (2.5 to 6.0), or high (6.1 to >12.0) pain threshold.³²

5.2.5 Analyses

Descriptive statistics including means and ranges were calculated for all variables to describe our sample. Differences in mean age, sex, PRWE score, vBMD, and JCA between the thumb CMC OA and healthy cohort were evaluated using independent samples t-test.

As a final step intended to guide future research, we qualitatively explored the responses to the secondary pain metrics (Body Map, MSI Somatic and Central, SLANSS, PPDT) for each of the participants in the CMC OA group. Using the cut scores described above for each indicator, participants were classed based on the most likely predominant driver of their pain experience, using the International Association for the Study of Pain categories of primarily Nociceptive, Neuropathic, or Nociplastic (Central) phenotypes.³³ The intention of this step was to explore potential pain mechanisms in our study cohort.

5.3 Results

5.3.1 Participant Demographics

The sample was composed of 18 participants: 9 healthy (4 female, mean age 72.9, range, 67 to 82 years), and 9 with thumb CMC OA (6 female, mean age 66.4, range, 41 to 83 years). Descriptive information (age, sex, clinical disease severity, subchondral vBMD, and JCA) are presented in Table 1. There were no differences between the healthy and thumb CMC OA cohorts in terms of age, sex, JCA (mm²), or the deepest layer of subchondral vBMD (mg K₂HPO₄/cm³) in MC1 and the first layer of subchondral vBMD (mg K₂HPO₄/cm³) in TPM (all p

> 0.05). The independent samples t-tests demonstrated that the healthy cohort had higher subchondral vBMD for all three bones and all normalized layers of bone, except for the first layer of the TPM. Results from the vBMD comparison are presented in Figure 1.

Table 5-1: Summary statistics and results of vBMD (mg/K₂HPO₄ cm³), at each anatomical site for each normalized depth.

		CMC OA (n = 9) Mean (range)	Healthy (n = 9) Mean (range)	P-value
Age (y)		64.2 (41.0 to 83.0)	72.9 (67.0 to 82.0)	0.13
Sex (% Female)		79	44	0.17
Clinical Severity (%)		34.2 (10.0 to 42.0)	4.2 (0 to 21.5)	<0.001
vBMD (SD)	Depth (mm)			
MC1	0 – 2.5	366.3 (113.0)	481.2 (68.7)	<0.05
	2.5 – 5.0	187.7 (77.7)	270.7 (59.4)	<0.05
	5.0 – 7.5	171.2 (8.4)	228.3 (53.5)	0.11
MC3	0 – 2.5	294.1 (40.4)	364.1 (83.4)	<0.05
	2.5 – 5.0	205.5 (35.6)	277.8 (64.7)	<0.05
	5.0 – 7.5	192.1 (41.3)	267.9 (72.5)	<0.05
TPM	0 – 1.25	483.7 (121.5)	414.9 (72.8)	0.17
	1.25 – 2.5	408.3 (122.7)	583.1 (86.7)	<0.005
	2.5 – 3.75	258.6 (71.1)	431.9 (118.9)	<0.005
	3.75 – 5.0	208.4 (52.2)	311.5 (98.0)	<0.05
	5.0 – 6.25	195.72 (45.2)	265.6 (81.4)	<0.05
JCA (mm ²)				
MC1		158.8 (62.2)	180.9 (29.9)	0.14
TPM		160.4 (63.2)	181.2 (33.4)	0.15

vBMD = volumetric bone mineral density; MC1 = 1st metacarpal; MC3 = 3rd metacarpal; TPM = trapezium; JCA = joint contact area

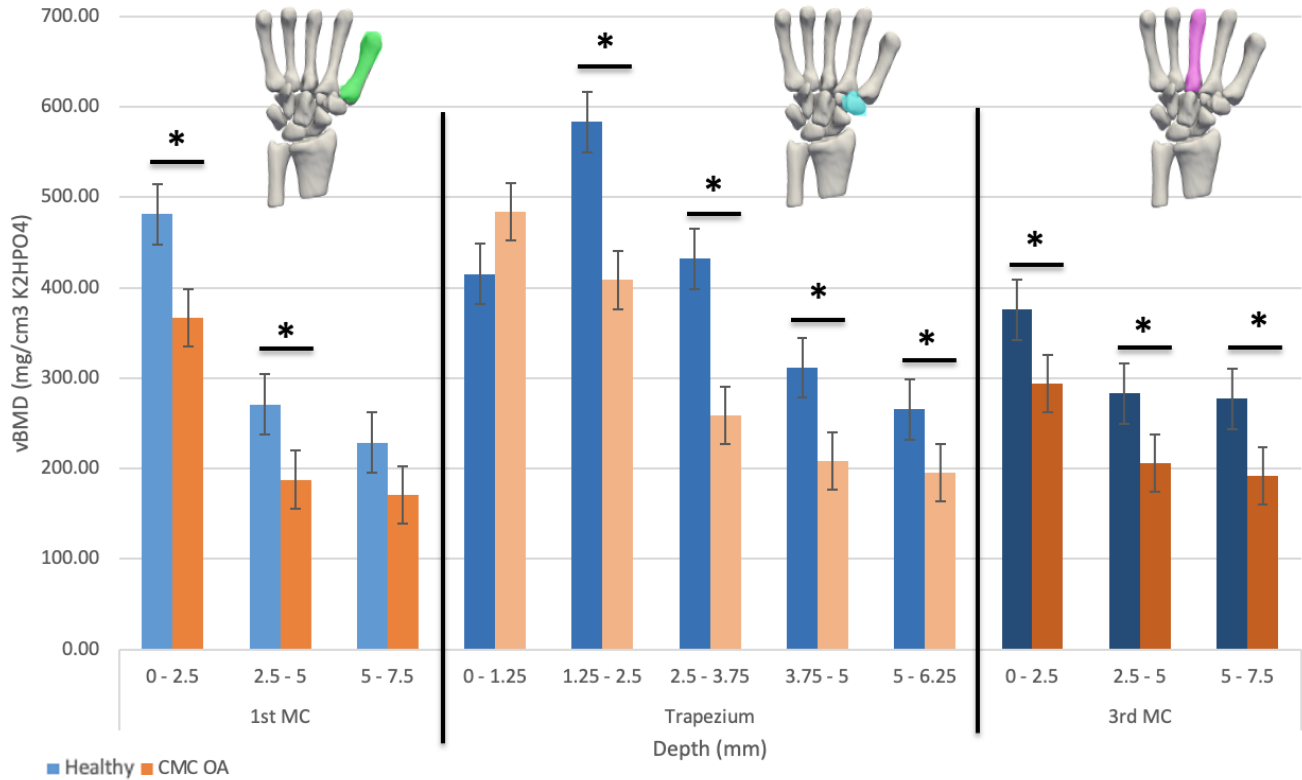


Figure 5-1: Volumetric BMD between the healthy cohort and thumb CMC OA cohort.

The healthy cohort had higher subchondral vBMD for all three bones and all normalized layers of bone, except for the first layer of the TPM. The black bar and asterisk indicate statistically significant differences ($p < 0.05$).

5.3.2 Pain Evaluation Exploratory Analysis

Based on the PROM scores obtained from nine patients with thumb CMC OA, we identified four pain phenotypes; localized nociceptive pain (n = 3), widespread nociceptive pain (n = 2), localized neuropathic pain (n = 2), and central nociplastic pain (n = 2). Figures 2 – 5 show descriptive information, including results from the PROMs, EL-grade, JCA, and vBMD for the TPM and MC1, for the patients classed within each of the four pain phenotypes. Overall, nociceptive pain (localized and widespread), was the dominant pain phenotype in our study cohort.

Across all thumb CMC OA patients, S-LANSS scores indicated that most participants (n = 6) were classified as low on the likelihood of presenting with pain of predominantly neuropathic origin, while three had a moderate likelihood. Two participants had an MSI Somatic score greater than 40%, suggesting dominant somatic pain symptoms, while only one had an MSI Central score greater than 40%, suggesting central- or non-somatic-dominant symptoms. The distribution of pain symptoms were evenly split between local (n = 4) versus widespread (n = 4) pain, while symptoms of numbness or heaviness was reported by five participants. Only one participant indicated no pain or numbness on the full body diagram. PPDT scores were low (n = 7) or moderate (n = 2) on the affected hand, with three participants demonstrating a low bilateral pain threshold. PPDTs over the tibialis anterior were moderate to high in all participants save for one who was ranked as low.

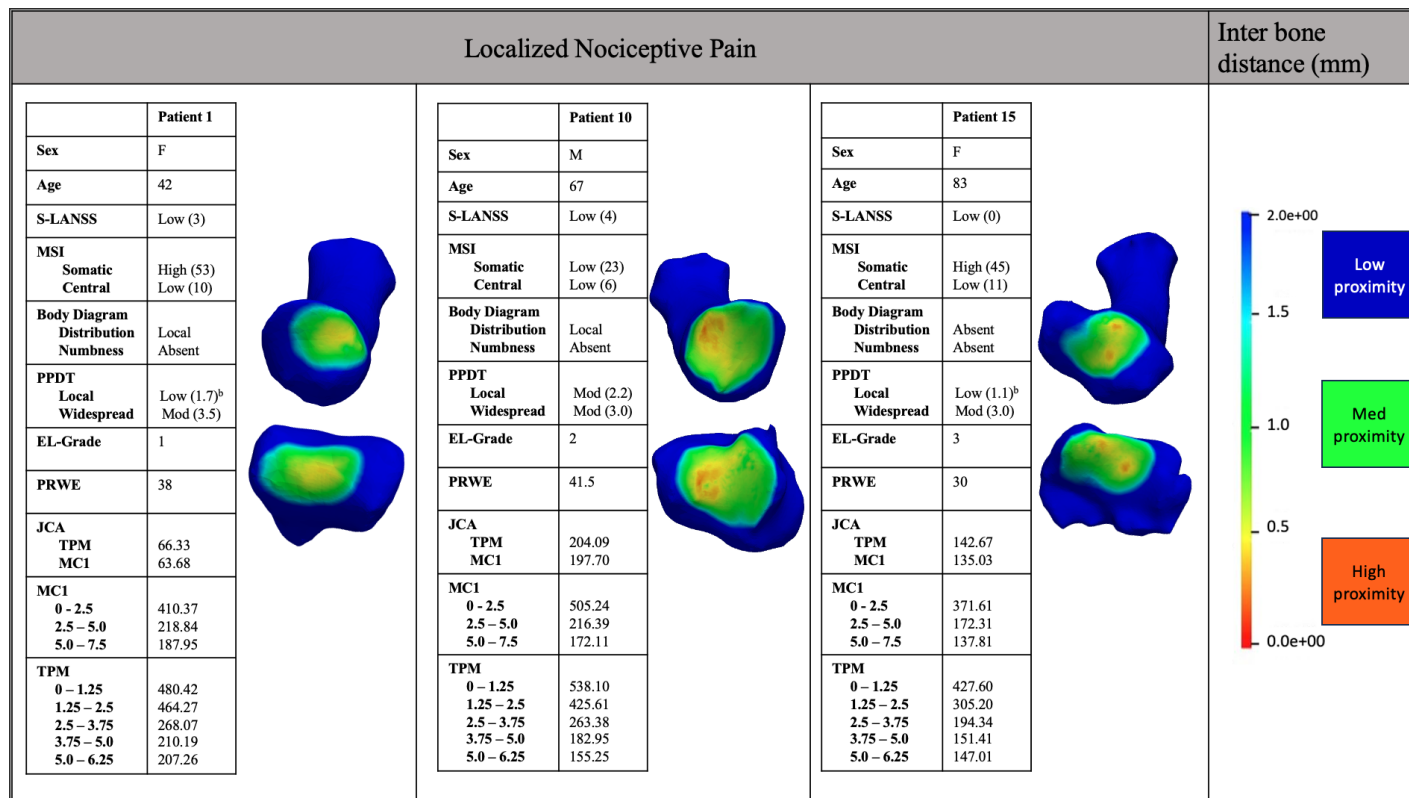


Figure 5-2: Localized nociceptive pain phenotype.

Three thumb CMC OA patients were classed as having localized nociceptive pain. S-LANSS scores were low, with dominant somatic symptoms on the MSI. The body diagram demonstrated local pain distribution in the absence of numbness, and local PPDT scores were considered low bilaterally or moderate. EL-grades ranged from early (1) to moderate (3) structural disease progression. PRWE scores were considered high, indicating significant pain and disability. JCA maps demonstrate high proximity in a volar-central location on the TPM and MC1, and vBMD measures indicate a higher vBMD in the first layer of the TPM for all layers and both bones.

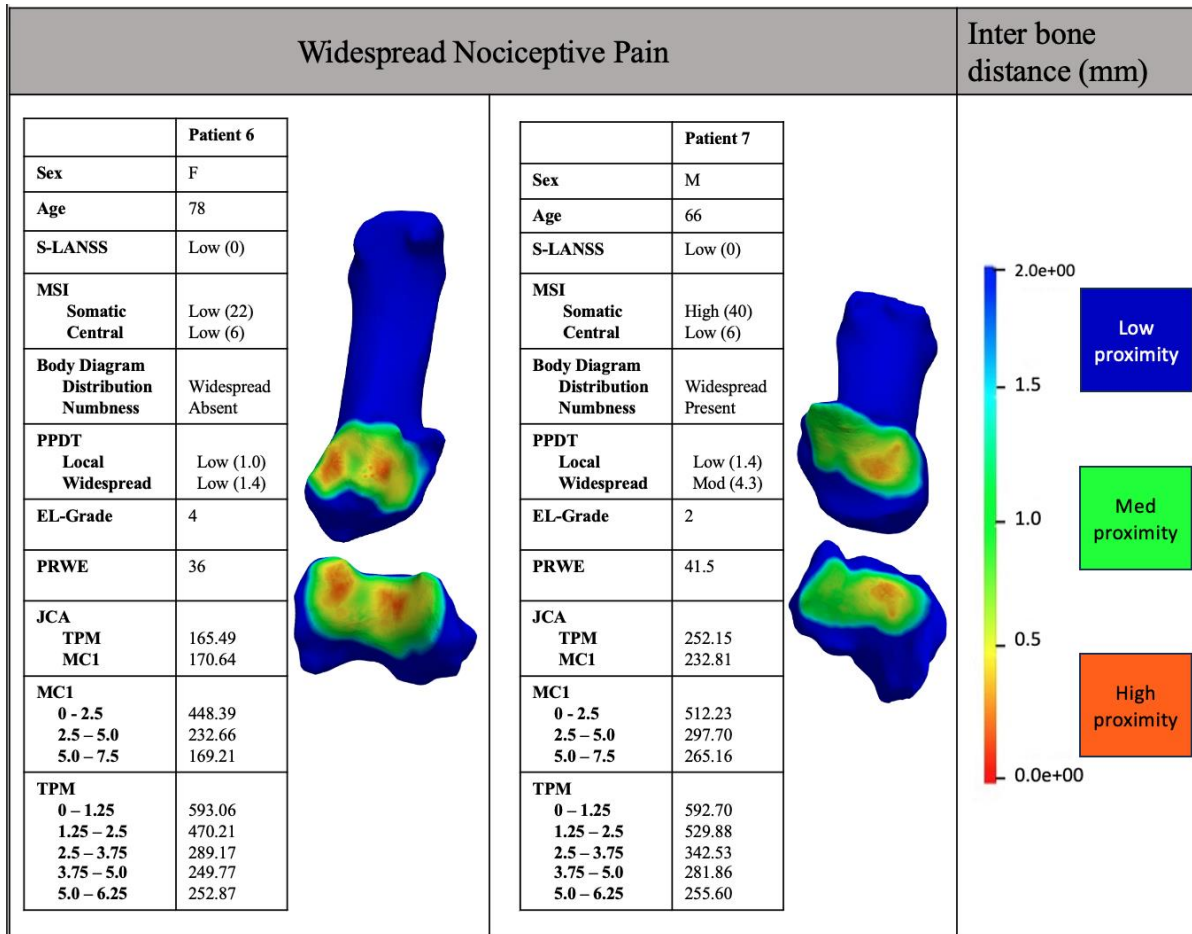


Figure 5-3: Widespread nociceptive pain phenotype.

Two thumb CMC OA patients were classed as having widespread nociceptive pain. S-LANSS scores were low (0), with dominant somatic symptoms on the MSI. The body diagram demonstrated widespread pain in the absence of numbness in one patient, and the presence of numbness in the other. Local and widespread PPDT scores were considered low to moderate, with EL-grades indicating early (2) or late (4) structural progression. PRWE scores were considered high, indicating significant pain and disability. JCA maps demonstrate high proximity in the central location on the TPM and MC1 in one patient, and high proximity in the dorsal-radial location on the TPM and MC1 in the other patient. vBMD measures indicate higher vBMD in the first layer of the TPM for all layers and both bones.

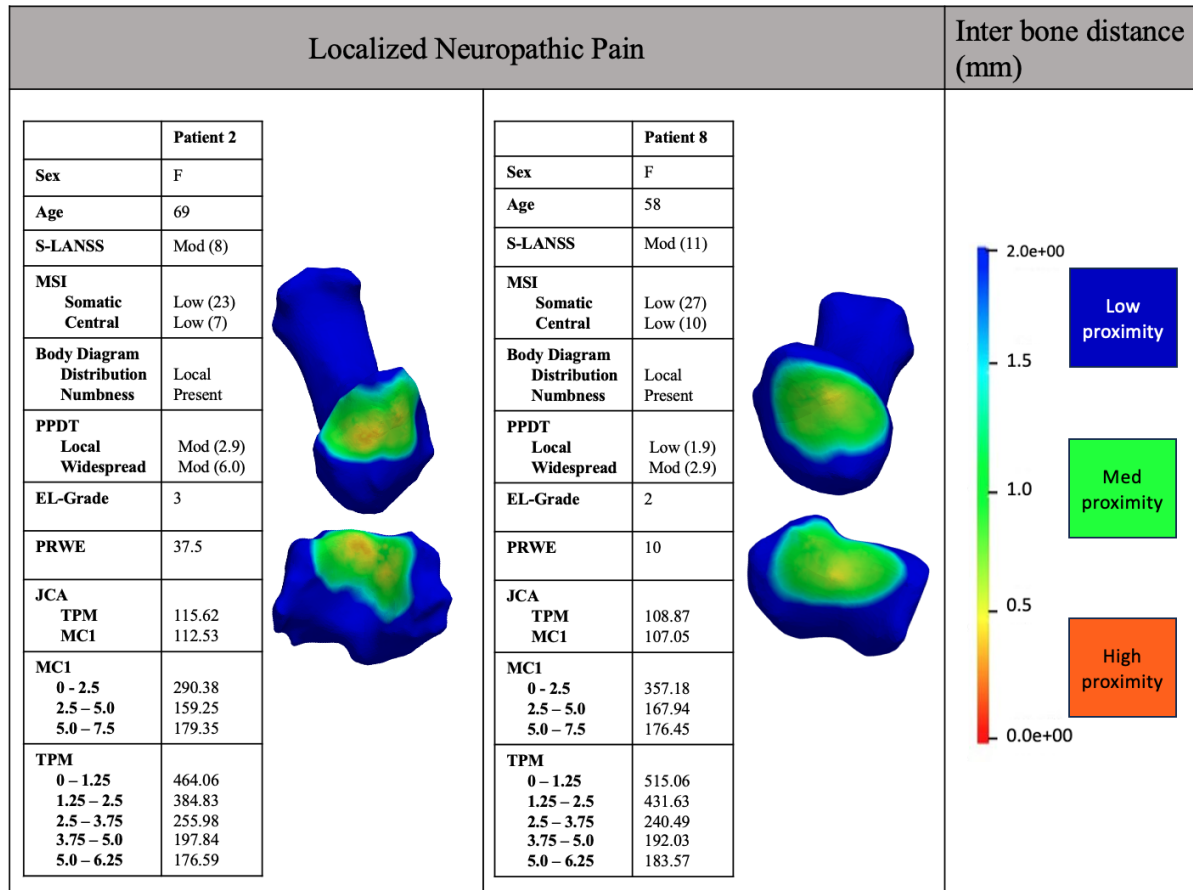


Figure 5-4: Localized neuropathic pain phenotype.

Two thumb CMC OA patients were classed as having pain of predominately localized neuropathic origin. S-LANSS scores were moderate, with low overall scores on the MSI. The body diagram demonstrated localized pain and numbness in both patients, with moderate local and widespread PPDT scores. EL-grade indicated moderate structural progression with grades of 3 and 2, and the PRWE scores were high (37.5) in one patient and low (10) in the other. JCA maps indicate high contact in the dorsal-central location of the TPM and MC1. vBMD measures indicate higher vBMD in the first layer of the TPM for all layers and both bones.

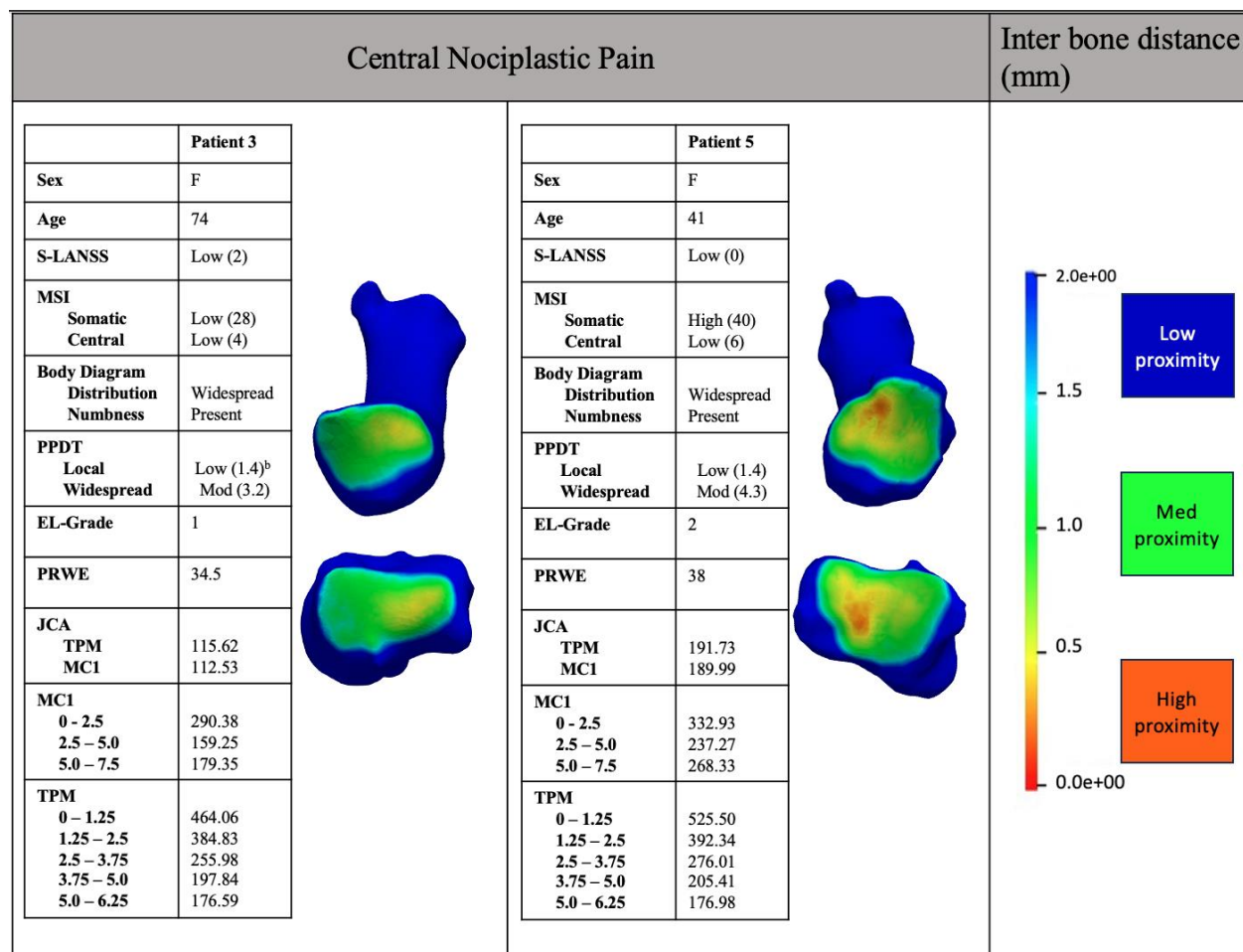


Figure 5-5: Central nociplastic pain phenotype.

Two thumb CMC OA patients were classed as having central nociplastic pain. S-LANSS scores were low, with dominant somatic symptoms in one patient and low overall MSI scores in the other. The body diagram indicated widespread distribution of pain and the presence of numbness for both patients. Local PPDT scores were low for both patients, and widespread scores were considered moderate. EL-grade indicated early structural progression with a grade of either 1 or 2, and the PRWE scores were high indicating significant pain and disability. JCA maps indicate high contact area in the volar-ulnar location of the TPM and MC1, and vBMD measures indicate a higher vBMD in the first layer of the TPM for all layers and both bones.

5.4 Discussion

The goal of Chapter 5 was to explore preliminary results on potential associations between self-rated severity of hand dysfunction and objective imaging-based biomarkers of joint pathology. Our preliminary results demonstrated that our thumb CMC OA cohort had an overall lower vBMD for all three bones and all depths of vBMD, except for the first layer of the TPM. We identified four pain phenotypes among our patient cohort and presented descriptive information for each patient within their proposed phenotype. Overall, a higher vBMD measure in the first layer of the TPM compared to the MC1 was consistent amongst all patients across all four phenotypes.

Previous research has described the TPM to be more affected by bony changes and cartilage loss than the MC1, likely due to the morphological features of the TPM.³⁴⁻³⁶ Our preliminary results demonstrated that the first layer of subchondral vBMD in the TPM is higher in our thumb CMC OA cohort compared to the healthy cohort, while all other regions of bone are lower in the thumb CMC OA cohort. Bone adaptation in the form of locally increased vBMD is suggestive of sclerosis, a bony change that commonly occurs late in the CMC OA disease state.²⁰ Our preliminary analysis includes a thumb CMC OA cohort with varying stages of OA, and it is therefore possible that patients with late-stage thumb CMC OA contributed to the increase in vBMD in this region. As the TPM is a short bone, the cortical bone thickness is likely to be smaller than that of the MC1, a long bone. The second layer of bone in the TPM is therefore likely to be made up of a higher proportion of trabecular bone; bone tissue that is more metabolically active and adaptive to change.³⁷ Altogether, our preliminary findings from TPM bone layers indicate that the TPM *may* experience bony changes before that of the MC1, serving as a potential factor in detecting early disease progression and providing reason to continue exploring this association.

Regional bone loading correlates to regional bone density, wherein bone tissue continually adapts and responds to meet changing mechanical demands.^{4,25,38} People with symptomatic CMC OA often modify daily activities, and therefore do not load their symptomatic hand.^{4,39,40} Activity modification and the relative disuse of the affected hand, thereby less loading on the joint, may contribute to lower subchondral vBMD in our thumb CMC OA cohort.^{4,39,40} As there were no statistically significant differences between demographics within our study cohorts, we can rule

out the possibility of differences in bone associated with aging or participant sex. Interestingly, the MC3 was also significantly lower in the thumb CMC OA cohort, suggesting an overall low subchondral vBMD that may not be specific to the site of thumb CMC OA. This finding aligns with activity modification, relative disuse, and a decreased loading on the symptomatic hand, however, requires more rigorous analysis to understand this association. Specifically, performing a within-subject bilateral comparison between subchondral vBMD in the MC3 of the affected and unaffected thumb will provide more insight into potential contributing factors to an overall low vBMD.

The participant profiles and pain phenotypes are intended to facilitate interpretation of the scores obtained from the PROMs, rather than endorse specific pain mechanisms. Overall, the results from the participant profiles align with previous work highlighting pain heterogeneity in OA.¹ Unlike OA-related structural changes, pain associated with OA is subjective and may involve both peripheral and central mechanisms.^{15,20} Joint nociception has been studied as a potential mechanism in knee OA-related pain research due to the correlation between BML, synovitis, and effusion. Specifically, scholars have demonstrated that the damage and remodelling of articular joint structures activates the afferent nerves (nociceptors) in the tissue, contributing to a lower pain threshold.^{14,15,41} Within our thumb CMC OA cohort, nociceptive pain was a dominant phenotype ranging from localized or widespread nociceptive pain, or central nociplastic pain. Our preliminary results therefore show promise towards a potential dominant pain mechanism within our study cohort.

Within each pain phenotype, participant demographics and imaging-based biomarker measures were similar. It is suspected that with a larger sample, underlying biological mechanisms will be further elucidated using our biomarkers. This work has the potential to highlight specific characteristics or trends within our biomarkers that differentiate between patients within each of the proposed pain phenotypes. Overall, our preliminary results demonstrate potential for understanding pain mechanisms in thumb CMC OA, with the hopes of facilitating more directed mechanism-based pain therapies and/or treatment.

5.5 Limitations

Several limitations should be considered when interpreting our findings. With only 18 participants in our study (nine of whom have thumb CMC OA), the results from this study are not intended to be generalizable or conclusive. As such, our findings are subject to several biases including outliers, a non-representative sample, skewed data, confounding factors, and the potential for others. This study was intended to be exploratory and hypothesis-generating to highlight potential relationships to explore further, however it is acknowledged that future work will require a larger sample size. Pain experience is a complex interplay between social, environmental, cultural, and physical influences. As such, mental health disorders may contribute to the overall pain experience. Although we did not include a questionnaire specific to mental health, the non-somatic symptoms sub score of the MSI has an almost perfect association with the PHQ-9²⁷, therefore addressing mental health contributors to the pain experience. It is also acknowledged that using cut scores from other scales to form our threshold values for the MSI Somatic and MSI Central sub scores present additional limitations. In an effort to rectify this limitation, we followed threshold values of other recognized scales that target somatic²⁸ and central²⁹ pain symptoms in similar work. In doing so, we acknowledge the potential that the scales have different underlying constructs, regardless of their seemingly similar contents. For future work, a thorough validation study on transferring such cut scores or threshold values would benefit this work, to capture the equivalence of the constructs each scale is measuring. Lastly, the normalized PPDT values for the hand were obtained from a study performed on the dorsal interosseous muscle of the hand in a healthy population, while the normalized PPDT values for the belly of the tibialis anterior were obtained from a study performed on whiplash associated disorder (WAD). This introduces the potential for overgeneralizing our results to different study cohorts.

5.6 Conclusion

Our preliminary results demonstrate significant differences in subchondral vBMD between our healthy and thumb CMC OA cohorts, with a significantly lower vBMD in the latter cohort. Overall, our preliminary findings show promise in detecting potential factors that may contribute to clinical disease severity, and the potential for targeted intervention and treatment strategies through our pain phenotypes. Future work will analyze these relationships in a larger,

longitudinal cohort to better characterize the impact of structural progression, vBMD and JCA changes on clinical disease severity and pain mechanisms. Through this, a more thorough understanding of the mechanisms underlying OA-related pain may lead to more directed mechanism-based pain therapies or interventions

5.7 References

1. Grassel S, Muschter D, Pitsillides A, Zaucke F. Recent advances in the treatment of osteoarthritis
Published online 2020. doi:10.12688/f1000research.22115.1
2. Health Canada. Arthritis in Canada an Ongoing Challenge. Published online 2003.
3. Chiarotto A, Fernandez-de-Las-Penas C, Castaldo M, Villafane JH. Bilateral pressure pain hypersensitivity over the hand as potential sign of sensitization mechanisms in individuals with thumb carpometacarpal osteoarthritis. *Pain Med.* 2013;14(10):1585-1592.
doi:https://dx.doi.org/10.1111/pme.12179
4. Schreiber JJ, McQuillan TJ, Halilaj E, et al. Changes in Local Bone Density in Early Thumb Carpometacarpal Joint Osteoarthritis. *Journal of Hand Surgery.* 2018;43(1):33-38.
doi:10.1016/j.jhsa.2017.09.004
5. Buhler M, Chapple CM, Stebbings S, Sangelaji B, Baxter GD. Effectiveness of splinting for pain and function in people with thumb carpometacarpal osteoarthritis: a systematic review with meta-analysis. *Osteoarthritis Cartilage.* 2019;27(4):547-559. doi:10.1016/J.JOCA.2018.09.012
6. Barr AJ, Campbell TM, Hopkinson D, Kingsbury SR, Bowes MA, Conaghan PG. A systematic review of the relationship between subchondral bone features, pain and structural pathology in peripheral joint osteoarthritis. *Arthritis Research & Therapy.* 2015;17(1).
doi:10.1186/S13075-015-0735-X
7. Eaton RG, Glickel SZ. Trapeziometacarpal Osteoarthritis: Staging as a Rationale for Treatment. *Hand Clin.* 1987;3(4):455-469. doi:10.1016/S0749-0712(21)00761-7
8. Jones G, Cooley HM, Bellamy N. A cross-sectional study of the association between Heberden's nodes, radiographic osteoarthritis of the hands, grip strength, disability and pain. *Osteoarthritis Cartilage.* 2001;9:606-611. doi:10.1053/joca.2001.0460
9. Dahaghin S, Bierma-Zeinstra SMA, Hazes JMW, Koes BW. Clinical Burden of Radiographic Hand Osteoarthritis: A Systematic Appraisal. Published online 2006. doi:10.1002/art.22109
10. Shapiro LM, McQuillan TJ, Kerkhof FD, Ladd A. Radiographic Progression of Thumb CMC Osteoarthritis: A Systematic Review. *J Hand Surg Glob Online.* 2020;2(6):343-348.
doi:10.1016/J.JHSG.2020.09.001

11. Wajon A, Ada L, Edmunds I. Surgery for thumb (trapeziometacarpal joint) osteoarthritis. *Cochrane Database of Systematic Reviews*. 2004;(1). doi:10.1002/14651858.CD004631
12. Villafañe JH, Cleland JA, Fernández-De-Las-Peñas C. The Effectiveness of a manual therapy and exercise protocol in patients with thumb carpometacarpal osteoarthritis: A randomized controlled trial. *Journal of Orthopaedic and Sports Physical Therapy*. 2013;43(4):204-213. doi:10.2519/JOSPT.2013.4524/ASSET/IMAGES/LARGE/JOSPT-204-FIG004.JPEG
13. Mesci N, Mesci E, Külçü D. Association of neuropathic pain with ultrasonographic measurements of femoral cartilage thickness and clinical parameters in patients with knee osteoarthritis. *J Phys Ther Sci*. 2016;28(8):2190. doi:10.1589/JPTS.28.2190
14. O'Neill TW, Felson DT. Mechanisms of Osteoarthritis (OA) Pain. *Curr Osteoporos Rep*. 2018;16(5):611. doi:10.1007/S11914-018-0477-1
15. Fu K, Robbins SR, McDougall JJ. Osteoarthritis: the genesis of pain. *Rheumatology*. 2018;57(suppl_4):iv43-iv50. doi:10.1093/RHEUMATOLOGY/KEX419
16. Walton DM, Elliott JM. *Musculoskeletal Pain - Assessment, Prediction and Treatment*. HANSPRING PUBLISHING LIMITED; 2019.
17. McDougall JJ, Albacete S, Schuelert N, et al. Lysophosphatidic acid provides a missing link between osteoarthritis and joint neuropathic pain. *Osteoarthritis Cartilage*. 2017;25(6):926-934. doi:10.1016/J.JOCA.2016.08.016
18. Naterstad IF, Bjordal JM, Joensen J, Saebo H, Stausholm Humaira; ORCID: <http://orcid.org/0000-0001-8882-014X> MBAOS. Reliability of pain pressure threshold algometry in persons with conservatively managed wrist fractures. *Physiother Res Int*. 2020;25(1):e1797. doi:<http://dx.doi.org/10.1002/pri.1797>
19. Walton D, MacDermid J, Nielson W, Teasell R, Chiasson M, Brown L. Reliability, Standard Error, and Minimum Detectable Change of Clinical Pressure Pain Threshold Testing in People With and Without Acute Neck Pain. *Journal of Orthopaedic & Sports Physical Therapy*. 2011;41(9):644-650. doi:10.2519/jospt.2011.3666
20. Kennedy CD, Manske MC, Huang JI. Classifications in Brief: The Eaton-Littler Classification of Thumb Carpometacarpal Joint Arthrosis. *Clin Orthop Relat Res*. 2016;474(12):2729-2733. doi:10.1007/S11999-016-4864-6/FIGURES/3

21. Robinson S, Straatman L, Lee TY, Suh N, Lalone E. Evaluation of four-dimensional computed tomography as a technique for quantifying carpal motion. *J Biomech Eng.* 2021;143(6). doi:10.1115/1.4050129
22. Lalone EA, McDonald CP, Ferreira LM, Peters TM, King GW, Johnson JA. Development of an image-based technique to examine joint congruency at the elbow. *Comput Methods Biomech Biomed Engin.* 2013;16(3):280-290. doi:10.1080/10255842.2011.617006
23. Straatman L, Knowles N, Suh N, Walton D, Lalone E. The Utility of Quantitative Computed Tomography to Detect Differences in Subchondral Bone Mineral Density Between Healthy People and People With Pain Following Wrist Trauma. *J Biomech Eng.* 2022;144(8). doi:10.1115/1.4053594
24. Crisco JJ, Moore DC, Marai GE, et al. Effects of distal radius malunion on distal radioulnar joint mechanics - An in vivo study. *Journal of Orthopaedic Research.* 2007;25(4):547-555. doi:10.1002/jor.20322
25. Straatman L, Norman E, Knowles N, Walton D, Suh N, Lalone E. Use it or lose it: The relationship between two image-based biomarkers in better understanding osteoarthritis progression in the wrist. *J Biomech.* 2023;161:111849. doi:10.1016/J.JBIOMECH.2023.111849
26. MacDermid JC. Development of a scale for patient rating of wrist pain and disability. *Journal of Hand Therapy.* 1996;9(2):178-183. doi:10.1016/S0894-1130(96)80076-7
27. Walton DM, Marsh J. The Multidimensional Symptom Index: A new patient-reported outcome for pain phenotyping, prognosis and treatment decisions. *European Journal of Pain.* 2018;22(7):1351-1361. doi:10.1002/EJP.1224
28. Gierk B, Kohlmann S, Kroenke K, et al. The Somatic Symptom Scale–8 (SSS-8): A Brief Measure of Somatic Symptom Burden. *JAMA Intern Med.* 2014;174(3):399-407. doi:10.1001/JAMAINTERNMED.2013.12179
29. Neblett R, Cohen H, Choi Y, et al. The Central Sensitization Inventory (CSI): Establishing Clinically Significant Values for Identifying Central Sensitivity Syndromes in an Outpatient Chronic Pain Sample. *J Pain.* 2013;14(5):438-445. doi:10.1016/J.JPAIN.2012.11.012
30. Bennett MI, Smith BH, Torrance N, Potter J. The S-LANSS score for identifying pain of predominantly neuropathic origin: Validation for use in clinical and postal research. *J Pain.* 2005;6(3):149-158. doi:10.1016/J.JPAIN.2004.11.007

31. Chesterton LS, Barlas P, Foster NE, Baxter GD, Wright CC. Gender differences in pressure pain threshold in healthy humans. *Pain*. 2003;101(3):259-266. doi:10.1016/S0304-3959(02)00330-5
32. Walton D, Macdermid J, Nielson W, Teasell R, Nailor T, Maheu P. A descriptive study of pressure pain threshold at 2 standardized sites in people with acute or subacute neck pain. *Journal of Orthopaedic and Sports Physical Therapy*. 2011;41(9):651-657. doi:10.2519/jospt.2011.3667
33. Raja SN, Carr DB, Cohen M, et al. The Revised IASP definition of pain: concepts, challenges, and compromises. *Pain*. 2020;161(9):1976. doi:10.1097/J.PAIN.0000000000001939
34. Nortwick S Van, Berger A, Cheng R, Lee J, Ladd AL. Trapezial Topography in Thumb Carpometacarpal Arthritis. *J Wrist Surg*. 2013;2(3):263. doi:10.1055/S-0033-1350088
35. North ER, Rutledge WM. The Trapezium-Thumb Metacarpal Joint: The Relationship of Joint Shape and Degenerative Joint Disease. 1983;15(2).
36. Morton AM, Peipert LJ, Moore DC, et al. Bone morphological changes of the trapezium and first metacarpal with early thumb osteoarthritis progression. *Clinical Biomechanics*. 2022;100:105791. doi:10.1016/j.clinbiomech.2022.105791
37. Madry H, van Dijk CN, Mueller-Gerbl M. The basic science of the subchondral bone. *Knee Surgery, Sports Traumatology, Arthroscopy*. 2010;18(4):419-433. doi:10.1007/s00167-010-1054-z
38. Brand RA. Biographical sketch: julius wolff, 1836-1902. *Clin Orthop Relat Res*. 2010;468(4):1047-1049. doi:10.1007/s11999-010-1258-z
39. Bagis S, Sahin G, Yapici Y, Cimen OB, Erdogan C. The effect of hand osteoarthritis on grip and pinch strength and hand function in postmenopausal women. *Clin Rheumatol*. 2003;22(6):420-424. doi:10.1007/S10067-003-0792-4/TABLES/5
40. McQuillan TJ, Kenney D, Crisco JJ, Weiss AP, Ladd AL. Weaker Functional Pinch Strength Is Associated With Early Thumb Carpometacarpal Osteoarthritis. *Clin Orthop Relat Res*. 2016;474(2):557-561. doi:10.1007/S11999-015-4599-9/TABLES/3
41. Neogi T. Clinical significance of bone changes in osteoarthritis. *Ther Adv Musculoskelet Dis*. 2012;4(4):259-267. doi:10.1177/1759720X12437354

42. French HP, Smart KM, Doyle F. Prevalence of neuropathic pain in knee or hip osteoarthritis: A systematic review and meta-analysis. *Semin Arthritis Rheum.* 2017;47(1):1-8. doi:10.1016/J.SEMARTHTRIT.2017.02.008

Chapter 6

6 General Discussion and Conclusions

This chapter summarizes the objectives and hypotheses proposed within each chapter, as well as a summary of the work that was completed to satisfy our objectives. The strengths and limitations of our work will also be discussed, and future directions that stem from the work completed.

6.1 Summary

The defining symptom associated with most clinical disorders of the hand and wrist, and often the major reason for seeking medical treatment, is pain. However, the mechanisms underlying chronic pain following musculoskeletal (MSK) trauma are complex, multifactorial, and remain largely unknown. While there have been numerous definitions of pain developed for the sake of understanding its myriad impacts, pain is one of the most multidimensional, complex, universal, human experiences, representing significant societal, economical, personal, and clinical burdens.¹ MSK pain is characterized as pain that often arises from the bones, muscles, ligaments, tendons, and other structures that support the body's MSK system. MSK pain is a highly prevalent and costly problem on global health care systems,² and is found to be a major cause of years living with pain and disability worldwide.³⁻⁵ The hand and wrist joint is one of the most complex, functionally important joints in the upper extremity.² Hand and wrist pain represent a significant proportion of overall MSK burden.² Although common, there is a lack of understanding surrounding the mechanisms underlying chronic pain after hand and wrist MSK trauma. As such, this thesis sought out to understand mechanisms underlying chronic pain in hand and wrist MSK pathologies, using imaging-based biomarkers and gold-standard pain evaluation techniques.

In Chapter 2, we sought to explore our first proposed mechanism to better understand underlying MSK-related pain: pain evaluation techniques. We explored the interacting influences of patient sex on multi-modal evaluation techniques that tap different domains

of the pain experience. We hypothesized that the correlation between sex-specific pain beliefs and clinical pain evaluation would be greater in biological females compared to their male counterparts. All participants completed the GREP, while healthy participants also underwent PPDT and CPT testing, and participants following an acute MSK injury completed the BPI. We found that in both study cohorts, there was no correlation between sex-specific pain beliefs and clinical pain evaluation within and between males and females. In the acute MSK trauma cohort, males were descriptively more accurate predictors of their clinical pain evaluation scores. However, inferential statistics did not show this to be a true difference greater than chance. Our results further acknowledge that pain beliefs, reports, and intervention strategies therein, will likely be different, on average, between males and females. This chapter further served design considerations for future work, wherein the GREP did not predict QST scores in this study cohort, and as such was not included in the latter studies.

In Chapter 3, we sought to explore our second proposed mechanism for better understanding MSK-related pain: imaging-based biomarkers. To do so, we demonstrated the utility of quantitative computed tomography (QCT) depth-specific analysis to compare subchondral volumetric bone mineral density (vBMD) between a healthy cohort ($n = 5$) and a cohort of participants with pain following various forms of wrist trauma ($n = 5$). We hypothesized that participants with pain following wrist trauma will have lower subchondral vBMD for all depths from the subchondral surface. Participants underwent bilateral CT scans of their hand and wrist accompanied by a calibration phantom with known material densities. Average vBMD was analyzed for 3 normalized layers of bone (0 to 2.5mm, 2.5 to 5mm, and 5 to 7.5mm) according to radiocarpal surface contact between bones. We found that the healthy cohort had a higher vBMD for all depth-specific layers of bone, while also demonstrating subject-specific differences (weighted average surface vector allowed for direct analysis of vBMD where joint contact was the highest), and joint-specific differences (differentiating between bone in the radiolunate (RL) and radioscapoid (RS) joints). Future work is required to understand how joint motion contributes to differences in vBMD, and as such was analyzed in the following chapter.

In Chapter 4, we incorporated another imaging-based biomarker as a proposed mechanism for understanding MSK-related pain: joint contact area (JCA). We sought to evaluate the correlation between kinematic JCA and subchondral vBMD in a cohort of healthy adults ($n = 20$), as it relates to depth from the subchondral surface. We hypothesized that a larger JCA will be significantly correlated to a higher subchondral vBMD measure, within all depth-specific layers, according to work performed in Chapter 3. Participants underwent bilateral CT scans of their hand and wrist accompanied by a calibration phantom, followed by a four-dimensional CT scan (4DCT) while performing maximum wrist extension to maximum flexion. Average vBMD was analyzed as introduced in Chapter 3, and kinematic JCA was determined for the RL and RS joints for every 10 degrees of motion from 40 degrees of extension to 40 degrees of flexion. We found that a higher vBMD was significantly associated with a larger JCA, specifically in the deeper regions of subchondral bone. Notably, JCA in wrist extension was significantly correlated to vBMD. Wrist extension is the position the wrist is most situated during activities of daily living, highlighting the correlation between joint motion and underlying bone. In addition, we found that sex contributed to the variance in vBMD measures, however age did not. Future work is required to understand the relationship between our imaging-based biomarkers in a clinical cohort of participants undergoing pathological change, and how these correlate to clinical symptoms as measured using pain evaluation techniques. These findings led us to our final chapter.

In Chapter 5, we sought to explore the association between structural and clinical severity, measured using our imaging-based biomarkers and pain evaluation techniques in a clinical cohort of patients with thumb carpometacarpal osteoarthritis (CMC OA) ($n = 9$) compared to healthy people ($n = 9$). Participants underwent static CT scans as introduced in Chapter 3 and Chapter 4, and completed a battery of patient-reported outcome measures (PROMs) targeting different pain mechanisms. Specifically, participants completed the patient-rated wrist evaluation (PRWE), the Multi-dimensional Symptom Index (MSI), the Short Form Leeds Assessment for Neuropathic Signs and Symptoms (S-LANSS), and a study-specific body diagram. Additionally, participants also underwent pressure pain detection threshold (PPDT) testing using a digital algometer. Average subchondral vBMD was analyzed in the first metacarpal (MC1) and

third metacarpal (MC3) using the same normalized layers described in Chapter 3, while the trapezium (TPM) was analyzed in five 1.25mm normalized layers (0 to 1.25mm, 1.25 to 2.50mm, 2.50 to 3.75mm, 3.75 to 5.0mm, and 5.0 to 6.25mm). Average JCA of the MC1 and TPM were taken for all participants. All PROMs were analyzed separately using conceptualized thresholds to characterize pain mechanisms. Our preliminary results demonstrated significant differences subchondral vBMD between our healthy and thumb CMC OA cohorts, with a significantly lower vBMD in the latter cohort. We identified four pain phenotypes within our thumb CMC OA cohort with regards to the scores obtained from the PROMs. The dominant phenotype was nociceptive pain, followed by the presence of neuropathic pain symptoms and central nociplastic pain symptoms. Our results demonstrate the heterogeneity of pain mechanisms associated with thumb CMC OA. Overall, our preliminary findings show promise in detecting potential biological factors that may contribute to clinical disease severity, and the potential for targeted intervention and treatment strategies therein.

Taken together, our work suggests that imaging-based biomarkers in conjunction with gold standard patient-reported outcomes provides novel information regarding mechanisms underlying MSK-related pain in the hand and wrist. Overall, identifying an imaging-based biomarker for chronic MSK pain in the hand and wrist stands to provide objectifiable information on the pathophysiology of chronic hand and wrist pain, with the hopes of transferability among other MSK-related pathologies. This has the potential to influence new mechanism-based pain intervention strategies to mitigate pain and suffering associated with MSK-related pathologies. We anticipate future investigations into a more comprehensive understanding of pain mechanisms in MSK-related pathologies will be required.

6.2 Future Directions

As predicted, this thesis challenges our understanding of biomarkers of pain, while also highlighting the benefits of combining two seemingly disparate fields of study, Health Sciences and Biomedical Engineering. Bridging the gap between these fields is foundational for investigating biomarkers that represent objective information on the mechanisms underlying chronic pain. While the results from our work have contributed

to our understanding of potential mechanisms underlying chronic MSK-related pain, they have also raised more questions regarding the relationship between structural and clinical disease progression and presentation. The works performed in this thesis are simply the tip of the iceberg and are not void of limitations.

Of note, a larger sample size would be beneficial for future work to validate the trends seen within our data. Although emerging trends were seen within the sample size acquired for each chapter of this thesis, it is likely that a larger sample size would serve to benefit more definitive conclusions. In Chapter 2, the sample size had sufficient power at $n = 128$. We acquired a total sample of $n = 161$, however as this work was a secondary analysis on previously collected data, we were unable to ensure a minimum of $n = 64$ participants within each group to maintain sufficient power. As such, our results are not conclusive and encourage future work in this area. In Chapter 3, we had a sample size of $n = 10$; five people post wrist fracture who were still experiencing pain and five healthy people. However, the objective of this study was to test potential applications of the proposed QCT analysis tool to refine the research protocol before conducting a larger study. The small sample size was sufficient in characterizing the difference between healthy people and people experiencing pain post-wrist fracture, using QCT. The intra-rater reliability sample size (or, the number of repetitions) was also sufficient, yielding an ICC of 0.99 through one rater manually segmenting the articular surfaces of interest (RL and RS) and obtaining the vBMD from one study participant, five times. Therefore, more data was not thought to affect these results. In Chapter 4, a sample size of $n = 20$ was sufficient in demonstrating relationships between our image-based biomarkers within our healthy cohort. The intra-rater reliability sample size (number of repetitions) was also sufficient, yielding an ICC of 0.91 through one rater obtaining kinematic JCA from one participant, five times. It is unlikely that a larger sample size would have affected these results. Lastly, In Chapter 5, we had 9 thumb CMC OA and 9 healthy participants. The objective of this final chapter was to highlight potential relationships and meaningful differences to explore further, rather than endorsing potential cause-and-effect relationships. Overall, it is acknowledged that a larger sample size would increase generalizability of our results by targeting a larger population of people with MSK-pain in the hand and wrist, as well as validate emerging trends seen within our work. As the

goal of this thesis was to highlight the potential applications for QCT analysis in detecting biomarkers underlying chronic MSK-pain, future work should continue using this methodology in a larger sample to further validate this work.

In addition, incorporating qualitative inquiries in conjunction with quantitative analysis would prove beneficial in understanding the patients experience with pain, and why some people may experience more severe clinical pain presentation with fewer structural progressive symptoms, and vice versa. To date, scholars are making a shift away from pain evaluation techniques that serve as a “one size fits all” approach and endorsing a more person-specific form of pain evaluation.⁷ Integrating qualitative methodologies may provide researchers with pertinent information not otherwise obtained using standardized pain evaluation techniques or through biomarkers. Additionally, this work may also benefit from a diverse group of patient partners who have lived experience with chronic pain following MSK-related pathologies. This has the potential to enhance our understanding of what’s important to the potential patients, how our research can embody their experience to better serve their needs, and expectations they may have from our research. Including a team of physiotherapists who work with patients with hand and wrist MSK-related disorders would also supplement this work, to better understand how our research can improve their work as clinicians, and how this specific research can be tailored to represent more pragmatic clinical scenarios.

Furthermore, our analysis was limited to bone and therefore did not include evaluation of soft tissues. The contribution of cartilage thickness and soft-tissues interactions, such as ligament laxity, on JCA was therefore not analyzed. Previous work within this laboratory has validated the measurement technique we used to calculate JCA, however it was performed in the elbow rather than the wrist.⁸ This thesis used JCA to estimate changes in bone movement throughout motion to show the usefulness of 4DCT and the impact of JCA on underlying subchondral bone. Therefore, while cartilage effects and other soft-tissue structures serve as a limitation, it did not invalidate the results from our study. Furthermore, subchondral vBMD is a measurement that is indirectly influenced by inflammatory markers that naturally occur in the bone and joint space following injury or pathological change.⁹ These markers could change the attenuation of the bone tissue, and

therefore artificially increase or decrease measures of vBMD. Previous knee literature has also identified inflammation as an underlying factor in pain sensitivity, wherein the presence of inflammation surrounding the joint capsule contributed to a lower pain threshold (higher pain sensitivity).¹⁰⁻¹² Future work should incorporate the analysis of inflammation within the joint, to rule out or identify these markers as potentially confounding factors for our subchondral vBMD and pain sensitivity metrics.

Lastly, this thesis only examined wrist motions during flexion and extension. As was analyzed in Chapters 3 and 4, the radiocarpal joint is critical to normal hand and wrist function. Formed by the articulations between the scaphoid, lunate and distal radius, the radiocarpal joint is responsible for more than half of the range of motion (ROM) in the wrist, therefore serving major functional and clinical importance. However, what is known about hand and wrist motion is limited to anatomically defined motions of flexion, extension, radial deviation, and ulnar deviation about the radiocarpal joint. Most wrist motion is a combination of all anatomically defined motions, such as the recently defined dart thrower's motion (DTM). In DTM, the wrist moves from radial extension to ulnar flexion, with less lunate and scaphoid motion compared to both flexion-extension and radial-ulnar deviation.¹³ DTM is commonly performed during myriad activities of daily living such as opening a jar, pouring water from a jug, drinking from a cup, throwing a ball, and many more.^{13,14} As such, DTM represents an important functional plane of motion in the wrist, and future work should therefore incorporate this motion when studying kinematic JCA in the wrist.

6.3 References

1. Raja SN, Carr DB, Cohen M, et al. The Revised IASP definition of pain: concepts, challenges, and compromises. *Pain*. 2020;161(9):1976.
doi:10.1097/J.PAIN.0000000000001939
2. Ferguson R, Riley ND, Wijendra A, Thurley N, Carr AJ, Bjf D. Wrist pain: a systematic review of prevalence and risk factors- what is the role of occupation and activity? *BMC Musculoskelet Disord*. 2019;20(1):1-13. doi:10.1186/S12891-019-2902-8/FIGURES/3
3. Phillips CJ. The Cost and Burden of Chronic Pain. *Rev Pain*. 2009;3(1):2-5.
doi:10.1177/204946370900300102
4. Woolf AD, Pfleger B. Burden of major musculoskeletal conditions. *Bull World Health Organ*. 2003;81(9):646-656. doi:10.1590/S0042-96862003000900007
5. Woolf AD. Global burden of osteoarthritis and musculoskeletal diseases. *BMC Musculoskeletal Disorders 2015 16:1*. 2015;16(1):1-1. doi:10.1186/1471-2474-16-S1-S3
6. Bruno F, Arrigoni F, Palumbo P, et al. The Acutely Injured Wrist. *Radiol Clin North Am*. 2019;57(5):943-955. doi:10.1016/j.rcl.2019.05.003
7. Walton DM, Elliott JM. *Musculoskeletal Pain - Assessment, Prediction and Treatment*. HANDSPRING PUBLISHING LIMITED; 2019.
8. Lalone EA, McDonald CP, Ferreira LM, Peters TM, King GW, Johnson JA. Development of an image-based technique to examine joint congruency at the elbow. *Comput Methods Biomech Biomed Engin*. 2013;16(3):280-290.
doi:10.1080/10255842.2011.617006
9. Meyer U, De Jong JJ, Bours SG, et al. Early changes in bone density, microarchitecture, bone resorption, and inflammation predict the clinical outcome 12 weeks after

- conservatively treated distal radius fractures: An exploratory study. *Journal of Bone and Mineral Research*. 2014;29(9):2065-2073. doi:10.1002/jbmr.2225
10. Fu K, Robbins SR, McDougall JJ. Osteoarthritis: the genesis of pain. *Rheumatology*. 2018;57(suppl_4):iv43-iv50. doi:10.1093/RHEUMATOLOGY/KEX419
 11. Mesci N, Mesci E, Külçü D. Association of neuropathic pain with ultrasonographic measurements of femoral cartilage thickness and clinical parameters in patients with knee osteoarthritis. *J Phys Ther Sci*. 2016;28(8):2190. doi:10.1589/JPTS.28.2190
 12. McDougall JJ, Albacete S, Schuelert N, et al. Lysophosphatidic acid provides a missing link between osteoarthritis and joint neuropathic pain. *Osteoarthritis Cartilage*. 2017;25(6):926-934. doi:10.1016/J.JOCA.2016.08.016
 13. Crisco JJ, Coburn JC, Moore DC, Akelman E, Weiss APC, Wolfe SW. In vivo radiocarpal kinematics and the dart thrower's motion. *Journal of Bone and Joint Surgery*. 2005;87(12 I):2729-2740. doi:10.2106/JBJS.D.03058
 14. Chen Z, Mat Jais IS, Teng SL, McGrouther DA. Understanding the biomechanics of the forearm during the dart thrower's motion. *Journal of Hand Surgery: European Volume*. Published online September 1, 2023. doi:10.1177/17531934231166351/ASSET/IMAGES/LARGE/10.1177_17531934231166351-FIG3.JPEG

Appendices

Appendices A: The Gender Role and Expectations of Pain Questionnaire (GREP)

ID No.: _____

Date: _____

1. How much do the following words describe you:

GREP

	Not At All	Very Little	Somewhat	A Lot	Extremely
Independent	<input type="checkbox"/>				
Emotional	<input type="checkbox"/>				
Aggressive	<input type="checkbox"/>				
Gentle	<input type="checkbox"/>				
Confident	<input type="checkbox"/>				
Weak	<input type="checkbox"/>				
Tough	<input type="checkbox"/>				
Giving	<input type="checkbox"/>				
Accepting	<input type="checkbox"/>				
Leader	<input type="checkbox"/>				
Competitive	<input type="checkbox"/>				
Determined	<input type="checkbox"/>				
Nurturing	<input type="checkbox"/>				
Sensitive	<input type="checkbox"/>				
Decisive	<input type="checkbox"/>				
Patient	<input type="checkbox"/>				

Here are 3 **different** aspects of how people can be different in how they experience pain. We will ask you about these below.

1. **Pain sensitivity** is the amount of injury or time required to cause pain.
2. **Pain endurance** is how much time passes before a person will seek relief from pain
3. **Willingness to report pain** is about whether a person is willing to tell others about their pain

2. Think about whether men or women are **usually different** in these aspects of pain. Put an **X in 1 box** on each of the 3 rows below to tell us **how much different** you think they are.

Who has more.....?	Comparing Typical Men and Women				
	Men have a lot more	Men have a little more	There is no difference	Women have a little more	Women have a lot more
Sensitivity to pain					
Endurance for pain					
Willingness to report pain					

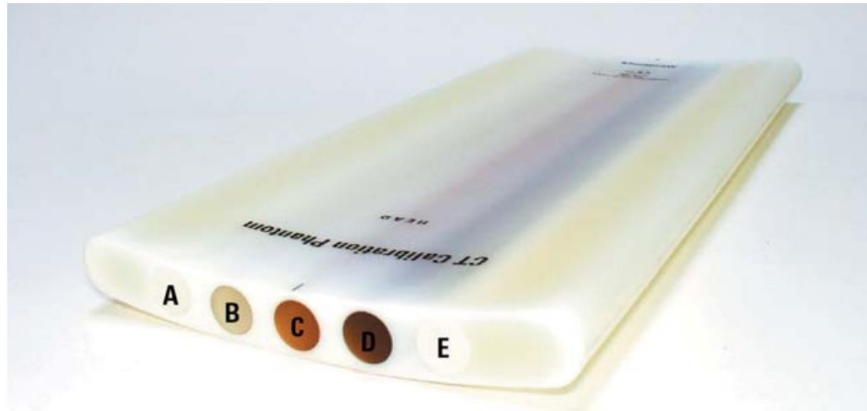
3. How would you **rate yourself** on these aspects of pain?

	Not At All	Very Little	Somewhat	A Lot	Extremely
I am sensitive to pain	<input type="checkbox"/>				
I can endure pain	<input type="checkbox"/>				
I am willing to report my pain	<input type="checkbox"/>				

4. How do you handle **pain compared to:**

	Better	No Difference	Worse
Typical Men	<input type="checkbox"/>	<input type="checkbox"/>	<input type="checkbox"/>
Typical Women	<input type="checkbox"/>	<input type="checkbox"/>	<input type="checkbox"/>

Appendices C: Calibration Phantom



Typical Composition of Various Solid Reference Materials		
Reference Rod	Eq. H ₂ O density (mg/cc)	Eq. K ₂ HPO ₄ density (mg/cc)
A	1012.2 +/- 2.3	-51.8 +/- 0.1
B	1057.0 +/- 1.9	-53.4 +/- 0.1
C	1103.6 +/- 1.7	58.9 +/- 0.1
D	1119.5 +/- 1.8	157.0 +/- 0.3
E	923.2 +/- 2.1	375.8 +/- 0.9

Image of the Model 3 CT calibration phantom, composed of a plastic base that contains five rods of reference material embedded in the base. The associated table demonstrates equivalent water and K₂HPO₄ densities. The reference material within the rods contains varying amounts of low (rod A) to high (rod E) atomic number materials.

Appendices D: The Patient-Rated Wrist Evaluation (PRWE)

PATIENT RATED WRIST EVALUATION

The questions below will help us understand how much difficulty you have had with your wrist in the past week. You will be describing your **average** wrist symptoms **over the past week** on a scale of 0-10. Please provide an answer for **ALL** questions. If you did not perform an activity, please **ESTIMATE** the pain or difficulty you would expect. If you have **never** performed the activity, you may leave it blank.

1. PAIN											
Rate the average amount of pain in your wrist over the past week by circling the number that best describes your pain on a scale from 0-10. A zero (0) means that you did not have any pain and a ten (10) means that you had the worst pain you have ever experienced or that you could not do the activity because of pain .											
RATE YOUR PAIN: Sample Scale **											
	0	1	2	3	4	5	6	7	8	9	10
	No Pain										Worst Ever
At rest	0	1	2	3	4	5	6	7	8	9	10
When doing a task with a repeated wrist movement	0	1	2	3	4	5	6	7	8	9	10
When lifting a heavy object	0	1	2	3	4	5	6	7	8	9	10
When it is at its worst	0	1	2	3	4	5	6	7	8	9	10
How often do you have pain?	0	1	2	3	4	5	6	7	8	9	10
	Never										Always
2. FUNCTION											
A. SPECIFIC ACTIVITIES											
Rate the amount of difficulty you experienced performing each of the items listed below - over the past week, by circling the number that describes your difficulty on a scale of 0-10. A zero (0) means you did not experience any difficulty and a ten (10) means it was so difficult you were unable to do it at all.											
Sample scale →	0	1	2	3	4	5	6	7	8	9	10
	No Difficulty										Unable To Do
Turn a door knob using my affected hand	0	1	2	3	4	5	6	7	8	9	10
Cut meat using a knife in my affected hand	0	1	2	3	4	5	6	7	8	9	10
Fasten buttons on my shirt	0	1	2	3	4	5	6	7	8	9	10
Use my affected hand to push up from a chair	0	1	2	3	4	5	6	7	8	9	10
Carry a 10lb object in my affected hand	0	1	2	3	4	5	6	7	8	9	10
Use bathroom tissue with my affected hand	0	1	2	3	4	5	6	7	8	9	10
B. USUAL ACTIVITIES											
Rate the amount of difficulty you experienced performing your usual activities in each of the areas listed below, over the past week, by circling the number that best describes your difficulty on a scale of 0-10. By "usual activities", we mean the activities you performed before you started having a problem with your wrist. A zero (0) means that you did not experience any difficulty and a ten (10) means it was so difficult you were unable to do any of your usual activities.											
Personal care activities (dressing, washing)	0	1	2	3	4	5	6	7	8	9	10
Household work (cleaning, maintenance)	0	1	2	3	4	5	6	7	8	9	10
Work (your job or usual everyday work)	0	1	2	3	4	5	6	7	8	9	10
Recreational activities	0	1	2	3	4	5	6	7	8	9	10

Appendices E: Letter of Information and Consent (Ch. 5)



Letter of Information and Consent

Version 1.5

June 15, 2023

Protocol Title: Integrating Joint Mechanics and Biology of Chronic Inflammation to Improve First Carpometacarpal Osteoarthritis Outcomes

Patient Group

Conflict of Interest:

Dr. Aaron Fenster, who is one of the co-investigators for this study and the director of the lab that developed and built the research device used in this study. Although there are currently no financial benefits related to this device, Dr. Fenster could benefit in the future from commercialization or other similar business endeavors.

Principal Investigator

Dr. Emily Lalone, Ph.D.
St. Joseph's Hospital, Tel: XXX-XXX-XXXX

Funding Source

Bone and Joint Health Institute
Canadian Institute of Health Research

What is the purpose?

You are being invited to voluntarily participate in a research study because you have recently, or are currently suffering from pain at the base of your thumb and are being treated at the Roth|McFarlane Hand and Upper Limb Clinic. The base of the thumb is one of the most common sites in the hand to experience pain and inflammation. Osteoarthritis can develop due to biomechanical abnormalities or injury to the joint. The biomechanical function of the joint, is the ways in which it moves and functions within the thumb. Ideally, the thumb will rotate smoothly without pain or discomfort. However, in some cases there are problems or 'abnormalities' with the cartilage, bone, and ligaments. It is thought that long term inflammation (swelling) plays a key role in the breakdown of the cartilage that covers and protects the underlying bone. This can lead to substantial pain, disability, and impairment. We are conducting this study to examine the association between joint mechanics and bone density, synovial blood flow (blood flow within the joint), and ligament laxity (muscle weakness) in the carpometacarpal joint of the thumb.

Study Procedures

Participation in this study is not part of your standard of care and is entirely optional. If you agree to participate, you will be asked to visit The Robarts Research Institute on four (4) separate occasions to have images taken, and complete a pain self-assessment survey, and pinch-grip task, and other brief tasks, which are described in detail below. In addition, we will collect and transfer your clinical x-ray images, and

pain sensitivity data from your most recent and follow-up visit to the Hand and Upper Limb Clinic to the study team at Western University. The clinical data will be stripped of any of your personal information before being transferred. The time required to complete all tasks and imaging during each visit to The Robarts Research Institute is approximately 60 minutes. You will also have your hand imaged using a hospital CT scanner during same day as the other study activities, or at a later time.

2D Ultrasound Imaging: Two-dimensional ultrasound Images will be acquired using a commercial ultrasound machine, an Aplioi800 by Canon Medical. An ultrasound probe designed by Canon Medical to image musculoskeletal (MSK) anatomy will be used to capture a few images of your thumb joint. The imaging including equipment set up time will take approximately 15 minutes of your time.

3D Ultrasound Imaging: Three-dimensional ultrasound images of the base of your thumb will be acquired with a research device and will take approximately 15 minutes. The device used in this study, was manufactured at Robarts Research Institute, see figure 1 on the next page. It is not an ultrasound machine, rather is essentially a tub and a motorized stage that connects to a clinical ultrasound machine, of that type used in the hospitals and clinics. The ultrasound machine is [an](#) Health Canada approved medical device; however, the 3D device has not been reviewed by Health Canada. For this component of the imaging, you will be seated with one arm resting in a rectangular tank of water, as shown in the picture below on page 3. The water will be heated above room temperature to a maximum of thirty-five degrees Celsius (less than body temperature). The ultrasound transducer that is connected to a lever will be brought down into the water above your arm, but not touching your arm. Several acquisition scans will be taken, by which a member of the research team will begin the motion of the ultrasound probe, that will move along its lever, while images are sent into the computer. The probe then moves by motor control back to its resting position.

Hand exercise: During the 3D Ultrasound acquisitions, you will perform repetitive resistance exercises for 30 seconds. 3D Ultrasound images will be acquired before the exercise and after to assess blood flow changes associated with hand exercise. Pain ratings will also be taken on a scale of 1-10 before and after exercise.

Pain Self-Assessment: You will also be asked to perform two physical tests. In one of the tests, you will pinch your pinky finger and thumb together and rate any pain on a scale of 1-10. For the other, you will be asked to squeeze a hand-held machine that measures grip strength so that we can measure the strength of your hand. In addition, there are four brief surveys that you will be asked to complete with the assistance of the research assistant. These paper surveys relate to your pain, and symptoms due to your thumb pain.

Pain Sensitivity Test: You will undergo a pressure pain detection threshold (PPDT) test using a digital algometer, in the same manner that was done during your clinical visit. Following a standardized procedure, the rubber tip of the algometer will be pressed on the painful area in the wrist indicated. You will cease the test when the pressure sensation changes to painful pressure. The risks associated with the quantitative sensitivity test are also minimal but involve a momentary increase in pain. The pain will dissipate following the removal of the rubber tip of the algometer. As with all data collection, we will cease the test if any pain/ discomfort.

Hand Measurement: We will use a tape measure to measure your hand. We will be measuring the width of your hand from both sides, the width from thumb to the other side, and the distance from the wrist to the index finger.

Pinch Grip Function Test: Following the thumb self-assessment test, you will be asked to perform three different pinch grip tests using a pinch dynamometer.

Hypermobility test: Following the pinch grip test, you will be asked to perform a few motions that will test your general hypermobility and measurements of the joint angles will be collected according to the Beighton scoring system.

CT Imaging: If chosen for CT imaging, joint CT images will be conducted at Roth | McFarlane Hand and Upper Limb Centre at St. Joseph's Health Care at one of your imaging appointments only. The CT scan will take approximately 30 mins.

We will contact you at 6 months, 1 year, and 2 years following your initial diagnosis to schedule those follow-up appointments.

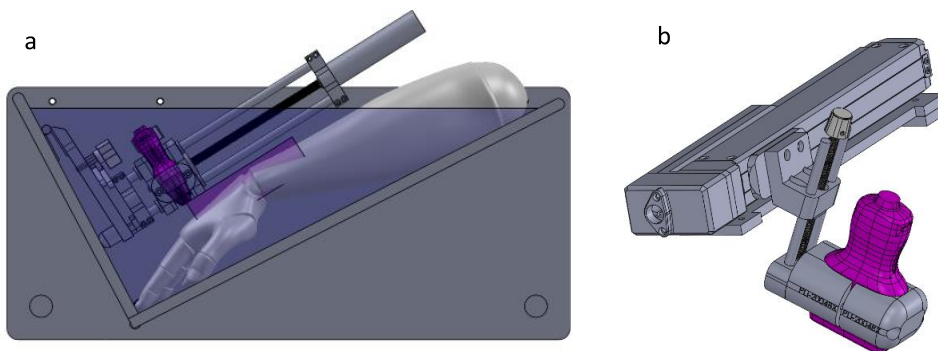


Figure 1 :a) Showing a CAD depiction of The 3D Ultrasound Wrist Imaging System, including the tub. b) A second linear stage is used to slide the ultrasound transducer at a right angle to the one in (a) to image the thumb in motion.

Potential risks of participating in this study:

For the CT, the risks involved in participating in this study are minimal but do involve exposure to ionizing radiation during the two x-ray and computed tomography (CT) scans. CT scan involves a minimal amount of radiation exposure when scanning the wrist joint. In total, you will undergo 4 CT scans. The total skin dose is 200 mSv from the wrist scans. The threshold for skin erythema from radiation exposure is 2000 mSv. Therefore, the skin dose 200 mSv from the research study is ten times lower than this threshold. You will be wearing a whole body lead apron, thyroid collar shield and leaded eye goggles.

The risks associated with the quantitative sensitivity test are also minimal, but involve a momentary increase in pain. The pain will dissipate following the removal of the rubber tip of the algometer. As with all data collection, we will cease the test if any pain/ discomfort arises to ensure your comfort.

Ultrasound imaging is a standard procedure that does not pose risk associated with the procedure.

As with all data collection, if you experience pain/discomfort during testing, we will stop testing to ensure your comfort.

Potential benefits of participating in this study:

You may not personally benefit from participation in this study. However, the results might improve outcomes following wrist injuries for future patients. The results of this research will benefit society by assessing the merit of using 3D ultrasound as a method of characterizing inflammation in CMC-1 OA patients. This is one step in the process of validating 3D ultrasound as a method of diagnosing and classifying inflammation and injury characteristics related to the thumb.

What will happen if I am experiencing pain/discomfort during my clinical assessment?

If you are experiencing any pain/discomfort or symptoms please tell the CT technician, ultrasound technician or the research team, who will immediately notify the Orthopedic Surgeon. The clinical team will continue to monitor you following completion of this study at the Hand and Upper Limb Centre. Preventative measures will be taken to reduce/avoid risk. Neither St Joseph's Health Care London, or the Principal Investigator can guarantee or assure that the stated risk, or other unknown consequences will not occur. If you become ill or injured as a direct result of participating in the study, the Principal Investigator will ensure that you receive medical care at no cost to you. By signing this consent form, you in no way, waive your legal rights.

How many people will be in this study?

There will be 100 local CMC-1 OA patients recruited in this study, along with up to 20 healthy volunteers.

Your Rights to Withdrawal from the Study

You may refuse to participate, refuse to answer any questions, or withdraw from the study at any time with no effect on your treatment. If your withdrawal is prior to the analysis of the imaging data, then the paper copies of the Letter of Information and consent will be stored per Lawson regulations, however your images will not be involved in analysis or dissemination in such manners as publications or conference presentations. Once data has been acquired and analyzed, withdrawal will not be an option. The analysis of your images will be included in the study and may be included in dissemination in such manners as publications or conference presentations. To withdraw from the study, you should tell Dr. Emily Lalone at XXX-XXX-XXXX.

Conditions Causing Withdrawal

You will be withdrawn from this study you become incapacitated or are unable to attend the follow-up imaging appointments within the 6-week, 1 year, or 2-year time period.

Will my results be kept confidential?

The overall results of the study will be available to you upon request and the information collected in the study will be confidential. By enrolling in this study, we will be collecting your name, initials, partial date of birth, sex, email, and telephone number using your hospital ID to retrieve your wrist-imaging records if they have been previously acquired. We will store the data for 15 years and Western Health Sciences Research Ethics Board and Lawson Quality Assurance and Program will have access to study files for monitoring purposes. Your individual results will be held in strict confidence. Your images that have been stripped of all personal information, may be included in publications, presentations, and shared with collaborators at external institutions. A master list is located in a locked cabinet within the lab which is also locked daily and will be stored.

Alternatives to Study Participants:

Participation in this study is voluntary. You may refuse to participate, refuse to answer any questions, or withdraw from the study at any time with no effect on your future care. You will receive a copy of this letter of information and consent from for your records. You do not have to waive any of your legal rights by signing this consent form.

Personal Costs Related to the Study

You will not incur any personal costs by participating in this study. In the event of a study related injury, you will receive medical care and treatment at no cost.

Reimbursement

You will receive \$25.00 compensation for each of the 4 visits to The Robarts Research Institute to cover parking and a snack.

Will my images be reviewed?

If the CT technologist or sonographer notices anything concerning or incidental findings in any of your images, they will share them with Dr. Assaf Kadar or Dr. Tom Appleton to review for any concerns that would require follow up. Dr. Kadar will mail the report to your family doctor. If a family doctor is not on file, you will be contacted directly by telephone.

Whom may you contact to find out more about this study?

You will be given a copy of this letter and the signed consent form. If you have questions about taking part in this study, you can directly contact

Dr. Emily Lalone, Principal Investigator.

Dr. Assaf Kadar, co-investigator.

If you have any questions/concerns about your rights as a research participant or the conduct of this study, please contact: St. Joseph's Health Care London Patient Relations Consultant at XXX-XXX-XXXX.

You will receive a copy of this letter to keep for future reference.



CONSENT FORM

Protocol Title: Integrating Joint Mechanics and Biology of Chronic Inflammation to Improve First Carpometacarpal Osteoarthritis Outcomes

Principal Investigator: Dr. Emily Lalone, Ph.D.
St. Joseph's Hospital, Tel: XXX-XXX-XXXX

I have read the letter of information, have had the nature of the study explained to me and all questions have been answered to my satisfaction and ***I agree to participate.***

For the Participant

Signature

Print name

Date

Signature of Translator (if applicable)

Print name of Translator

Date

Person Obtaining Consent

Signature

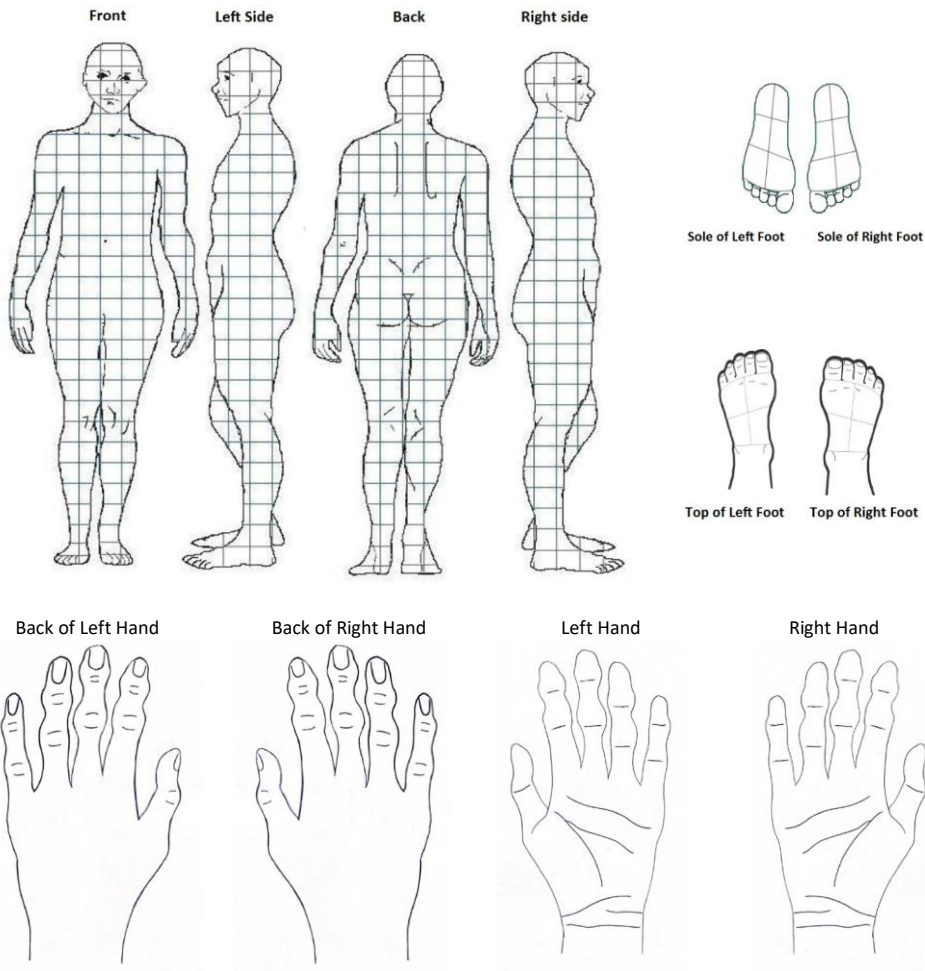
Print name

Date

Appendices F: Study Specific Body Diagram

On the diagrams below, please indicate the areas in which you are *currently* feeling symptoms.

1. First, **shade (color)** the areas in which you are feeling pain.
2. Next, **circle** the areas in which you are feeling tingling, pricking, or burning.
3. Finally, **place and 'N'** near the areas where you are feeling numbness, heaviness, or other sensations.



Appendices G: The Multidimensional Symptom Index (MSI)

ID No.: _____ Date: _____

Multidimensional Symptom Index

When answering, please consider only those symptoms that you believe are due to the condition for which you are seeking treatment.

Do this part first ↓					Then this part ↓			
How often does this bother you?					When it occurs, how intense is it? If you never experience that symptom, don't circle a number here			
Does your condition cause:	Never	Rarely	Often	Always	Barely noticeable, doesn't really bother me	Intense enough that I notice it, but can usually carry on without much effort	Quite intense, requiring real effort or support to push through it	So intense I have to stop what I am doing and seek relief
1. Sharp or shooting pain	0	1	2	3	1	2	3	4
2. General dull achiness	0	1	2	3	1	2	3	4
3. Stiffness or restricted movement	0	1	2	3	1	2	3	4
4. Weakness, clumsiness or giving way	0	1	2	3	1	2	3	4
5. Increased sensitivity to light, noise, certain odors or temperature	0	1	2	3	1	2	3	4
6. Numbness or pins & needles	0	1	2	3	1	2	3	4
7. Fatigue	0	1	2	3	1	2	3	4
8. Fogginess (difficulty concentrating or remembering things)	0	1	2	3	1	2	3	4
9. Poor appetite or nausea	0	1	2	3	1	2	3	4
10. Nervousness, anxiety or sadness	0	1	2	3	1	2	3	4

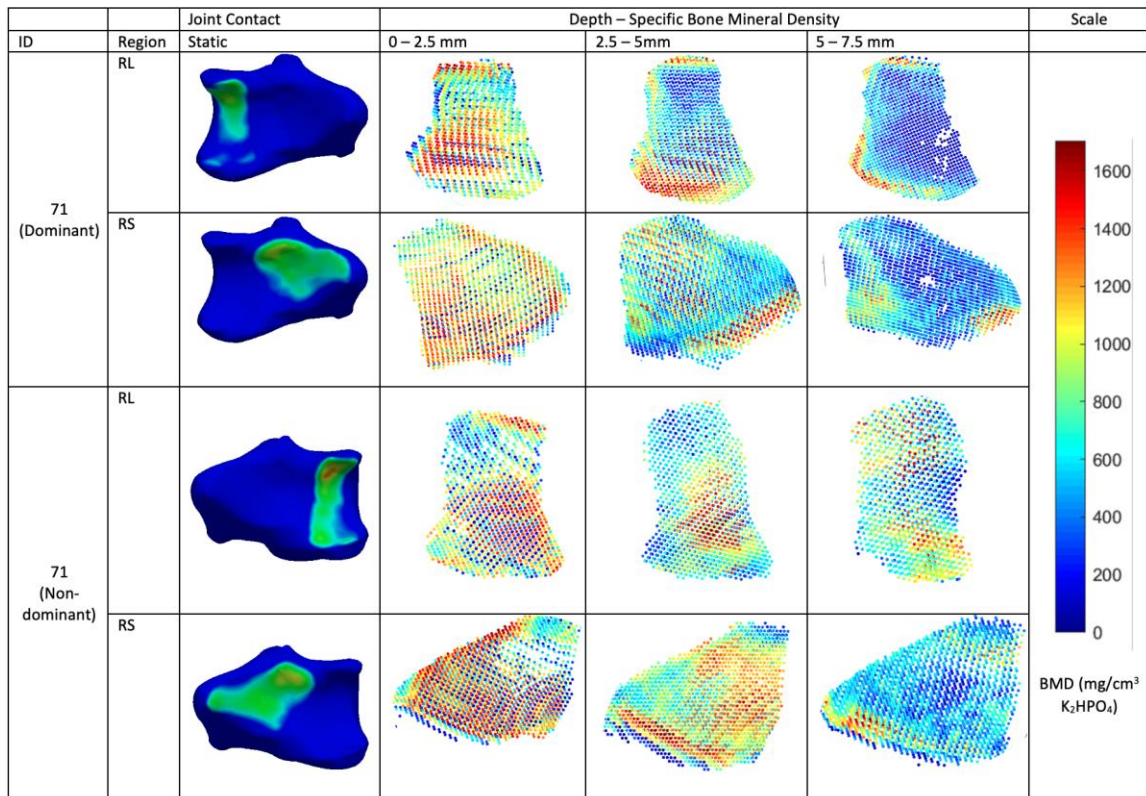
Appendices H: The Self-Reported Leeds Assessment of Neuropathic Signs and Symptoms (S-LANSS)

S-LANSS

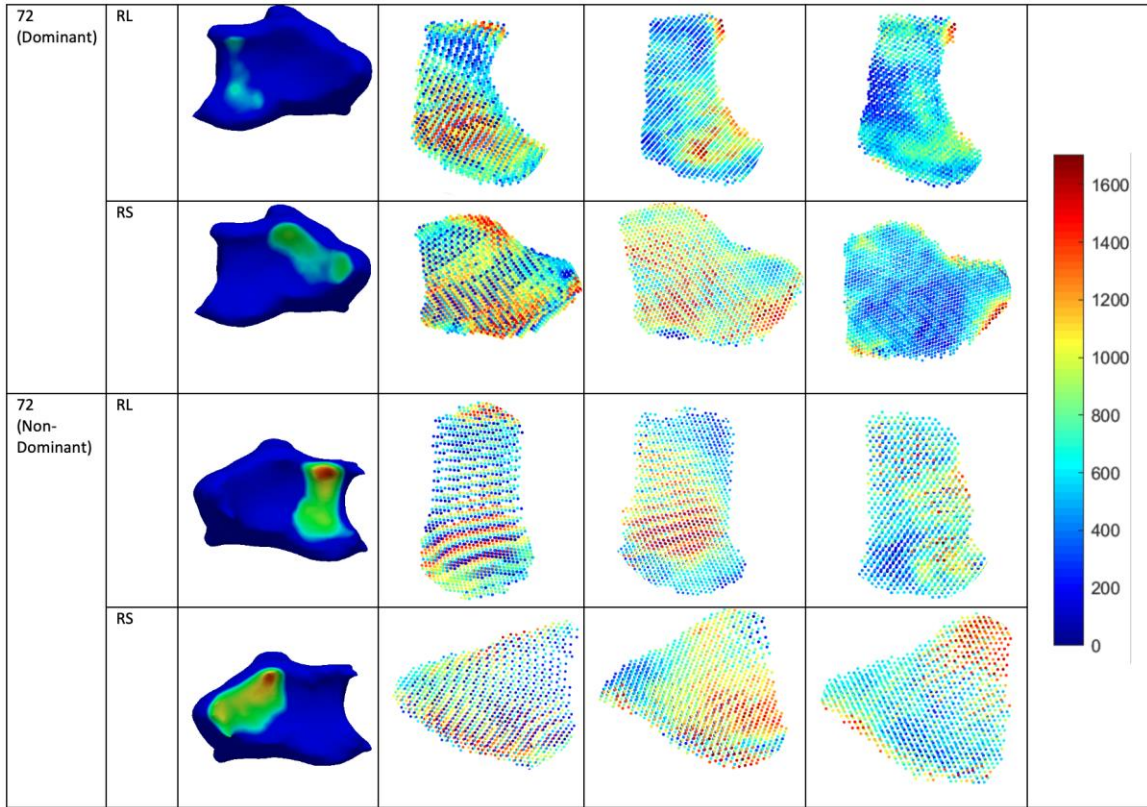
Think about how the pain you have experienced as a result of your accident has felt over the last week. Please tick (✓) the descriptions that best match your pain. These descriptions may, or may not, match your pain, no matter how severe it feels.

1. In the area where you have pain, do you also have 'pin and needles', tingling or prickling sensations?	<input type="checkbox"/> NO I don't get the sensation	<input type="checkbox"/> YES I do get these sensations (5)
2. Does the painful area change colour (perhaps looks mottled or more red) when the pain is particularly bad?	<input type="checkbox"/> NO The pain does not affect the colour of my skin	<input type="checkbox"/> YES I have noticed that the pain does make my skin different from normal (5)
3. Does your pain make the affected skin abnormally sensitive to touch? Getting unpleasant sensations or pain when lightly stroking the skin might describe this.	<input type="checkbox"/> NO The pain does not make my skin in that area abnormally sensitive to touch	<input type="checkbox"/> YES My skin in that area is particularly sensitive to touch (3)
4. Does your pain come on suddenly and in bursts for no apparent reason when you are completely still? Words like 'electric shocks', jumping and bursting might describe this.	<input type="checkbox"/> NO My pain doesn't really feel like this	<input type="checkbox"/> YES I get these sensations often (2)
5. In the area where you have pain, does your skin feel unusually hot like a burning pain?	<input type="checkbox"/> NO I don't have burning pain	<input type="checkbox"/> YES I get these sensations often (1)
6. Gently <u>rub</u> the painful area with your index finger and then rub a non-painful area (for example the skin further away from the area, or on the opposite side). How does this rubbing feel in the painful area?	<input type="checkbox"/> The pain area feels no different from the non-painful area	<input type="checkbox"/> I feel discomfort, like pins and needles, tingling or burning in the painful area that is different from the non-painful area (5)
7. Gently <u>press</u> on the painful area with your finger then gently press in the same way onto a non-painful area like you did in the last question. How does this feel in the painful area?	<input type="checkbox"/> The pain area feels no different from the non-painful area.	<input type="checkbox"/> I feel numbness or tenderness in the painful area that is different from the non-painful area (3)

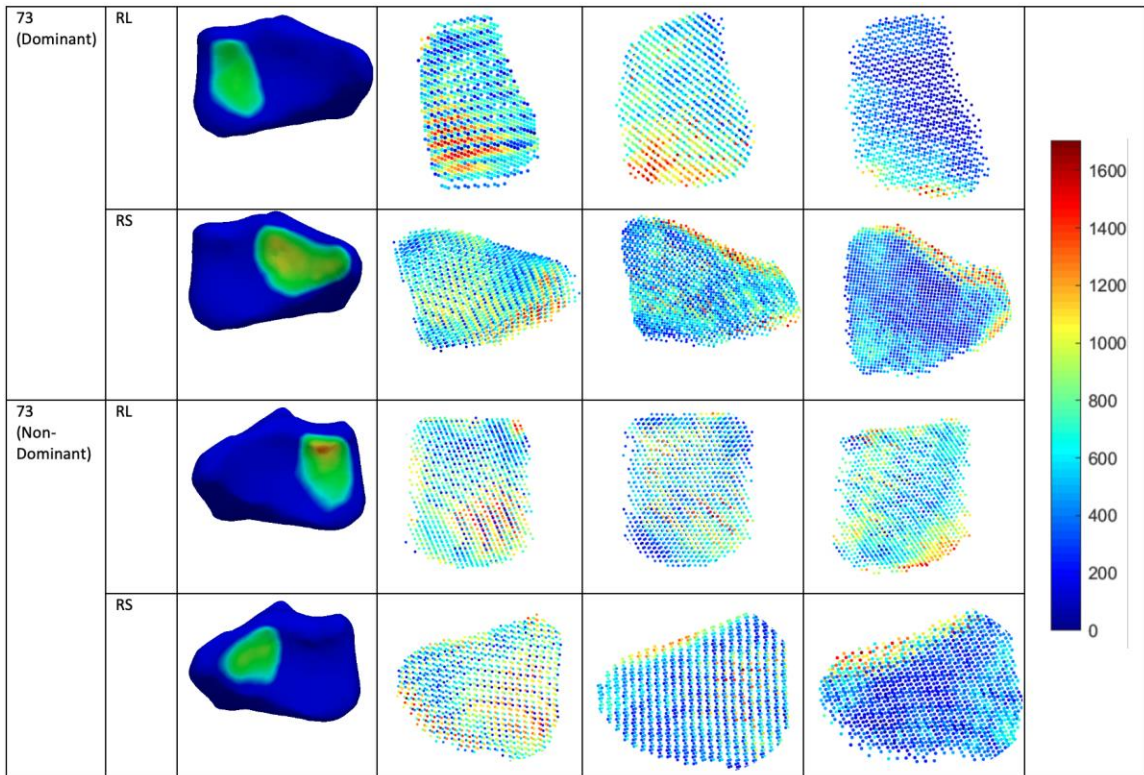
Appendices I: Additional static subject-specific JCA and subchondral vBMD maps from Chapter 3 – Healthy Participants



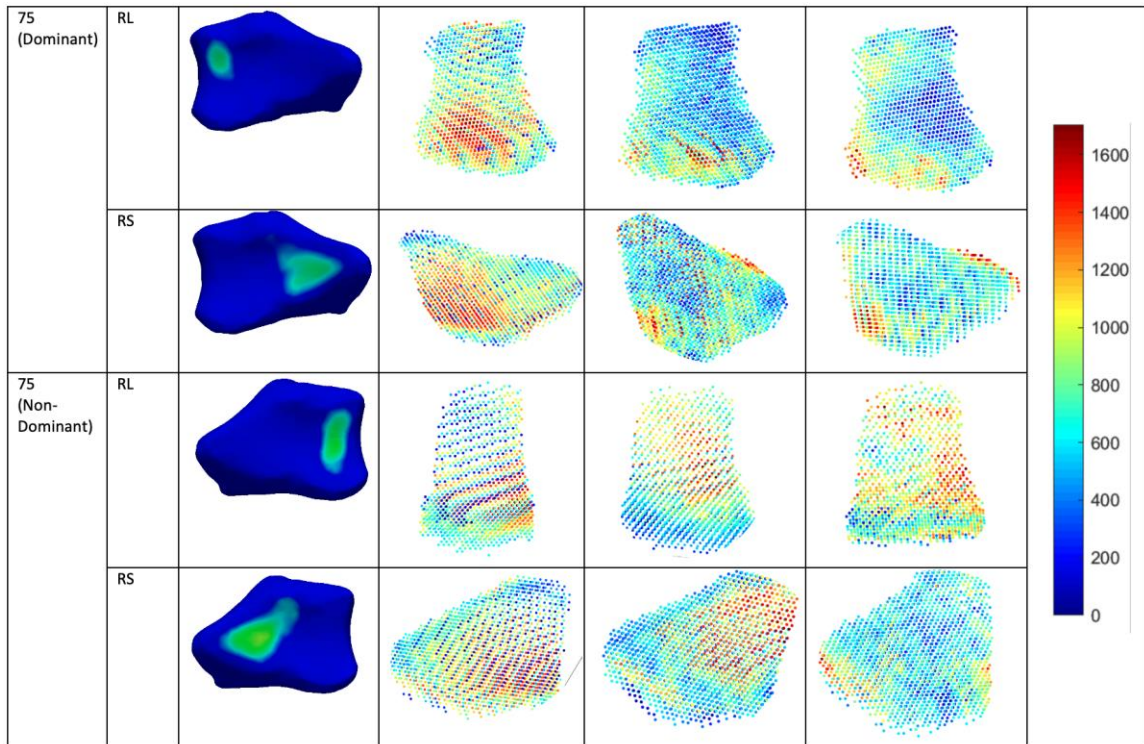
Appendices I-1: Static maps from 111702-71.



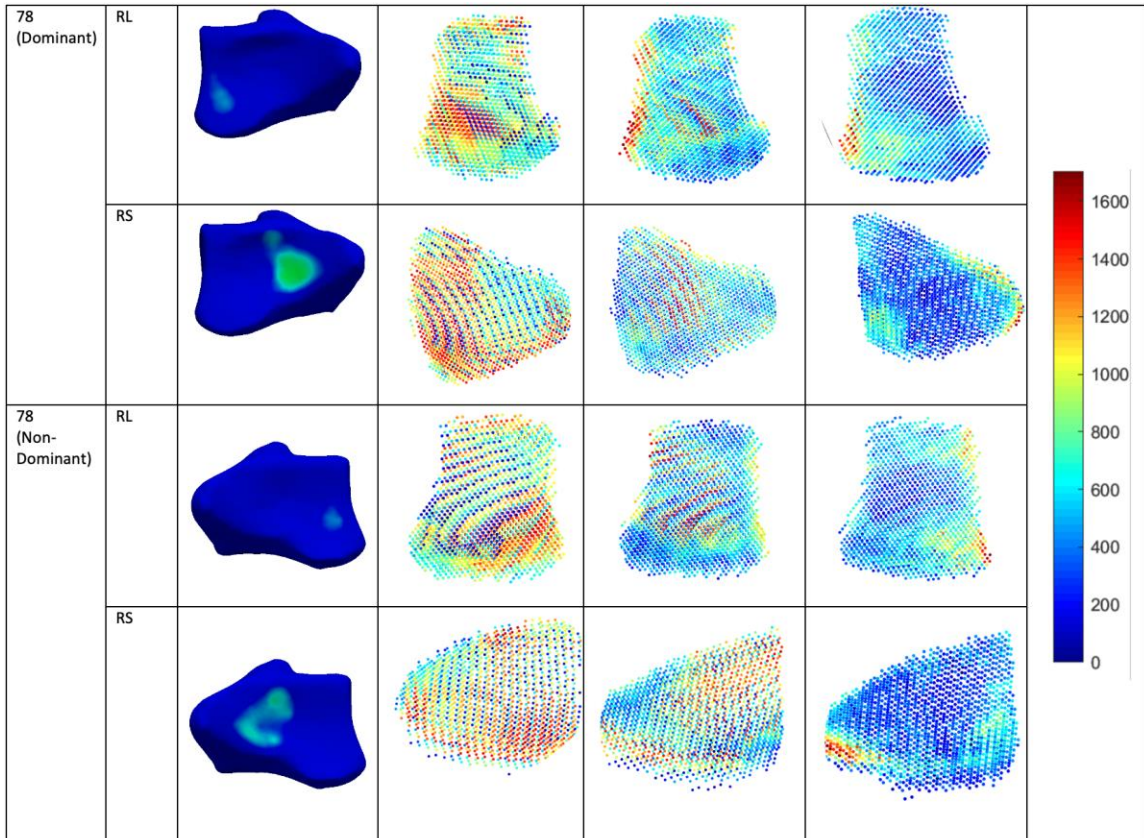
Appendices I-2: Static maps from 111702-72.



Appendices I-3: Static maps from 111702-73.

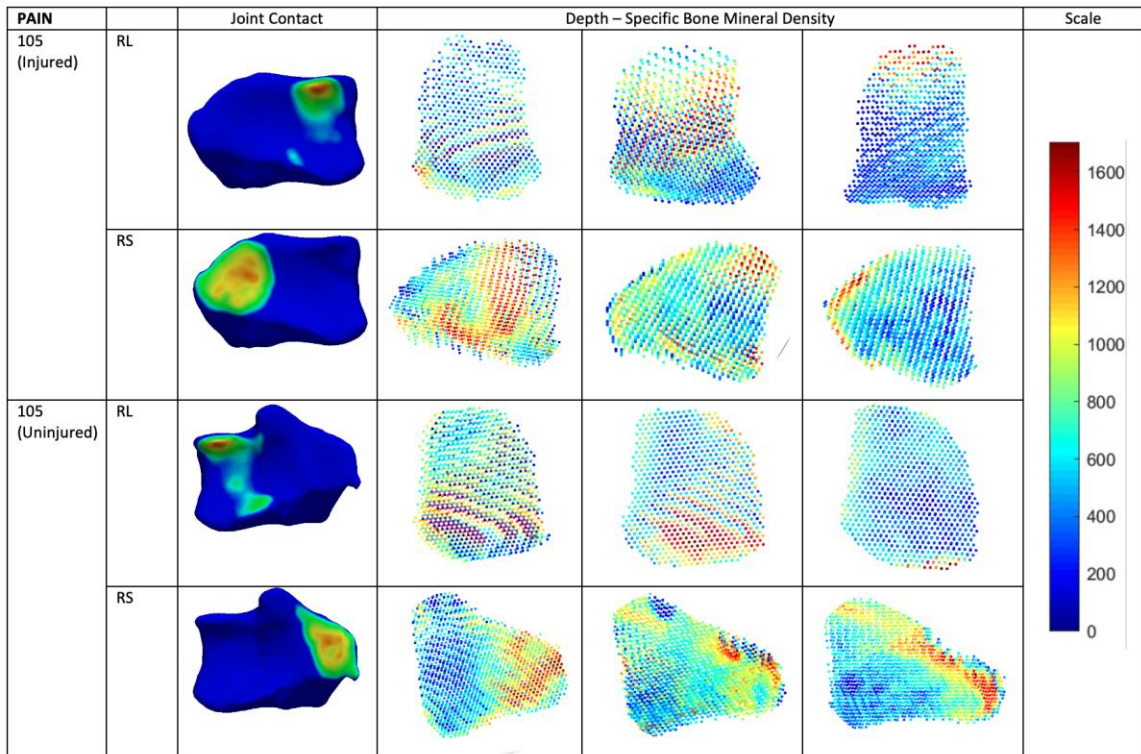


Appendices I-4: Static maps from 111702-75.

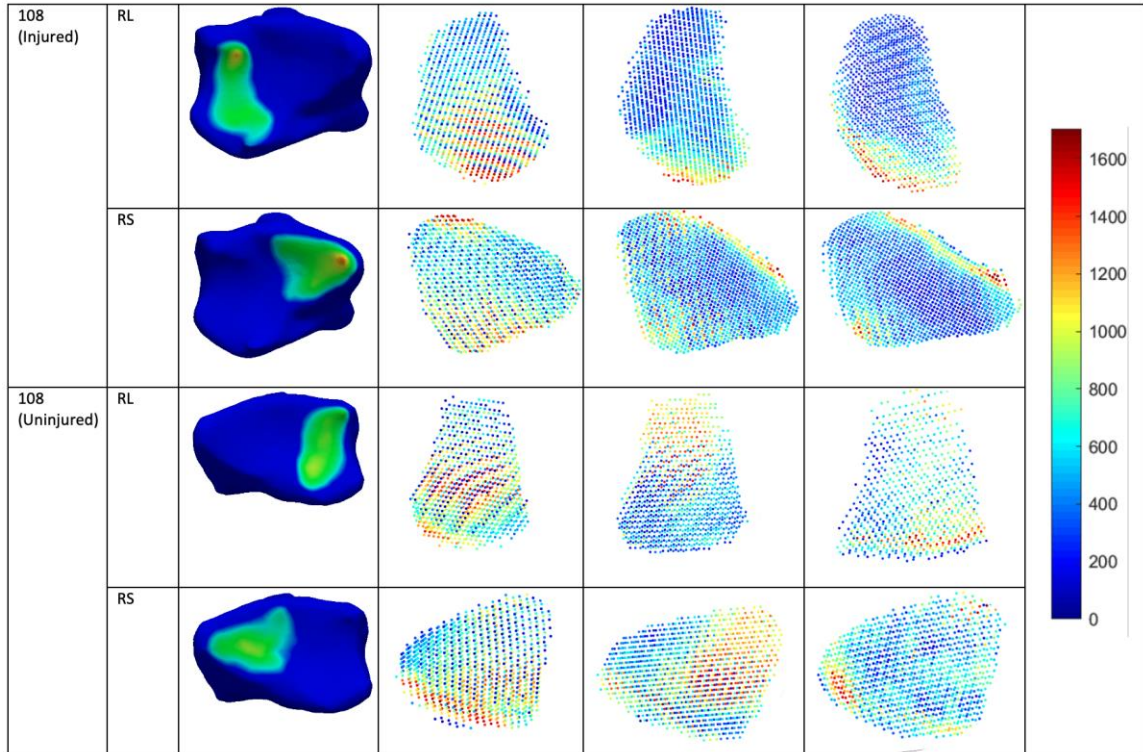


Appendices I-5: Static maps from 111702-78.

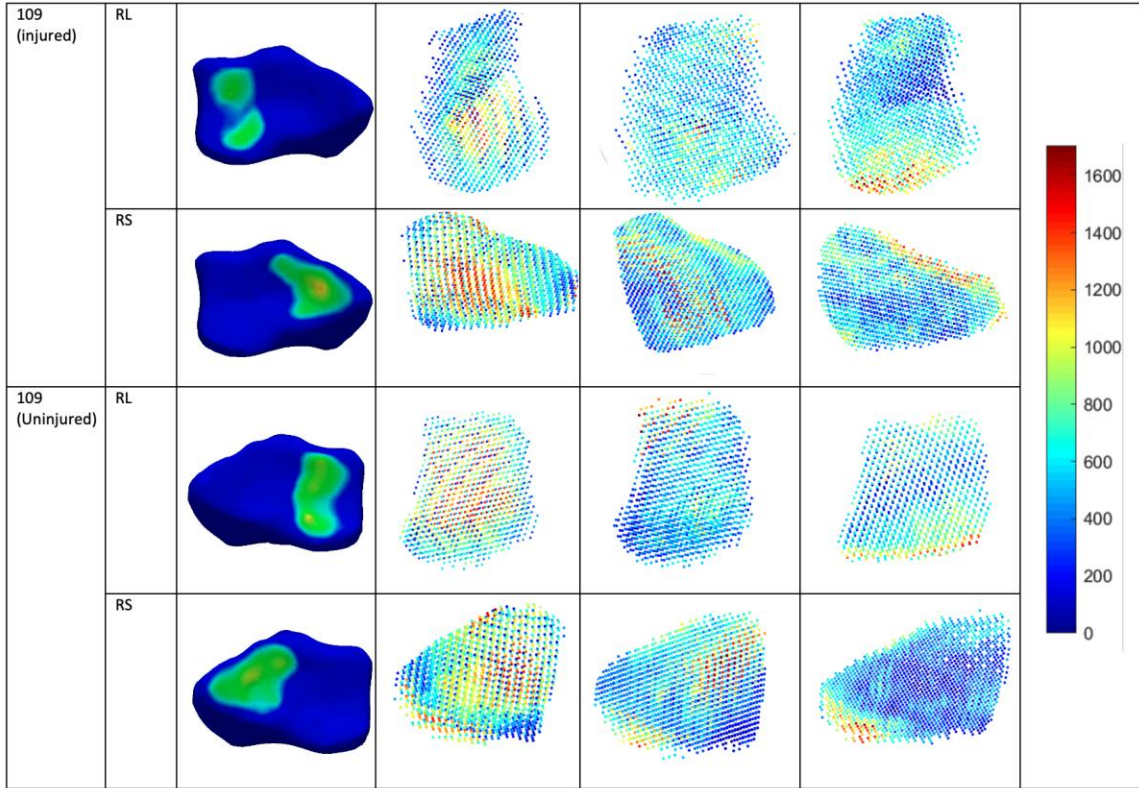
Appendices J: Additional static subject-specific JCA and subchondral vBMD maps from Chapter 3 – Wrist Trauma Participants



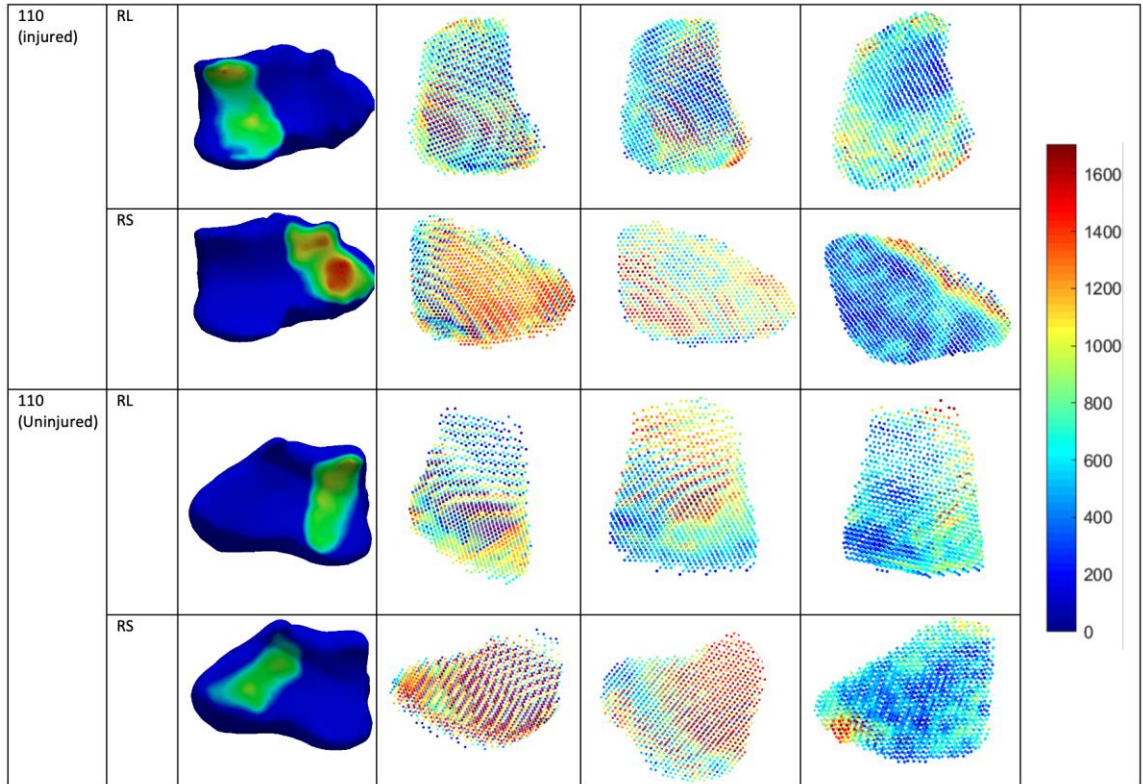
Appendices J-1: Static maps from 111702-105.



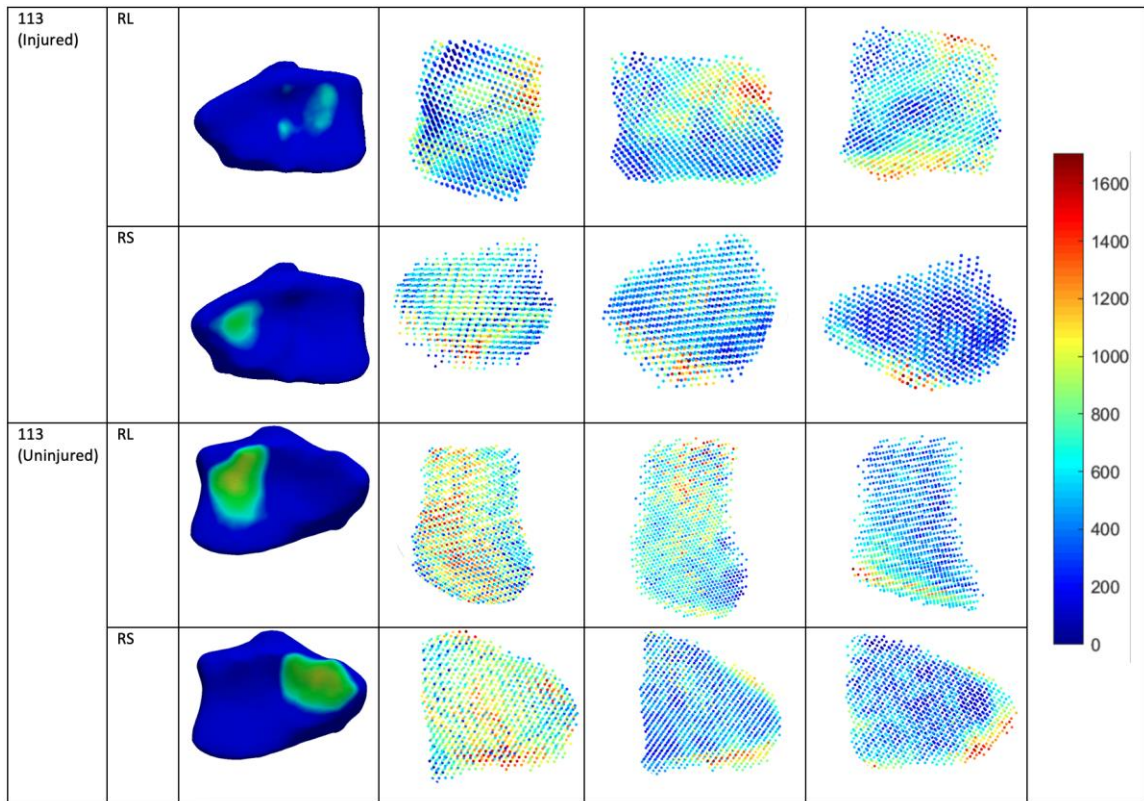
Appendices J-2: Static maps from 111702-108.



Appendices J-3: Static maps from 111702-109.

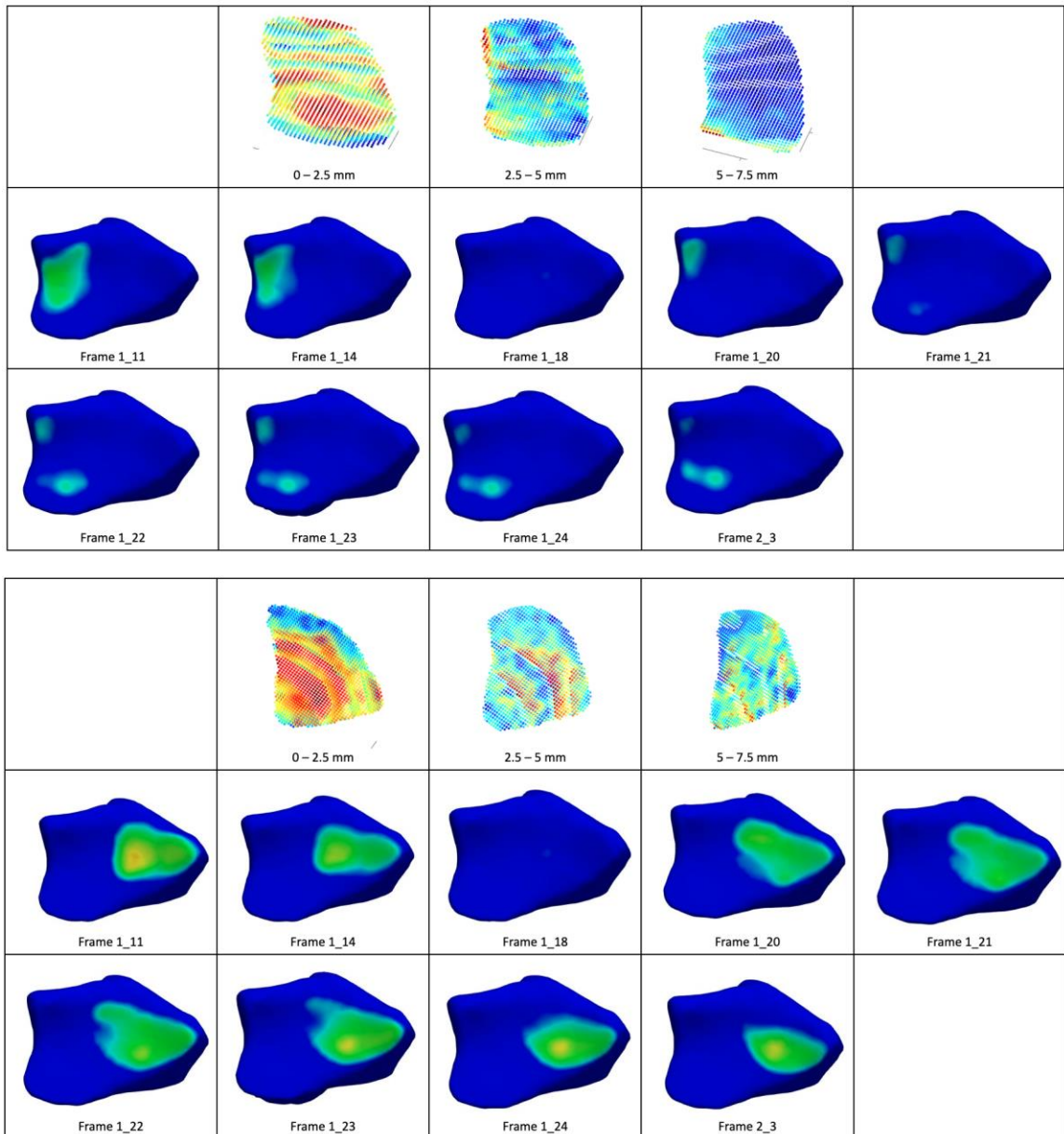


Appendices J-4: Static maps from 111702-110.

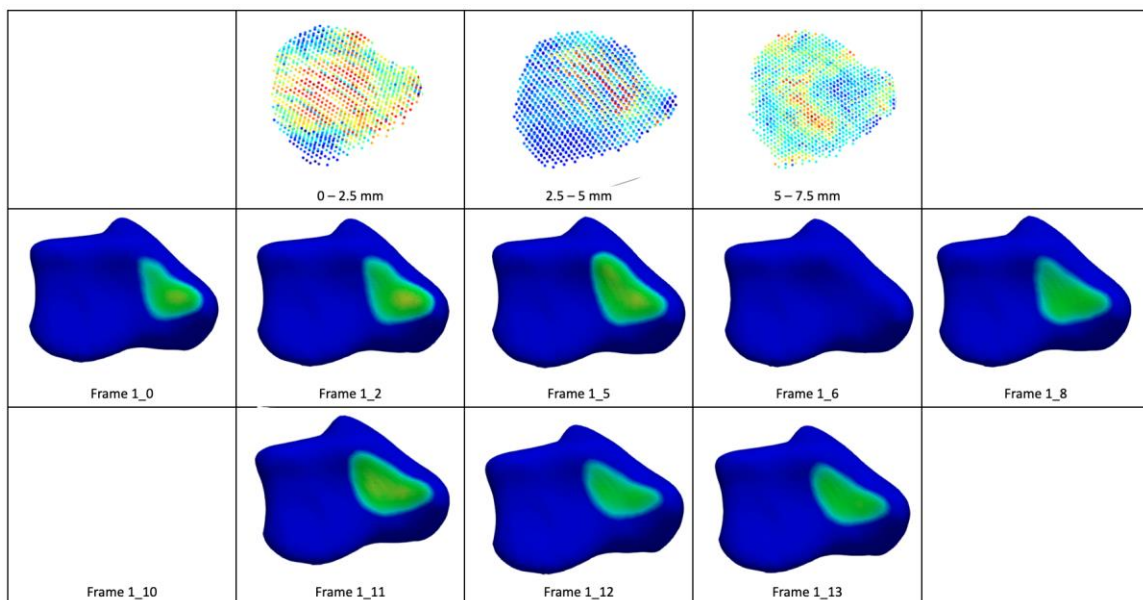
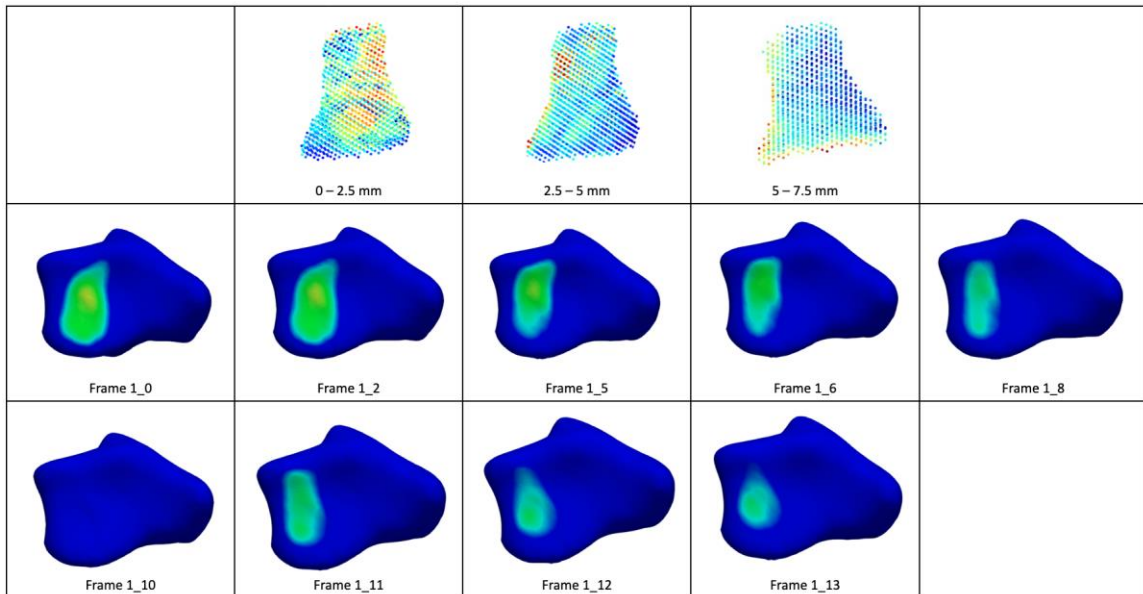


Appendices J-5: Static maps from 111702-113.

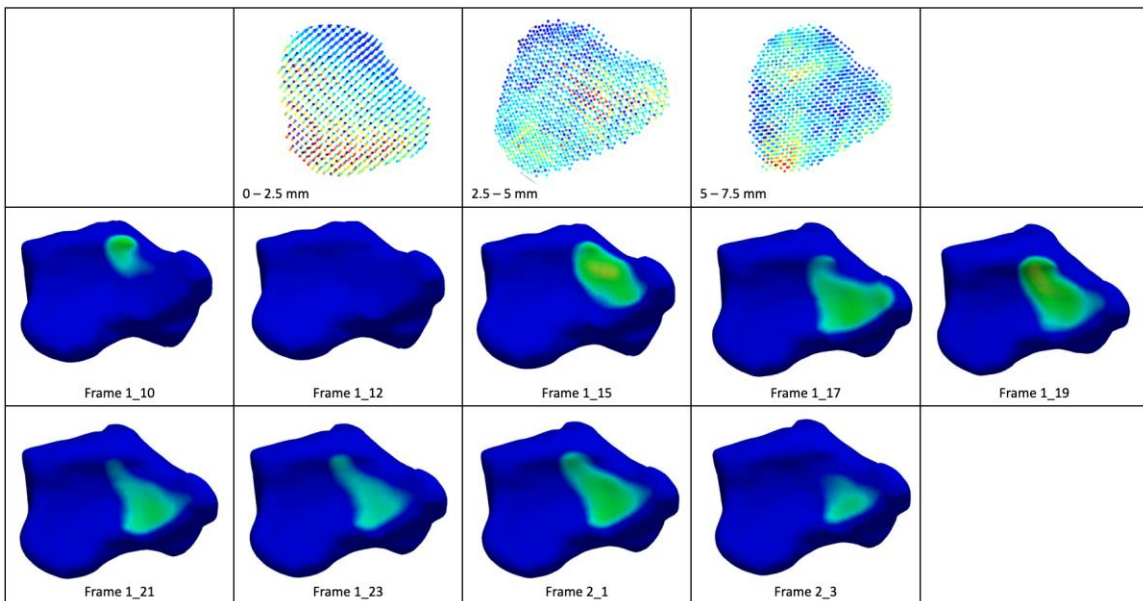
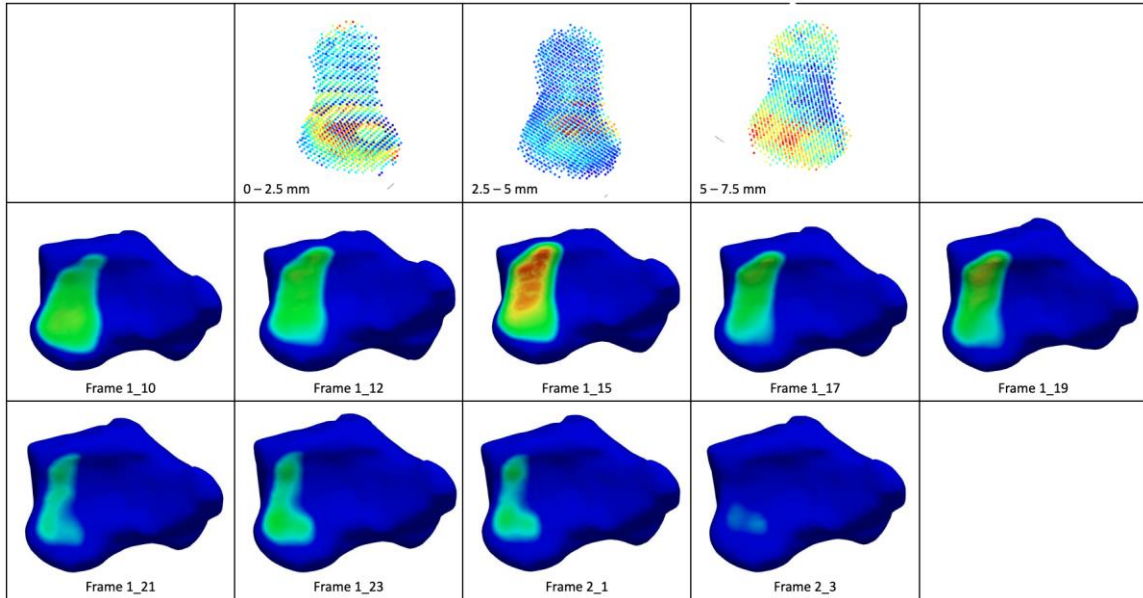
Appendices K: Additional kinematic subject-specific JCA and subchondral vBMD maps from Chapter 4 – Healthy Participants



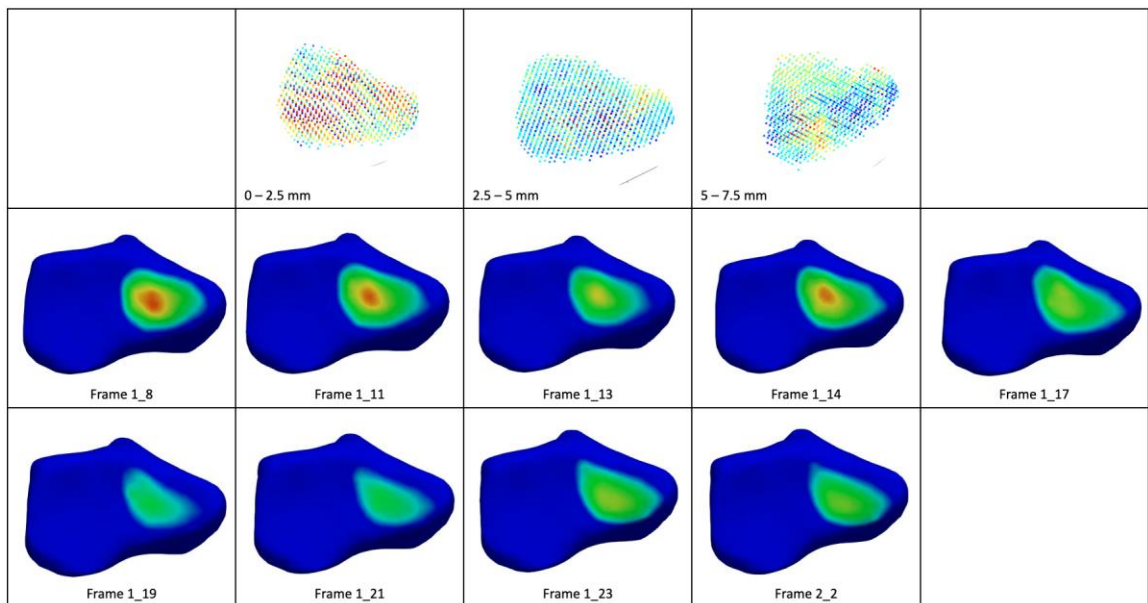
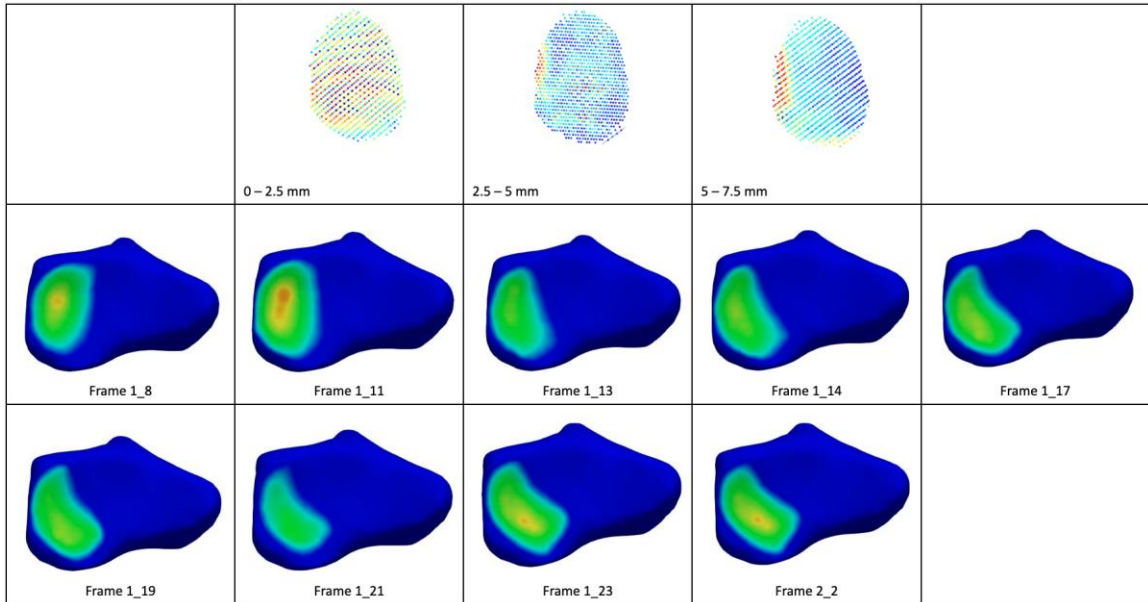
Appendices K-1: Kinematic maps from 111702-13R-Radiolunate joint (top) and radioscaphoid joint (bottom).



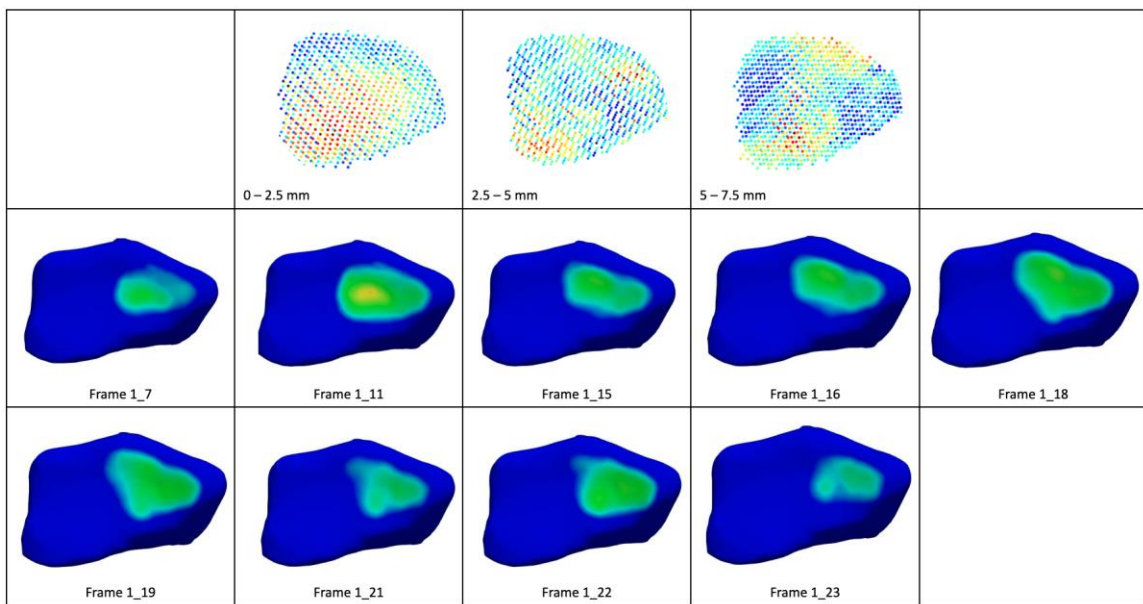
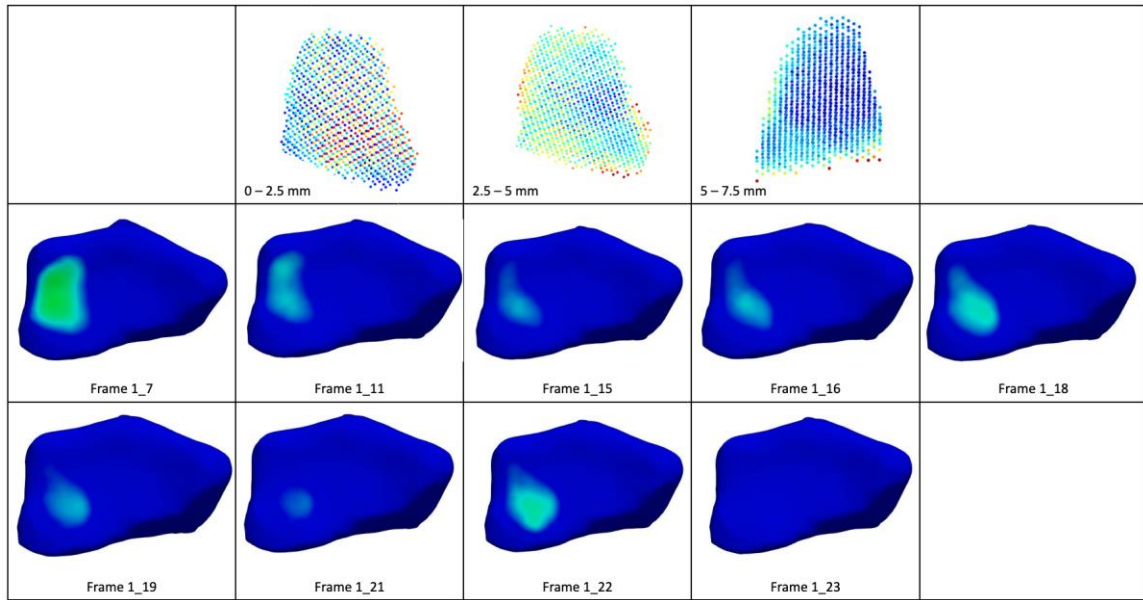
Appendices K-2: Kinematic maps from 111702-21R-Radiolunate joint (top) and radioscaphoid joint (bottom).



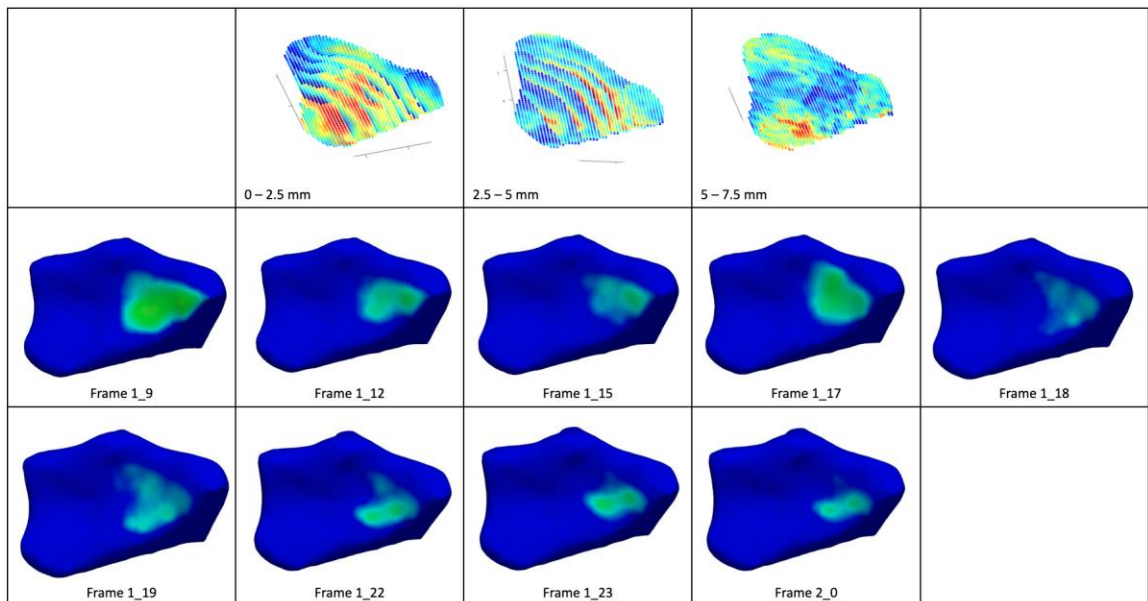
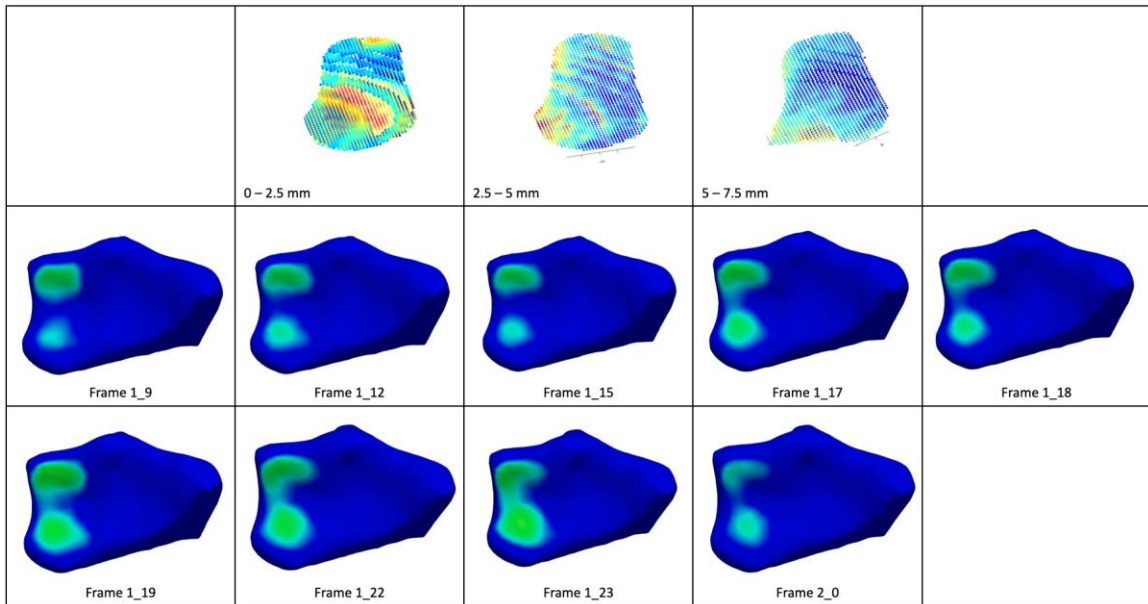
Appendices K-3: Kinematic maps from 111702-24R- Radiolunate joint (top) and radiosaphoid joint (bottom).



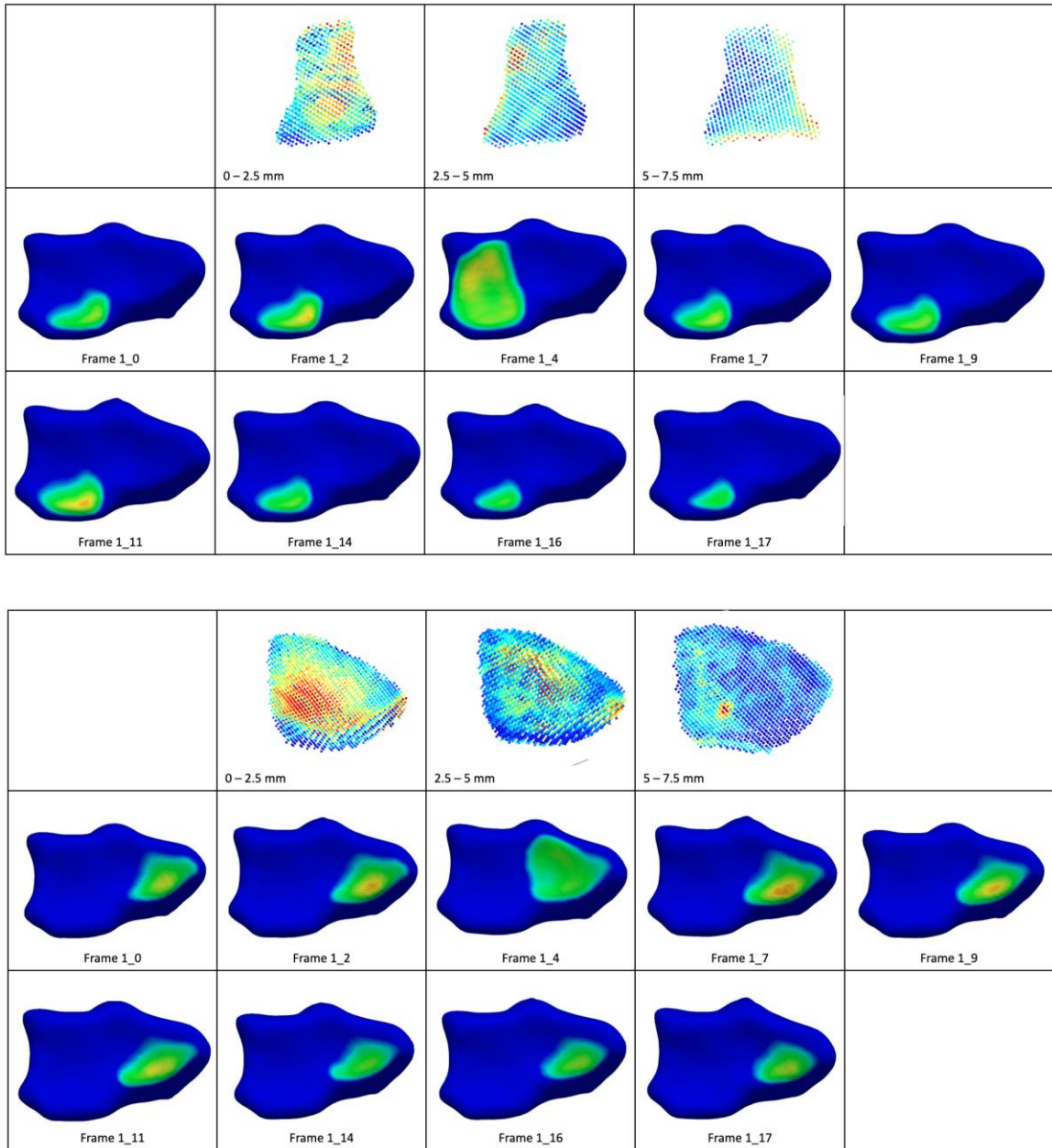
Appendices K-4: Kinematic maps from 111702-28R-Radiolunate joint (top) and radioscaphoid joint (bottom).



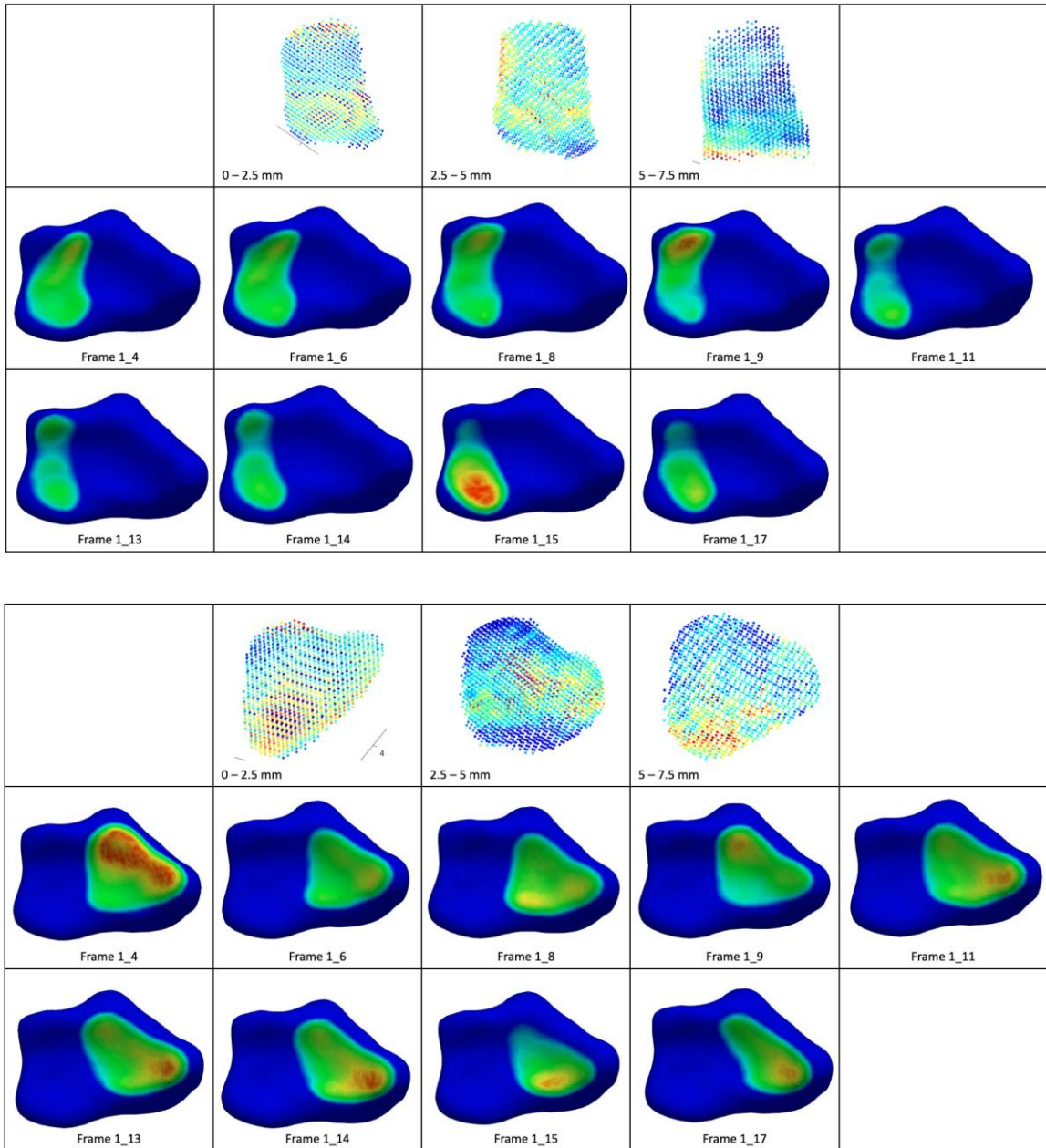
Appendices K-5: Kinematic maps from 111702-29R-Radiolunate joint (top) and radioscaphoid joint (bottom).



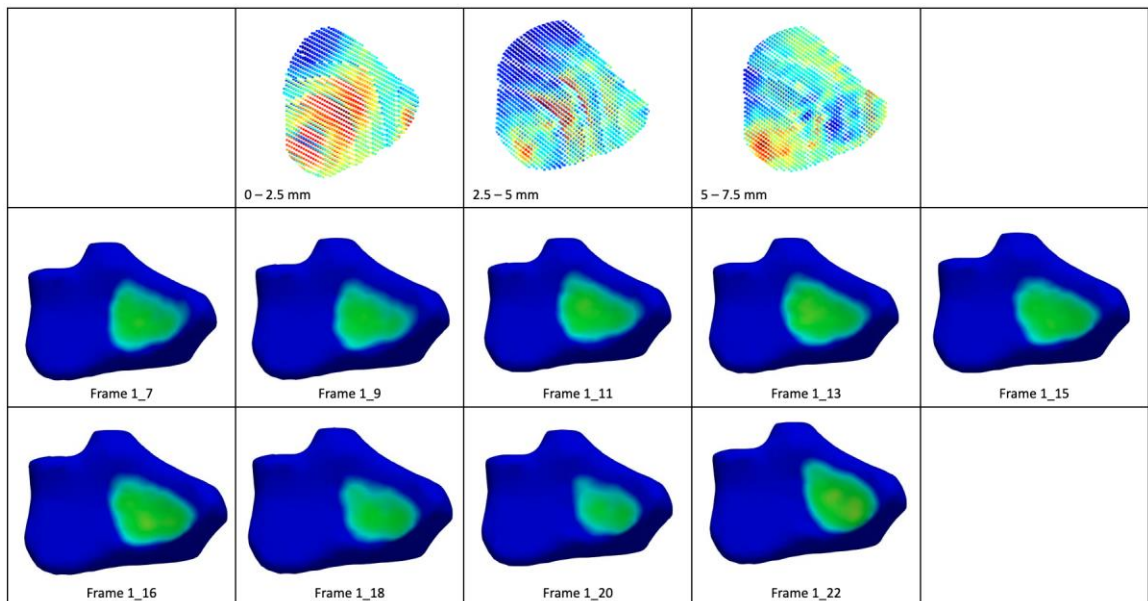
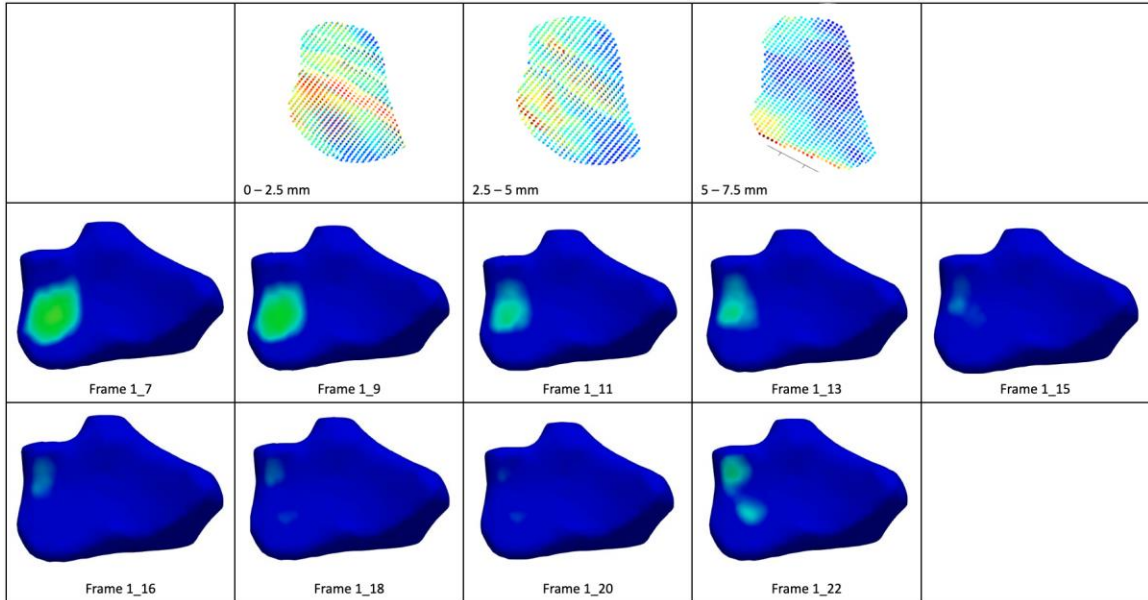
Appendices K-6: Kinematic maps from 111702-41R-Radiolunate joint (top) and radioscaphoid joint (bottom).



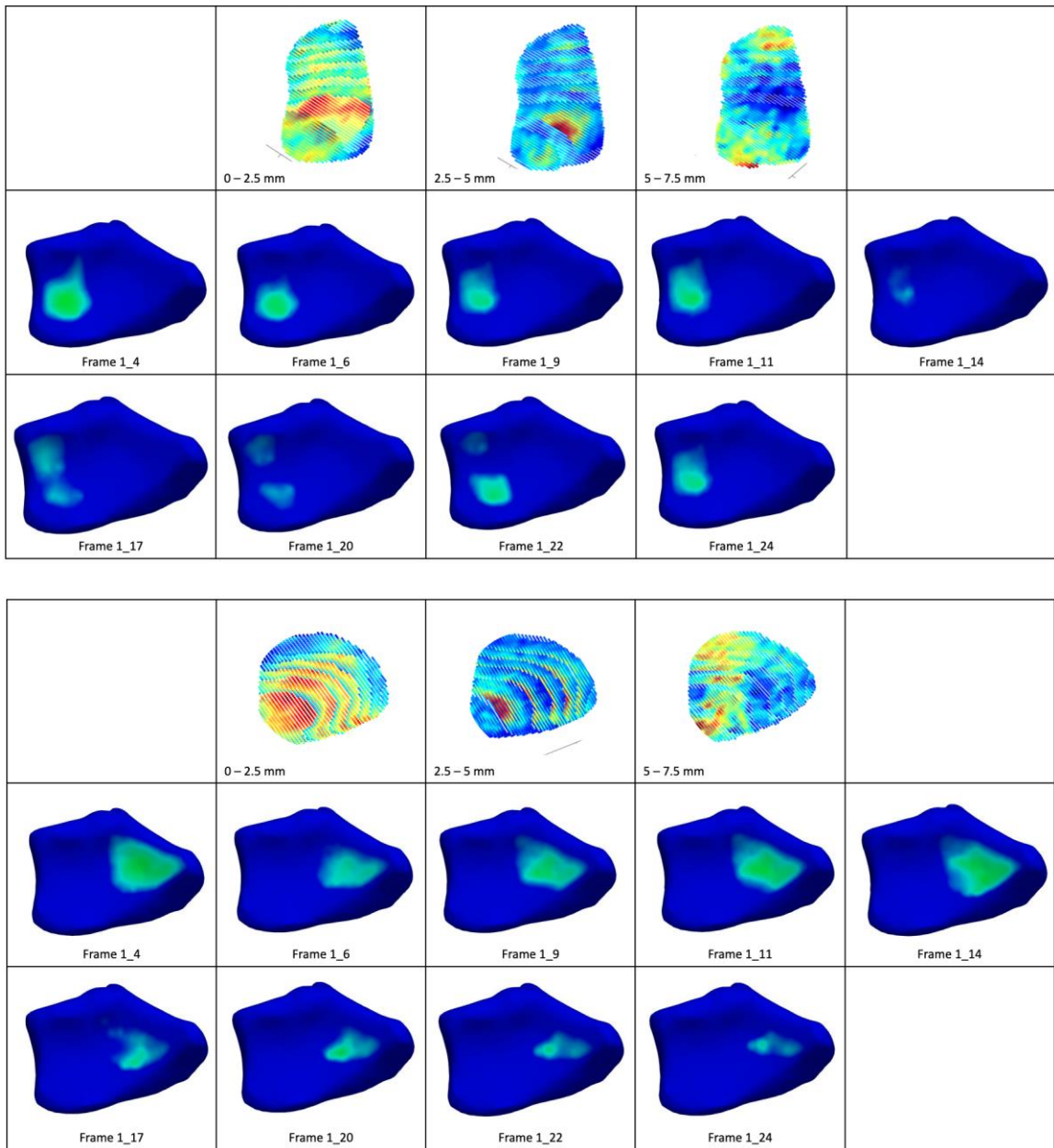
Appendices K-7: Kinematic maps from 111702-42R-Radiolunate joint (top) and radioscaphoid joint (bottom).



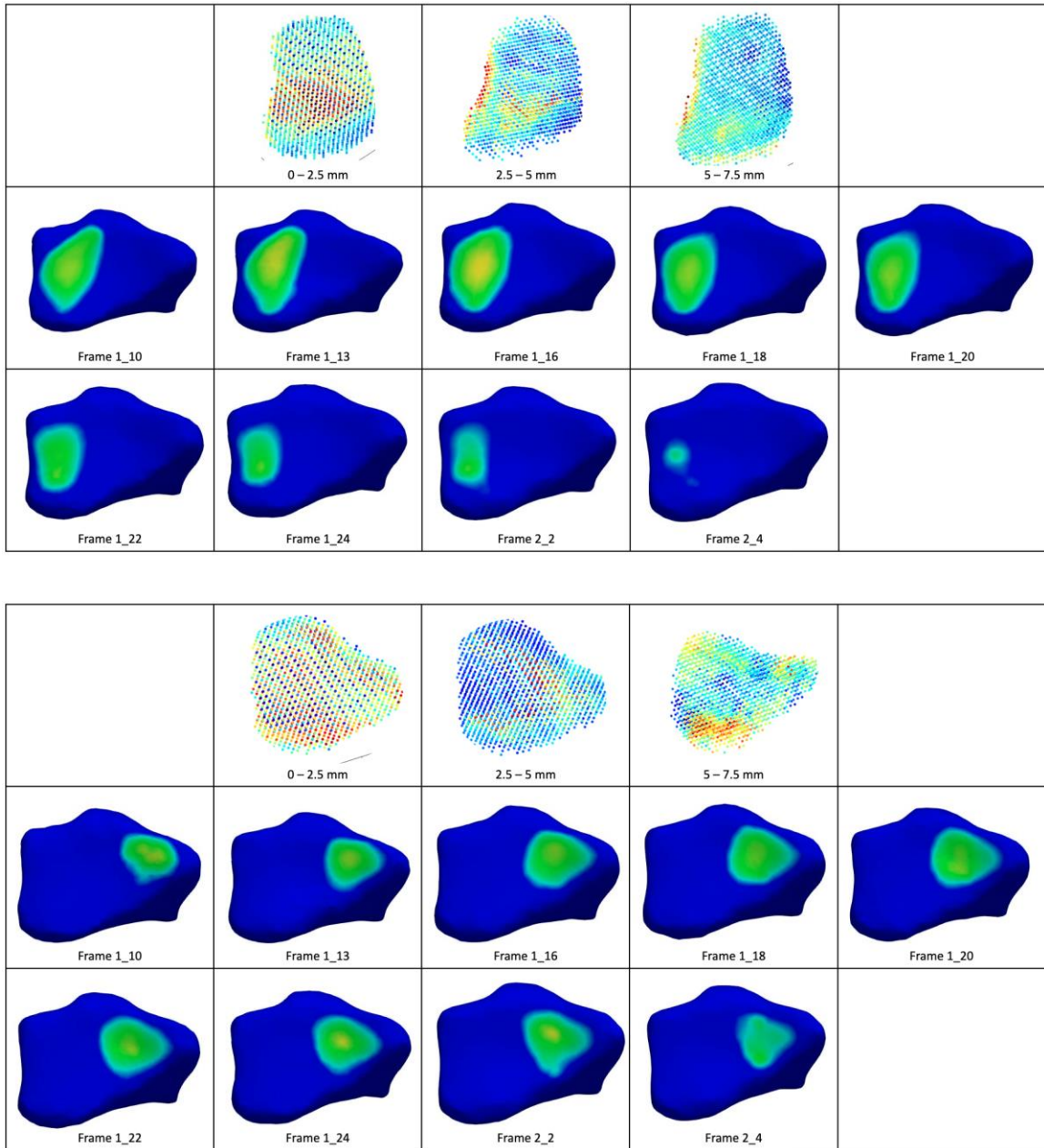
Appendices K-8: Kinematic maps from 111702-43R-Radiolunate joint (top) and radioscaphoid joint (bottom).



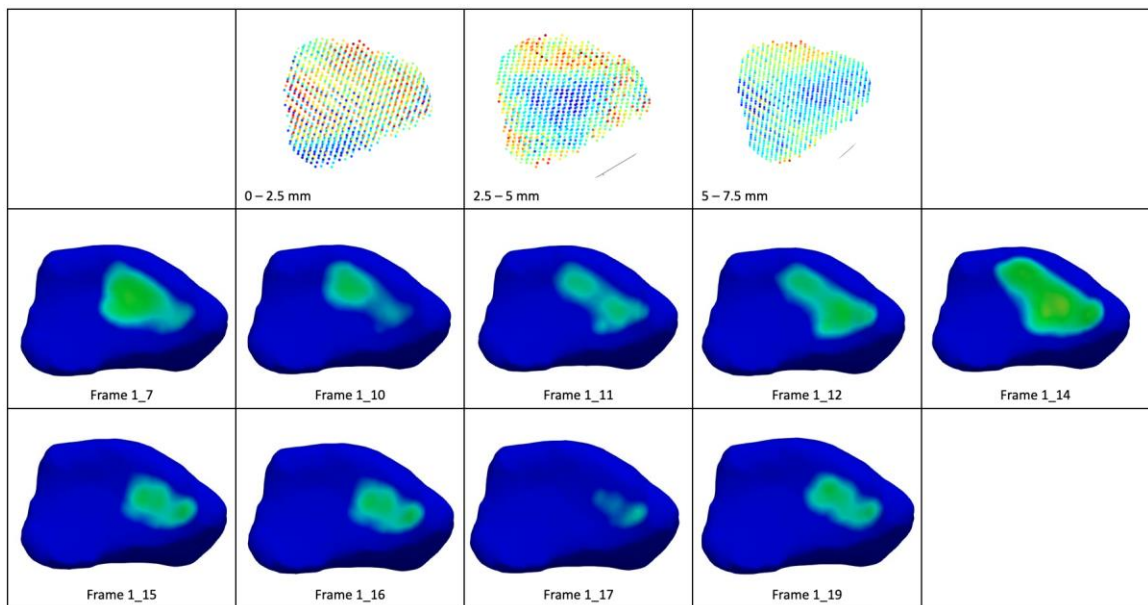
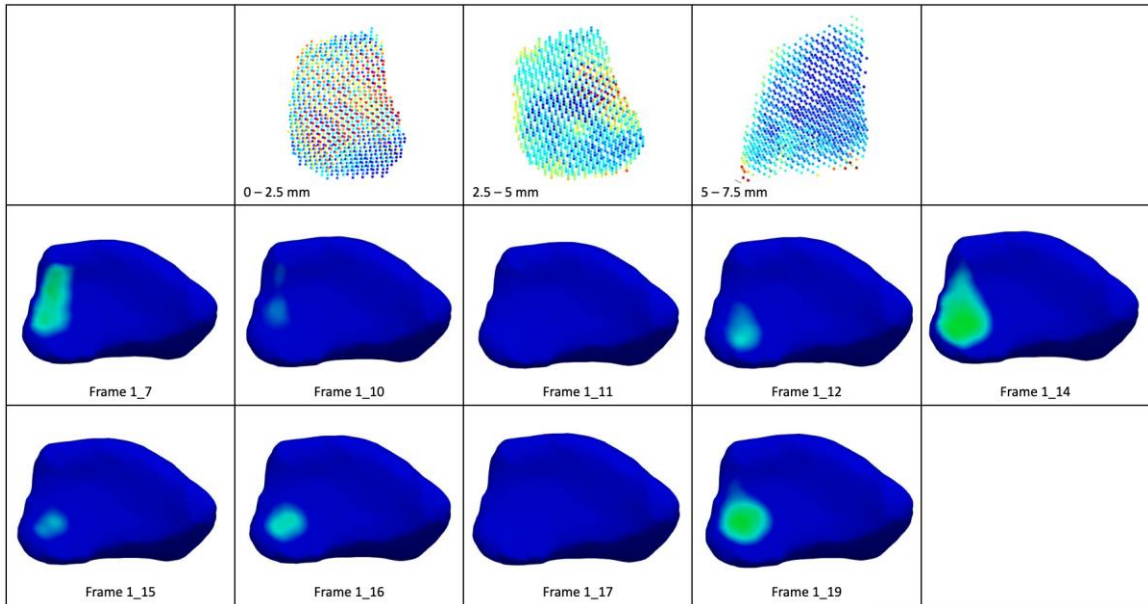
Appendices K-9: Kinematic maps from 111702-44R-Radiolunate joint (top) and radioscaphoid joint (bottom).



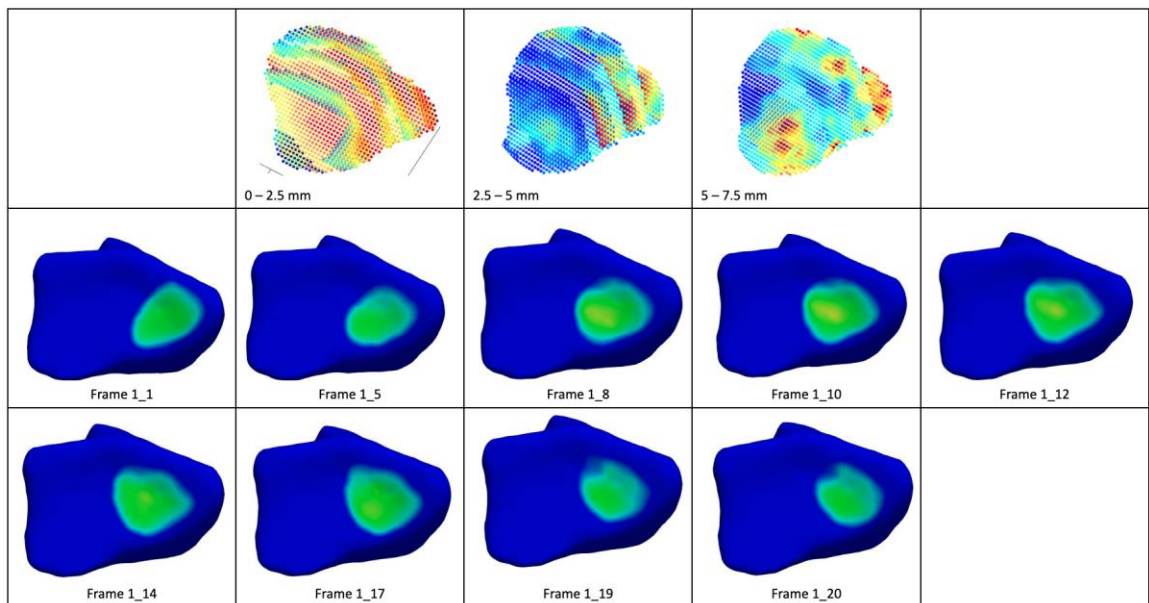
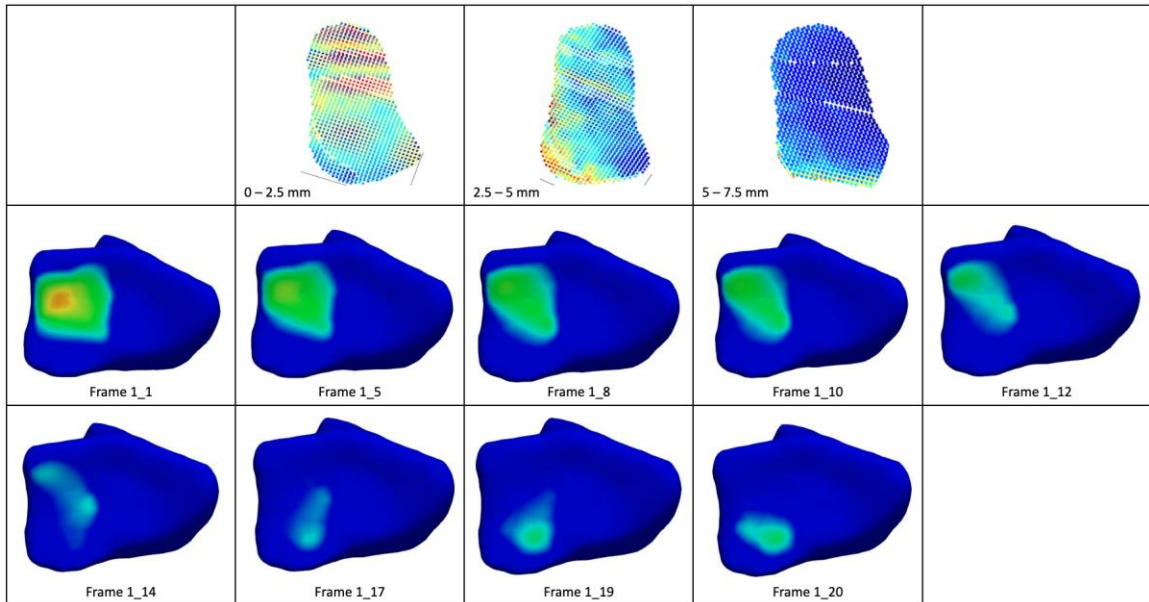
Appendices K-10: Kinematic maps from 111702-51R-Radiolunate joint (top) and radioscaphoid joint (bottom).



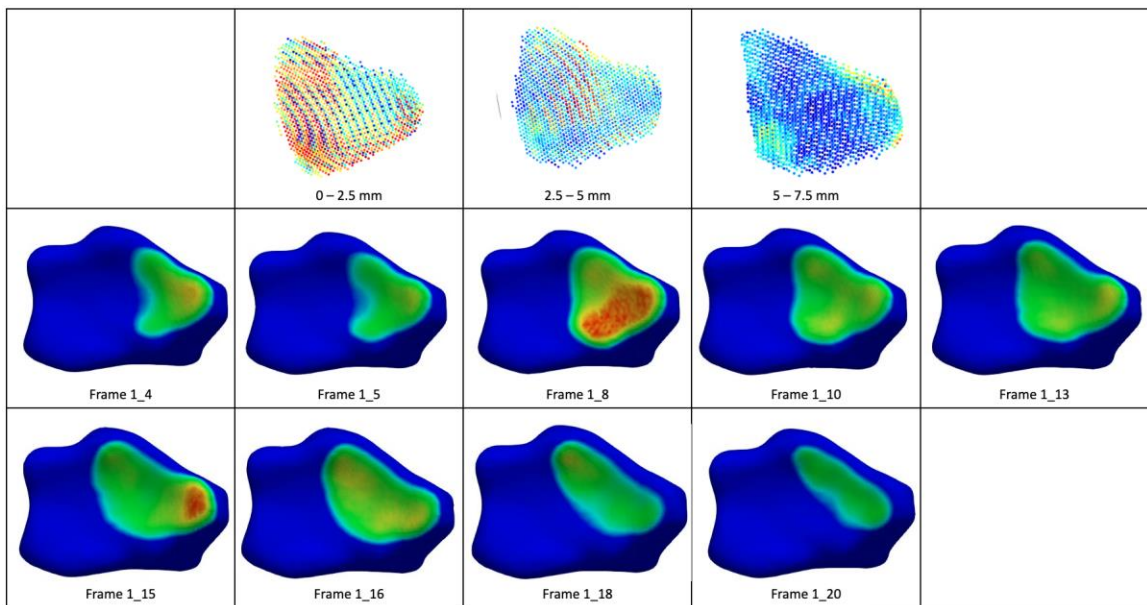
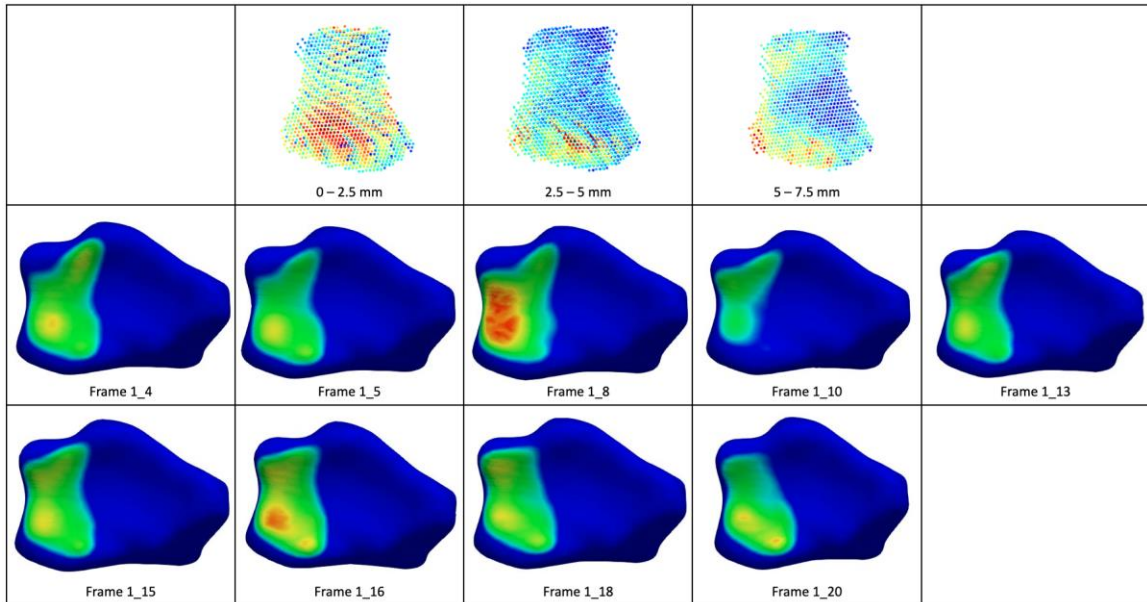
Appendices K-11: Kinematic maps from 111702-52R-Radiolunate joint (top) and radioscaphoid joint (bottom).



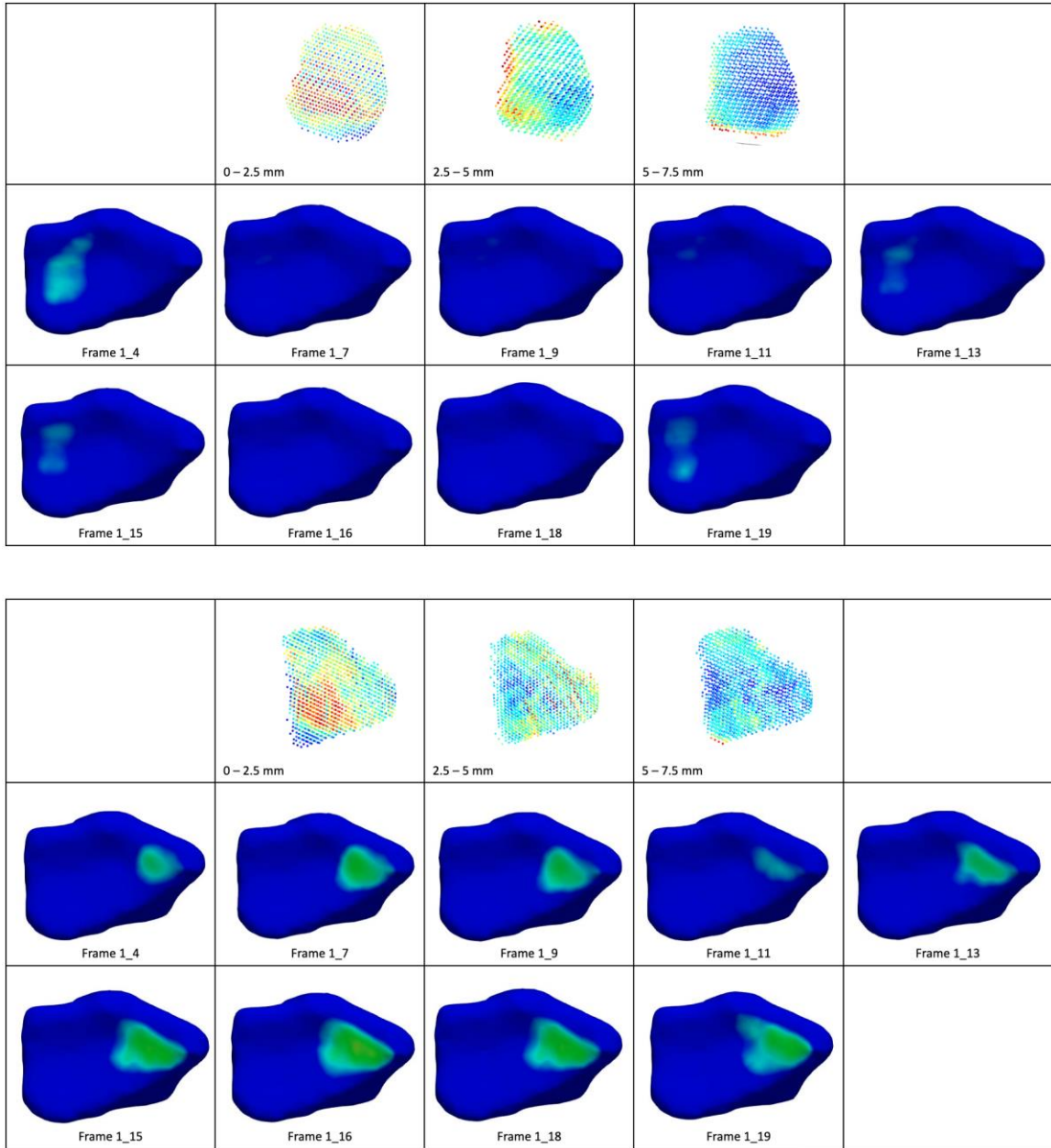
Appendices K-12: Kinematic maps from 111702-53R-Radiolunate joint (top) and radioscaphoid joint (bottom).



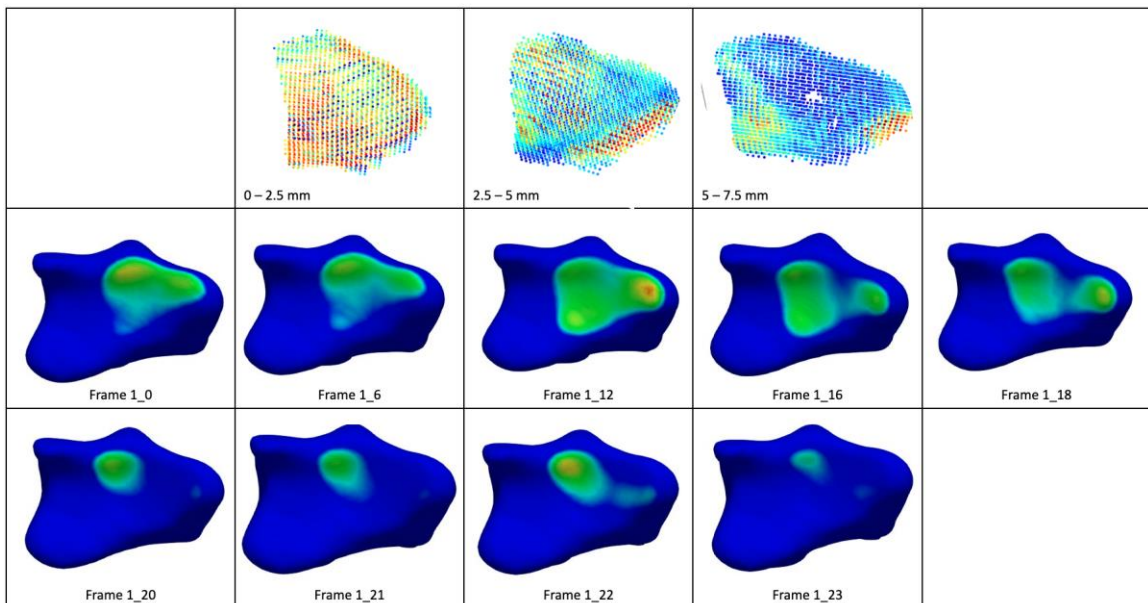
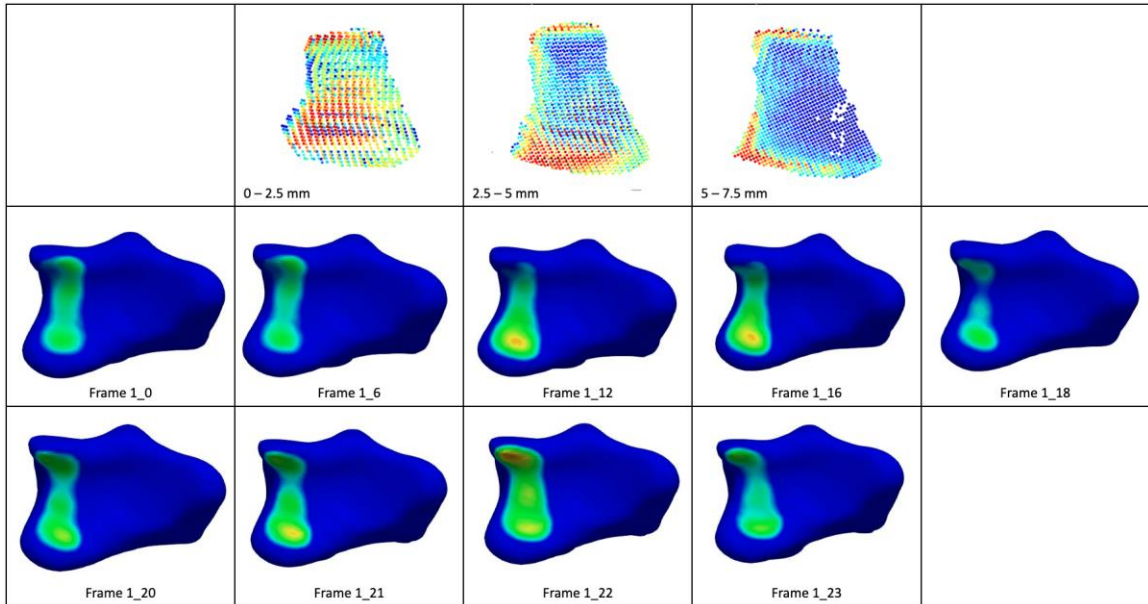
Appendices K-13: Kinematic maps from 111702-54R-Radiolunate joint (top) and radioscaphoid joint (bottom).



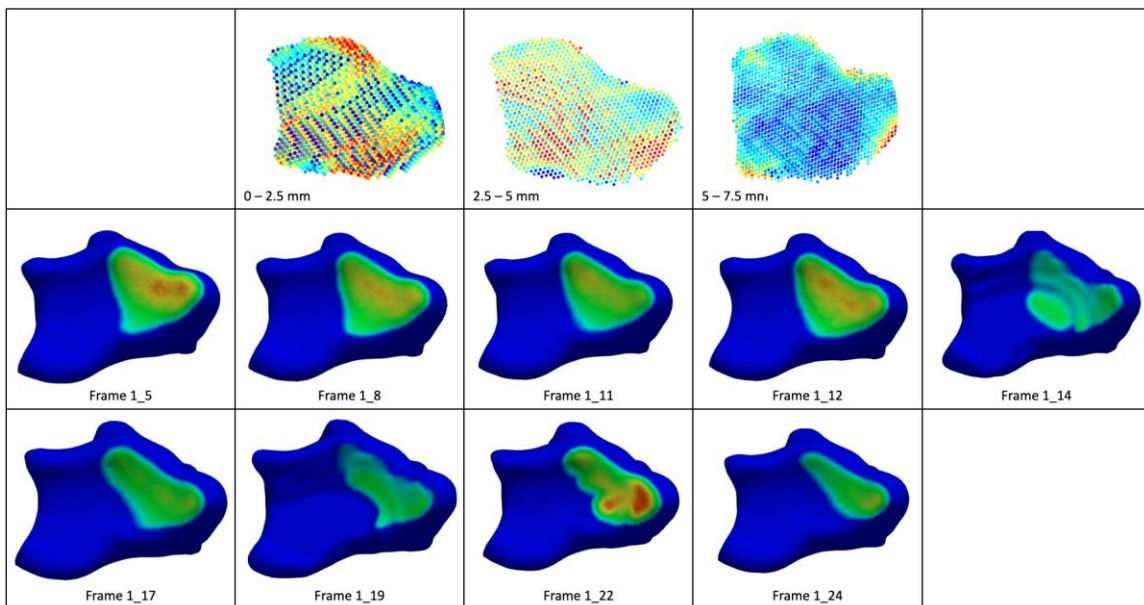
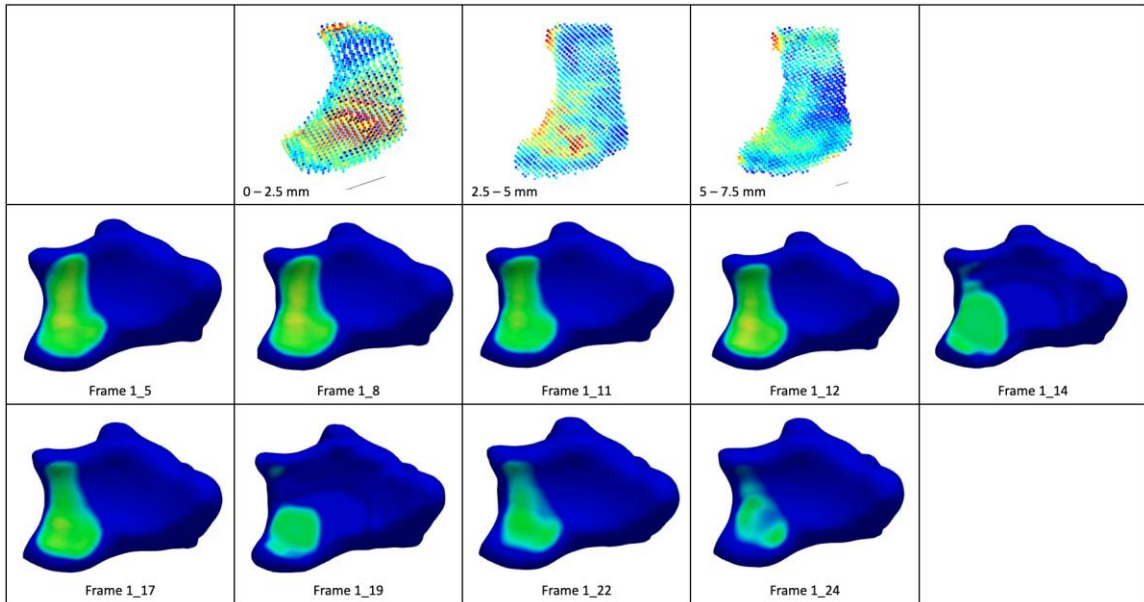
Appendices K-14: Kinematic maps from 111702-56R-Radiolunate joint (top) and radioscaphoid joint (bottom).



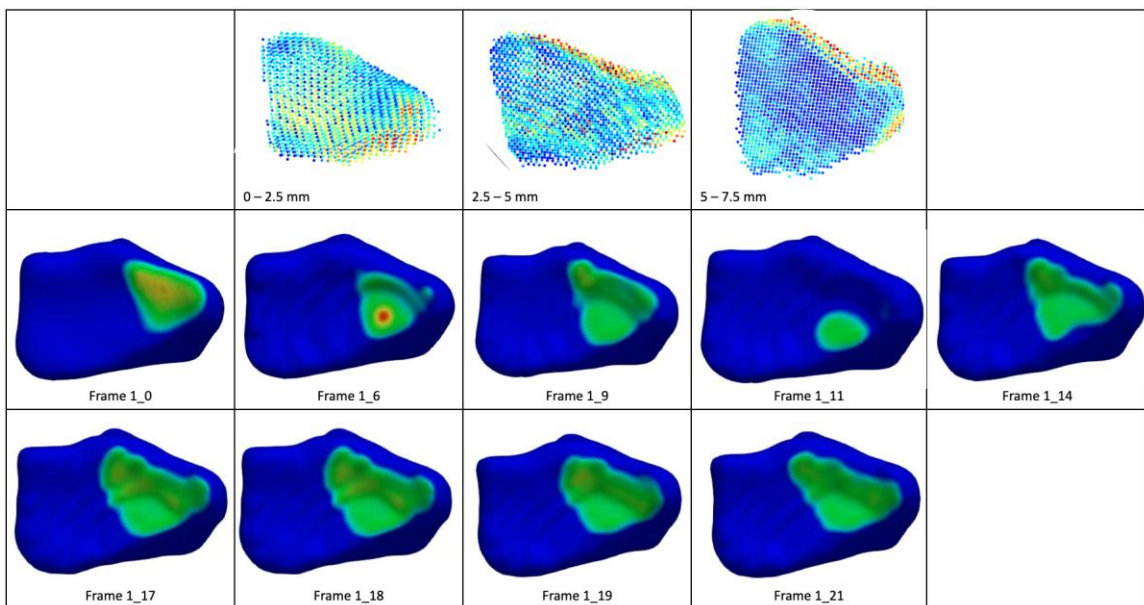
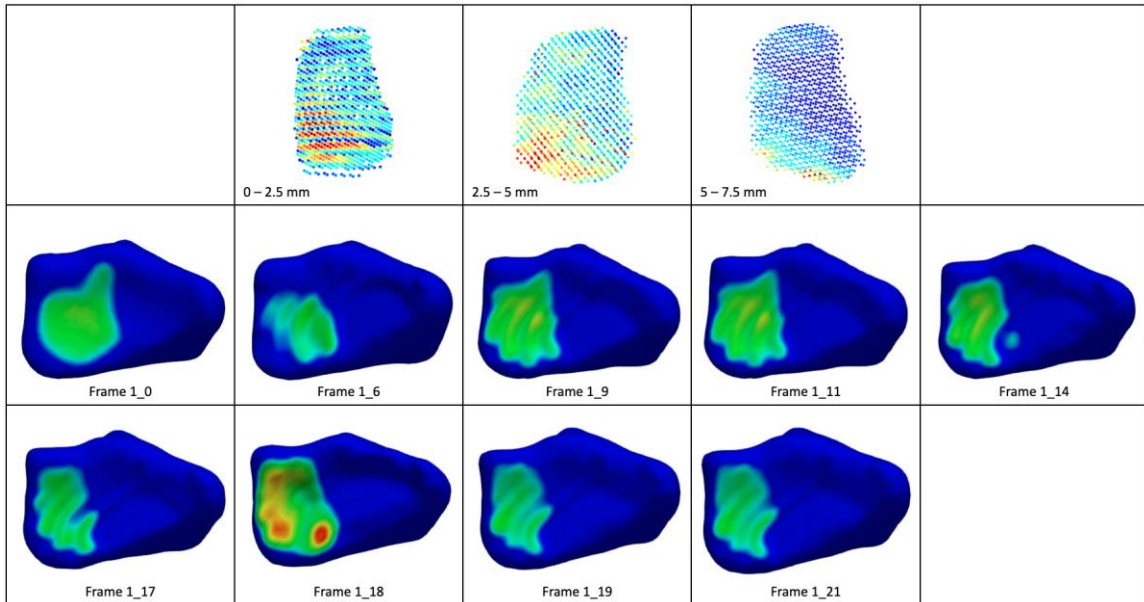
Appendices K-15: Kinematic maps from 111702-58R-Radiolunate joint (top) and radioscaphoid joint (bottom).



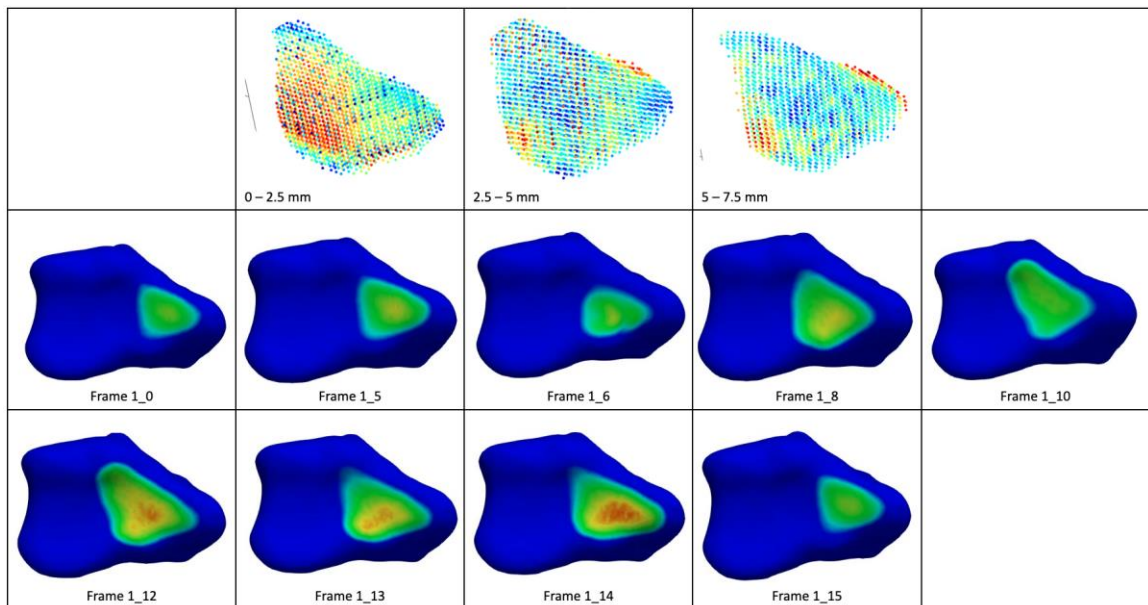
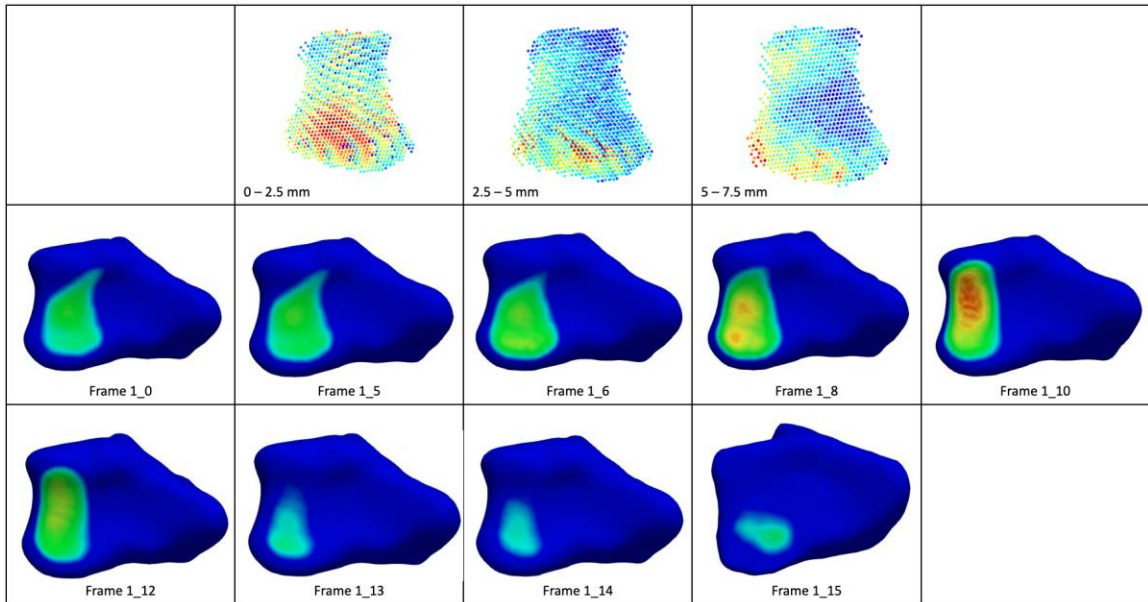
Appendices K-16: Kinematic maps from 111702-71R-Radiolunate joint (top) and radioscaphoid joint (bottom).



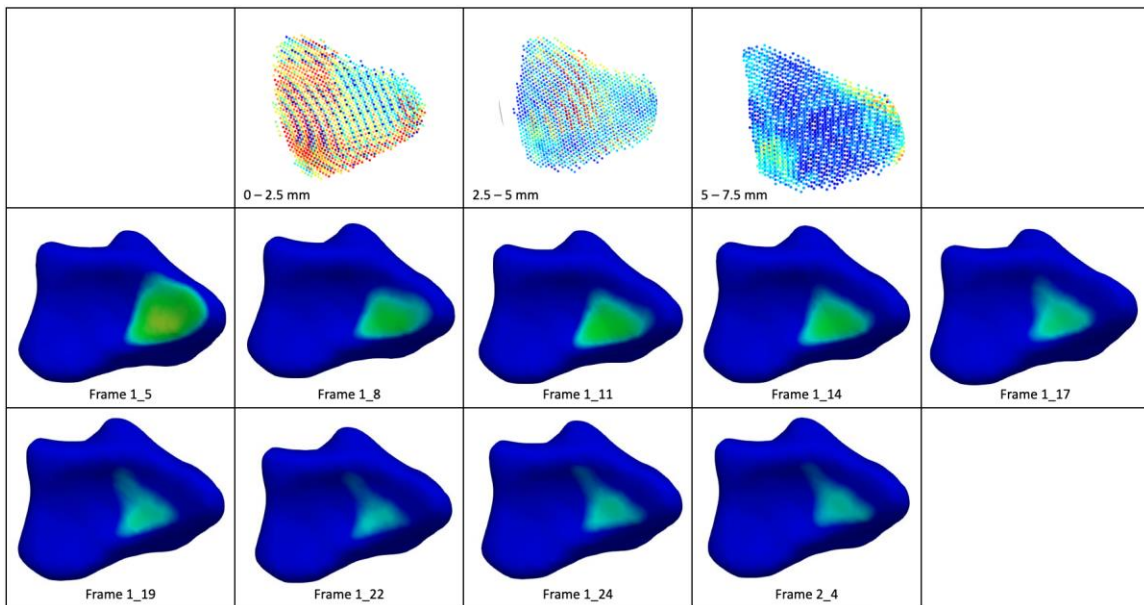
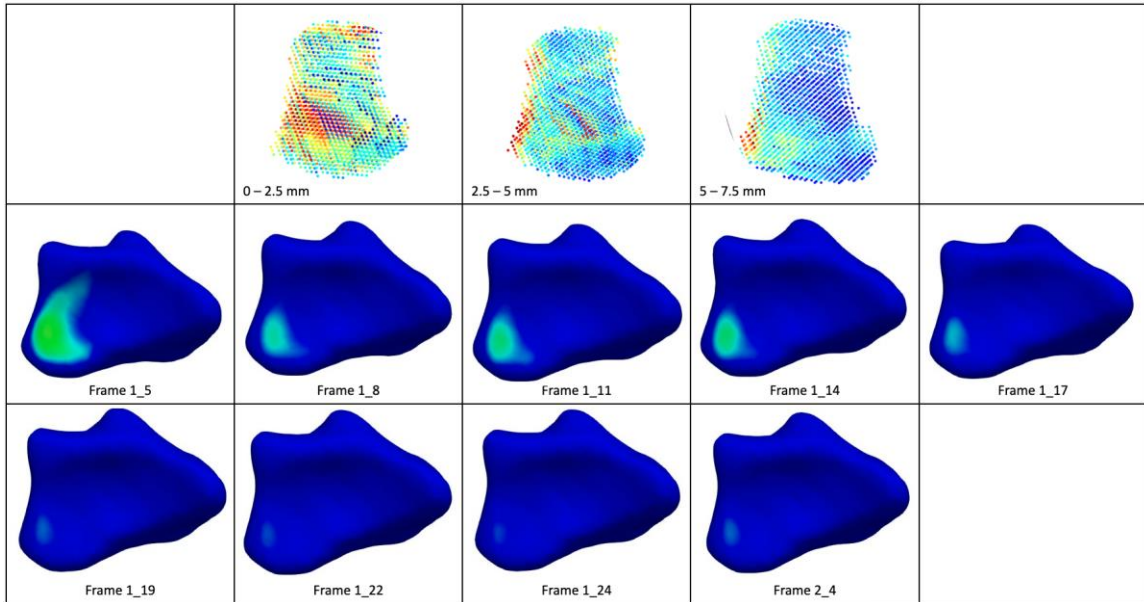
Appendices K-17: Kinematic maps from 111702-72R-Radiolunate joint (top) and radioscaphoid joint (bottom).



Appendices K-18: Kinematic maps from 111702-73R-Radiolunate joint (top) and radioscaphoid joint (bottom).



Appendices K-19: Kinematic maps from 111702-75R-Radiolunate joint (top) and radioscaphoid joint (bottom).



Appendices K-20: Kinematic maps from 111702-78R-Radiolunate joint (top) and radioscaphoid joint (bottom).

Curriculum Vitae

Name: Lauren Straatman, Ph.D. Candidate

**Post-secondary
Education and
Degrees:** University of Toronto
Toronto, Ontario, Canada
2014 - 2019 B.A.

The University of Western Ontario
London, Ontario, Canada
2019 – transferred into Ph.D.

The University of Western Ontario
London, Ontario, Canada
2020 - 2023 Ph.D.

HONORS/ AWARDS/ RECOGNITIONS

- Province of Ontario Graduate Scholarship – 2020-2021, 2022-2023, 2023-2024 (\$15,000/ year).
- Transdisciplinary Bone and Joint Training Award – 2021-2022, 2022-2023 (\$10,000/ year).
- Arthritis Society Canada Ph.D. Salary Award – 2022-2024 (\$35,000/ year).
- Top Paper Award Nominee – Canadian Orthopedic Research Society – 2023 (“The Relationship between Image-Based Biomarkers to Better Understand Osteoarthritis Progression in the Wrist”).
- Top PhD Presenter in Collaborative Specializations in Musculoskeletal Health Research – 2022 (\$200).
- Top PhD Oral Presentation Award – Graduate Research Conference – 2021, 2022 (\$200).
- 2nd Place Poster Presentation – Canadian Bone and Joint Conference – 2020 (\$275).
- Top Masters Oral Presentation – Graduate Research Conference – 2020 (\$100).

RELATED WORK EXPERIENCE

Teaching Assistant – Western University:

- Enabling Health and Well-Being through Occupation – Undergraduate Level
September 2019 – December 2020
- Introduction to Research Methods – Graduate Level
September 2020 – December 2023
- Systemic Approach to Functional Anatomy – Undergraduate Level
September 2022 – December 2022

Undergraduate Research Assistant – The Hand and Upper Limb Center at St. Joseph's Hospital

- **May 2015 – August 2015:** Responsibilities included editing CT scans using an advanced segmentation tool for graduate students to use for patient-specific and medical-imaging based research.

Supervisor: Dr. James Johnson

- **May 2016 – August 2016:** Assisting graduate students with their projects using computer software such as Python, Matlab, and Mimics, as well as editing and running programs on CT scans of the carpal bones in the hand as well as helping to prepare cadaveric specimens for testing.

Supervisors: Dr. James Johnson and Dr. Emily Lalone

- **May 2017 – August 2017:** My responsibilities were split between 2 labs; responsibilities included editing and running programs on CT scans of the carpal bones in the hand as well as helping to prepare cadaveric specimens for testing. At the biomechanics lab on Western University campus, I assisted in experimentation, and processing the video data from experiments to quantify joint motion.

Supervisors: Dr. Emily Lalone and Sara Holland (MSc).

- **May 2018 – August 2018:** Responsibilities included assisting graduate students with their projects using Dartfish Video Analysis Software to quantify joint motion in the hand using video data from testing days. The data was used to develop a Grip Configuration Model that can be used to develop assistive devices. The testing days involved working with participants with and without hand osteoarthritis and running them through a series of tasks of daily living. I presented my own research from this project at the Western Engineering

Undergraduate Summer Research Day where I placed first in the thesis presentation.

Supervisors: Dr. Emily Lalone and Sara Holland (MSc).

OTHER RELATED EXPERIENCE

- President of Health and Rehabilitation Science Graduate Research Society
September 2021-2023.
- VP Social Representative of Health and Rehabilitation Science Graduate Research Society
September 2020-2021

PUBLICATIONS

1. **Straatman, L.**, Norman, E., Knowles, N., Walton, D., & Lalone, E. (2023). Use it or lose it: The relationship between two image-based biomarkers in better understanding osteoarthritis progression in the wrist. *Journal of Biomechanics*, <https://doi.org/10.1016/j.jbiomech.2023.111849>.
2. **Straatman, L.**, Lukacs, M., Grewal, R., Carlesso, L., Walton, D., & Lalone, E. (2023). A systematic review of the psychometric properties of pressure pain detection threshold in evaluating mechanical pain threshold in people with hand or wrist injuries. *Journal of Hand Therapy*, <https://doi.org/10.1016/j.jht.2023.06.008>.
3. **Straatman, L.**, Lukacs, M., Lee, J., Ghodrati, M., Lalone, E., & Walton, D. (2022). Are people good prognosticators of their own pain? An Exploration of the Relationship between Sex-Specific Pain Beliefs and Clinical Pain Evaluation. *Musculoskeletal Science and Practice Journal*, <https://doi.org/10.1016/j.msksp.2022.102667>.
4. **Straatman, L.**, Knowles, N., Suh, N, Walton, D & Lalone, E. (2021). Utility of Quantitative CT (QCT) To Detect Differences in Subchondral Bone Mineral Density Between Healthy People and People with Pain Following Wrist Trauma. *Journal of Biomechanical Engineering*, <https://doi-org.proxy1.lib.uwo.ca/10.1115/1.4053594>.
5. Robinson, S., **Straatman, L.**, Lee, T., Suh, N., & Lalone, E. (2021). Evaluation of Four-Dimensional Computed Tomography as a Technique for Quantifying Carpal Motion. *Journal of Biomechanical Engineering*, <https://doi-org.proxy1.lib.uwo.ca/10.1115/1.4050129>.

6. Holland, S., **Straatman, L.**, Sinden, K., MacDermid, J., & Lalone, E. (2020). The Development of a Novel Grip Motion Analysis Technique using the Dartfish Movement Analysis Software to Evaluate Hand Movements during Activities of Daily Living. *Medical Engineering and Physics*, <https://doi.org/10.1016/j.medengphy.2020.09.010>.
7. Holland, S., MacDermid, J., **Straatman, L.**, Sinden, K., & Lalone, E. (2018). Upper Limb Motion Demands of Tasks of Daily Living: Application of Dartfish Movement Analysis Software. *Journal of Hand Therapy*.

MANUSCRIPTS IN PREPARATION

1. DuToit, C., Hutter, M., Dima, R., Mudathir, R., **Straatman, L.**, Chun, J., Fenster, A., & Lalone, E. 3D Ultrasound for Monitoring Thumb Osteoarthritis Patients: A Pilot Longitudinal Study of Imaging Biomarkers.

PRESENTATIONS AT SCIENTIFIC MEETINGS

1. Use it or lose it: The Relationship between Kinematic Joint Contact and Depth-Specific Subchondral Bone Mineral Density (2023). Canadian Orthopaedic Research Conference, Calgary, Canada. *This work was selected to be a part of the Top Canadian Research Paper Session, eligible for a Founder's Award.*
2. Use it or lose it: The Relationship between Kinematic Joint Contact and Subchondral Volumetric Bone Mineral Density (2023). Canadian Arthritis Research Conference, Toronto, Canada.
3. The Relationship between Kinematic Joint Contact and Subchondral Bone Mineral Density (2023). Ontario Biomechanics Conference, Waterloo, Canada.
4. Use it or lose it: The Relationship between Kinematic Joint Contact and Subchondral Volumetric Bone Mineral Density (2023). Orthopedic Research Society Conference, Dallas, United States of America.
5. An Exploration of the Relationship Between Kinematic Joint Contact and Subchondral Volumetric Bone Mineral Density: Preliminary Results (2022). Canadian Bone and Joint Conference, London, Canada.
6. An Exploration of the Relationship between Kinematic Joint Contact and Subchondral Volumetric BMD (2022). Imaging Network Ontario, Toronto, Canada.
7. The Exploration of the Relationship between Kinematic Joint Contact and Subchondral Bone Mineral Density (2022). Orthopaedic Research Conference, Miami, United States of America.

8. An Exploration of the Relationship Between Kinematic Joint Contact and Subchondral Volumetric Bone Mineral Density (2022). Canadian Orthopaedic Research Society Conference, Quebec, Canada.
9. The Development of Image-Based Biomarkers using 4DCT scans to Differentiate between Healthy and Previously Fractured Wrists (2021). The Canadian Pain Society Annual Scientific Meeting, *Virtual*, Canada.
10. The Development of Imaged-Based Biomarkers to Elucidate Mechanisms Underpinning Pain Post Wrist Fracture (2021). Orthopaedic Research Society Conference, *Virtual*, Canada.
11. An Exploration of the Relationship between Subjective and Objective Pain (2020). Canadian Bone and Joint Conference, London, Canada.
12. The Development of Two Image-Based Biomarkers to Elucidate Mechanisms Underpinning Pain Post Wrist Fracture (2020). IASP World Congress of Pain, Amsterdam, Netherlands. *Accepted before conference cancellation due to COVID-19.*
13. The Development of Diagnostic Platform to Detect at Risk Patients Following Wrist Fracture in the Prevention of Complex Regional Pain Syndrome (2020). Health and Rehabilitation Sciences Graduate Research Conference, London, Canada.
14. Grip Configuration in People with and without Hand Osteoarthritis during Tasks of Daily Living: Application of Dartfish Analysis Software (2018). Undergraduate Research Day, London, Canada.